

Cover Page



Universiteit Leiden



The handle <http://hdl.handle.net/1887/18932> holds various files of this Leiden University dissertation.

Author: Vrij, Jeroen de

Title: Improvement of oncolytic adenovirus vectors through genetic capsid modifications

Issue Date: 2012-05-10

Improvement of Oncolytic Adenovirus Vectors through Genetic Capsid Modifications

Jeroen de Vrij

Cover: The cover illustrates the ongoing developments in the field of oncolytic adenovirology. The mechanism of action of an oncolytic adenovirus is illustrated by the virus particles attacking the crab. The crab is the international symbol of cancer. Cancer was originally named *karkinoma* (Greek for *krab*) by Hippocrates, to whom the growth of a tumor with its sprouting blood vessels reminded on the legs and claws of a crab. As indicated, different types of capsid modifications are being explored to establish tumor-targeting, for example through adding a heterologous polypeptide to the fiber protein or to protein IX. The staircase symbolizes the 'road towards successful oncolytic virus therapies'. The helical form of the staircase illustrates the importance of introducing genetic modifications in the DNA genome of oncolytic adenoviruses.

Copyright © 2012 J. de Vrij, Zoeterwoude, The Netherlands. All rights reserved. No part of this publication may be reproduced or transmitted in any form, without permission from the copyright owner.

The cover includes modified art work from Aruana16 (the crab) and Megainarmy (the spiral stairs) (copyrights were obtained at www.shutterstock.com), and from Jort Vellinga (adenovirus particles) (copyrights were obtained from J. Vellinga).

ISBN: 978-94-6182-092-1

Layout & printing: Off Page, www.offpage.nl

Printing of this thesis was financially supported by the J.E. Jurriaanse Stichting

Improvement of Oncolytic Adenovirus Vectors through Genetic Capsid Modifications

PROEFSCHRIFT

ter verkrijging van
de graad van Doctor aan de Universiteit Leiden,
op gezag van Rector Magnificus prof. mr. P.F. van der Heijden,
volgens besluit van het College voor Promoties
te verdedigen op donderdag 10 mei 2012
klokke 13:45 uur

door

Jeroen de Vrij
geboren te Stolwijk
in 1979

PROMOTIECOMMISSIE

Promotor: Prof. dr. R.C. Hoeben
Overige leden: Prof. dr. A.J. van Zonneveld
Prof. dr. C.H. Bangma (Erasmus Medisch Centrum, Rotterdam)
Dr. G. van der Pluijm

The research presented in this thesis was performed at the department of Molecular Cell Biology, Leiden University Medical Center, Leiden, The Netherlands.
The work described in this thesis was supported by the European Union through the 6th Framework Program GIANT (contract no. 512087).

TABLE OF CONTENTS

Chapter 1	General introduction	7
Chapter 2	Adenovirus-derived vectors for prostate cancer gene therapy	31
Chapter 3	Efficient incorporation of a functional hyper-stable single-chain antibody fragment protein-IX fusion in the adenovirus capsid	51
Chapter 4	Adenovirus targeting to HLA-A1/MAGE-A1-positive tumor cells by fusing a single-chain T-cell receptor with minor capsid protein IX	65
Chapter 5	A cathepsin-cleavage site between the adenovirus capsid protein IX and a tumor-targeting ligand improves targeted transduction	87
Chapter 6	An oncolytic adenovirus redirected with a tumor-specific T-cell receptor	107
Chapter 7	Enhanced transduction of CAR-negative cells by protein IX-gene deleted adenovirus 5 vectors	125
Chapter 8	General discussion	145
Addendum	Summary	157
	Nederlandstalige samenvatting	159
	Dankwoord	161
	List of publications	162
	Curriculum Vitae	164

CHAPTER 1

GENERAL INTRODUCTION

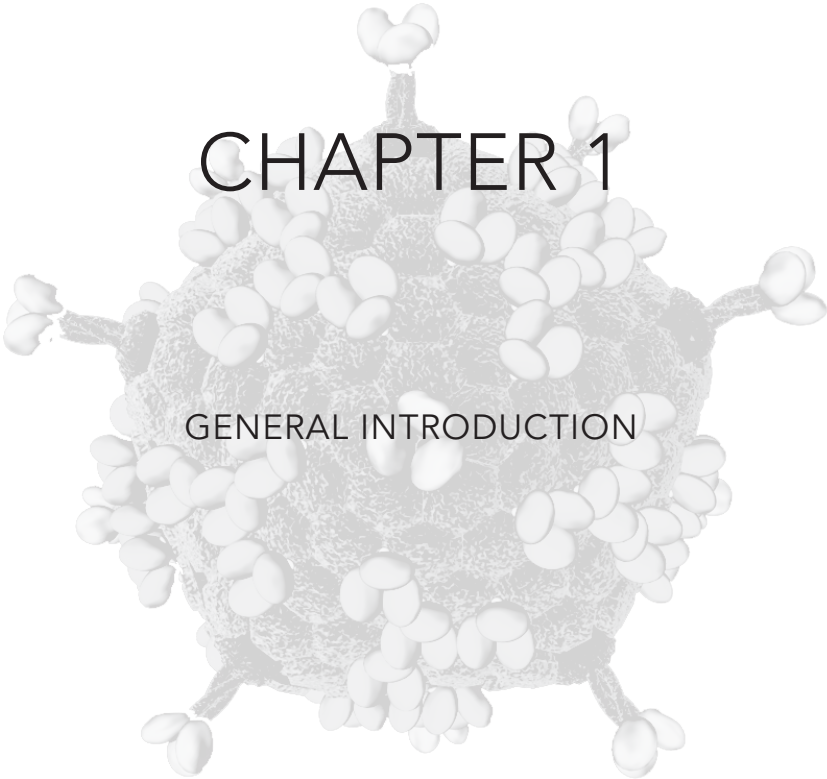




TABLE OF CONTENTS

1.1 Aims and outline of this thesis	9
1.2 Biology of Human Adenovirus Type 5	10
1.2.1 Virion architecture	11
1.2.2 Cellular infection route	12
1.2.3 Replication	13
1.2.4 Capsid protein IX	14
1.3 Adenovirus vectors for cancer therapy	16
1.3.1 Replication-deficient vectors	17
1.3.2 Conditionally-Replicating Adenoviruses (CRAds)	18
1.3.3 Capsid modifications for targeting and detargeting	20
1.3.4 Random approaches to vector development	22

1.1 AIMS AND OUTLINE OF THIS THESIS

Aims

1. To establish the production of HAdV-5 particles decorated with protein IX-fused polypeptide ligands that have proven potential for tumor targeting, such as single-chain antibody fragments, single-chain T-cell receptors, or Affibody molecules.
2. To investigate the targeting efficacy and specificity of protein IX-ligand decorated HAdV-5 vectors to tumor cell lines.
3. To investigate the targeting of HAdV-5 to cancer-testis antigens through fusing a single-chain T-cell receptor with protein IX or fiber molecules.
4. To analyze the effect on transduction of incorporating cathepsin-cleavage sites in between HAdV-5 protein IX and its fused targeting ligand.
5. To obtain insight into the biological consequences of protein IX modification.

Outline

Chapter 1 provides a general introduction on HAdV-5, which is the best-studied adenovirus serotype and the serotype most-often used for the construction of oncolytic vectors for cancer gene therapies. Important aspects on the biology of HAdV-5 are summarized, including the virion architecture, the infection route, and the replication mechanism. A separate paragraph is devoted to the minor capsid protein IX of HAdV-5, taking into account the important role of this protein in this thesis. Chapter 1 also provides a general overview on oncolytic adenovirus vectors. Vector modification strategies aiming at improved efficacy are described, as well as strategies for reducing transduction of non-target tissues. The ins and outs are provided for replication-deficient HAdV-5 vectors, as well as for the more recently developed Conditionally Replicating Adenoviruses (CRAds).

In Chapter 2 the most recent advances in oncolytic adenovirus technology are described, focusing on vectors for prostate-cancer treatment. The most prominent bottlenecks for successful cancer gene therapy with oncolytic viruses are reviewed, and potential solutions to overcome these hurdles are outlined.

Chapters 3, 4, and 5 describe the usability of the adenovirus minor capsid protein IX as an anchor for genetically fusing tumor targeting ligands.

The feasibility of fusing large and complex polypeptides to protein IX is described in Chapter 3. As a model ligand the hyper-stable single-chain antibody fragment 13R4 was chosen, which binds with high affinity to β -galactosidase. Incorporation of protein IX-13R4 polypeptides in the virus capsid was achieved with our previously developed "protein-IX screening" system, encompassing the transduction of a protein IX-13R4 producing helper cell line with a protein IX gene-deleted HAdV-5 vector, followed by harvesting and purification of the progeny viruses. Incorporation efficiency and functionality of 13R4 in the capsid of the HAdV-5 vector is discussed.

As a next step, using the same ligand incorporation strategy, a tumor-targeting ligand was fused with protein IX (Chapter 4). Since cancer-testis (CT) antigens have been described to be truly tumor-specific (except for their expression in the testis) it was decided to fuse protein IX with a single-chain T-cell receptor (scTCR) directed

against the CT antigen MAGE-A1, in complex with HLA-A1. Efficacy of targeting to HLA-A1/MAGE-A1 positive melanoma cell lines is described, as well as various assays to analyze the specificity of targeting.

Chapter 5 describes the results on HAdV-5 viruses targeted to tumor cells through fusion of a high-affinity binding Affibody molecule to protein IX, and the effects of incorporating a cathepsin-cleavage site (ccs) in between protein IX and the Affibody molecule. Previous findings by us and by others suggested that protein IX-mediated targeting using 'high-affinity binders' (like Affibody molecules) as ligand is limited by inefficient release of protein IX-fused ligands from their cognate receptors in the endosome. This would result in inefficient endosomal escape of the virus particles. Chapter 5 comprises an extensive comparison between HAdV-5 viruses containing either wild type protein IX, protein IX-Affibody, or protein IX-ccs-Affibody in the capsid. The transduction efficiency is compared in monolayer cultures, 3-dimensional spheroid cultures, and in SKOV-3 tumors grown on the chorioallantoic membrane of embryonated chicken eggs.

In addition to the analyses of the protein IX-scTCR loaded HAdV-5 vectors, as described in Chapter 4, the usability of the HLA-A1/MAGE-A1 specific scTCR for HAdV-5 targeting was also tested in the context of fusion with the fiber protein (Chapter 6). The adenoviral fiber knob, which is responsible for attachment to the Coxsackie virus and Adenovirus Receptor (CAR) on target cells, was replaced by the scTCR molecule and an extrinsic trimerization motif in a replication-competent HAdV-5 vector. The efficacy and specificity of targeting is presented through comparison of cell killing in a panel of melanoma cell lines.

Functional consequences of deleting the protein IX gene from HAdV-5 vectors are described in Chapter 7. The findings provide novel insights into the biological role of protein IX, and may be of relevance for future development and clinical implementation of protein IX-modified HAdV-5 vectors.

Chapter 8 provides a general discussion on the potency of protein IX-mediated tumor targeting for the development of improved oncolytic HAdV-5 vectors. Recommendations for further preclinical studies are included. Also, an overview is given on the newest insights and developments in preclinical testing of oncolytic AdV vectors in general. The anticipated essence of various model systems for future vector analyses is described.

1.2 BIOLOGY OF HUMAN ADENOVIRUS TYPE 5

Adenovirus was first isolated in the 1950s from adenoid tissue-derived cell cultures. These primary cell cultures were often noted to spontaneously degenerate over time, and human adenoviruses (HAdV), (belonging to the family Adenoviridae, genus Mastadenovirus) are now known to be a common cause of asymptomatic respiratory tract infection that produces *in vitro* cytolysis in these tissues. Based on serological parameters, hemagglutination parameters, restriction enzyme digestion patterns, and nucleotide sequence analyses, 55 types of HAdV have been described (51 'serotypes' identified by traditional immunochemical methods, and 4 'types' defined by genomics). These have been classified in seven species, A to G. Most HAdV serotypes cause mild diseases in immunologically healthy people, but some serotypes

can cause considerable morbidity, especially in individuals who are compromised immunologically (e.g. transplant patients) or nutritionally (e.g. gastrointestinal infections in children in the developing world).

Adenoviruses are icosahedral, non-enveloped viruses of approximately 90 nm in size, belonging to the largest non-enveloped viruses. Recently, the structure of a HAdV has been solved at the atomic level, providing the largest high-resolution model ever.^{1,2} Research on adenoviruses has yielded ample knowledge on various cell biology mechanisms, such as RNA splicing.³ Also, laboratory experiments on adenoviruses and their derived vectors has come along with the development of important molecular-biological techniques like the calcium-phosphate DNA transfection method.⁴

Various aspects, including the relative safety, the well-known biology, and the suitability for genetic modification, have made vectors derived from HAdV type 5 (belonging to the species C HAdVs) the currently most-often used vehicles for viral gene-delivery. HAdV-5 vectors have been used extensively as vaccine, and have shown great potential for *ex vivo* and *in vivo* gene therapies for treatment of hereditary diseases or cancer.

1.2.1 Virion architecture

A fully mature HAdV-5 particle, with an approximate mass of 150 MDa, consists of an icosahedral capsid of 20 facets and a core, as schematically depicted in **Fig. 1**. The pentons, hexons and fibers form the so-called major proteins of the adenovirus capsid. The minor proteins of the capsid are proteins IIIa, VI, VIII and IX. The core consists of a double-stranded linear DNA genome (36 kb in size) and of several proteins: proteins IVa2, V, VII, terminal protein (TP), mu, and the adenovirus protease.^{5,6} The HAdV-5 genome contains transcriptional units referred to as early (regions E1 to E4), intermediate (regions pIX and IVa2) and late (regions L1 to L5) depending on their temporal expression, relative to the onset of viral DNA replication.

The fiber protein in the capsid has been identified as the main cell binding protein, with the cell surface protein bound being the coxsackievirus and adenovirus receptor (CAR).⁷ CAR binds to the fiber knob domain, which is located at the carboxyl-terminus of the fiber shaft domain. The fiber tail is mounted on the vertex protein penton base. Penton base is located on each vertex and has protruding arginine-glycine-aspartic acid (RGD)-domains that are involved in secondary cell binding and the initiation of virus endocytosis through integrin binding.^{8,9} Penton base has also been suggested to play a role in endosomal escape of virus particles, evidenced by the blocking of adenovirus induced endosomal lysis by α -penton antibodies and addition of soluble penton.^{10,11} The bulk of the capsid consists of 240 copies of trimeric hexon, contributing to approximately 50% of the mass of the capsid.¹² The hexon content of a capsid can be divided in two subgroups. The groups of nine (GON) are a group of hexons that is frequently observed after dissociation of the capsid.¹³ The non-GON belonging hexons are the peripentonal hexons. These are, as the name suggests, the hexons in direct contact with the penton bases. Each trimeric hexon has three towering structures on top, with a cavity in between that can be bound by coagulation factor X in HAdV-5.^{14,15}

Most minor capsid proteins have an assigned capsid localization, but their mechanism of function has often not yet been fully resolved. Protein IIIa was found to be important

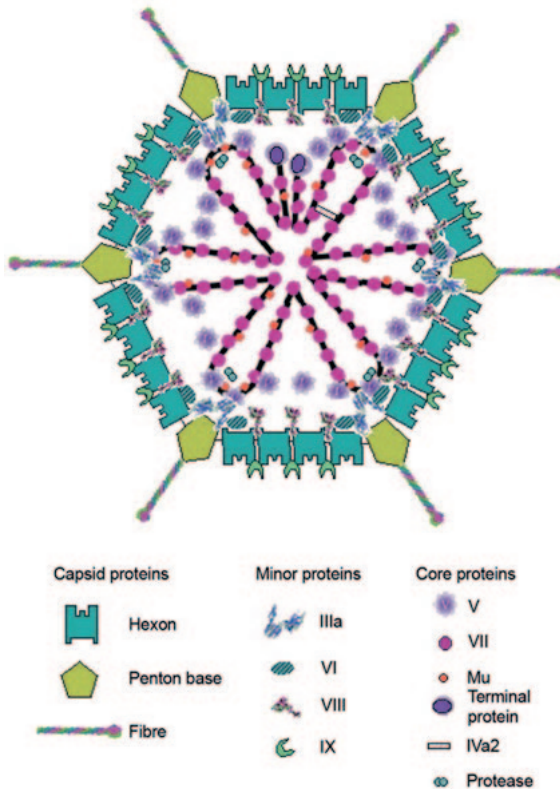


Figure 1. Schematic representation of the adenovirus structure. Taken from Russell.⁶

for packaging the viral DNA as well as capsid maturation and localizes on the inner side of the pentons.¹⁶ Protein VI has been localized to the inner cavity of hexons and has a function in hexon transport into the nucleus during virus assembly, as well as being involved in the lysis of endosome membranes.¹⁷⁻¹⁹ Protein VIII (assigned to the inner capsid) is thought to provide the capsid stability but the exact functions remains to be solved.²⁰ A description on the smallest but most abundant minor capsid protein, protein IX, is provided in more detail below, since this protein plays a major role in this thesis.

1.2.2 Cellular infection route

Different receptors are involved in adenovirus cell binding.²¹ The main receptor for adenoviruses is CAR, which binds to the fiber knob.⁷ Alternatively, species B adenoviruses utilize different receptors, that is, CD46 for species B1 (serotypes 16, 21, 35, 50), desmoglein 2 for species B2 (serotypes 3, 7, 14), and CD46 or desmoglein 2 for species B3 (serotype 11).²² Furthermore, cell surface sialic acid molecules can be utilized as a receptor by various serotypes, such as HAdV-37 from species D.^{23,24} Recently, a new mechanism of cellular uptake was discovered for HAdV-5, via the interaction of hexon with coagulation factor X (FX). This mechanism appears to be a major cause for the uptake of systemically introduced HAdV-5 vectors in the liver, through the binding of virus-bound FX to heparan sulphate molecules on hepatocytes.^{14,15,25} However, it

remains to be established how important the latter mechanism is for transduction of liver cells in humans. After the initial docking of a HAdV-5 particle to its primary receptor, various secondary interactions can occur, the most prominent one being the interaction of RGD domains of penton base with integrins $\alpha_v\beta_3$ or $\alpha_v\beta_5$.^{8,9} Also heparan sulphate proteoglycans have been identified as cell surface molecules for secondary interactions, through binding to the fiber shaft.²⁶ Shortly after cell binding the fiber is shed.^{27,28} The interaction of penton base RGD domains with cellular integrins induces a conformational change of penton base monomers, suggested to be necessary for fiber release or for breaking contacts with the surrounding hexons, allowing the fiber or the penton base to be released.²⁹ Integrin aggregation through penton-base binding localizes the virus to clathrin coated endosomes, the main entry route for adenovirus.³⁰ Integrin binding also activates various intracellular signaling routes, including the MAPK/p38 and the p85/p110 PI(3) kinase routes, which is thought to influence susceptibility of adenovirus uptake by the canonical routes and by other endocytosis pathways such as macropinocytosis.^{31,32} Once the virus is in the clathrin-coated endosome and the environment acidifies, the release of pVI triggers endosomal escape.^{18,19} Once in the cytosol, HAdV-5 binds molecular motors that move over microtubules; a minus end directed motor (kinesin) and a plus end directed motor (dynein). These motors are engaged in a tug of war principle, resulting in speeds of movement of micrometers per minute.^{33,34} Hexon seems to be the protein responsible for binding kinesins and dyneins.³⁵ Whether the movements of the viral particle occur according to a stochastic tug of war principle or whether all movements are coordinated is still subject of debate.³⁶ Alternatively, microtubule independent transport has been reported, suggesting other cytosolic transport mechanisms.^{37,38} When the partially dismantled HAdV-5 particle reaches the nucleus, it binds the nuclear pore complex and is further dismantled.³⁹ Subsequently, the viral DNA is imported and transcription of genes can be initiated.

1.2.3 Replication

The adenoviral genes can be classified in three groups, based on their time of transcription after infection: the early genes (E1A, E1B, E2, E3, and E4), the intermediate genes (pIX and IVa2), and the late genes (L1 to L5).⁴⁰ Genes are transcribed from both DNA strands and the majority of RNA transcripts are subject to complex splicing patterns. The first messengers to be transcribed after infection are the E1A transcripts. The E1A proteins induce the cell to enter the cell cycle, necessary for replication of the adenoviral DNA, through binding cellular proteins including the retinoblastoma gene product Rb. The E1B-55kD protein binds p53, thereby preventing apoptosis or blockage of the cell cycle. The E2 proteins (terminal protein, DNA-polymerase, and single-stranded DNA binding protein) are involved in viral DNA replication, the E3 proteins play essential roles in down-regulating the host immune response against HAdVs, and the E4 proteins have multiple functions in the regulation of viral transcription, replication and mRNA transport. The late genes encode the capsid proteins, with the exception of capsid protein IX, which is a product from an intermediate gene.

1.2.4 Capsid protein IX

The 14.3 kDa protein IX is the smallest of the HAdV capsid proteins. Protein IX is unique to the Mastadenoviruses and is, in contrast to the other capsid proteins, absent in the other adenovirus genera. During the viral replication cycle, the transcription of protein IX messenger RNAs is, for unknown reasons, initiated relatively early after infection, as compared to the mRNAs of the other capsid proteins.⁴⁰ Each virus facet contains 12 molecules of protein IX, resulting in a total of 240 molecules per virion. The protein has three conserved regions, as shown by amino acid alignment, located at the amino-terminus, the middle part, and the carboxyl-terminus of protein IX. The amino-terminal regions of protein IX are positioned in the cavities between the hexon tops of hexons that belong to a GON. Each cavity contains the amino-termini of three molecules of protein IX.⁴¹ The recent determination of the HAdV-5 structure, by means of cryoelectron microscopy and x-ray analyses, has revealed the carboxyl-terminus of protein IX to be present in the capsid as quadrimeric coiled-coils, at a location previously assigned to the minor capsid protein IIIa.^{1,2,42,43} The orientation of the four coiled-coils is parallel for three of the coils, originating from one facet of the capsid, and anti-parallel for one coil, originating from a neighbouring facet.^{1,2,43} Taken together, these assignments result in a large network of protein IX, spanning the entire capsid (**Fig. 2**).

Despite many years of research the definite function of protein IX is still to be assigned. The protein highly likely acts as capsid cement, since deletion of the protein causes thermal instability.⁴⁴ The amino-terminus appears to be exclusively responsible for incorporation of protein IX in the virus capsid and for providing the capsid its thermal stability, probably through stabilizing the GONs.⁴⁵ Besides its postulated role in providing the virion stability, protein IX seems to play a role in viral DNA packaging, as suggested by the finding that viruses lacking protein IX have a strong reduction in infectivity if the genome is larger than 95% of wild-type size (>35 kb).^{46,47} The carboxyl-terminus of protein IX, which can be deleted from HAdV-5 without affecting thermostability, has been suggested to be essential for post-infection interactions of protein IX with cellular factors, resulting in a stimulatory effect on promoters of early viral genes.⁴⁸ However, this effect, which was found in a non-viral context, was subsequently toned down by another study, showing no significant effect of protein IX on viral transcription in the context of viral infection.⁴⁹

Interestingly, protein IX was reported to form clear amorphous bodies in the nucleus, strongly resembling the so-called PML (promyelocytic leukemia protein) bodies in terms of size and protein contents (including PML and sp100).⁵⁰ Deleting the carboxyl-terminus of protein IX abrogated the capacity of protein IX to form PML bodies. Appreciating the importance in cellular biology of PML bodies, for example functioning in regulation of cell cycle and cell growth, it was tempting to speculate on a role of (the carboxyl terminus of) protein IX in host cell modulation.⁵⁰ However, such a role has not been confirmed in subsequent experiments. The relevance of the PML-protein IX bodies in HAdV-5 biology is questionable, based on results obtained in our laboratory (De Vrij, unpublished data, **Fig. 3**). To our surprise, expression of protein IX in normal diploid cells (VH10 cells (primary foreskin fibroblasts) and mesenchymal stem cells (MSCs)) results in protein IX localization in both cytoplasm and nucleus, with significant accumulation of the protein at certain cytoplasmic locales. Protein

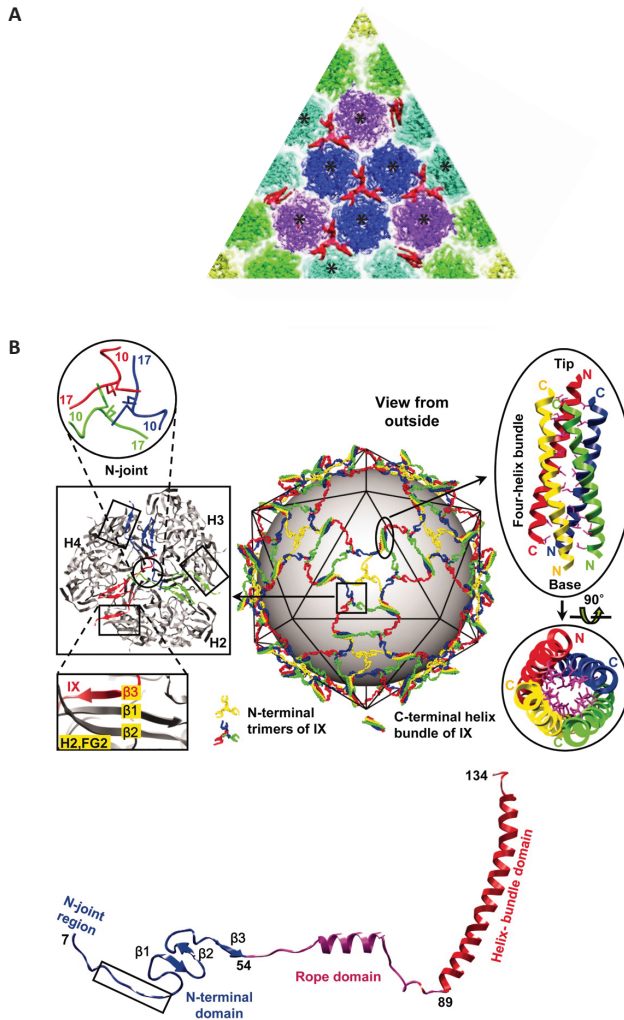


Figure 2. Capsid structure of HAAdV-5. (a) Protein density on an exterior region of the capsid, roughly corresponding to one icosahedral facet. The model was created through overlaying a cryo-electron microscopy model of the entire virus particle (at 6-Å resolution) with X-ray crystallography structures of individual proteins. Penton base monomers are indicated in yellow, and hexons are indicated in green (position 1), cyan (position 2), blue (position 3), and magenta (position 4). Protein IX densities, as four trimeric regions and three helical bundles, are indicated in red. Hexons belonging to a group of nine (GON) are marked with an asterisk (*). Figure adapted from Saban *et al.*⁴² (b) CryoEM (at 3.6-Å resolution) reveals a physical network of protein IX in the capsid, lashing together hexons into GON tiles. Left insets: Ribbon models of the N-terminal domains of three protein IX monomers (blue, green, and red), overlaying the models of three adjacent hexon monomers (H2, H3, and H4) (gray). The N-terminus of protein IX is in close proximity to the FG2 region of a hexon monomer (lower left inset). Right insets: Ribbon models of the C-terminal domains of protein IX. Four C-terminal domains form a bundle consisting of three parallel α -helices and one antiparallel α -helix. The helices are linked by a ladder of hydrophobic residues (leucines and valines) (magenta). Bottom inset: Ribbon model of protein IX showing three distinguished domains as well as the N-joint region. Figure adapted from Liu *et al.*¹

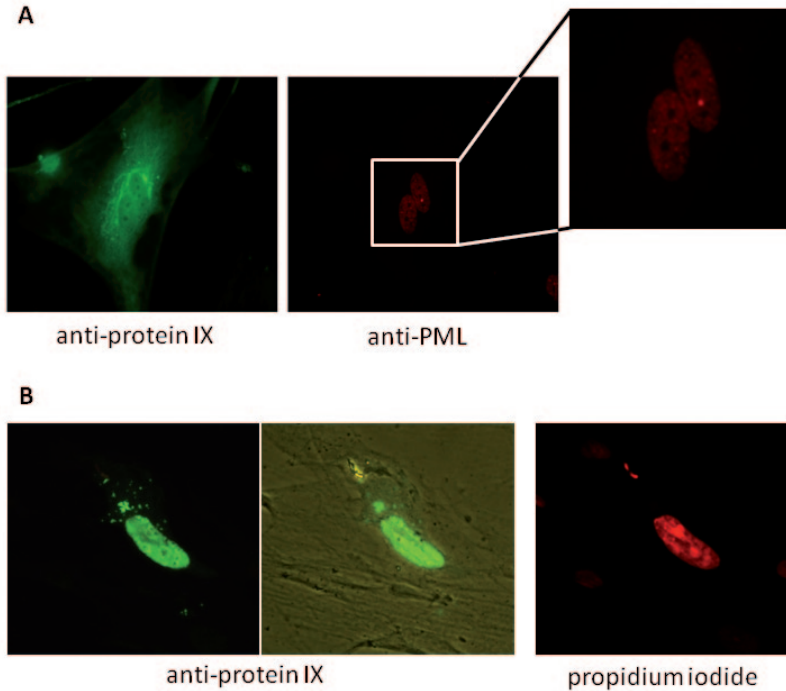


Figure 3. Subcellular localization of protein IX in mesenchymal stem cells, as visualized by immunohistochemistry. **(a)** Detection of protein IX and promyelocytic leukemia (PML) protein after establishing lentiviral vector-mediated heterologous expression of protein IX. The cells were fixed with acetone-methanol (1:1). Staining was performed by means of primary incubation with the antibodies α -protein IX (rabbit, polyclonal)⁵¹ and α -PML (5E10; mouse, monoclonal),⁵² followed by secondary incubation with α -rabbit-FITC and α -mouse-Alexa594, respectively. **(b)** Detection of protein IX after infection with HAdV-5. Infection was performed with 10 virus particles per cell. The cells were fixed with acetone-methanol (1:1), at 72 hours post infection. Staining was performed through subsequent incubations with antibodies α -protein IX (rabbit, polyclonal) and α -rabbit-FITC. The nuclei were stained with propidium iodide.

IX appeared not to co-localize with PML. In the context of HAdV-5 infection in these primary cell cultures, protein IX localizes to the nucleus, regularly forming ring-like structures. In contrast, and in line with the results published by Rosa-Calatrava *et al.*,⁵⁰ protein IX formed nuclear bodies in transformed cell lines like A549 alveolar epithelium cells. These observations argue against a role of protein IX in nuclear sequestration of PML in non-transformed cells.

1.3 ADENOVIRUS VECTORS FOR CANCER THERAPY

Genetically modified adenoviruses have been explored extensively as gene-transfer vehicle for the purpose of gene therapy or vaccination.⁵³ Several characteristics make adenoviruses highly suitable as gene-transfer vehicle: a relatively low level of pathogenicity; a high stability of the viral DNA genome, thereby preventing the

development of heterogeneous populations of 'quasispecies'; the ability to transduce dividing as well as quiescent cells; the well known biology and uncomplicated genetic modification; the availability of technologies for production of clinical-grade virus batches with high titers and high purity. Adenoviruses can be used either as replication-deficient or replication-competent vectors. The replication-deficient vectors can be used as gene delivery vehicle for gene augmentation therapy (e.g. through delivery of genes that are mutated in the vector-receiving patient) or cancer therapy (e.g. through delivery of prodrug-activating genes). Also, replication-deficient vectors are being used (with proven efficacy and safety) as vaccine vector to induce immune responses against antigenic polypeptides that are displayed on the viral capsid or encoded for by the viral vector.⁵⁴ More recently, replication-competent adenovirus vectors, or Conditionally Replicating Adenoviruses (CRAdS), have been developed, exploiting the lytic infection cycle of the virus to kill tumor cells. Various modifications can be introduced to CRAdS to provide tumor cell selective replication.

Currently, the large majority of adenovirus vectors for cancer therapies are derived from HAdV of serotype 5, mainly as a result of its well known biology and its proven safety. In the next paragraphs a general overview is given on the development of HAdV-5-derived vectors for cancer therapy, describing replication-deficient as well as replication-competent vectors. An extensive outline is provided on rational design approaches towards improved oncolytic HAdVs, such as capsid modifications for targeting and detargeting purpose. Preclinical developments on random approaches, such as bioselection with mutagen-induced viral libraries, are summarized as well.

1.3.1 Replication-deficient vectors

Different types, or 'generations', of replication-deficient HAdV-5 vectors have been developed. The first-generation vectors have the E1 region deleted.⁵⁵ This deletion renders the recombinant virus replication-defective, providing an important safety feature. The production of E1-deleted vectors is dependent on specialized helper cells that provide the E1 functions *in trans*. The most frequently used helper cell lines are the 293 cell line (human embryonic kidney cells transformed with sheared HAdV5 DNA)⁵⁶ and the 911 and PER.C6 cell lines (human embryonic retinoblasts transformed with a plasmid carrying a defined portion of the adenovirus genome).^{57,58} By combining removal of the E1 region with removal of the E3 region, which encodes for proteins involved in evasion of the immune system and is dispensable for vector growth *in vitro*, approximately 7500 base pairs of heterologous DNA can be accommodated in HAdV-5 vectors.

The first-generation HAdV-5 vectors appeared to be suboptimal for certain gene-delivery applications, mainly as a result of the induction of a strong cell-mediated immune response.⁵⁹ These responses appeared to be a result of viral protein expression. As a consequence second-generation HAdV-5 vectors were made in which deletions or mutations were introduced in the E2 and E4 region. These modifications resulted in a substantial reduction of the cellular immune response and, as a consequence, prolonged transgene expression.⁵⁵ Also third-generation or 'high-capacity' HAdV-5 vectors have been developed, which are devoid of all viral genes and can accommodate up to 35 kilo bases of heterologous DNA.^{55,60} The only remaining viral sequences are the inverted terminal repeats (ITRs) and the packaging signal. Production of high-

capacity vectors requires the usage of a helper virus to provide all viral functions and structural proteins *in trans*. Elegant systems have been developed to prevent the presence of helper virus contaminants in the final high-capacity vector preparation. As intended, high-capacity HAdV vectors have a strongly improved duration of transgene expression as compared to first- or second-generation HAdV vectors, as a result of a reduced cellular immune response.⁵⁵

As evidenced by various studies, the first-generation HAdV-5 vectors are inferior to the higher-generation vectors in these gene-delivery applications that require the *in vivo* expression of large heterologous genes for prolonged times. However, the usage of replication-deficient vectors for the (short-term) expression of oncolytic genes in cancer cells not necessarily requires the usage of higher-generation vectors. First-generation vectors can perfectly accommodate the majority of anti-tumor transgenes and, importantly, induce immune responses that might be of benefit for the efficacy of the therapy (e.g. through induction of a cellular immune response against tumor antigens). Examples of anti-tumor transgenes are genes encoding for prodrug converting enzymes (e.g. the Herpes Simplex Virus thymidine-kinase (HSV-TK) for activating gancyclovir, the bacterial nitroreductase for activating CB1954), immune stimulatory cytokines (IL-2, IL-12, GM-CSF, IL-24), or apoptotic proteins (e.g. p53).⁶¹ Specificity of transgene expression can be provided through the inclusion of tissue-specific promoters.

To improve the specificity and efficacy of AdV vectors, a large variety of capsid modifications is being pursued. Such modifications aim, on one hand, on the enhancement of tumor cell transduction (e.g. through fusing tumor-targeting polypeptides to the viral capsid) and, on the other hand, on reduced transduction of non-target cells or tissues. Transductional targeting and detargeting approaches will be discussed in Paragraph 1.2.3.

1.3.2 Conditionally-Replicating Adenoviruses (CRAds)

Past clinical trials have defined major limitations of replication-deficient vectors for cancer gene therapy, as a result of their inability to infect the majority of cells within a clinically presented three-dimensional solid tumor mass.⁶² Conditionally Replicating Adenoviruses (CRAds) are designed to overcome this limitation by making use of the natural ability of HAdV-5 to kill their host cells upon its spread throughout a tissue. To provide specificity of cell killing, CRAds are designed in such a way to restrict their replicative ability to tumor cells. Besides the direct lytic effect of CRAds, their induction of cell death might cause anti-tumor immune responses as a positive bystander effect.^{63,64} Future research is necessary to fully delineate the effects of CRAD therapies on the patient's immune system.

CRAds are rendered tumor-specific by taking advantage of cancer-specific cellular changes. It was found by Berk *et al.* that disruption of the HAdV-5 E1B-55K gene in the mutant *d11520* yielded specific replication in cancer cells.⁶⁵ Based on previous experiments showing an ability of E1B-55K to interact with the tumor-suppressor protein p53, it was initially thought that the tumor selectivity of *d11520* was due to p53 being mutated in cancer cells. However, *d11520* was found to replicate in p53-expressing cancer cells as well.^{66,67} Despite the controversy on the mechanism behind the tumor cell preference, E1B-55K deleted CRAds are paradigm for designing of today's oncolytic

vectors. The *d11520* virus has been tested in a variety of cancer clinical trials (under its commercial name ONYX-015) including head and neck cancer,⁶⁸ oral carcinoma,⁶⁹ colorectal carcinoma metastases to the liver,⁷⁰ hepatocellular carcinoma⁷¹ and glioma.⁷² These studies have demonstrated safety, with well tolerated doses of up to 2×10^{12} particles (by various routes of injection) and tumor-selective replication. The efficacy as a single agent has been relatively limited to date (0-14% local tumor regression rates), but encouraging anti-tumor activity has been demonstrated in combination with chemotherapy.⁷³ A very similar virus, H101, has been registered for clinical use in China.

Cancer cell-specific CRAds can also be made by mutating the E1A gene.⁷⁴ A 24-bp deletion was found to prevent E1A from binding to the cellular protein Rb for induction of the cellular S-phase. As a consequence, replication depends on the inactivation of Rb through other means (e.g. hyperphosphorylation) which is the case in most types of cancer. Clinical safety and efficacy of E1A Δ 24 CRAds is subject of current research. Recently, the maximum tolerated dose, toxicity spectrum, clinical activity, and biological effects were evaluated for a E1A Δ 24 CRAd (named Ad5- Δ 24-RGD) in patients with ovarian cancer.⁷⁵ Besides having the 24-bp deletion, to establish tumor-selectivity, this CRAd also contained an RGD-domain fused to the fiber, to enhance efficacy of the treatment. The approach appeared to be safe, and a minor antitumor response was found.

As an alternative to the E1 deletions, CRAds can be created through the incorporation of tissue-specific promoters to control the expression of essential viral genes. As an example, expression of the viral E1A gene can be controlled by the recombinant prostate-specific PPT sequence, which is composed of a prostate-specific antigen (PSA) enhancer, a prostate-specific membrane antigen (PSMA) enhancer and a T cell receptor gamma-chain alternate reading frame protein (TARP) promoter.⁷⁶ As a result, the AdV vector replicates exclusively in normal and neoplastic prostate epithelial cells.

A large variety of modifications is being explored, to further improve the efficacy and specificity of CRAds. Similar to the replication-deficient vectors, the CRAd genome can be armed with 'cell killing transgenes', which may improve the efficacy of tumor eradication. As an example, arming the *d11520* virus with the HSV-TK/Ganciclovir system results in increased survival rates in mice with subcutaneous colon cancer xenografts.⁷⁷ Alternatively, CRAds with improved clinical performance may be obtained by the insertion of genes coding for proteins with antitumor effect on the tumor micro-environment, such as angiogenesis inhibition or immune activation.⁷⁸ To improve the specificity and safety of CRAds, their replication can be blocked in non-target cells by incorporating microRNA (miRNA)-binding sequences in viral genes. In this way, multiple binding sites for a hepatocyte-specific miRNA, mir-122, have been placed in the 3' untranslated region of the E1A gene of a CRAd, leading to the absence of E1A gene expression (and viral replication) in murine hepatocytes and a significant reduction in hepatotoxicity.^{79,80}

Furthermore, capsid modifications for targeting and detargeting approaches are pursued, as will be discussed in the next paragraph.

1.3.3 Capsid modifications for targeting and detargeting

Studies on oncolytic HAdV-5-based vectors, in preclinical- as well as early phase clinical settings, have demonstrated the necessity of introducing modifications in the viral capsid to improve the efficacy and safety in the complex environment of a patient's tumor.

One important efficacy-limiting aspect is the low-level expression of the CAR receptor on many tumor cells, necessitating capsid modifications to alter the wild-type tropism of HAdV-5.^{81,82} Development of modified vectors that can infect CAR-negative cells has mainly focused on the genetic incorporation of heterologous ligands in the fiber protein, or on 'fiber-swap' strategies in which the HAdV-5 fiber is replaced by a fiber from another HAdV serotype.⁸³ Although effective, the applicability of incorporating large and complex ligands (e.g. single-chain antibody fragments) into fiber locales might be limited, since such modifications in many cases result in virus replication with low titers.²¹ This drawback has prompted the identification of other capsid proteins (hexon, penton base, protein IIIa, and minor capsid protein IX) as usable locales for incorporating heterologous peptides (reviewed by Vellinga *et al.*⁵).

An interesting locale for the fusion of polypeptides is the minor capsid protein IX. Fusing polypeptides to the carboxyl-terminus of protein IX does not reduce the viral titers upon *in vitro* production, and has no effect on the stability of the virus particles.⁴⁵ It was found that the presentation of protein IX-fused peptides can be improved through incorporating a 75-Ångstrom alpha-helical spacer in between protein IX and the peptide.⁸⁴ Using the protein IX-spacer sequence as anchor, highly efficient coverage of the virions with heterologous peptides can be obtained with incorporation efficiencies close to the theoretical maximum of 240 molecules per virion, depending on the size and complexity of the polypeptide. The feasibility of targeting HAdV-5 to tumor cells through fusing tumor-targeting ligands to protein IX has subsequently been investigated, as described in detail in this thesis.

Nowadays, elegant systems are available for creating genetically modified HAdV-5 vectors, which enable cloning and recombination steps in a bacterial context instead of in human cell lines. Still, genetic modification of the HAdV-5 genome is a time- and effort consuming process, limiting the rapid screening of polypeptide moieties for their capsid incorporation ability. For this reason, screening-facilitating systems have been developed based on the propagation of HAdV-5 vectors on cell lines expressing heterologous peptides fused to a capsid protein. Such systems have been used successfully for expedited functional assessment of modified variants of protein IX and fiber.^{85,86}

An alternative to genetically modifying the viral vector for transductional purposes has been provided by 'adapter strategies', applying bispecific targeting moieties that on one hand bind to the virus (in general to the fiber knob domain), and on the other hand to a molecule on the target cell. As an example, HAdV-5 vectors have been efficiently retargeted to HER2/neu expressing tumor cells through using designed ankyrin repeat proteins (DARPs) as bivalent adapter molecules.⁸⁷ The adapter technology has several potential advantages with respect to the genetic modification technology, in that it enables the relatively rapid screening of targeting ligands, and provides a production platform for the preparation of high-titer batches of HAdV-5 vectors that are efficiently decorated with large and complex targeting

ligands. However, special care will be required to ensure the preparation of clinical batches with defined characteristics, for example assuring low variability of ligand incorporation efficiencies between different vector preparations.

The above described modifications aim at enhanced transduction of tumor cells through coupling tumor-targeting ligands to the HAdV-5 capsid. Another strategy to improve the potency of oncolytic HAdV-5 vectors is by detargeting the vector from non-target tissues. As discussed in more detail in the next chapter, last years have witnessed an enhanced understanding on the *in vivo* mechanisms behind the disappointing anti-tumor efficacies of oncolytic HAdV-5 vectors in early-phase clinical trials. One aspect thwarting effective therapy is the high prevalence of pre-existing humoral immunity against HAdV-5 in the human population, resulting in rapid clearance of the vectors from the blood. Additionally, strong innate immune responses, e.g. by natural killer cells, are observed after intratumoral or systemic injection of oncolytic HAdV-5 vectors. Another bottleneck, especially hampering the efficacy of systemically delivered oncolytic HAdV-5 vectors, is the rapid clearance from the blood stream as a result of sequestration in the liver. It has recently been found that binding of HAdV-5 to blood coagulation factor (F) X, results in uptake of the vectors by hepatocytes in the liver.^{14,15} FX appears to bind to viral capsid epitopes of the hexon protein, and bridges the virus to heparan sulphate proteoglycans on hepatocytes. Besides the FX-hepatocyte mediated removal of oncolytic HAdV-5 vectors, the vectors are also cleared from the blood by liver-residing macrophages (Kupffer cells).⁸⁸ Binding of the vectors to complement proteins, natural antibodies and platelets seems to play an important role in the uptake by these scavenging macrophages.^{89,90} Another problem to tackle is the binding of HAdV-5 vectors to erythrocytes.^{91,92} This binding appears to be specific for human erythrocytes, and has therefore not been noticed previously during vector analyses in rodent models. Last years have seen enormous pre-clinical improvements in the efficacy of HAdV-5 based oncolytic vectors, through applying novel types of modifications leading to improved transductional targeting and detargeting. One highly promising example is the ability to genetically modify viral hexon sequences to abolish uptake of virus particles by hepatocytes, thereby enhancing gene transfer to target cells.^{93,94}

Additionally, strategies have been developed to reduce off-target binding by shielding the adenovirus vector particles with chemical polymers.⁹⁵ In animal models, this technology significantly increases the circulation time of HAdV-5 vectors in the blood stream, and simultaneously reduces liver toxicity.^{96,97} Similar to targeting of the 'naked' vector particles, the polymer coatings can also be modified to achieve targeting to tumor cells.⁹⁸ Research is ongoing to further improve the polymer coating technology, for example aiming at 'low pH triggered de-shielding' to facilitate proper intracellular routing of polymer coated virus particles after their uptake in the endosome. As an alternative to the polymer coatings, 'carrier cells' might be utilized to shield HAdV-5 vectors from efficacy-limiting moieties. Various cell types with intrinsic tumor-homing properties, such as mesenchymal stem cells, T cells, and monocytes, are currently under investigation.⁹⁹

Taken together, a large array of new targeting and detargeting approaches has been developed to facilitate improved performance of oncolytic HAdV-5 vectors. The most up-to-date developments in the field of oncolytic HAdV-5 vector engineering,

as well as prominent aspects that require further optimization, are outlined in more detail in Chapter 2.

1.3.4 Random approaches to vector development

As described in the previous sections, a plethora of rational design approaches is being pursued to develop AdV vectors with improved performance. However, last years have witnessed a renewed interest in the more traditional 'directed evolution' method of oncolytic vector development; the random creation of virus mutants followed by bioselection of the best-performing viruses. This approach has yielded improved oncolytic HAdVs with genomic mutations that would have never been picked up using rational design approaches. These findings not only benefit to the development of improved oncolytic HAdVs, but also enhance our knowledge on HAdV biology.

Following a mutagenesis and bioselection approach, Yan *et al.* plaque purified two mutants, ONYX-201 and ONYX-203, from a pool of randomly mutated HAdV-5 that was repeatedly passaged in the human colorectal cancer cell line HT29.¹⁰⁰ The mutants replicated more rapidly in HT29 cells than wild-type HAdV-5, and lysed HT29 cells up to 1,000-fold more efficiently. The enhanced cytotoxicity was also observed in other human cancer cell lines, but not in a number of normal primary human cells, indicating a strong enhancement of the therapeutic index of ONYX-201 and ONYX-203. Although the virus mutants contained multiple single-base-pair mutations, they shared a mutation at nucleotide 8350, which was shown to be essential for the observed phenotype. This mutation was mapped to the i-leader sequence of the HAdV-5 genome, which is (for unknown reasons) present as a 440-nucleotide leader sequence in the majority of HAdV-5 major-late transcripts. The i-leader contains an open reading frame encoding for a 16 kDa-sized protein.¹⁰¹ The mutation at nucleotide 8350 introduces a stopcodon, resulting in a truncation of 21 amino acids from the C terminus of the i-leader protein. In parallel to these results, another i-leader mutant HAdV-5 was isolated by Subramanian and coworkers in a screen for large plaques on A549 alveolar epithelium cells.¹⁰² Although the exact mechanism behind the improved oncolytic performance of i-leader mutated HAdV-5 remains to be investigated, the potential of this type of mutation was recently underscored by Van den Hengel *et al.*, who demonstrated enhanced cytopathic activity of i-leader mutated HAdV-5 in glioma cell lines and primary glioma cultures.¹⁰³

Using similar mutagenesis and bioselection approaches, another type of HAdV-5 mutant with enhanced antitumor efficacy was found by Gros *et al.*¹⁰⁴ The propagation of a mutagenized HAdV-5 stock in human tumor xenografts led to the isolation of a mutant virus displaying a large-plaque phenotype *in vitro* and an enhanced antitumor activity *in vivo*. A truncating mutation in the viral E3-19K gene, resulting in relocalization of the E3-19K protein from the endoplasmic reticulum to the plasma membrane, appeared to be responsible for the mutant's enhanced antitumor efficacy. The aberrant protein localization appeared to enhance the cellular influx of calcium ions, thereby deregulating calcium homeostasis and inducing membrane permeabilization.

Recently, Uil *et al.* presented another type of directed evolution, through serial passaging of HAdV-5 in cancer cells in the context of a 'sloppy' viral polymerase protein.¹⁰⁵ To this aim, the authors first identified mutations in the viral polymerase protein that lead to viral replication with increased mutation rate. The strongest identified mutators, all

having a mutation in the single-strand DNA binding region of the exonuclease domain, were exploited to generate HAdV-5 mutants with improved cytolytic activity in tumor cells. A common mutation was identified, located in a splice acceptor site preceding the gene for the adenovirus death protein (ADP). Accordingly, high and untimely expression of ADP was observed, presumably causing the enhanced cytotoxicity.

Kuhn and coworkers have used a directed evolution approach to obtain chimeric oncolytic adenoviruses, that consist of components from different HAdV serotypes.¹⁰⁶ An array of serotypes, representing HAdV species B to F, was pooled and passaged on tumor cell lines under conditions that invite recombination. By using this methodology, a highly potent oncolytic HAdV-3/HAdV-11p chimeric virus (named ColoAd1) was obtained. ColoAd1 demonstrated greatly enhanced potency and selectivity, as compared to its parent serotypes and ONYX/015, in colon cancer cell cultures and in a mouse tumor model.

The proven potential of random selection approaches has triggered researchers to combine this type of approach with rational design. As such, improved HAdV vectors targeted to prostate cancer cells have been isolated after genetically incorporating random peptides at viral capsid locales flanking the tumor-targeting polypeptide sequence.¹⁰⁷

Directed evolution approaches are expected to lead to the isolation of novel and improved oncolytic HAdVs. Performing such strategies in clinically relevant model systems will be of great interest, acknowledging the large repertoire of efficacy-limiting *in vivo* aspects of oncolytic viral therapy, with many aspects having non-resolved mechanisms of action.

REFERENCES

1. Liu H, Jin L, Koh SB, Atanasov I, Schein S, Wu L *et al.* Atomic structure of human adenovirus by cryo-EM reveals interactions among protein networks. *Science* 2010; **329**: 1038-1043.
2. Reddy VS, Natchiar SK, Stewart PL, Nemerow GR. Crystal structure of human adenovirus at 3.5 Å resolution. *Science* 2010; **329**: 1071-1075.
3. Berget SM, Moore C, Sharp PA. Spliced segments at the 5' terminus of adenovirus 2 late mRNA. *Proc Natl Acad Sci U S A* 1977; **74**: 3171-3175.
4. Graham FL, van der Eb AJ. A new technique for the assay of infectivity of human adenovirus 5 DNA. *Virology* 1973; **52**: 456-467.
5. Vellinga J, Van der Heijdt S, Hoeben RC. The adenovirus capsid: major progress in minor proteins. *J Gen Virol* 2005; **86**: 1581-1588.
6. Russell WC. Adenoviruses: update on structure and function. *J Gen Virol* 2009; **90**: 1-20.
7. Bergelson JM, Cunningham JA, Droguett G, Kurt-Jones EA, Krithivas A, Hong JS *et al.* Isolation of a common receptor for Coxsackie B viruses and adenoviruses 2 and 5. *Science* 1997; **275**: 1320-1323.
8. Wickham TJ, Mathias P, Cheresch DA, Nemerow GR. Integrins alpha v beta 3 and alpha v beta 5 promote adenovirus internalization but not virus attachment. *Cell* 1993; **73**: 309-319.
9. Chiu CY, Mathias P, Nemerow GR, Stewart PL. Structure of adenovirus complexed with its internalization receptor, alphavbeta5 integrin. *J Virol* 1999; **73**: 6759-6768.
10. Seth P. Adenovirus-dependent release of choline from plasma membrane vesicles at an acidic pH is mediated by

- the penton base protein. *J Virol* 1994; **68**: 1204-1206.
11. Wickham TJ, Filardo EJ, Cheresh DA, Nemerow GR. Integrin alpha v beta 5 selectively promotes adenovirus mediated cell membrane permeabilization. *J Cell Biol* 1994; **127**: 257-264.
 12. Maizel JV, Jr., White DO, Scharff MD. The polypeptides of adenovirus. II. Soluble proteins, cores, top components and the structure of the virion. *Virology* 1968; **36**: 126-136.
 13. Smith KO, Gehle WD, Trousdale MD. Architecture of the Adenovirus Capsid. *J Bacteriol* 1965; **90**: 254-261.
 14. Kalyuzhnyi O, Di Paolo NC, Silvestry M, Hofferr SE, Barry MA, Stewart PL et al. Adenovirus serotype 5 hexon is critical for virus infection of hepatocytes *in vivo*. *Proc Natl Acad Sci U S A* 2008; **105**: 5483-5488.
 15. Waddington SN, McVey JH, Bhella D, Parker AL, Barker K, Atoda H et al. Adenovirus serotype 5 hexon mediates liver gene transfer. *Cell* 2008; **132**: 397-409.
 16. San Martin C, Glasgow JN, Borovjagin A, Beatty MS, Kashentseva EA, Curiel DT et al. Localization of the N-terminus of minor coat protein IIIa in the adenovirus capsid. *J Mol Biol* 2008; **383**: 923-934.
 17. Wodrich H, Guan T, Cingolani G, Von Seggern D, Nemerow G, Gerace L. Switch from capsid protein import to adenovirus assembly by cleavage of nuclear transport signals. *EMBO J* 2003; **22**: 6245-6255.
 18. Wiethoff CM, Wodrich H, Gerace L, Nemerow GR. Adenovirus protein VI mediates membrane disruption following capsid disassembly. *J Virol* 2005; **79**: 1992-2000.
 19. Silvestry M, Lindert S, Smith JG, Maier O, Wiethoff CM, Nemerow GR et al. Cryo-electron microscopy structure of adenovirus type 2 temperature-sensitive mutant 1 reveals insight into the cell entry defect. *J Virol* 2009; **83**: 7375-7383.
 20. Liu GQ, Babiss LE, Volkert FC, Young CS, Ginsberg HS. A thermolabile mutant of adenovirus 5 resulting from a substitution mutation in the protein VIII gene. *J Virol* 1985; **53**: 920-925.
 21. Arnberg N. Adenovirus receptors: implications for tropism, treatment and targeting. *Rev Med Virol* 2009; **19**: 165-178.
 22. Wang H, Li ZY, Liu Y, Persson J, Beyer I, Moller T et al. Desmoglein 2 is a receptor for adenovirus serotypes 3, 7, 11 and 14. *Nat Med* 2011; **17**: 96-104.
 23. Arnberg N, Kidd AH, Edlund K, Nilsson J, Pring-Akerblom P, Wadell G. Adenovirus type 37 binds to cell surface sialic acid through a charge-dependent interaction. *Virology* 2002; **302**: 33-43.
 24. Burmeister WP, Guilligay D, Cusack S, Wadell G, Arnberg N. Crystal structure of species D adenovirus fiber knobs and their sialic acid binding sites. *J Virol* 2004; **78**: 7727-7736.
 25. Jonsson MI, Lenman AE, Frangsmyr L, Nyberg C, Abdullahi M, Arnberg N. Coagulation factors IX and X enhance binding and infection of adenovirus types 5 and 31 in human epithelial cells. *J Virol* 2009; **83**: 3816-3825.
 26. Bayo-Puxan N, Cascallo M, Gros A, Huch M, Fillat C, Alemany R. Role of the putative heparan sulfate glycosaminoglycan-binding site of the adenovirus type 5 fiber shaft on liver detargeting and knob-mediated retargeting. *J Gen Virol* 2006; **87**: 2487-2495.
 27. Greber UF, Willetts M, Webster P, Helenius A. Stepwise dismantling of adenovirus 2 during entry into cells. *Cell* 1993; **75**: 477-486.
 28. Nakano MY, Boucke K, Suomalainen M, Stidwill RP, Greber UF. The first step of adenovirus type 2 disassembly occurs at the cell surface, independently of endocytosis and escape to the cytosol. *J Virol* 2000; **74**: 7085-7095.
 29. Lindert S, Silvestry M, Mullen TM, Nemerow GR, Stewart PL. Cryo-electron microscopy structure of an adenovirus-integrin complex indicates conformational changes in both penton base and integrin. *J Virol* 2009; **83**: 11491-11501.
 30. Varga MJ, Weibull C, Everitt E. Infectious entry pathway of adenovirus type 2. *J Virol* 1991; **65**: 6061-6070.
 31. Meier O, Boucke K, Hammer SV, Keller S, Stidwill RP, Hemmi S et al. Adenovirus triggers macropinocytosis and endosomal leakage together with

- its clathrin-mediated uptake. *J Cell Biol* 2002; **158**: 1119-1131.
32. Meier O, Greber UF. Adenovirus endocytosis. *J Gene Med* 2004; **6 Suppl 1**: S152-163.
 33. Suomalainen M, Nakano MY, Keller S, Boucke K, Stidwill RP, Greber UF. Microtubule-dependent plus- and minus end-directed motilities are competing processes for nuclear targeting of adenovirus. *J Cell Biol* 1999; **144**: 657-672.
 34. Kelkar SA, Pfister KK, Crystal RG, Leopold PL. Cytoplasmic dynein mediates adenovirus binding to microtubules. *J Virol* 2004; **78**: 10122-10132.
 35. Gazzola M, Burckhardt CJ, Bayati B, Engelke M, Greber UF, Koumoutsakos P. A stochastic model for microtubule motors describes the *in vivo* cytoplasmic transport of human adenovirus. *PLoS Comput Biol* 2009; **5**: e1000623.
 36. Kural C, Kim H, Syed S, Goshima G, Gelfand VI, Selvin PR. Kinesin and dynein move a peroxisome *in vivo*: a tug-of-war or coordinated movement? *Science* 2005; **308**: 1469-1472.
 37. Glotzer JB, Michou AI, Baker A, Saltik M, Cotten M. Microtubule-independent motility and nuclear targeting of adenoviruses with fluorescently labeled genomes. *J Virol* 2001; **75**: 2421-2434.
 38. Yea C, Dembowy J, Pacione L, Brown M. Microtubule-mediated and microtubule-independent transport of adenovirus type 5 in HEK293 cells. *J Virol* 2007; **81**: 6899-6908.
 39. Trotman LC, Mosberger N, Fornerod M, Stidwill RP, Greber UF. Import of adenovirus DNA involves the nuclear pore complex receptor CAN/Nup214 and histone H1. *Nat Cell Biol* 2001; **3**: 1092-1100.
 40. Flint SJ. Organization and expression of viral genes in adenovirus-transformed cells. *Int Rev Cytol* 1982; **76**: 47-65.
 41. Furcinitti PS, van Oostrum J, Burnett RM. Adenovirus polypeptide IX revealed as capsid cement by difference images from electron microscopy and crystallography. *EMBO J* 1989; **8**: 3563-3570.
 42. Saban SD, Silvestry M, Nemerow GR, Stewart PL. Visualization of alpha-helices in a 6-angstrom resolution cryoelectron microscopy structure of adenovirus allows refinement of capsid protein assignments. *J Virol* 2006; **80**: 12049-12059.
 43. Fabry CM, Rosa-Calatrava M, Moriscot C, Ruigrok RW, Boulanger P, Schoehn G. The C-terminal domains of adenovirus serotype 5 protein IX assemble into an antiparallel structure on the facets of the capsid. *J Virol* 2009; **83**: 1135-1139.
 44. Colby WW, Shenk T. Adenovirus type 5 virions can be assembled *in vivo* in the absence of detectable polypeptide IX. *J Virol* 1981; **39**: 977-980.
 45. Vellinga J, van den Wollenberg DJ, van der Heijdt S, Rabelink MJ, Hoeben RC. The coiled-coil domain of the adenovirus type 5 protein IX is dispensable for capsid incorporation and thermostability. *J Virol* 2005; **79**: 3206-3210.
 46. Ghosh-Choudhury G, Haj-Ahmad Y, Graham FL. Protein IX, a minor component of the human adenovirus capsid, is essential for the packaging of full length genomes. *EMBO J* 1987; **6**: 1733-1739.
 47. Sargent KL, Ng P, Eveleigh C, Graham FL, Parks RJ. Development of a size-restricted pIX-deleted helper virus for amplification of helper-dependent adenovirus vectors. *Gene Ther* 2004; **11**: 504-511.
 48. Lutz P, Rosa-Calatrava M, Kedinger C. The product of the adenovirus intermediate gene IX is a transcriptional activator. *J Virol* 1997; **71**: 5102-5109.
 49. Sargent KL, Meulenbroek RA, Parks RJ. Activation of adenoviral gene expression by protein IX is not required for efficient virus replication. *J Virol* 2004; **78**: 5032-5037.
 50. Rosa-Calatrava M, Grave L, Puvion-Dutilleul F, Chatton B, Kedinger C. Functional analysis of adenovirus protein IX identifies domains involved in capsid stability, transcriptional activity, and nuclear reorganization. *J Virol* 2001; **75**: 7131-7141.
 51. Caravokyri C, Leppard KN. Constitutive episomal expression of polypeptide IX (pIX) in a 293-based cell line complements the deficiency of pIX mutant adenovirus type 5. *J Virol* 1995; **69**: 6627-6633.

52. Stuurman N, de Graaf A, Floore A, Josso A, Humbel B, de Jong L et al. A monoclonal antibody recognizing nuclear matrix-associated nuclear bodies. *J Cell Sci* 1992; **101 (Pt 4)**: 773-784.
53. Fallaux FJ, Hoeben RC. Safety of recombinant adenoviruses produced on adenovirus-transformed human cells. *Dev Biol (Basel)* 2001; **106**: 489-496; discussion 497, 501-411.
54. Lasaro MO, Ertl HC. New insights on adenovirus as vaccine vectors. *Mol Ther* 2009; **17**: 1333-1339.
55. Imperiale MJ, Kochanek S. Adenovirus vectors: biology, design, and production. *Curr Top Microbiol Immunol* 2004; **273**: 335-357.
56. Graham FL, Smiley J, Russell WC, Nairn R. Characteristics of a human cell line transformed by DNA from human adenovirus type 5. *J Gen Virol* 1977; **36**: 59-74.
57. Fallaux FJ, Kranenburg O, Cramer SJ, Houweling A, Van Ormondt H, Hoeben RC et al. Characterization of 911: a new helper cell line for the titration and propagation of early region 1-deleted adenoviral vectors. *Hum Gene Ther* 1996; **7**: 215-222.
58. Fallaux FJ, Bout A, van der Velde I, van den Wollenberg DJ, Hehir KM, Keegan J et al. New helper cells and matched early region 1-deleted adenovirus vectors prevent generation of replication-competent adenoviruses. *Hum Gene Ther* 1998; **9**: 1909-1917.
59. Yang Y, Wilson JM. Clearance of adenovirus-infected hepatocytes by MHC class I-restricted CD4+ CTLs *in vivo*. *J Immunol* 1995; **155**: 2564-2570.
60. Kochanek S, Clemens PR, Mitani K, Chen HH, Chan S, Caskey CT. A new adenoviral vector: Replacement of all viral coding sequences with 28 kb of DNA independently expressing both full-length dystrophin and beta-galactosidase. *Proc Natl Acad Sci U S A* 1996; **93**: 5731-5736.
61. Bachtarzi H, Stevenson M, Fisher K. Cancer gene therapy with targeted adenoviruses. *Expert Opin Drug Deliv* 2008; **5**: 1231-1240.
62. Yamamoto M, Curiel DT. Current issues and future directions of oncolytic adenoviruses. *Mol Ther* 2010; **18**: 243-250.
63. Geutskens SB, van der Eb MM, Plomp AC, Jonges LE, Cramer SJ, Ensink NG et al. Recombinant adenoviral vectors have adjuvant activity and stimulate T cell responses against tumor cells. *Gene Ther* 2000; **7**: 1410-1416.
64. Alemany R, Cascallo M. Oncolytic viruses from the perspective of the immune system. *Future Microbiol* 2009; **4**: 527-536.
65. Barker DD, Berk AJ. Adenovirus proteins from both E1B reading frames are required for transformation of rodent cells by viral infection and DNA transfection. *Virology* 1987; **156**: 107-121.
66. Goodrum FD, Ornelles DA. p53 status does not determine outcome of E1B 55-kilodalton mutant adenovirus lytic infection. *J Virol* 1998; **72**: 9479-9490.
67. Turnell AS, Grand RJ, Gallimore PH. The replicative capacities of large E1B-null group A and group C adenoviruses are independent of host cell p53 status. *J Virol* 1999; **73**: 2074-2083.
68. Nemunaitis J, O'Brien J. Head and neck cancer: gene therapy approaches. Part 1: adenoviral vectors. *Expert Opin Biol Ther* 2002; **2**: 177-185.
69. Wadler S, Kaufman H, Horwitz M, Morley S, Kirn D, Brown R et al. The dl1520 virus is found preferentially in tumor tissue after direct intratumoral injection in oral carcinoma. *Clin Cancer Res* 2005; **11**: 2781-2782; author reply 2782.
70. Reid T, Galanis E, Abbruzzese J, Sze D, Andrews J, Romel L et al. Intra-arterial administration of a replication-selective adenovirus (dl1520) in patients with colorectal carcinoma metastatic to the liver: a phase I trial. *Gene Ther* 2001; **8**: 1618-1626.
71. Habib N, Salama H, Abd El Latif Abu Median A, Isac Anis I, Abd Al Aziz RA, Sarraf C et al. Clinical trial of E1B-deleted adenovirus (dl1520) gene therapy for hepatocellular carcinoma. *Cancer Gene Ther* 2002; **9**: 254-259.
72. Chiocca EA, Abbed KM, Tatter S, Louis DN, Hochberg FH, Barker F et al. A phase I open-label, dose-escalation, multi-institutional trial of injection with an E1B-Attenuated adenovirus, ONYX-015, into the peritumoral region

- of recurrent malignant gliomas, in the adjuvant setting. *Mol Ther* 2004; **10**: 958-966.
73. Kirn D. Oncolytic virotherapy for cancer with the adenovirus dl1520 (Onyx-015): results of phase I and II trials. *Expert Opin Biol Ther* 2001; **1**: 525-538.
 74. Fueyo J, Gomez-Manzano C, Alemany R, Lee PS, McDonnell TJ, Mitlianga P et al. A mutant oncolytic adenovirus targeting the Rb pathway produces anti-glioma effect *in vivo*. *Oncogene* 2000; **19**: 2-12.
 75. Kimball KJ, Preuss MA, Barnes MN, Wang M, Siegal GP, Wan W et al. A phase I study of a tropism-modified conditionally replicative adenovirus for recurrent malignant gynecologic diseases. *Clin Cancer Res* 2010; **16**: 5277-5287.
 76. Dzojic H, Cheng WS, Essand M. Two-step amplification of the human PPT sequence provides specific gene expression in an immunocompetent murine prostate cancer model. *Cancer Gene Ther* 2007; **14**: 233-240.
 77. Wildner O, Blaese RM, Morris JC. Therapy of colon cancer with oncolytic adenovirus is enhanced by the addition of herpes simplex virus-thymidine kinase. *Cancer Res* 1999; **59**: 410-413.
 78. Shashkova EV, Kuppuswamy MN, Wold WS, Doronin K. Anticancer activity of oncolytic adenovirus vector armed with IFN-alpha and ADP is enhanced by pharmacologically controlled expression of TRAIL. *Cancer Gene Ther* 2008; **15**: 61-72.
 79. Ylosmaki E, Hakkarainen T, Hemminki A, Visakorpi T, Andino R, Saksela K. Generation of a conditionally replicating adenovirus based on targeted destruction of E1A mRNA by a cell type-specific MicroRNA. *J Virol* 2008; **82**: 11009-11015.
 80. Cawood R, Chen HH, Carroll F, Bazan-Peregrino M, van Rooijen N, Seymour LW. Use of tissue-specific microRNA to control pathology of wild-type adenovirus without attenuation of its ability to kill cancer cells. *PLoS Pathog* 2009; **5**: e1000440.
 81. Hemmi S, Geertsens R, Mezzacasa A, Peter I, Dummer R. The presence of human coxsackievirus and adenovirus receptor is associated with efficient adenovirus-mediated transgene expression in human melanoma cell cultures. *Hum Gene Ther* 1998; **9**: 2363-2373.
 82. Li D, Duan L, Freimuth P, O'Malley BW, Jr. Variability of adenovirus receptor density influences gene transfer efficiency and therapeutic response in head and neck cancer. *Clin Cancer Res* 1999; **5**: 4175-4181.
 83. Glasgow JN, Everts M, Curiel DT. Transductional targeting of adenovirus vectors for gene therapy. *Cancer Gene Ther* 2006; **13**: 830-844.
 84. Vellinga J, Rabelink MJ, Cramer SJ, van den Wollenberg DJ, Van der Meulen H, Leppard KN et al. Spacers increase the accessibility of peptide ligands linked to the carboxyl terminus of adenovirus minor capsid protein IX. *J Virol* 2004; **78**: 3470-3479.
 85. Vellinga J, Uil TG, de Vrij J, Rabelink MJ, Lindholm L, Hoeben RC. A system for efficient generation of adenovirus protein IX-producing helper cell lines. *J Gene Med* 2006; **8**: 147-154.
 86. Uil TG, de Vrij J, Vellinga J, Rabelink MJ, Cramer SJ, Chan OY et al. A lentiviral vector-based adenovirus fiber-pseudotyping approach for expedited functional assessment of candidate retargeted fibers. *J Gene Med* 2009; **11**: 990-1004.
 87. Dreier B, Mikheeva G, Belousova N, Parizek P, Boczek E, Jelesarov I et al. Her2-specific multivalent adapters confer designed tropism to adenovirus for gene targeting. *J Mol Biol* 2011; **405**: 410-426.
 88. Lieber A, He CY, Meuse L, Schowalter D, Kirillova I, Winther B et al. The role of Kupffer cell activation and viral gene expression in early liver toxicity after infusion of recombinant adenovirus vectors. *J Virol* 1997; **71**: 8798-8807.
 89. Stone D, Liu Y, Shayakhmetov D, Li ZY, Ni S, Lieber A. Adenovirus-platelet interaction in blood causes virus sequestration to the reticuloendothelial system of the liver. *J Virol* 2007; **81**: 4866-4871.
 90. Xu Z, Tian J, Smith JS, Byrnes AP. Clearance of adenovirus by Kupffer cells is mediated by scavenger receptors, natural antibodies, and complement. *J Virol* 2008; **82**: 11705-11713.

91. Carlisle RC, Di Y, Cerny AM, Sonnen AF, Sim RB, Green NK *et al.* Human erythrocytes bind and inactivate type 5 adenovirus by presenting Coxsackie virus-adenovirus receptor and complement receptor 1. *Blood* 2009; **113**: 1909-1918.
92. Seiradake E, Henaff D, Wodrich H, Billet O, Perreau M, Hippert C *et al.* The cell adhesion molecule "CAR" and sialic acid on human erythrocytes influence adenovirus *in vivo* biodistribution. *PLoS Pathog* 2009; **5**: e1000277.
93. Alba R, Bradshaw AC, Parker AL, Bhella D, Waddington SN, Nicklin SA *et al.* Identification of coagulation factor (FX) binding sites on the adenovirus serotype 5 hexon: effect of mutagenesis on FX interactions and gene transfer. *Blood* 2009; **114**: 965-971.
94. Alba R, Bradshaw AC, Coughlan L, Denby L, McDonald RA, Waddington SN *et al.* Biodistribution and retargeting of FX-binding ablated adenovirus serotype 5 vectors. *Blood* 2010; **116**: 2656-2664.
95. Kreppel F, Kochanek S. Modification of adenovirus gene transfer vectors with synthetic polymers: a scientific review and technical guide. *Mol Ther* 2008; **16**: 16-29.
96. Fisher KD, Stallwood Y, Green NK, Ulbrich K, Mautner V, Seymour LW. Polymer-coated adenovirus permits efficient retargeting and evades neutralising antibodies. *Gene Ther* 2001; **8**: 341-348.
97. Green NK, Herbert CW, Hale SJ, Hale AB, Mautner V, Harkins R *et al.* Extended plasma circulation time and decreased toxicity of polymer-coated adenovirus. *Gene Ther* 2004; **11**: 1256-1263.
98. Morrison J, Briggs SS, Green NK, Thoma C, Fisher KD, Kehoe S *et al.* Cetuximab retargeting of adenovirus via the epidermal growth factor receptor for treatment of intraperitoneal ovarian cancer. *Hum Gene Ther* 2009; **20**: 239-251.
99. Russell SJ, Peng KW. The utility of cells as vehicles for oncolytic virus therapies. *Curr Opin Mol Ther* 2008; **10**: 380-386.
100. Yan W, Kitzes G, Dormishian F, Hawkins L, Sampson-Johannes A, Watanabe J *et al.* Developing novel oncolytic adenoviruses through bioselection. *J Virol* 2003; **77**: 2640-2650.
101. Symington JS, Lucher LA, Brackmann KH, Virtanen A, Pettersson U, Green M. Biosynthesis of adenovirus type 2 i-leader protein. *J Virol* 1986; **57**: 848-856.
102. Subramanian T, Vijayalingam S, Chinnadurai G. Genetic identification of adenovirus type 5 genes that influence viral spread. *J Virol* 2006; **80**: 2000-2012.
103. van den Hengel SK, de Vrij J, Uil TG, Lamfers ML, Sillevius Smitt PA, Hoeben RC. Truncating the i-leader open reading frame enhances release of human adenovirus type 5 in glioma cells. *Virology* 2011; **8**: 162.
104. Gros A, Martinez-Quintanilla J, Puig C, Guedan S, Mollevi DG, Alemany R *et al.* Bioselection of a gain of function mutation that enhances adenovirus 5 release and improves its antitumoral potency. *Cancer Res* 2008; **68**: 8928-8937.
105. Uil TG, Vellinga J, de Vrij J, van den Hengel SK, Rabelink MJ, Cramer SJ *et al.* Directed adenovirus evolution using engineered mutator viral polymerases. *Nucleic Acids Res* 2010; **39**: e30.
106. Kuhn I, Harden P, Bauzon M, Chartier C, Nye J, Thorne S *et al.* Directed evolution generates a novel oncolytic virus for the treatment of colon cancer. *PLoS One* 2008; **3**: e2409.
107. Wu P, Kudrolli TA, Chowdhury WH, Liu MM, Rodriguez R, Lupold SE. Adenovirus targeting to prostate-specific membrane antigen through virus-displayed, semirandom peptide library screening. *Cancer Res* 2010; **70**: 9549-9553.

CHAPTER 2

ADENOVIRUS-DERIVED VECTORS FOR PROSTATE CANCER GENE THERAPY

J de Vrij¹, RA Willemsen², L Lindholm³, RC Hoeben¹,
and the GIANT consortium*

¹Department of Molecular Cell Biology, Leiden University Medical Center,
Leiden, The Netherlands, ²Tumor Immunology Group, Department of Medical
Oncology, Erasmus MC-Daniel den Hoed, Rotterdam, The Netherlands and
³Got-A-Gene AB, Kullavik, Sweden.

Human Gene Therapy 2010; 21:795-805

* The GIANT consortium consists of: CH Bangma¹, C Barber¹⁴, JP Behr¹¹, S Briggs², R Carlisle³,
WS Cheng², IJC Dautzenberg⁴, C de Ridder¹, H Dzojic², P Erbacher¹², M Essand², K Fisher¹³,
A Frazier⁹, LJ Georgopoulos¹⁴, I Jennings¹⁴, S Kochanek⁵, D Koppers-Lalic⁴, R Kraaij¹, F Kreppel⁵,
M Magnusson⁷, N Maitland⁹, P Neuberger¹³, R Nugent¹⁴, M Ogris¹⁰, JS Remy¹¹, M Scaife¹⁴, E Schenk-Braat¹,
E Schooten¹, L Seymour², M Slade¹⁴, P Szyjanowicz¹⁴, T Totterman², TG Uil⁴, K Ulbrich⁶,
L van der Weel¹, W van Weerden⁸, E Wagner¹⁰, G Zuber¹¹.

¹Erasmus MC University Medical Centre, Rotterdam, The Netherlands, ²Uppsala University, Uppsala, Sweden,
³University of Oxford, Oxford, U.K., ⁴Leiden University Medical Center, Leiden, The Netherlands, ⁵University
of Ulm, Ulm, Germany, ⁶Academy of Sciences of Czech Republic, Prague, Czech Republic, ⁷Got-a-Gene
AB, Kullavik, Sweden, ⁸Scuron, Rotterdam, The Netherlands, ⁹Procore, York, U.K., ¹⁰Ludwig-Maximilians-
Universität, Munich, Germany, ¹¹Universite Louis Pasteur de Strasbourg, Illkirch, France, ¹²Polyplus
Transfection, Illkirch, France, ¹³Hybrid Systems, Oxford, U.K., and ¹⁴University of York, York, U.K.

ABSTRACT

Prostate cancer is a leading cause of death among men in Western countries. Whereas the survival rate approaches 100% for patients with localized cancer, the results of treatment in patients with metastasized prostate cancer at diagnosis are much less successful. The patients are usually presented with a variety of treatment options, but therapeutic interventions in prostate cancer are associated with frequent adverse side effects. Gene therapy and oncolytic virus therapy may constitute new strategies. Already a wide variety of preclinical studies has demonstrated the therapeutic potential of such approaches, with oncolytic prostate-specific adenoviruses as the most prominent vector. The state of the art and future prospects of gene therapy in prostate cancer are reviewed, with a focus on adenoviral vectors. We summarize advances in adenovirus technology for prostate cancer treatment and highlight areas where further developments are necessary.

INTRODUCTION

Although many viruses are being evaluated as oncolytic agents, human adenoviruses (HAdVs) are among the most popular to be developed. There are several good reasons for making HAdV vectors such a popular choice. Recombinant HAdV vectors have a good safety profile as a gene therapy vector, can be produced under GMP conditions, and various commercially operating manufacturing facilities are available, allowing research groups access to batches of HAdV vectors that meet the required quality standards. In addition, the wild-type HAdVs from which vectors are derived are only mildly pathogenic.¹ Although HAdV genomes are stable enough to prevent the rapid development of heterogeneous populations of so-called quasispecies, they are easily amendable by genetic modification. Genetically modified HAdVs with altered host range (“targeted viruses”) have been generated by engineering new polypeptide ligands in the capsids of the particles, yielding viruses that preferentially infect specific cell or tissue types. In parallel, by engineering mutations at known receptor-binding sites in the capsid, “detargeted” HAdV vectors have been generated to reduce transduction of nontarget tissues. Also, HAdVs can be modified to carry therapeutic or reporter transgenes.² Numerous and diverse transgenes have been inserted in E1-deleted HAdVs to be exploited as cytolytic agents. Such therapeutic transgenes include genes encoding prodrug-activating enzymes (e.g., herpes simplex virus thymidine kinase for activating ganciclovir, cytosine deaminase for activating 5-fluorocytosine, bacterial nitroreductase activating CB1954), genes encoding immune-stimulatory cytokines (interleukin [IL]-2, IL-12, granulocyte-macrophage colony-stimulating factor [GM-CSF], and IL-24), or genes encoding proteins inducing apoptosis (e.g., p53). More recently, conditionally replicating adenoviruses (CRAds) have been developed. Such viruses rely on the lytic replication cycle of HAdVs for tumor cell killing. Viral replication in the tumor increases the local vector concentration and may lead to spread of the virus within the tumor. In addition, HAdV may provide a danger signal that stimulates an antitumor immune response.³ Successful preclinical studies have led to various phase I clinical trials of replication-defective as well as conditionally replication-competent HAdV vectors in prostate cancer.^{4,5} So far these studies have confirmed the good safety profile of HAdV vectors. Taken together, these factors have made adenoviral vectors a prime candidate for developing viral oncolytic agents.

GETTING THE VIRUS TO THE TUMOR

Intratumoral injection

An important lesson learned from preclinical and clinical research in cancer gene therapy is that efficient transduction of the cancer cells in the tumor is essential for efficacious treatment. Tumors are heterogeneous and contain a stromal compartment and extracellular matrix components that form physical barriers within the tumor (Fig. 1). Therefore even direct intratumoral administration of viral anticancer agents is often disappointingly inefficient. Expression of the receptor used by most HAdVs to enter the cell, that is, the coxsackievirus and adenovirus receptor (CAR), is often scanty. The high interstitial fluid pressure within most tumors causes a convective flow from the tumor. This inhibits the passive diffusion of viral particles into the tumor. The

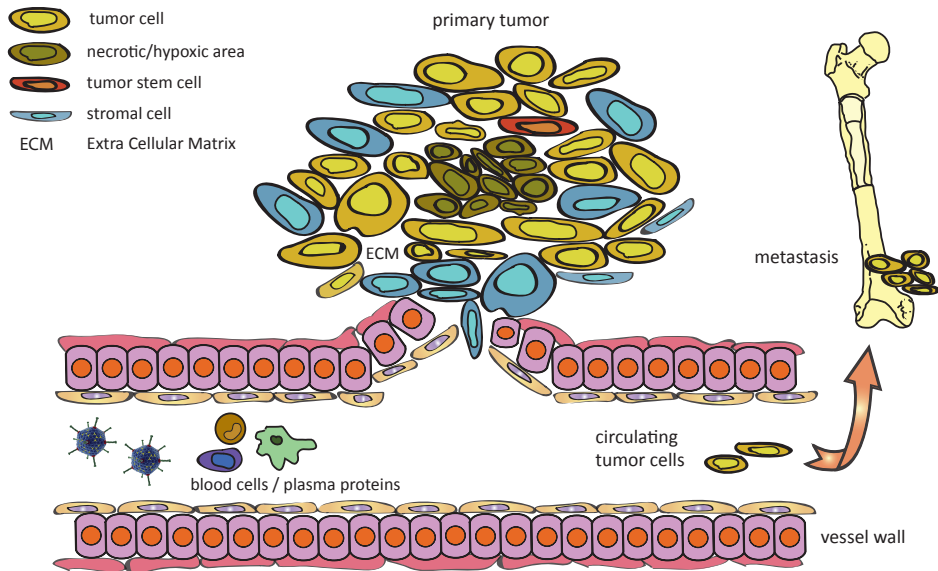


Figure 1. Schematic representation of the tumor structure and the hurdles to efficient adenoviral vector-mediated prostate cancer gene therapy. Several efficacy-lowering aspects are encountered on systemic or intratumoral delivery of adenoviral vectors to prostate cancer. Systemic delivery of vector particles to the primary tumor site and to metastasized tumor cells is hampered by innate and humoral immunity, sequestration from the blood stream through the binding of blood cells or plasma proteins, and limited permeability of blood vessels. The heterogeneous composition of the primary tumor mass results in inefficient penetration into the tumor and insufficient transduction of the neoplastic cells.

extracellular matrix may form physical barriers that prevent efficient spread of viral vectors.⁶⁻⁸ In elegant studies, Jain and co-workers demonstrated that destruction of the matrix by collagenase treatment or overexpression of matrix metalloproteinases (MMP)-1 and -8 increases the volume distribution of oncolytic herpesviruses.^{9,10} The volume distribution can also be increased by multiple injections, or by convection-enhanced delivery procedures.

Vascular delivery

Theoretically, vascular delivery of vectors may lead to a larger distribution of viruses within the tumor. Also, it could provide an option for transducing (micro)metastatic tumors. However, vascular delivery, too, has been frustratingly inefficient so far. This is attributable to a wide variety of factors. Direct contact between malignant cells and the oncolytic HAdV may be difficult to obtain. Often blood vessels are confined to the tumor stroma, and therefore several layers of stromal cells must be passed before malignant cells are reached by vascularly applied therapeutic agents.^{6,7}

HAdV vectors may become unavailable to the tumor by promiscuous association with nontarget tissues such as the liver. The primary receptor of many HAdVs is the CAR. After ligation of the adenoviral fiber with the CAR an integrin-binding RGD motif in the penton base binds $\alpha_v\beta_3$ - or $\alpha_v\beta_5$ -integrins. This promotes adenovirus

internalization. Both CAR and the integrins are widely expressed on cells in the human body, resulting in transduction of nontarget tissues.¹¹ Intriguingly, mutation of the CAR-binding site of the fiber and the RGD motif in the penton base was found not to reduce liver transduction, and on intravascular administration adenoviruses were still efficiently sequestered by Kupffer cells in the liver.¹² Subsequently it became evident that the interaction of the virus with host blood cells and plasma proteins is critical. Studies suggest that these interactions dictate the particle biodistribution of adenovirus *in vivo*. Various plasma proteins and in particular vitamin K-dependent coagulation factors IX and X can bind to hexon proteins in the capsid, and bridge the virus to receptors in the liver.^{13,14} In this respect there is variability between human adenoviral serotypes. Whereas the serotypes commonly used as vector, that is, HAdV-5 and -2, strongly bind factor X, others such as serotype 26 and 46 do not.^{15,16} Therefore (hexons of) different serotypes, or non-clotting factor-binding derivatives of the HAdV-5 hexon, can be used to decrease the loss of vector particles in the liver and to improve bioavailability to the tumors. Indeed, such mutations significantly decrease liver transduction of HAdV-5 vectors in mice.^{15,16} The HAdV-5 fiber harbors a site with high affinity for heparan sulfate proteoglycans; however, mutation of the binding motif KTKK barely affects liver transduction in mice.^{12,17}

Not only these interactions with clotting factors thwart efficient tumor cell transduction, but so do neutralizing immunoglobulins. A majority of humans have preexisting humoral neutralizing activity against HAdV-5 and HAdV-2 as a result of prior exposure to these viruses. Intravascular administration of adenovirus to recipients with preexisting humoral immunity will strongly reduce gene transfer. The use of vectors derived from HAdV with a low seroprevalence in the general population, or from nonhuman adenoviruses, may reduce the magnitude of the problem.¹⁸

An unexpected finding came with the observation that human, in contrast to murine, erythrocytes bind HAdV-5. Human erythrocytes present CAR at their surface, which stably interacts with HAdV-5 particles.^{19,20} Also human, but not murine, erythrocytes present complement receptor-1 (CR1), which binds HAdV-5 in the presence of antibodies and complement.¹⁹ Transplantation of human erythrocytes into immune deficient mice extended the blood circulation time of HAdV-5, reduced liver transduction, and decreased extravasation of the virus into human xenograft tumors. Similarly, HAdV-5 showed extended circulation and decreased liver transduction in transgenic mice presenting either CAR or CR1 on their erythrocytes. Erythrocytes may therefore restrict HAdV-5 infection in humans, independent of antibody status, presenting another challenge to HAdV-5-based anticancer viruses.^{19,20} Although much insight has been acquired on the interaction of adenoviruses with blood cells and plasma proteins, many other areas of virus-host interactions remain underexplored and in general we understand little of it.

Shielding vector particles from neutralizing immunity

Although formidable, the challenges of vascular delivery summarized previously may not be insurmountable. One approach potentially leading to improvements in delivery of adenoviral vectors for cancer gene therapy involves chemical coating of the vector particles. This approach is based on established and clinically applicable technology of packaging drugs or therapeutic biologicals in synthetic polymers. It is hoped that

this can lead to improved pharmacological parameters, such as improved solubility and stability, reduced dosing frequency, potentially reduced toxicity, and extended circulation time. Amongst others, poly[N-(2-hydroxypropyl)-methacrylamide] and polyethylene glycol (PEG) are often used to covalently coat therapeutics.²¹

Coating with multivalent polymers based on poly[N-(2-hydroxypropyl)-methacrylamide] abrogated normal HAdV-5 infectious tropism.²² In addition, neutralization by antibodies was decreased up to 50-fold, and the resulting polymer-coated adenoviral particles have a greatly extended plasma circulation time in mice.^{22,23} Although normal tropism was blocked, polymer-coated adenovirus accumulated within a solid subcutaneous tumor 40 times more efficiently than unmodified virus, and mediated higher levels of transgene expression within tumors. This has been attributed to the enhanced permeability and retention effect, which leads to the nonspecific accumulation of circulating macromolecules within tumors.²⁴

After blocking, infectivity can be restored by linking targeting peptides onto the surface of the polymer-coated viruses. Addition of a synthetic -SIKVAV- peptide, which binds α_6 -integrin, can restore viral infectivity of PC-3 cells. Competition assays confirmed that entry of retargeted viruses was mediated via the incorporated ligand. Intravenous administration of retargeted viruses to tumor-bearing mice resulted in slower plasma clearance and greatly reduced liver tropism, and hence toxicity compared with unmodified virus, while maintaining reporter gene expression in the tumor.²⁵ Similarly, polymer-coated HAdV could be targeted with cetuximab to target the epidermal growth factor (EGF) receptor.²⁶ The data demonstrate that the polymer-coating technology is compatible with peptide-based tumor targeting.

Other groups used coating of adenoviral particles with polyethylene glycol (PEG) molecules for particle shielding, and showed that this allows escape from neutralizing antibodies and to some extent allowed vector readministration. In this respect the size of the PEG molecules matters. With the use of large PEG molecules (e.g., 20-kDa PEG), vector particles were detargeted from muscle after local delivery and from liver after systemic delivery in mouse models. Surprisingly, fully detargeted PEGylated adenoviral vectors still induced strong cellular and humoral immune responses to vector-encoded transgene products. PEGylation does not affect the kinetics of transgene product-specific cytotoxic immune responses.²⁷ These data have been corroborated by Barry and collaborators, who demonstrated that PEGylation with 20-kDa PEG was as efficient at detargeting adenovirus from Kupffer cells and hepatocytes as virus predosing and warfarinization.²⁸⁻³¹ Bioluminescence imaging of viral distribution in a xenograft model in nude mice demonstrated that PEGylation with 20-kDa PEG reduced liver infection 19- to 90-fold. Tumor transduction levels were similar for 20-kDa PEGylated and un-PEGylated vectors. Anticancer efficacy after a single intravenous injection was retained at the level of unmodified vector in large established LNCaP prostate carcinoma xenografts, resulting in complete elimination of tumors in all animals and long-term tumor-free survival.³¹ It should be noted that the protective effects of PEGylation could be more pronounced in the presence of human erythrocytes, as PEGylation will also reduce association with CAR and complement receptor I. Taken together, these data suggest that chemical shielding of HAdV particles is a powerful approach to prevent interaction of HAdV particles with blood proteins, erythrocytes, and nontarget tissues, and thereby may

increase the bioavailability, and as a result the uptake of viruses into tumors, by enhanced permeability and retention.

Vascular permeability

To further stimulate extravasation of vector particles, new physiological regulators of vascular permeability (i.e., vascular endothelial growth factor [VEGF]) may be used. This strategy allows enhanced transduction of striated muscle by combining intravenous AAV6-vector administration with infusion of VEGF.³² Alternatively, strategies are being developed that employ the endothelial receptor-mediated transcytosis pathway. The transferrin receptor is an example of a receptor that binds transferrin and its associated iron, resulting in caveolar uptake of the complex. Via a series of vesicles these complexes are transported across the endothelium and released at the basolateral side. Curiel and co-workers provided evidence that this pathway can be used by adenoviruses. By using a bifunctional adaptor, for example, a soluble CAR-transferrin fusion protein, the particles could be taken up by Caco-2 cells and transported across a polarized monolayer.³³ These data suggest that adenoviruses can be redirected to the transcytosis pathway, although it remains to be established how efficiently this route can be recruited in the tumor endothelium.

Targeting adenoviruses

Many strategies have been pursued to improve gene transfer into CAR-negative cells. In addition to the use of non-CAR-binding serotypes and fiber-swap vectors,^{34,35} recombinant HAdV vectors with altered tropism have also been generated by engineering new ligands for cellular receptors into surface loops of capsid components. The favorite locations have been the C terminus and the HI loop of the knob domain of the fiber, the RGD loop of the penton base protein, and the L1 loop of the hexon. Although effective, the applicability of this approach was initially limited by the restricted tolerance for inserting new ligands at these positions.¹¹ In addition, new ligands that are to be incorporated genetically into adenoviral vectors must be able to fold correctly in the reducing environment of the mammalian cell cytoplasm. This excludes most ligands dependent on disulfide bond formation for proper folding such as epidermal growth factor and most single-chain variable fragments.³⁶ Promising candidate ligands are Affibody molecules (Affibody AB, Bromma, Sweden), which are affinity proteins based on a 58-amino acid three-helix bundle structure, termed "Z," that is derived from the immunoglobulin-binding domain of staphylococcal protein A. Display libraries have been constructed on the basis of randomization of 13 surface accessible amino acids in the Z domain, from which novel Affibody molecules to desired targets have been selected. These Affibodies can be efficiently used for genetic retargeting of adenovirus.^{36,37} Although initial experiments were thwarted by structural constraints, Lindholm and collaborators managed to insert two Affibodies in tandem in the HI loop, by connecting them via small flexible linkers. This resulted in HAdV-5 vectors genetically retargeted with a HER2/neu-specific Affibody molecule inserted in the HI loop of the fiber knob of a CAR-binding-ablated fiber.³⁸ With this technology, vectors can be generated by incorporating two Affibody molecules with different specificities.³⁹ Camelid and human single-domain antibody fragments may be applicable in a similar manner.⁴⁰

In another approach, the knob and shaft of the fiber have been replaced by an artificial trimerization domain, which was linked to an heterologous receptor-binding ligand.⁴¹⁻⁴³ Via this strategy Willemssen and co-workers managed to retarget HAdV-5 to tumor cells by replacing the shaft and knob of HAdV-5 by a single-chain T cell receptor specific for HLA-A1 molecules that present a MAGE-A1 peptide.⁴⁴ Similar single-chain T cell receptors have been fused to the C terminus of the minor capsid protein IX.⁴⁵ Immunoaffinity studies suggested that the C termini of protein IX molecules are positioned near the capsid surface.^{46,47} This has been confirmed by cryoelectron microscopy studies, which suggest that the C termini are located near the peripentonal hexons. Here the leucine zipper domain in the C-terminal part of protein IX interacts with the zipper of other molecules, forming a coiled coil.⁴⁸⁻⁵⁰ These protein IX-protein IX associations are not necessary for pIX-capsid incorporation and thermostability of the particles.⁵¹

If ligands are to be fused with pIX, a spacer may expose the ligands above the outer surface of hexon capsomers to ensure its accessibility to cellular receptors. Vellinga and co-workers have demonstrated that linkers up to a length of 75 Å can be added to the C terminus of protein IX without affecting the incorporation of protein IX into the capsid.⁵² Indeed, a wide variety of targeting polypeptides could be functionally incorporated by genetic fusion at the C terminus of protein IX. In this way small targeting peptides, a hyperstable single-chain Fv, and a single-chain T cell receptor could be functionally incorporated into the capsid.^{45,52-54} In addition, other functional proteins were incorporated in the adenoviral capsid through linkage to pIX, such as fluorescent proteins that allow particle tracing by fluorescence microscopy.^{55,56}

An elegant combination of genetic modification and chemical modification has been developed by Kreppel and co-workers. HAdV-5 vectors were genetically modified to contain cysteines at solvent-exposed positions in the capsid.⁵⁷ The introduced thiol groups are highly reactive, and procedures were established for their controlled covalent coupling to protein and nonprotein ligands. Depending on the chemistry used, ligands could be coupled by formation of thioether or disulfide bonds. The latter method yields viruses that release the coupled ligand in the endosome. In addition, thiol groups in the fiber knob were still accessible after amino PEGylation, allowing PEG shielding to be combined with targeting by ligand coupling to the thiol groups.⁵⁷ Coupling of transferrin to engineered cysteine residues at the C terminus of protein IX allowed targeting of HAdV particles in mice *in vivo*.⁵⁸ This validates the applicability of the technique in procedures involving intravenous administrations of adenoviral vectors.

Taken together, these data show that HAdV vector technology has matured and constitutes a functional and robust platform for generating shielded, retargeted vectors that can be used for developing oncolytic HAdV vectors for cancer gene therapy.

Targetable receptors in prostate cancer

With the targeting platform in place, a key question concerns which receptors could be targeted in prostate cancer. Extensive target exploration has yielded several cell surface receptors that are expressed preferentially or specifically in prostate cancer cells.

A prime candidate is prostate-specific membrane antigen (PSMA). It is expressed both on benign and malignant prostate cells. It is a type 2 membrane receptor, which

can be efficiently internalized. The ligands that trigger internalization remain to be identified.⁵⁹ Nearly all prostate tumors and prostate cancer cells express PSMA and increased expression correlates with aggressive tumors.⁶⁰ PSMA is also upregulated after androgen deprivation in model systems whereas other markers such as prostate-specific antigen (PSA) are decreased after androgen withdrawal.⁶¹ PSMA can serve as a tissuespecific target for adenoviral vectors.⁶² Retargeting of viral particles to prostate cancer cell lines was obtained through the attachment of bispecific molecules, which consisted of conjugates between an anti-adenoviral fiber knob Fab' fragment and anti-PSMA monoclonal antibodies.⁶²

Besides PSMA, various other cell surface molecules have been demonstrated to be upregulated in prostate cancer, such as prostate stem cell antigen (PSCA). Successful targeting to PSCA-expressing prostate cancer cells has been achieved for genetically engineered T cells that have been equipped with a chimeric T cell receptor recognizing PSCA.⁶³ These findings support the exploration of PSCA targeting in the context of prostate cancer-targeted oncolytic viruses.

The urokinase-type plasminogen activator receptor (uPAR) has also been exploited for targeting of oncolytic viruses to prostate cancer cells. uPAR is overexpressed in tumors as well as in stromal cells of multiple malignancies, including prostate cancer.^{64,65} uPAR is involved in tumor angiogenesis. For example, tumor cell-conditioned media can upregulate endothelial uPAR expression.⁶⁶ The principle of targeting tumor endothelium by aiming at uPAR, rather than at the cancer cells themselves, is highly attractive, because such an approach may lead to improved viral trafficking from the bloodstream into the tumor tissue. HAdV targeting to uPAR is feasible.⁶⁷ More recently, tumor and vascular targeting of an oncolytic measles virus has been achieved.⁶⁸

In addition, other cell surface molecules are upregulated in the tumor vasculature, including members of the vascular endothelial growth factor receptor (VEGFR) family. Both VEGFR1 (Flt-1) and VEGFR2 (Flk-1) are selectively expressed on endothelial cells and are highly upregulated in proliferating (angiogenic) capillary cells of numerous types of prostate tumor.⁶⁹ The potential of VEGFR2 as a target has been shown in studies on systemic targeting of drug-loaded microspheres to subcutaneous prostate tumors in mice, which demonstrated significant inhibition of tumor growth after conjugation of anti-VEGFR2 antibodies to the microspheres.⁷⁰

One class of potentially specific receptors is the group of tumor-specific cancer testis (CT) antigens.⁷¹ Peptides of these CT antigens are presented on the cell surface in complex with major histocompatibility class (MHC) I molecules. With the exception of their expression in the testis, an immune-privileged site due to the absence of MHC expression, the CT antigens are expressed exclusively in cancer cells. Proof-of-principle of targeting adenoviral vectors to CT antigens has been shown by genetically fusing viral capsid proteins with single-chain T cell receptors, which could specifically recognize the melanoma-specific CT antigen MAGE-A1 in complex with HLA-A1.^{44,45} Multiple cancer CT antigens have been found in patients with prostate cancer, including SSX-2 and MAD-CT-1 and -2.^{72,73} A peptide present in the majority of MAGE-A gene family members could serve as an ideal target as most tumors, both solid and blood-borne, express at least one member of this MAGE-A gene family.⁷⁴ In addition to cell surface antigens, intracellular antigens, for example, PSA, have now become available for targeting and warrant further exploration as targets for gene therapy vectors.^{72,73}

Combining the selective power of phage display, which allows for the testing of tens of billions of individual clones, with high-throughput selection of Fabs with peptide-MHC complex-binding capacity will yield new human “T cell receptor (TCR)-like” Fab fragments that specifically target viruses to tumor cells expressing intracellular tumor antigens.⁷⁵

Prostate-targeted conditionally replicative adenoviruses

HAdVs have been generated that replicate specifically in certain cell types. In HAdV infection, the E1A gene acts as the master switch that activates the viral gene expression cascade. Therefore, by controlling E1A expression with a tumor- or tissue-specific promoter, viral replication can be restricted to certain cell types. Along these lines, Essand and collaborators developed a series of prostate-specific adenoviruses that replicate exclusively in normal and neoplastic prostate epithelial cells.⁷⁶⁻⁷⁸ In these vectors expression of E1A is controlled by the recombinant prostate-specific PPT sequence. The PPT sequence is composed of a prostate-specific antigen (PSA) enhancer, a prostate-specific membrane antigen (PSMA) enhancer, and a T cell receptor γ -chain alternate reading frame protein (TARP) promoter. The PSMA enhancer, which upregulates PSMA expression in androgen-depleted prostate cancer cells, also ensures that the PPT sequence is active under androgen-deprived conditions. The mouse H19 insulator (I), with enhancer-blocking activity, was placed upstream of PPT to protect it from interfering signals from the adenoviral backbone.^{76,77} The most advanced version, the so-called Ad[i/PPT-E1A, E3] virus, induced regression of aggressively growing LNCaP tumors, and yielded significantly prolonged survival for treated mice compared with the control groups.⁷⁸

Not only can E1 regulation be used to restrict replication to cancer cells, but the strategy has also been used to prevent expression of E1A, and thereby expression of other viral genes, in sensitive nontarget tissues. HAdV5 vectors can mediate significant hepatotoxicity. To prevent viral gene expression in hepatocytes, multiple binding sites for a hepatocyte-specific microRNA, miR-122, were placed in the 30 untranslated region of the E1A gene.^{79,80} miR-122 is highly and selectively expressed in hepatocytes and this modification might prevent expression of E1A within hepatocytes, and hepatotoxicity, while maintaining its replicative capacity in tumor cells. Animals receiving a lethal dose of wild-type Ad5 (5×10^{10} viral particles/mouse) showed substantial hepatic genome replication and extensive liver pathology, whereas inclusion of miR-122 binding sites decreased replication 50-fold and virtually abrogated liver toxicity, demonstrating the efficiency of the approach.⁸⁰ These examples demonstrate that we can endow replicating HAdV vectors with tumor cell selectivity, while protecting sensitive nontarget tissues.

NEW DIRECTIONS

A robust technology platform for cancer-targeted and oncolytic HAdV vector generation has been established. Many elegant tools and techniques have been developed with well-chosen experiments to show their proof-of-concept. However, it seems fair to state that most improvements have been incremental and only a few

of the vectors that showed promise in preclinical studies have reached the stage of clinical evaluation. So, where do we go from here? In what fields are new developments necessary to fulfill the promise of efficacious prostate cancer-targeted HAdV vectors? It may be useful to step back, reflect, and place our activities in perspective.

Rational design or evolution of new oncolytic viruses?

So far, most vectorologists have followed a “rational design” or reverse-genetics approach for building new therapeutic vectors. In other words, on the basis of a *priori* knowledge of virus biology, tumor cell biology, and pharmaceutical parameters, we have built our new vectors to have the desired phenotype and to perform as anticipated. This approach has been most useful and has delivered most of the vectors that are in use in clinical gene therapy to date. Nevertheless, one should realize that this is not the classical approach in microbiology.

Classical virology studies viruses by employing selection strategies to isolate mutants with desired phenotypes and to study these to obtain insight into viral genetics and virus biology. There has been a revival of interest in the classical, more evolutionary approaches involving bioselection strategies for developing improved HAdV oncolytic vectors. Yan and co-workers have provided a fine example of the power of this approach.⁸¹ *In vitro* chemical mutagenesis of HAdV-5 was combined with a bioselection strategy. This yielded a mutant virus that replicated more efficiently in the HT29 colorectal tumor cells that were used for selection. The mutation truncates an open reading frame in the late *i*-leader transcript. Not only in HT29, but also in several other tumor cell lines, replication was enhanced by the causative *i*-leader mutation at nucleotide 8350 of the HAdV-5 genome.⁸¹ Along similar lines, Gros and co-workers used *in vivo* bioselection and obtained an E3/19K mutant with enhanced antitumoral potency.⁸² By selecting for HAdVs with large-plaque phenotypes, Subramanian and coworkers isolated a series of mutants, including mutants in the *i*-leader and in the E3/19K gene.⁸³ Taken together, these data suggest that the oncolytic activity of wild-type HAdV-5 can be enhanced by mutations.

Hermiston and collaborators took this approach a step further.⁸⁴ On the basis of the notion that there is no evidence that HAdV-5 is the optimal start point for selecting more potent oncolytic HAdVs, they pooled an array of HAdV serotypes. These pools were passaged under conditions that invite recombination between serotypes. They isolated a mutant, designated coloAd1, which replicates more efficiently than any wild-type virus in human colon cancer cells. Characterization of coloAd1 revealed that it is a complex hybrid between HAdV-3 and -11p.⁸⁴ It is evident that none of the bioselected viruses would have been created on the basis of preexisting knowledge. In fact, we have no clear understanding why these mutants replicate so much better in the cell systems that were used for their isolation. This underscores the potential of the classical strategy. It is to be expected that evolutionary approaches involving bioselections will become more widely applied. These approaches will yield new viruses, and the characterization of these viruses may provide new insights concerning critical aspects of virus and tumor cell biology. Uil and co-workers reported an approach that employs modified adenoviral polymerases with deficits in the polymerase proofreading function. This strategy will facilitate the isolation of more complex HAdV mutants for cancer gene therapy.⁸⁵

Taken together, it seems reasonable to anticipate that adenoviral mutations that have been isolated by bioselection procedures will soon be incorporated in clinically applicable oncolytic adenoviruses.

Cellular delivery of viruses

Many studies have demonstrated that the delivery of vector particles into tumors is inefficient. Both intratumoral and vascular delivery are thwarted by a variety of factors (see above), and therefore new delivery methods are essential. An attractive option is to use cells with the capacity to migrate to tumors as delivery vehicles for oncolytic viruses. In this strategy the tumor-targeting cells are loaded with viruses and administered to the patient. After migration the cells should hand off the cell-associated viruses or, if the virus replicates in the delivery cells, their progeny. In this way viruses should be delivered to tumor cells. Several cell types can migrate to tumors *in vivo*, including cytokine-induced killer cells, tumor antigen-specific T cells, macrophages, endothelial progenitor cells, and mesenchymal stem cells.⁸⁶ In addition, virus-loaded dendritic cells have been used to eradicate tumor cells from tumor-draining lymph nodes.⁸⁷

Cellular delivery of viral anticancer agents may also circumvent the effects of neutralizing immunity.⁸⁸ This is evidenced in a study employing human reoviruses as the oncolytic agent. In reovirus-immune mice with B16tk lymph node melanoma metastases, *in vivo* delivery of free reovirus to the melanoma was ineffective, whereas effective antitumor responses and long-term tumor clearance were obtained if mature dendritic cells as well as T cells were used as carriers.⁸⁷ This and other studies suggest that cellular delivery is feasible and may be applicable for the delivery of viral oncolytic agents at tumor sites. It should be noted that cellular delivery adds a new level of complexity to clinical gene therapy studies and is logistically challenging.

Tumor stem cells as new targets?

With the aid of such new technologies, that is, the bioselection-based strategies for vector improvement, and cell-based methods for vector delivery, new cancer gene therapeutics and therapeutic strategies may be developed that ensure efficient vector delivery into the tumors. It is known that tumors are usually markedly heterogeneous, consisting of complex mixtures of cancer cells with various grades of differentiation. A cell type that has attracted much attention is the tumor-initiating cell, or cancer stem cell. The tumor-initiating cell is a cell with the capacity to self-renew and differentiate into any of the lineages of cancer cells that comprise a tumor.⁸⁹ Presumably the tumor-initiating cells are derived from organ stem cells.⁹⁰ The latter are long-lived and change over the course of time by accumulating (epi)genetic alterations. In this model, the characteristics of a cancer-initiating cell, and therefore of the resulting tumor, depend (in part) on these alterations. The cancer stem cell population in a tumor may govern crucial tumor processes such as progression, invasion, and metastasis. Therapy resistance may be the consequence if a particular treatment does not effectively eradicate the cancer stem cell population. It may therefore be important to ensure that new oncolytic agents have the capacity to transduce and kill cancer stem cells.

Nonviral delivery of viral genomes

Systemic approaches for cancer gene therapy have been focused on delivering viruses to the tumor. With advances in the field of nonviral gene delivery, an alternative approach became feasible.⁹¹ Rather than delivering intact viruses to the tumor cells, a strategy is followed in which viral genomes are delivered. If transferred into cells, HAdV DNA can yield replicating virus. Although not particularly efficient, infectious HAdV can be reproducibly recovered from cell cultures on transfer of naked DNA.

The field of nonviral gene transfer has seen impressive advances in increased tumor accumulation of transgenes,⁹² but so far the therapeutic consequences remain to be improved. Individual steps in gene delivery need further improvement, especially those relating to intracellular trafficking of the complexes. This includes the timely release of the DNA complex from the targeting ligand, efficient escape from the endosomal compartment, and proper delivery of the genes into the nucleus.⁹³⁻⁹⁵ Furthermore, innate immunity must be evaded. Integration of controlled-release technologies into targeted gene delivery systems will provide more effective gene delivery systems.⁹⁶⁻⁹⁸

With the delivery of viral genomes we could benefit from the best of two worlds. Nonviral vectors may be easier to produce and formulate, and may deliver their payload more reproducibly at the tumor site than viral vectors. If used for the delivery of viral genomes, tumor-selective replicating viruses may be generated on site, which can spread in the tumor and exert their therapeutic action, without causing collateral damage to nontarget tissues. It remains doubtful, however, that HAdV is the best choice of virus for such strategies.

New therapeutic genes

New transgenes in the vectors may enhance therapeutic efficacy. An intriguing class of prodrug-activating genes is based on deoxyribonucleoside kinases (dNKs). These enzymes catalyze the phosphorylation of deoxyribonucleosides to deoxyribonucleoside monophosphates and thereby provide the cell with deoxyribonucleoside triphosphates. The dNKs catalyze the first, and often rate-limiting, step of nucleoside analog activation. These enzymes are therefore promising candidates to be used in combination with nucleotide analogs as prodrug-enzyme combinations. Bioselection yielded mutants of the *Drosophila melanogaster*-derived dNK with enhanced sensitivity to a range of clinically approved nucleotide analogs, such as 30-azido-30-deoxythymidine (AZT), arabinosylcytosine (AraC), ddA, and ddC.^{99,100} These mutants efficiently sensitized glioblastoma, osteosarcoma, and breast cancer cells to clinically accepted drugs.¹⁰⁰ The use of approved nucleoside analogs may facilitate swift acceptance of the strategy.

FUTURE PROSPECTS

We have witnessed an enormous expansion of the gene transfer technology required for cancer gene therapy. Initial clinical safety studies have demonstrated the validity of the concept, and the feasibility of current approaches.¹⁰¹ The viral vectors used in the clinical studies reported so far have been well tolerated and safe. Robust technology platforms have been established and many of the factors currently thwarting prostate cancer gene therapy have been identified. New platforms for preclinical evaluation of

new oncolytic vectors are available.¹⁰² Combining the technologies and building on new insights from prostate cancer biology and virology will facilitate the generation of new vectors that will, it is hoped, be as safe as current vectors, but more efficacious. With these we may keep the promise of gene therapists to provide new and effective treatment for malignant neoplastic disease in general and prostate cancer in particular.

ACKNOWLEDGEMENTS

This work was supported by the European Union through the 6th Framework Program GIANT (contract no. 512087).

REFERENCES

1. Van der Vliet PC and Hoeben RC. Adenoviruses. In *DNA Replication and Human Disease* ed. DePamphilis, ML, ed. (Cold Spring Harbor Laboratory Press, Cold Spring Harbor, New York) 2006; 645-661.
2. Bachtarzi H, Stevenson M, Fisher K. Cancer gene therapy with targeted adenoviruses. *Expert Opin Drug Deliv* 2008; **5**:1231-1240.
3. Geutskens SB, van der Eb MM, Plomp AC, Jonges LE, Cramer SJ, Ensink NG et al. Recombinant adenoviral vectors have adjuvant activity and stimulate T cell responses against tumor cells. *Gene Ther* 2000; **7**:1410-1416.
4. Figueiredo ML, Kao C, Wu L. Advances in preclinical investigation of prostate cancer gene therapy. *Mol Ther* 2007; **15**:1053-1064.
5. Freytag SO, Stricker H, Movsas B, Kim JH. Prostate cancer gene therapy clinical trials. *Mol Ther* 2007; **15**:1042-1052.
6. Kuppen PJ, van der Eb MM, Jonges LE, Hagenaars M, Hokland ME, Nannmark U et al. Tumor structure and extracellular matrix as a possible barrier for therapeutic approaches using immune cells or adenoviruses in colorectal cancer. *Histochem Cell Biol* 2001; **115**:67-72.
7. Li ZY, Ni S, Yang X, Kiviat N, Lieber A. Xenograft models for liver metastasis: Relationship between tumor morphology and adenovirus vector transduction. *Mol Ther* 2004; **9**:650-657.
8. Mok W, Stylianopoulos T, Boucher Y, Jain RK. Mathematical modeling of herpes simplex virus distribution in solid tumors: implications for cancer gene therapy. *Clin Cancer Res* 2009; **15**:2352-2360.
9. McKee TD, Grandi P, Mok W, Alexandrakis G, Insin N, Zimmer JP et al. Degradation of fibrillar collagen in a human melanoma xenograft improves the efficacy of an oncolytic herpes simplex virus vector. *Cancer Res* 2006; **66**:2509-2513.
10. Mok W, Boucher Y, Jain RK. Matrix metalloproteinases-1 and -8 improve the distribution and efficacy of an oncolytic virus. *Cancer Res* 2007; **67**:10664-10668.
11. Arnberg N. Adenovirus receptors: implications for tropism, treatment and targeting. *Rev Med Virol* 2009; **19**:165-178.
12. Di Paolo NC, van Rooijen N, Shayakhmetov DM. Redundant and synergistic mechanisms control the sequestration of blood-born adenovirus in the liver. *Mol Ther* 2009; **17**:675-684.
13. Kalyuzhniy O, Di Paolo NC, Silvestry M, Hofherr SE, Barry MA, Stewart PL et al. Adenovirus serotype 5 hexon is critical for virus infection of hepatocytes *in vivo*. *Proc Natl Acad Sci USA* 2008; **105**:5483-5488.
14. Waddington SN, McVey JH, Bhella D, Parker AL, Barker K, Atoda H, et al. Adenovirus serotype 5 hexon mediates liver gene transfer. *Cell* 2008; **132**:397-409.

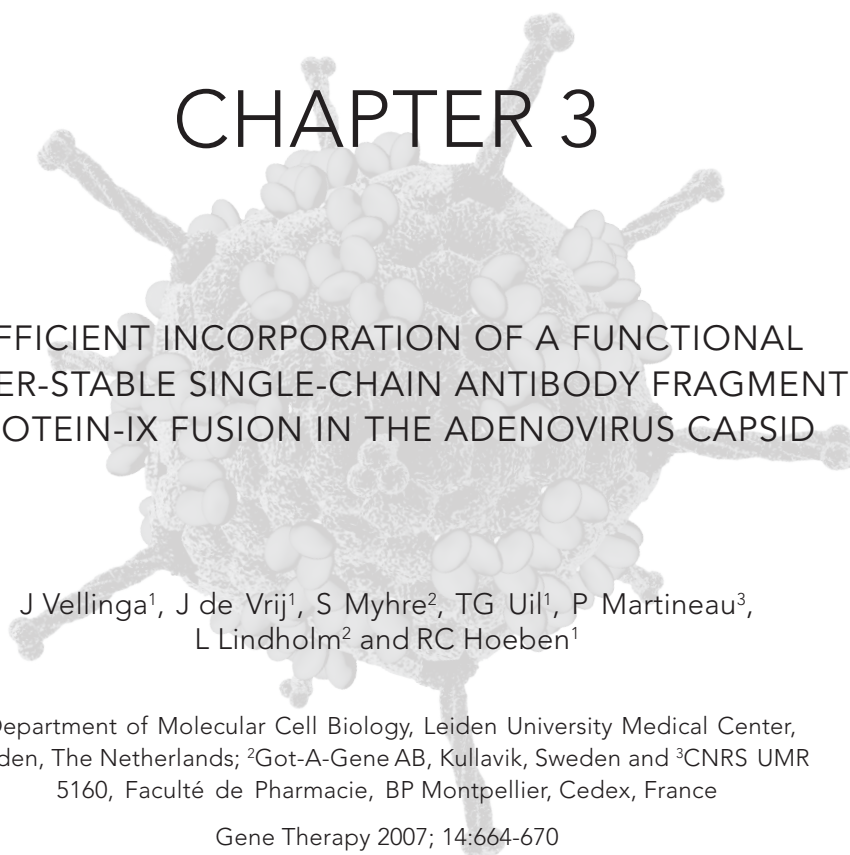
15. Waddington SN, Parker AL, Havenga M, Nicklin SA, Buckley SM, McVey JH et al. Targeting of adenovirus serotype 5 (Ad5) and 5/47 pseudotyped vectors *in vivo*: fundamental involvement of coagulation factors and redundancy of CAR binding by Ad5. *J Virol* 2007; **81**:9568-9571.
16. Alba R, Bradshaw AC, Parker AL, Bhella D, Waddington SN, Nicklin SA et al. Identification of coagulation factor (FX) binding sites on the adenovirus serotype 5 hexon: effect of mutagenesis on FX interactions and gene transfer. *Blood* 2009; **114**:956-971.
17. Kritz AB, Nicol CG, Dishart KL, Nelson R, Holbeck S, Von Seggern DJ et al. Adenovirus 5 fibers mutated at the putative HSPG-binding site show restricted retargeting with targeting peptides in the HI loop. *Mol Ther* 2007; **15**:741-749.
18. Abbink P, Lemckert AA, Ewald BA, Lynch DM, Denholtz M, Smits S et al. Comparative seroprevalence and immunogenicity of six rare serotype recombinant adenovirus vaccine vectors from subgroups B and D. *J Virol* 2007; **81**:4654-4663.
19. Carlisle RC, Di Y, Cerny AM, Sonnen AF, Sim RB, Green NK et al. Human erythrocytes bind and inactivate type 5 adenovirus by presenting Coxsackie virus-adenovirus receptor and complement receptor 1. *Blood* 2009; **113**:1909-1918.
20. Seiradake E, Henaff D, Wodrich H, Billet O, Perreau M, Hippert C et al. The cell adhesion molecule "CAR" and sialic acid on human erythrocytes influence adenovirus *in vivo* biodistribution. *PLoS Pathog* 2009; **5**:e1000277.
21. Kreppel F and Kochanek. Modification of adenovirus gene transfer vectors with synthetic polymers: a scientific review and technical guide. *Mol Ther* 2008; **16**:16-29.
22. Fisher KD, Stallwood Y, Green NK, Ulbrich K, Mautner V, Seymour LW. Polymer-coated adenovirus permits efficient retargeting and evades neutralising antibodies. *Gene Ther* 2001; **8**:341-348.
23. Green NK, Herbert CW, Hale SJ, Hale AB, Mautner V, Harkins R et al. Extended plasma circulation time and decreased toxicity of polymer-coated adenovirus. *Gene Ther* 2004; **11**:1256-1263.
24. Matsumura Y and Maeda H. A new concept for macromolecular therapeutics in cancer chemotherapy: mechanism of tumoritropic accumulation of proteins and the antitumor agent smancs. *Cancer Res* 1986; **46**:6387-6392.
25. Stevenson M, Hale AB, Hale SJ, Green NK, Black G, Fisher KD, et al. Incorporation of a laminin-derived peptide (SIKVAV) on polymer-modified adenovirus permits tumor-specific targeting via alpha6-integrins. *Cancer Gene Ther* 2007; **14**:335-345.
26. Morrison J, Briggs SS, Green NK, Thoma C, Fisher KD, Kehoe S et al. Cetuximab retargeting of adenovirus via the epidermal growth factor receptor for treatment of intraperitoneal ovarian cancer. *Hum Gene Ther* 2009; **20**:239-251.
27. Wortmann A, Vohringer S, Engler T, Corjon S, Schirmbeck R, Reimann J et al. Fully detargeted polyethylene glycol-coated adenovirus vectors are potent genetic vaccines and escape from pre-existing anti-adenovirus antibodies. *Mol Ther* 2008; **16**:154-162.
28. Hofherr SE, Mok H, Gushiken FC, Lopez JA, Barry MA. Polyethylene glycol modification of adenovirus reduces platelet activation, endothelial cell activation, and thrombocytopenia. *Hum Gene Ther* 2007; **18**:837-848.
29. Hofherr SE, Shashkova EV, Weaver EA, Khare R, Barry MA. Modification of adenoviral vectors with polyethylene glycol modulates *in vivo* tissue tropism and gene expression. *Mol Ther* 2008; **16**:1276-1282.
30. Weaver EA and Barry MA. Effects of Shielding Adenoviral Vectors with Polyethylene Glycol (PEG) on Vector-specific and Vaccine-mediated Immune Responses. *Hum Gene Ther* 2008; **19**:1369-1382.
31. Doronin K, Shashkova EV, May S, Hofherr S, Barry MA. Chemical modification with high molecular weight polyethylene glycol reduces transduction of hepatocytes and increases efficacy of intravenously delivered oncolytic adenovirus. *Hum Gene Ther* 2009; **20**:975-988.

32. Gregorevic P, Blankinship MJ, Allen JM, Crawford RW, Meuse L, Miller DG et al. Systemic delivery of genes to striated muscles using adeno-associated viral vectors. *Nat Med* 2004; **10**:828-834.
33. Zhu ZB, Makhija SK, Lu B, Wang M, Rivera AA, Preuss M et al. Transport across a polarized monolayer of Caco-2 cells by transferrin receptor-mediated adenovirus transcytosis. *Virology* 2004; **325**:116-128.
34. Murakami M, Ugai H, Belousova N, Pereboev A, Dent P, Fisher PB, et al. Chimeric adenoviral vectors incorporating a fiber of human adenovirus 3 efficiently mediate gene transfer into prostate cancer cells. *Prostate* 2009; **70**:362-376.
35. Sandberg L, Papareddy P, Silver J, Bergh A, Mei YF. Replication-competent Ad11p vector (RCAd11p) efficiently transduces and replicates in hormone-refractory metastatic prostate cancer cells. *Hum Gene Ther* 2009; **20**:361-373.
36. Lindholm L, Henning P, Magnusson MK. Novel strategies in tailoring human adenoviruses into therapeutic cancer gene-therapy vectors. *Future Virol* 2008; **3**:45-59.
37. Henning P, Magnusson MK, Gunneriusson E, Hong SS, Boulanger P, Nygren PA et al. Genetic modification of adenovirus 5 tropism by a novel class of ligands based on a three-helix bundle scaffold derived from staphylococcal protein A. *Hum Gene Ther* 2002; **13**:1427-1439.
38. Magnusson MK, Henning P, Myhre S, Wikman M, Uil TG, Friedman M et al. Adenovirus 5 vector genetically re-targeted by an Affibody molecule with specificity for tumor antigen HER2/neu. *Cancer Gene Ther* 2007; **14**:468-479.
39. Myhre S, Henning P, Friedman M, Stahl S, Lindholm L, Magnusson MK. Re-targeted adenovirus vectors with dual specificity; binding specificities conferred by two different Affibody molecules in the fiber. *Gene Ther* 2009; **16**:252-261.
40. Harmsen MM and De Haard HJ. Properties, production, and applications of camelid single-domain antibody fragments. *Appl Microbiol Biotechnol* 2007; **77**:13-22.
41. Krasnykh V, Belousova N, Korokhov N, Mikheeva G, Curiel DT. Genetic targeting of an adenovirus vector via replacement of the fiber protein with the phage T4 fibrin. *J Virol* 2001; **75**:4176-4183.
42. Magnusson MK, Hong SS, Boulanger P, Lindholm L. Genetic retargeting of adenovirus: novel strategy employing "deknobbing" of the fiber. *J Virol* 2001; **75**:7280-7289.
43. Schagen FH, Graat HC, Carette JE, Vellinga J, van Geer MA, Hoeben RC et al. Replacement of native adenovirus receptor-binding sites with a new attachment moiety diminishes hepatic tropism and enhances bioavailability in mice. *Hum Gene Ther* 2008; **19**:783-794.
44. Sebestyén Z, de Vrij J, Magnusson M, Debets R, Willemsen R. An oncolytic adenovirus redirected with a tumor-specific T-cell receptor. *Cancer Res* 2007; **67**:11309-11316.
45. de Vrij J, Uil TG, van den Hengel SK, Cramer SJ, Koppers-Lalic D, Verweij MC et al. Adenovirus targeting to HLA-A1/MAGE-A1-positive tumor cells by fusing a single-chain T-cell receptor with minor capsid protein IX. *Gene Ther* 2008; **15**:978-989.
46. Akalu A, Liebermann H, Bauer U, Granzow H, Seidel W. The subgenus-specific C-terminal region of protein IX is located on the surface of the adenovirus capsid. *J Virol* 1999; **73**:6182-6187.
47. Vellinga J, Van der Heijdt S, Hoeben RC. The adenovirus capsid: major progress in minor proteins. *J Gen Virol* 2005b; **86**:1581-1588.
48. Scheres SH, Marabini R, Lanzavecchia S, Cantele F, Rutten T, Fuller SD et al. Classification of single-projection reconstructions for cryo-electron microscopy data of icosahedral viruses. *J Struct Biol* 2005; **151**:79-91.
49. Saban SD, Silvestry M, Nemerow GR, Stewart PL. Visualization of alpha-helices in a 6-angstrom resolution cryoelectron microscopy structure of adenovirus allows refinement of capsid protein assignments. *J Virol* 2006; **80**:12049-12059.
50. Fabry CM, Rosa-Calatrava M, Moriscot C, Ruigrok RW, Boulanger P et al. The C-terminal domains of adenovirus

- serotype 5 protein IX assemble into an antiparallel structure on the facets of the capsid. *J Virol* 2009; **83**:1135-1139.
51. Vellinga J, van den Wollenberg DJ, Van der Heijdt S, Rabelink MJ, Hoeben RC. The coiled-coil domain of the adenovirus type 5 protein IX is dispensable for capsid incorporation and thermostability. *J Virol* 2005a; **79**:3206-3210.
 52. Vellinga J, Rabelink MJ, Cramer SJ, van den Wollenberg DJ, Van der Meulen H, Leppard KN et al. Spacers increase the accessibility of peptide ligands linked to the carboxyl terminus of adenovirus minor capsid protein IX. *J Virol* 2004; **78**:3470-3479.
 53. Vellinga J, Uil TG, de Vrij J, Rabelink MJ, Lindholm L, Hoeben RC. A system for efficient generation of adenovirus protein IX-producing helper cell lines. *J Gene Med* 2006; **8**:147-154.
 54. Vellinga J, de Vrij J, Myhre S, Uil T, Martineau P, Lindholm L et al. Efficient incorporation of a functional hyperstable single-chain antibody fragment protein-IX fusion in the adenovirus capsid. *Gene Ther* 2007; **14**:664-670.
 55. Le LP, Everts M, Dmitriev IP, Davydova JG, Yamamoto M, Curiel DT. Fluorescently labeled adenovirus with pIX-EGFP for vector detection. *Mol Imaging* 2004; **3**:105-116.
 56. Meulenbroek RA, Sargent KL, Lunde J, Jasmin BJ, Parks RJ. Use of adenovirus protein IX (pIX) to display large polypeptides on the virion--generation of fluorescent virus through the incorporation of pIX-GFP. *Mol Ther* 2004; **9**:617-624.
 57. Kreppel F, Gackowski J, Schmidt E, Kochanek S. Combined genetic and chemical capsid modifications enable flexible and efficient de- and retargeting of adenovirus vectors. *Mol Ther* 2005; **12**:107-117.
 58. Corjon S, Wortmann A, Engler T, van Rooijen N, Kochanek S, Kreppel F. Targeting of adenovirus vectors to the LRP receptor family with the high-affinity ligand RAP via combined genetic and chemical modification of the pIX capsomere. *Mol Ther* 2008; **16**:1813-1824.
 59. Wang X, Yin L, Rao P, Stein R, Harsch KM, Lee Z et al. Targeted treatment of prostate cancer. *J Cell Biochem* 2007; **102**:571-579.
 60. Tasch J, Gong M, Sadelain M, Heston WD. A unique folate hydrolase, prostate-specific membrane antigen (PSMA): a target for immunotherapy? *Crit Rev Immunol* 2001; **21**:249-261.
 61. Israeli RS, Powell CT, Corr JG, Fair WR, Heston WD. Expression of the prostate-specific membrane antigen. *Cancer Res* 1994; **54**:1807-1811.
 62. Kraaij R, van Rijswijk AL, Oomen MH, Haisma HJ, Bangma CH. Prostate specific membrane antigen (PSMA) is a tissue-specific target for adenoviral transduction of prostate cancer *in vitro*. *Prostate* 2005; **62**:253-259.
 63. Morgenroth A, Cartellieri M, Schmitz M, Gunes S, Weigle B, Bachmann M et al. Targeting of tumor cells expressing the prostate stem cell antigen (PSCA) using genetically engineered T-cells. *Prostate* 2007; **67**:1121-1131.
 64. Romer J, Nielsen BS, Ploug M. The urokinase receptor as a potential target in cancer therapy. *Curr Pharm Des* 2004; **10**:2359-2376.
 65. Li Y and Cozzi PJ. Targeting uPA/uPAR in prostate cancer. *Cancer Treat Rev* 2007; **33**:521-527.
 66. Seghezzi G, Marelli R, Mandriota SJ, Nolli ML, Mazzieri R, Mignatti P. Tumor cell-conditioned medium stimulates expression of the urokinase receptor in vascular endothelial cells. *J Cell Physiol* 1996; **169**:300-308.
 67. Drapkin PT, O'Riordan CR, Yi SM, Chiorini JA, Cardella J, Zabner J et al. Targeting the urokinase plasminogen activator receptor enhances gene transfer to human airway epithelia. *J Clin Invest* 2000; **105**:589-596.
 68. Jing Y, Tong C, Zhang J, Nakamura T, Iankov I, Russell SJ et al. Tumor and vascular targeting of a novel oncolytic measles virus retargeted against the urokinase receptor. *Cancer Res* 2009; **69**:1459-1468.
 69. Kollermann J and Helpap B. Neuroendocrine differentiation and short-term neoadjuvant hormonal treatment of prostatic carcinoma with special regard to tumor regression. *Eur Urol* 2001; **40**:313-317.

70. Lu J, Jackson JK, Gleave ME, Burt HM. The preparation and characterization of anti-VEGFR2 conjugated, paclitaxel-loaded PLLA or PLGA microspheres for the systemic targeting of human prostate tumors. *Cancer Chemother Pharmacol* 2008; **61**:997-1005.
71. Costa FF, Le BK, Brodin B. Concise review: cancer/testis antigens, stem cells, and cancer. *Stem Cells* 2007; **25**:707-711.
72. Hoepfner LH, Dubovsky JA, Dunphy EJ, McNeel DG. Humoral immune responses to testis antigens in sera from patients with prostate cancer. *Cancer Immunol* 2006; **6**:1.
73. Dubovsky JA and McNeel DG. Inducible expression of a prostate cancer-testis antigen, SSX-2, following treatment with a DNA methylation inhibitor. *Prostate* 2007; **67**:1781-1790.
74. Scanlan MJ, Gure AO, Jungbluth AA, Old LJ, Chen YT. Cancer/testis antigens: an expanding family of targets for cancer immunotherapy. *Immunol Rev* 2002; **188**:22-32.
75. Willemsen R, Chames P, Schooten E, Gratama JW, Debets R. Selection of human antibody fragments directed against tumor T-cell epitopes for adoptive T-cell therapy. *Cytometry A* 2008; **73**:1093-1099.
76. Cheng WS, Dzovic H, Nilsson B, Totterman TH, Essand M. An oncolytic conditionally replicating adenovirus for hormone-dependent and hormone-independent prostate cancer. *Cancer Gene Ther* 2006; **13**:13-20.
77. Dzovic H, Cheng WS, Essand M. Two-step amplification of the human PPT sequence provides specific gene expression in an immunocompetent murine prostate cancer model. *Cancer Gene Ther* 2007; **14**:233-240.
78. Danielsson A, Dzovic H, Nilsson B, Essand M. Increased therapeutic efficacy of the prostate-specific oncolytic adenovirus Ad[*l*/PPT-E1A] by reduction of the insulator size and introduction of the full-length E3 region. *Cancer Gene Ther* 2008; **15**:203-213.
79. Ylosmaki E, Hakkarainen T, Hemminki A, Visakorpi T, Andino R, Saksela K. Generation of a conditionally replicating adenovirus based on targeted destruction of E1A mRNA by a cell type-specific MicroRNA. *J Virol* 2008; **82**:11009-11015.
80. Cawood R, Chen HH, Carroll F, Bazan-Peregrino M, van Rooijen N, Seymour LW. Use of tissue-specific microRNA to control pathology of wild-type adenovirus without attenuation of its ability to kill cancer cells. *PLoS Pathog* 2009; **5**:e1000440.
81. Yan W, Kitzes G, Dormishian F, Hawkins L, Sampson-Johannes A, Watanabe J et al. Developing novel oncolytic adenoviruses through bioselection. *J Virol* 2003; **77**:2640-2650.
82. Gros A, Martinez-Quintanilla J, Puig C, Guedan S, Mollevi DG, Alemany R et al. Bioselection of a gain of function mutation that enhances adenovirus 5 release and improves its antitumoral potency. *Cancer Res* 2008; **68**:8928-8937.
83. Subramanian T, Vijayalingam S, Chinnadurai G. Genetic identification of adenovirus type 5 genes that influence viral spread. *J Virol* 2006; **80**:2000-2012.
84. Kuhn I, Harden P, Bauzon M, Chartier C, Nye J, Thorne S et al. Directed evolution generates a novel oncolytic virus for the treatment of colon cancer. *PLoS One* 2008; **3**:e2409.
85. Uil TG, Vellinga J, de Vrij J, van den Hengel SK, Rabelink MJ, Cramer SJ et al. Directed adenovirus evolution using engineered mutator viral polymerases. *Nucl Acids Res* 2011; **39**:e30.
86. Power AT and Bell JC. Taming the Trojan horse: optimizing dynamic carrier cell/oncolytic virus systems for cancer biotherapy. *Gene Ther* 2008; **15**:772-779.
87. Ilett, E.J., Prestwich, R.J., Kottke, T., Errington, F., Thompson, J.M., Harrington, K.J et al. Dendritic cells and T cells deliver oncolytic reovirus for tumour killing despite pre-existing anti-viral immunity. *Gene Ther* 2009; **16**:689-699.
88. Power AT, Wang J, Falls TJ, Paterson JM, Parato KA, Lichty BD et al. Carrier cell-based delivery of an oncolytic virus circumvents antiviral immunity. *Mol Ther* 2007; **15**:123-130.
89. Lobo NA, Shimono Y, Qian D, Clarke MF. The biology of cancer stem cells.

- Annu Rev Cell Dev Biol* 2007; **23**:675-699.
90. Collins AT and Maitland NJ. Prostate cancer: Regeneration of interest in the prostate. *Nat Rev Urol* 2009; **6**:184-186.
 91. Carlisle RC, Briggs SS, Hale AB, Green NK, Fisher KD, Etrych T et al. Use of synthetic vectors for neutralising antibody resistant delivery of replicating adenovirus DNA. *Gene Ther* 2006; **13**:1579-1586.
 92. Wolff JA and Rozema DB. Breaking the bonds: non-viral vectors become chemically dynamic. *Mol Ther* 2008; **16**:8-15.
 93. Ogris M, Kotha AK, Tietze N, Wagner E, Palumbo FS, Giammona G et al. Novel biocompatible cationic copolymers based on polyaspartylhydrazide being potent as gene vector on tumor cells. *Pharm Res* 2007; **24**:2213-2222.
 94. Russ V, Elfberg H, Thoma C, Kloeckner J, Ogris M, Wagner E. Novel degradable oligoethylenimine acrylate ester-based pseudodendrimers for *in vitro* and *in vivo* gene transfer. *Gene Ther* 2008; **15**:18-29.
 95. Schwerdt A, Zintchenko A, Concia M, Roesen N, Fisher KD, Lindner LH et al. Hyperthermia induced targeting of thermosensitive gene carriers to tumors. *Hum Gene Ther* 2008; **19**:1283-1292.
 96. Meyer M and Wagner E. Recent developments in the application of plasmid DNA-based vectors and small interfering RNA therapeutics for cancer. *Hum Gene Ther* 2006; **17**:1062-1076.
 97. Philipp A, Meyer M, Wagner E. Extracellular targeting of synthetic therapeutic nucleic acid formulations. *Curr Gene Ther* 2008; **8**:324-334.
 98. Schaffert D and Wagner E. Gene therapy progress and prospects: synthetic polymer-based systems. *Gene Ther* 2008; **15**:1131-1138.
 99. Knecht W, Munch-Petersen B, Piskur J. Identification of residues involved in the specificity and regulation of the highly efficient multisubstrate deoxyribonucleoside kinase from *Drosophila melanogaster*. *J Mol Biol* 2000; **301**:827-837.
 100. Knecht W, Rozpedowska E, Le BC, Willer M, Gojkovic Z, Sandrini MP et al. *Drosophila* deoxyribonucleoside kinase mutants with enhanced ability to phosphorylate purine analogs. *Gene Ther* 2007; **14**:1278-1286.
 101. Schenk E, Essand M, Bangma CH, and members of the GIANT FP6 Consortium. Clinical adenoviral gene therapy for prostate cancer. *Hum Gene Ther* 2009; **21**:807-813.
 102. Maitland NJ, Chambers K, Georgopoulos L, Simpson-Holley M, Leadley R, Evans H, et al. Gene transfer vectors targeted to human prostate cancer: Do we need better preclinical testing systems? *Hum Gene Ther* 2009; **21**:815-827.



CHAPTER 3

EFFICIENT INCORPORATION OF A FUNCTIONAL HYPER-STABLE SINGLE-CHAIN ANTIBODY FRAGMENT PROTEIN-IX FUSION IN THE ADENOVIRUS CAPSID

J Vellinga¹, J de Vrij¹, S Myhre², TG Uil¹, P Martineau³,
L Lindholm² and RC Hoeben¹

¹Department of Molecular Cell Biology, Leiden University Medical Center,
Leiden, The Netherlands; ²Got-A-Gene AB, Kullavik, Sweden and ³CNRS UMR
5160, Faculté de Pharmacie, BP Montpellier, Cedex, France

Gene Therapy 2007; 14:664-670

ABSTRACT

Recombinant adenoviruses are frequently used as gene transfer vehicles for therapeutic gene delivery. Strategies to amend their tropism include the incorporation of polypeptides with high affinity for cellular receptors. Single-chain antibodies have a great potential to achieve such cell type specificity. In this study, we evaluated the efficiency of incorporation of a single-chain antibody fused with the adenovirus minor capsid protein IX in the capsid of adenovirus type 5 vectors. To this end, the codons for the single-chain antibody fragment (scFv) 13R4 were fused with those encoding of pIX via a 75-Angstrom spacer sequence. The 13R4 is a hyper-stable single-chain antibody directed against β -galactosidase, which was selected for its capacity to fold correctly in a reducing environment such as the cytoplasm. A lentiviral vector was used to stably express the pIX.flag.75.13R4.MYC.HIS fusion gene in 911 helper cells. Upon propagation of pIX-gene deleted HAdV-5 vectors on these cells, the pIX-fusion protein was efficiently incorporated in the capsid. Here, the 13R4 scFv was functional as was evident from its capacity to bind its ligand β -galactosidase. These data demonstrate that the minor capsid protein IX can be used as an anchor for incorporation of single-chain antibodies in the capsids of adenovirus vectors.

INTRODUCTION

Human Adenovirus (HAdV)-derived vectors are among the most frequently used gene delivery vehicles for human gene therapy and vaccination.¹ Much effort has been devoted to improve the cell-type specificity of gene delivery. Whereas the use of bispecific antibodies has been employed with considerable success, retargeting of adenovirus vectors by genetic incorporation of cell-specific ligands and single-chain antibodies proved more difficult. Many attractive ligands for insertion into the virus capsid elements for retargeting purposes are molecules that are normally excreted from the cells, such as epidermal growth factor (EGF), antibodies, and their derivatives, for example, single-chain antibody fragments (scFv).^{2,3} An important hurdle is that many of such polypeptide ligands are normally routed via the protein secretory pathway, whereas the adenovirus particles assemble in the nucleus. Hence, the ligands fused with capsid proteins lack the post-translational modifications that may be essential for their function.^{2,4} The reducing environment in the cytoplasm, which prevents the formation of disulphide bridges, and the absence of accessory factors to help these proteins to fold correctly, avert their maturation to functional proteins.⁵ Indeed, studies in which scFv were fused with capsid proteins were not very successful.^{2,6,7} However, some antibodies can be produced in a soluble form in the cytoplasm and retain their activity. These are called hyper-stable single-chain antibodies.⁸⁻¹² Recently, such hyper-stable scFv have been incorporated in HAdV particles on de-knobbed, fibritin-foldon trimerized fibers.⁴ Although the exact location of pIX in the adenovirus capsid is under revision,¹³⁻¹⁶ we and others have shown that this minor protein is an efficient platform for retargeting and imaging moieties.¹⁷⁻²¹ Here, we demonstrate efficient and functional incorporation of the hyper-stable scFv 13R4 that was fused with the minor capsid protein IX via a 75-Angstrom spacer. The scFv 13R4 originates from a naïve human phage display library²² and was isolated after random mutagenesis by error-prone polymerase chain reaction, and selection for increased cytoplasmic solubility.⁹ We show that 13R4 fused with pIX via the 75-Angstrom spacer is accessible on the surface of purified viruses. Moreover, the 13R4 is functional in the capsid as evidenced from its capacity to bind *E. coli* β -galactosidase.

3

RESULTS

For incorporation of the 13R4 scFv in the adenovirus capsid a fusion gene was constructed in which the coding region of pIX was fused via the flag epitope with the codons for a 75-Angstrom spacer, and with the codons for the 13R4 scFv (**Fig. 1a**). The resulting fusion gene coding for pIX.flag.75.13R4.MYC.HIS was inserted into the lentiviral expression vector pLV-CMV-IRES-NPTII.²³ A schematic outline of the vector is provided in **Fig. 1b**. To test the pIX.flag.75.13R4.MYC.HIS production after lentivirus transduction, 911 cells were exposed to LV-CMV-pIX.flag.75.13R4.MYC.HIS-IRES-NPTII at 40 ng p24 per 10⁵ cells (911-pIX.flag.75.13R4.MYC.HIS). Forty-eight hours post-transduction, the 911-pIX.flag.75.13R4.MYC.HIS cells were fed fresh medium with 200 μ g ml⁻¹ G418. No clonal cells were isolated, as the lentiviral transduction leads to a polyclonal cell line that produce homogenous levels pIX, sufficient to restore fully the heat-stable phenotype of the HAdV particle.²³ Immunohistochemistry analysis showed

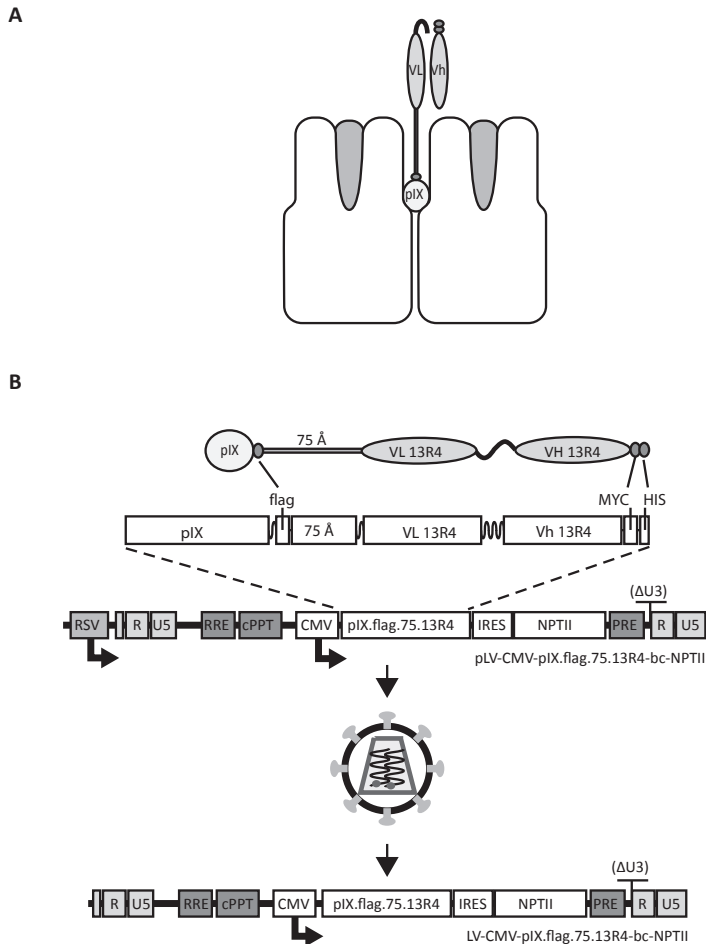


Figure 1. (a) Schematic representation of the pIX.flag.75.13R4.MYC.HIS fusion protein exposing the 13R4 scFv above the hexon capsomers. (b) Schematic representation of the lentiviral system. The lentiviral vectors used in this study are so-called SIN vectors,³⁵ and contain the Rev-responsive element sequence,³⁶ the central poly-purine tract (cPPT)^{33,37,38} and the human hepatitis B virus-derived post-transcriptional regulatory element. The encephalomyocarditis virus internal ribosomal entry site (IRES) was obtained from pTM3,³⁹ the NPTII coding region was isolated from pEGFPn2 (Clontech, Leusden, The Netherlands).

homogeneous amounts of the fusion proteins in the transduced cells (**Fig. 2a**). The pIX.flag.75.13R4.MYC.HIS amounts produced by the transduced 911 cells are similar to the pIX level produced by 911 cells during infection with a wt HAdV-5 (**Fig. 2b**).²³

Next, we tested the incorporation of pIX.flag.75.13R4.MYC.HIS into the capsid of the HAdV-5 vector HAdV-5ΔpIX.CMV.GFP/LUC.²³ This vector lacks a functional pIX gene and carries the enhanced green fluorescent protein (eGFP) and the firefly luciferase (LUC) reporter genes under control of two separate cytomegalovirus (CMV)-promoters. HAdV-5ΔpIX.CMV.GFP/LUC viruses were propagated on the 911-pIX.flag.75.13R4.

MYC.HIS cell line, harvested and purified via the conventional CsCl purification method. During purification, particle-associated pIX molecules were separated from the non-associated pIX, as variants of pIX that cannot be incorporated into the capsid do not co-purify with the particles of CsCl gradients.^{19,24} To examine the amount of pIX.flag.75.13R4.MYC.HIS in the particles, 5×10^9 CsCl-gradient purified particles were analyzed by Western analysis (**Fig. 2c**). The amount of pIX.flag.75.13R4.MYC.HIS in the pIX.flag.75.13R4.MYC.HIS-loaded HAdV-5 Δ pIX.CMV.GFP/LUC particles is similar to the amounts in wt HAdV-5 particles.

To test if the 13R4.MYC.HIS fusion protein was accessible on the outside of the viral capsid, the purified pIX.flag.75.13R4.MYC.HIS-loaded HAdV-5 Δ pIX.CMV.GFP/LUC particles were subjected to immunoelectron microscopy. The presence of the 13R4.MYC.HIS fusion protein was visualized using penta-HIS antibodies and gold-conjugated prot.A (**Fig. 2d**). Wt HAdV-5 particles were used as negative control. There was no gold label found on the negative control, whereas viruses loaded with the 13R4.MYC.HIS show specific binding of the gold-conjugated prot.A.

To study if incorporation of the pIX.flag.75.13R4.MYC.HIS could restore the heat stability of the pIX-gene deleted viruses, HAdV-5 Δ pIX.CMV.GFP/LUC was propagated on 911-pIX.flag.75.13R4.MYC.HIS cells. Similarly, HAdV-5 Δ pIX.CMV.GFP/LUC and HAdV-5.CMV.GFP/LUC were propagated on 911 cells as negative and positive control, respectively. Heat-inactivation analysis demonstrated that although the particles were fully loaded, the pIX.flag.75.13R4.MYC.HIS protein could not restore heat stability of the pIX-gene deleted virus (**Fig. 2e**).

To study the functionality of the scFv in the capsid, we assayed the ligand (β -galactosidase)-binding capability of the 13R4 on the surface of the adenovirus. To this end, CsCl purified pIX.flag.75.13R4.MYC.HIS-loaded HAdV-5 Δ pIX.CMV.GFP/LUC and wt HAdV-5 were separately mixed with 100 μ g β -galactosidase. The viruses were purified using continuous CsCl density gradients to separate free β -galactosidase from the β -galactosidase bound to the 13R4 on the surface of the adenoviral particles. To examine if the 13R4 scFv was able to bind β -galactosidase, both viruses were analyzed by Western analysis (**Fig. 3a**) and immunoelectron microscopy (**Fig. 3b**). Both assays showed that β -galactosidase was bound specifically to viruses loaded with the 13R4 scFv.

For another approach to study the ligand (β -galactosidase)-binding capability of the 13R4 on the surface of the adenovirus, the pIX.flag.75.13R4.MYC.HIS-loaded HAdV-5 Δ pIX.CMV.GFP/LUC particles were trapped in DAKO IDEIA microwells and incubated with β -galactosidase. The DAKO kit was developed for demonstration of HAdV in clinical specimens. It contains microwell strips pre-coated with an anti HAdV antibody. After blocking and washing, the particles were exposed to the substrate (ONPG). Compared to wt HAdV-5, the particles that contain the pIX.flag.75.13R4.MYC.HIS molecules showed significant β -galactosidase activity (**Fig. 4**), demonstrating that the 13R4 scFv can bind β -galactosidase on the surface of the virions. From the absorbance value of 0.5, a path length of 0.6 cm, and a molar absorption of $\sim 4500 \text{ M}^{-1} \text{ cm}^{-1}$,²⁵ we can calculate that the concentration of *o*-nitrophenol formed is $1.85 \times 10^{-4} \text{ M}$, which corresponds to 37 nmoles in the sample volume. As the reaction was developed for one h, this is the equivalent of $37/60 = 0.6$ Miller units.²⁵ Since the *E.coli* β -galactosidase has a specific activity of 58,000 U / nmole of monomer, there is

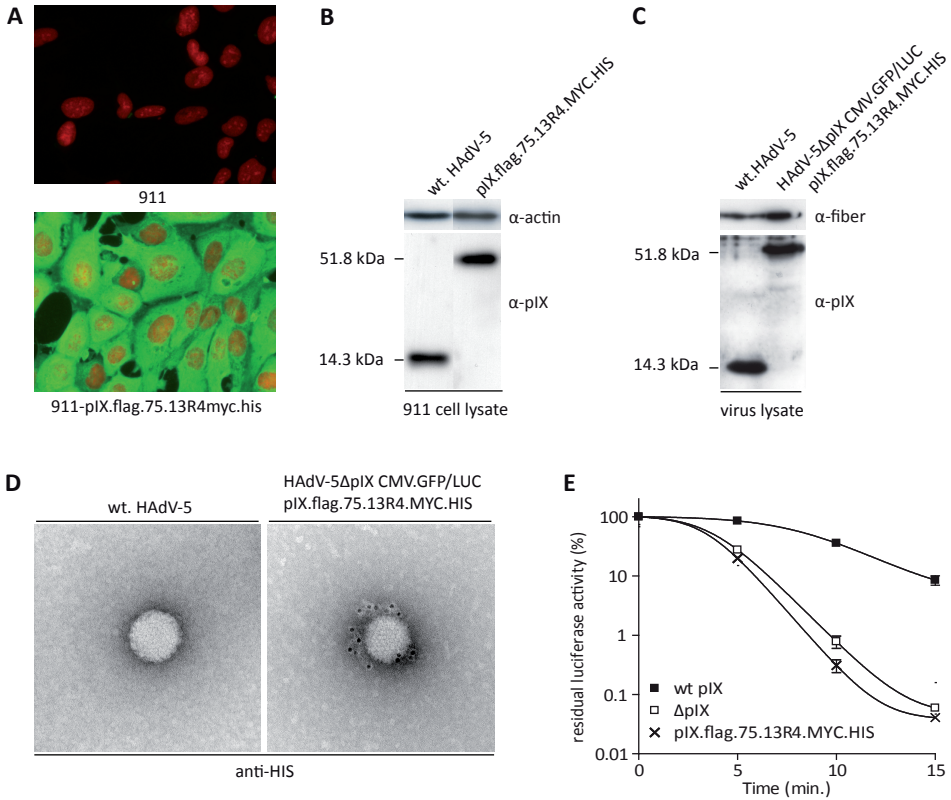


Figure 2. (a) Immunohistochemistry assay for detection of the pIX.flag.75.13R4.MYC.HIS produced by the 911-pIX.flag.75.13R4.MYC.HIS cells. The production of pIX.flag.75.13R4.MYC.HIS was visualized using mouse anti-flag and FITC-labeled goat-anti-mouse antibodies. The nuclei were stained using propidium iodide. (b) Western analysis of pIX.flag.75.13R4.MYC.HIS levels in the 911-pIX.flag.75.13R4.MYC.HIS cells. The pIX.flag.75.13R4.MYC.HIS amount in the complementing cell line 911-pIX.flag.75.13R4.MYC.HIS was compared with the pIX amounts during wt HAdV-5 infection. The Western analysis was performed using anti pIX serum.²³ (c) Western analysis of the incorporation efficiency of pIX.flag.75.13R4.MYC.HIS. To test the incorporation efficiency of pIX.flag.75.13R4.MYC.HIS produced by the 911-pIX.flag.75.13R4.MYC.HIS cells, HAdV-5ΔpIX.CMV.GFP/LUC was propagated on the cell line, purified by CsCl centrifugation, and protein lysate of the purified virus sample was made for Western analysis. The amount of the pIX fusion proteins in HAdV-5ΔpIX.CMV.GFP/LUC propagated on 911-pIX.flag.75.13R4.MYC.HIS was compared with wt HAdV-5, with anti-pIX serum and, as a virus-particle loading control, the 4D2 antibody directed against the fiber protein. (d) Immunoelectron microscopic analysis of HAdV-5ΔpIX.CMV.GFP/LUC loaded with pIX.flag.75.13R4.MYC.HIS. To test the accessibility of the HIS epitope on viruses loaded with pIX.flag.75.13R4.MYC.HIS were bound on copper grids. The HIS epitope was detected with penta-HIS antibody, followed by rabbit anti-mouse immunoglobulin and gold-labeled Prot.A. (e) Heat stability of HAdV-5ΔpIX.CMV.GFP/LUC with pIX.flag.75.13R4.MYC.HIS in their capsid. HAdV-5ΔpIX.CMV.GFP/LUC was propagated on 911-pIX.flag.75.13R4.MYC.HIS cells. Similarly, HAdV-5ΔpIX.CMV.GFP/LUC and HAdV-5.CMV.GFP/LUC were propagated on 911 cells as negative and positive control, respectively. Freeze-thaw lysates were incubated at 45°C for various times. Residual infectious virus titers were estimated by determining the capacity of the virus to induce LUC activity in U2OS cells 24 h after infection. The results are presented as percentages of residual LUC activity. Each bar represents the cumulative mean \pm s.d. of triplicate analyses.

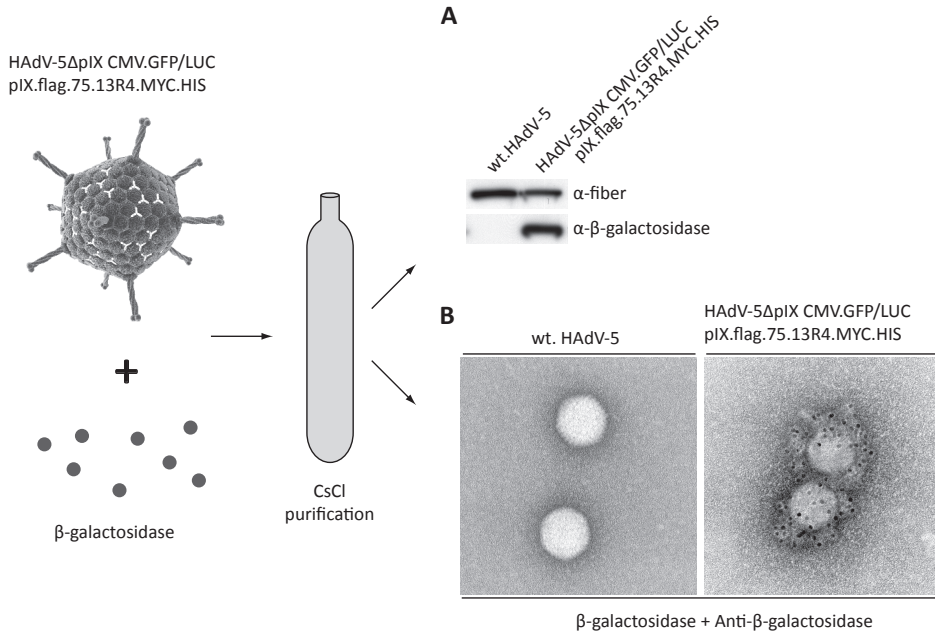


Figure 3. To test if the HAdV-5ΔpIX.CMV.GFP/LUC particles loaded with pIX.flag.75.13R4.MYC.HIS were able to bind specifically β-galactosidase on the outside of the virion, viruses were mixed with β-galactosidase and purified via the standard CsCl purification protocol. **(a)** Western analysis. The captured β-galactosidase was detected using anti-β-galactosidase. Wt HAdV-5 was used as negative control. **(b)** Immunoelectron microscopic analysis of β-galactosidase bound to HAdV-5ΔpIX.CMV.GFP/LUC loaded with pIX.flag.75.13R4.MYC.HIS. The β-galactosidase was only detected on the viruses that carried the 13R4 scFv fused to pIX.

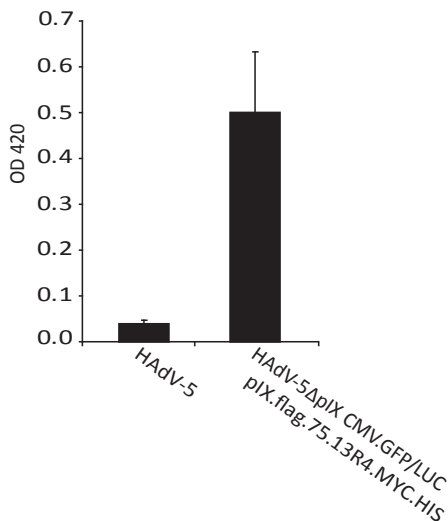


Figure 4. DAKO IDEIA β-galactosidase binding assay. To measure the binding capability of 13R4 on the surface of the virion to its native ligand β-galactosidase, the HAdV-5ΔpIX.CMV.GFP/LUC loaded with pIX.flag.75.13R4.MYC.HIS were incubated with β-galactosidase and trapped on a DAKO IDEIA strip. The bound β-galactosidase was detected by measuring OD420 (left y-axis) after adding ONPG together with the Z-buffer ($n = 3$). As negative control an identical number of wt HAdV-5 particles were used.

in the well $0.61/58,000 = 1.05 \times 10^{-5}$ nmoles of monomer, that is 2.6×10^{-6} nmoles of β -galactosidase tetramer, or 1.6×10^9 β -galactosidase tetramers. The DAKO wells used to capture the adenoviruses seem to be saturated between 1×10^6 and 5×10^6 viruses (data obtained from Dako Diagnostics; <http://www.dako.co.uk/products>). This means that about $1.6 \times 10^9 / 5 \times 10^6 = 320$ to $1.6 \times 10^9 / 10^6 = 1600$ β -galactosidase tetramers would be bound to each particle. As each particle contains 240 pIX molecules in the capsid, this number suggests that the majority of the inserted scFv is active and accessible in the capsid.

DISCUSSION

Here, we demonstrate the functional incorporation of a hyper-stable scFv (13R4), directed against β -galactosidase, fused with pIX into the adenovirus capsid. To test whether the pIX.flag.75.13R4.MYC.HIS (51.8 kDa) is able to incorporate into the viral capsid, a 911 cell line was created that produced the pIX.flag.75.13R4.MYC.HIS proteins. To this end 911 cells were exposed to the lentiviral vector LV-CMV-pIX.flag.75.13R4.MYC.HIS-IRES-NPTII. The production of pIX.flag.75.13R4.MYC.HIS proteins in the 911 cells was homogeneous as was seen earlier with pIX and pIX.flag.75.MYC proteins.²³ Propagation of HAdV-5 Δ pIX.CMV.GFP/LUC on the 911-pIX.flag.75.13R4.MYC.HIS cells did result in virus production levels that are similar to the levels obtained after propagation on the standard 911 helper cell line. Western analysis showed that pIX.flag.75.13R4.MYC.HIS was incorporated into the HAdV-5 Δ pIX.CMV.GFP/LUC as efficient as wt pIX (14.3 kDa) in wt HAdV-5 particles. Infection experiments using HAdV-5 Δ pIX.CMV.GFP/LUC with or without pIX.flag.75.13R4.MYC.HIS on 911 helper cells resulted in similar LUC levels 24 h post-infection (data not shown). Despite the complete loading, the particles that have the pIX.flag.75.13R4.MYC.HIS incorporated in their capsid are not heat stable. This may be attributed to sterical hindrance, as we have seen similar effects with large pIX-fusion proteins (data not shown).

These data demonstrate that insertions of ligands up to at least 2.5 times the molecular weight of wt pIX can be incorporated into the capsid without decreasing the incorporation efficiency and without impairing the fiber and penton-base-mediated internalization. Retaining the capacity of the arginine glycine aspartic acid (RGD) motif in the penton-base to bind α v integrins may be important for retargeted viruses, and may depend on the ligand used for retargeting.

The 13R4.MYC.HIS fusion protein was located on the surface of the adenovirus capsid as shown by immunoelectron microscopy. The number of gold particles on the adenovirus particles appeared to be less than in previous studies using pIX.flag.75.MYC.^{19,23} This might be due to the differences between the antibodies used for detection of the epitopes. Furthermore, the structure of the 13R4 scFv could have impaired the accessibility of the C-terminal HIS epitope. Alternatively, the positively charged HIS tag may have associated with the acidic-loop regions of the hexon molecules, making them less accessible to antibodies.

Both by Western analysis and by immunoelectron microscopy, we demonstrated that HAdV-5 Δ pIX.CMV.GFP/LUC particles loaded with pIX.flag.75.13R4.MYC.HIS

bind β -galactosidase, whereas wt HAdV-5 does not. The detection of β -galactosidase in both assays was carried out using the GAL-13 antibody. This antibody does not recognize denatured or reduced β -galactosidase (data from Sigma–Aldrich; <http://www.sigmaaldrich.com/sigma/datasheet/g8021dat.pdf>). Nevertheless, in our Western analysis, we were able to detect β -galactosidase using this antibody. The results of the DAKO IDEIA β -galactosidase binding assay using the HAdV-5 Δ pIX.CMV.GFP/LUC particles loaded with pIX.flag.75.13R4.MYC.HIS show binding of native β -galactosidase tetramers. The capacity to bind β -galactosidase was specific for the particles harboring the pIX.flag.75.13R4.MYC.HIS molecules. We estimated that approximately 320-1600 β -galactosidase tetramers are bound per virus particle. As the particle contains 240 pIX molecules in the capsid, this number suggests that the majority of the inserted scFv is active and accessible in the capsid. This is the first time that it has been shown that pIX can be used as anchor to incorporate large targeting ligands such as the model scFv 13R4 into the HAdV-5 capsid.

Unfortunately, the β -galactosidase cannot be used as receptor on cell surfaces. This makes it difficult to show formally that the scFv can mediate adenovirus retargeting. Future studies using for retargeting biological relevant scFv, such as the scFv- α HER2,²⁶ will show the applicability of these retargeting moieties. Alternatively, 13R4 can be used as scaffold for loop grafting.²⁷

Hyper-stable scFv can be produced without the need of stabilizing disulfide bounds. The development of techniques that facilitate the creation of large libraries of hyper-stable scFv will be of great importance for use in therapeutic agents such as gene transfer vectors described in this study. Traditional techniques involve isolation of V_H and V_L domains to construct scFv from an original hybridoma or *in vitro* display systems to screen and select for specific scFv that consequently should be tested for their ability to fold into functional scFv in the cytoplasm. Although these techniques have been shown effective for standard scFv, they rarely yield of the hyper-stable scFv variants. Other techniques such as intracellular antigen capturing and complementarity determining regions (CDR) grafting are promising approaches to create effective scFv that can be used for retargeting of adenoviruses to specific cells or tissues.²⁸⁻³⁰

The efficient incorporation of the relatively large 13R4.MYC.HIS fusion protein is promising for future retargeting strategies. The fact that the model scFv used in this study is biological active on the surface of the adenovirus is supporting the feasibility of retargeting adenovirus vectors by inserting of scFv that are directed against specific cellular receptors. However, it should be noticed that formal proof of effective retargeting via these pIX modifications still needs to be provided. In this light, it is important to be aware that the efficiency of retargeting can depend on the capsid protein to which the scFv is added.¹⁸ Therefore, it is necessary to compare side by side the retargeting efficiency with a single scFv fused with different capsid proteins (i.e. pIX and fiber).

MATERIALS AND METHODS

Cells

The HAdV-5 E1-transformed cell line 911³¹ was maintained at 37°C in a humidified atmosphere of 5% CO₂ in Dulbecco's modified Eagle's medium (Gibco-BRL, Breda, The

Netherlands) supplemented with 8% fetal bovine serum (Gibco-BRL) and 0.3% glucose (JT Baker, Deventer, The Netherlands). The 911 cells were used to propagate and titer adenovirus vectors. Infections of the cells with HAAdVs were carried out in infection medium containing 2% horse serum.

Production of recombinant lentiviruses

The lentiviral vectors used in this study were described before.²³ The lentivirus vectors were derived from the plasmid pLV-CMV-eGFP. Plasmid pLV-CMV-pIX.flag.75.13R4.MYC.HIS-IRES-NPTII has been constructed by standard cloning procedures.²³ The gene for pIX.flag.75 was obtained from the pCDNA3.1-based construct pAd5pIX.MYC.flag.75.MYC.¹⁹ The gene encoding the scFv 13R4 was subcloned from the plasmid pPM163R4.⁹ The lentiviral vectors were produced and quantified as described previously.^{23,32} For titer estimations was assumed that 1 ng p24 equals to 2×10^3 transducing units in an infection assay.³³

Lentiviral transduction

For transduction, the lentiviral supernatant was added to fresh medium together with $8 \mu\text{g ml}^{-1}$ Polybrene (Sigma Aldrich, Zwijndrecht, The Netherlands). After overnight incubation, the medium was replaced with fresh medium. Cells transduced with lentiviral vectors containing the neomycin selection gene were cultured in medium supplemented with 200 mg l^{-1} G418 (Invitrogen, Breda, The Netherlands).

Adenovirus vectors

The HAAdV-CMV.GFP/LUC and HAAdV-5 Δ pIX.CMV.GFP/LUC were made as described previously.¹⁹ The vectors carry a GFP and a firefly LUC transgene, each under the control of the human CMV immediate-early promoter. HAAdV-5 was obtained from the virus collection of the Department of Molecular Cell Biology of the Leiden University Medical Center. The concentration of the adenovirus particles was measured by a standard OD260 protocol.³⁴ Heat-inactivation studies of adenoviruses were performed as described previously.²⁴

Western analysis

Cell lysates were made in radioimmunoprecipitation assay lysis buffer (50 mM Tris.Cl pH7.5, 150 mM NaCl, 0.1% sodium dodecyl sulfate, 0.5% DOC and 1% NP40). Protein concentrations were measured via the standard method with the bicinchoninic acid protein assay (Pierce, Perbio Science BV, Etten-Leur, The Netherlands). Virus lysates were prepared by adding 5×10^9 virus particles directly to Western sample buffer. The Western blotting and detection procedures have been previously described.^{19,23} For detection of β -galactosidase, the monoclonal anti- β -galactosidase clone GAL-13 was used (1:2000, Sigma Aldrich, Zwijndrecht, The Netherlands).

Immunohistochemistry assays

For immunohistochemistry assays, the 911-pIX.flag.75.13R4 cells were grown on glass cover slips in 6-well plates, fixed in methanol, washed with phosphate-buffered saline (PBS) containing 0.05% Tween-20, and incubated with primary antibody, anti-flag (anti-FLAG M2 Affinity Gel Freezer-Safe; Sigma Aldrich Chemie, Zwijndrecht, The

Netherlands) (1:1000 diluted in PBS, 3% bovine serum albumin (BSA)) for 60 min at room temperature. The cells were washed and incubated with secondary fluorescein isothiocyanate (FITC)-conjugated goat anti-mouse serum (1:100 diluted in PBS, 3% BSA) for 30 min at room temperature. Nuclei were visualized using propidium iodide. Subsequently, the cells were washed and mounted on object glasses using Dabco / Glycerol (Glycerol, 0.02M Tris.Cl pH8.0 and 1 $\mu\text{g ml}^{-1}$ 2,4-diamidino-2-phenylindole). Cells were visualized with a Leica DM-IRBE microscope.

β -galactosidase binding

CsCl purified viruses (1 x 10¹¹ particles per well) were incubated with 100 μg β -galactosidase (Sigma Aldrich, Zwijndrecht, The Netherlands) for 60 min on room temperature. Subsequently, the viruses were subjected to a continuous CsCl density gradient protocol during adenovirus purification. The purified viruses were further analyzed via Western analysis and immunoelectron microscopy. For the DAKO IDEIA β -galactosidase binding assay, purified viruses (5 x 10⁹ particles per well) were trapped together with β -galactosidase (Sigma Aldrich, Zwijndrecht, The Netherlands) on DAKO IDEIA microwell strips (Dako Ltd, Ely, UK). After 60 min incubation on room temperature, the microwell strips were washed eight times according to the IDEIA kit instructions. After adding 60 μl ONPG (stock was 4 mg / ml in sodium-phosphate buffer, pH7.5) (Sigma Aldrich, Zwijndrecht, The Netherlands) and 60 μl Z-buffer (100 mM NaH₂PO₄ / Na₂HPO₄ pH7.5; 10 mM KCl; 1 mM MgSO₄ and 50 mM 2-mercaptoethanol), the reaction was stopped after 60 min by adding 50 μl Na₂CO₃ (stock was 1 M Na₂CO₃). The ONPG incubations were performed at 37°C. The conversion of ONPG as a measurement for β -galactosidase activity was determined by assaying the OD420.

Immunoelectron microscopy

The presence of the modified pIX molecules in the viral capsids and the presence of β -galactosidase on the surface of the viral particles was visualized with antisera and gold-labeled protein-A as described.¹⁹ For the detection of the HIS epitope, the penta-HIS antibody was used (QIAGEN Benelux BV, Venlo, The Netherlands) (1:200 diluted in PBS-2% BSA). For detection of β -galactosidase, the same antibody was used as for Western analysis (1:200 diluted in PBS-2% BSA). Subsequently, these samples were fixed in 1.5% glutaraldehyde in cacodylate buffer and negatively stained with 1% uranyl acetate for 15 min. The viruses were examined with a Philips CM-10 transmission electron microscope at 100 kV.

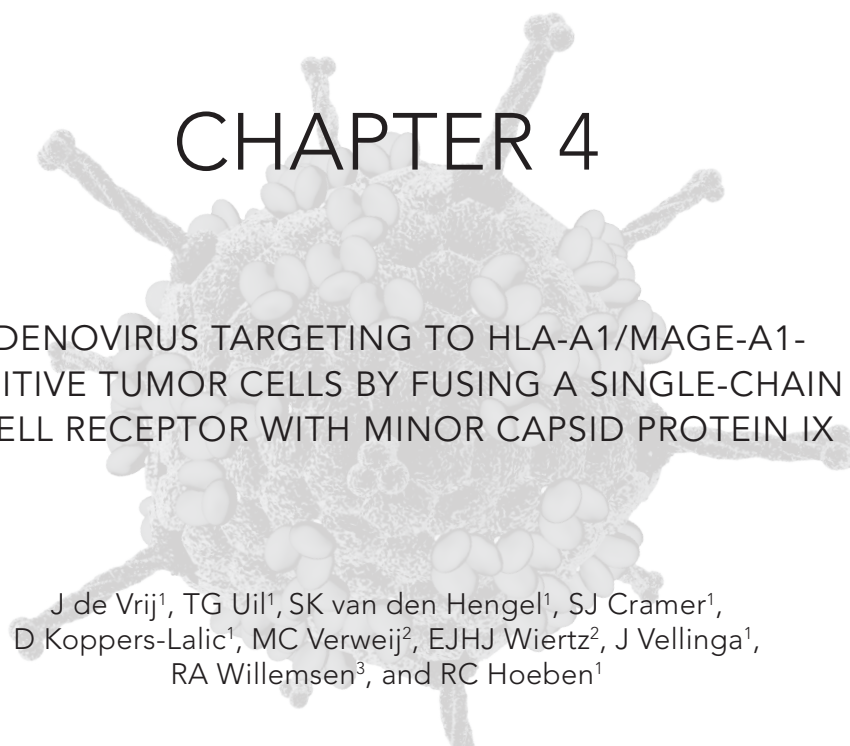
ACKNOWLEDGEMENTS

We thank Ronald WAL Limpens (Leiden University Medical Center) for help with immuno-affinity electron microscopy, and participants in the GIANT program for stimulating discussions. This work was supported by the Technology Foundation STW (program LGN66.3977), and the European Union through the 6th Framework Program GIANT (Contract no.: 512087).

REFERENCES

1. St George JA. Gene therapy progress and prospects: adenoviral vectors. *Gene Ther* 2003; **10**:1135-1141.
2. Magnusson MK, Hong SS, Henning P, Boulanger P, Lindholm L. Genetic retargeting of adenovirus vectors: functionality of targeting ligands and their influence on virus viability. *J Gene Med* 2002; **4**:356-370.
3. Biocca S, Ruberti F, Tafani M, Pierandrei-Amaldi P, Cattaneo A. Redox state of single chain Fv fragments targeted to the endoplasmic reticulum, cytosol and mitochondria. *Biotechnology (N Y)* 1995; **13**:1110-1115.
4. Hedley SJ, Auf der MA, Hohn S, Escher D, Barberis A, Glasgow JN, et al. An adenovirus vector with a chimeric fiber incorporating stabilized single chain antibody achieves targeted gene delivery. *Gene Ther* 2006; **13**:88-94.
5. Cattaneo A, Biocca S. The selection of intracellular antibodies. *Trends Biotechnol* 1999; **17**:115-121.
6. Wickham TJ. Genetic targeting of adenoviral vectors. In: Curiel DT, Douglas JT (eds). *Vector targeting for therapeutic gene delivery*. Wiley-Liss: Hoboken, 2002, pp.143-170.
7. Curiel DT. Strategies to alter the tropism of adenoviral vectors via genetic capsid modification. In: Curiel DT, Douglas JT (eds). *Vector targeting for therapeutic gene delivery*. Wiley-Liss: Hoboken, 2002, pp. 171-200.
8. Tavladoraki P, Girotti A, Donini M, Arias FJ, Mancini C, Morea V, et al. A single-chain antibody fragment is functionally expressed in the cytoplasm of both *Escherichia coli* and transgenic plants. *Eur J Biochem* 1999; **262**:617-624.
9. Martineau P, Jones P, Winter G. Expression of an antibody fragment at high levels in the bacterial cytoplasm. *J Mol Biol* 1998; **280**:117-127.
10. Ohage EC, Wirtz P, Barnikow J, Steipe B. Intrabody construction and expression. II. A synthetic catalytic Fv fragment. *J Mol Biol* 1999; **291**:1129-1134.
11. Proba K, Worn A, Honegger A, Pluckthun A. Antibody scFv fragments without disulfide bonds made by molecular evolution. *J Mol Biol* 1998; **275**:245-253.
12. Jung S, Honegger A, Pluckthun A. Selection for improved protein stability by phage display. *J Mol Biol* 1999; **294**:163-180.
13. Saban SD, Nepomuceno RR, Gritton LD, Nemerow GR, Stewart PL. CryoEM structure at 9 Å resolution of an adenovirus vector targeted to hematopoietic cells. *J Mol Biol* 2005; **349**:526-537.
14. Marsh MP, Campos SK, Baker ML, Chen CY, Chiu W, Barry MA. CryoEM of protein IX-modified adenoviruses suggests a new position for the C-terminus of protein IX. *J Virol* 2006; **80**:11881-11886.
15. Fabry CM, Rosa-Calatrava M, Conway JF, Zubieta C, Cusack S, Ruigrok RW, et al. A quasi-atomic model of human adenovirus type 5 capsid. *EMBO J* 2005; **24**:1645-1654.
16. Saban SD, Silvestry M, Nemerow GR, Stewart PL. Visualization of α -helices in a 6 Å resolution cryoEM structure of adenovirus allows refinement of capsid protein assignments. *J Virol* 2006; **80**:12049-12059.
17. Vellinga J, van der Heijdt S, Hoeben RC. The adenovirus capsid: major progress in minor proteins. *J Gen Virol* 2005; **86**:1581-1588.
18. Campos SK, Barry MA. Comparison of adenovirus fiber, protein IX, and hexon capsomeres as scaffolds for vector purification and cell targeting. *Virology* 2006; **349**:453-462.
19. Vellinga J, Rabelink MJ, Cramer SJ, van den Wollenberg DJ, Van der MH, Leppard KN, et al. Spacers increase the accessibility of peptide ligands linked to the carboxyl terminus of adenovirus minor capsid protein IX. *J Virol* 2004; **78**:3470-3479.
20. Campos SK, Parrott MB, Marsh M, Chiu W, Barry MA. Metabolically biotinylated viruses for vector targeting, virus purification, and capsid imaging. *Mol Ther* 2004; **9**:S390.
21. Le LP, Everts M, Dmitriev IP, Davydova JG, Yamamoto M, Curiel DT. Fluorescently labeled adenovirus with pIX-EGFP for vector detection. *Mol Imaging* 2004; **3**:105-116.

22. Vaughan TJ, Williams AJ, Pritchard K, Osbourn JK, Pope AR, Earnshaw JC, et al. Human antibodies with sub-nanomolar affinities isolated from a large non-immunized phage display library. *Nat Biotechnol* 1996; **14**:309-314.
23. Vellinga J, Uil TG, de Vrij J, Rabelink MJ, Lindholm L, Hoeben RC. A system for efficient generation of adenovirus protein IX-producing helper cell lines. *J Gene Med* 2006; **8**:147-154.
24. Vellinga J, van den Wollenberg DJ, van der Heijdt S, Rabelink MJ, Hoeben RC. The coiled-coil domain of the adenovirus type 5 protein IX is dispensable for capsid incorporation and thermostability. *J Virol* 2005; **79**:3206-3210.
25. Miller JH. *A Short Course in Bacterial Genetics*. Cold Spring Harbor Laboratory Press, Cold Spring Harbor, NY: 2006.
26. Lombardi A, Sperandei M, Cantale C, Giacomini P, Galeffi P. Functional expression of a single-chain antibody specific for the HER2 human oncogene in a bacterial reducing environment. *Protein Expr Purif* 2005; **44**:10-15.
27. Jung S, Pluckthun A. Improving *in vivo* folding and stability of a single-chain Fv antibody fragment by loop grafting. *Protein Eng* 1997; **10**:959-966.
28. der Maur AA, Zahnd C, Fischer F, Spinelli S, Honegger A, Cambillau C, et al. Direct *in vivo* screening of intrabody libraries constructed on a highly stable single-chain framework. *J Biol Chem* 2002; **277**:45075-45085.
29. Ewert S, Honegger A, Pluckthun A. Stability improvement of antibodies for extracellular and intracellular applications: CDR grafting to stable frameworks and structure-based framework engineering. *Methods* 2004; **34**:184-199.
30. Worn A, Pluckthun A. Stability engineering of antibody single-chain Fv fragments. *J Mol Biol* 2001; **305**:989-1010.
31. Fallaux FJ, Kranenburg O, Cramer SJ, Houweling A, van Ormondt H, Hoeben RC, et al. Characterization of 911: a new helper cell line for the titration and propagation of early region 1-deleted adenoviral vectors. *Hum Gene Ther* 1996; **7**:215-222.
32. Carlotti F, Bazuine M, Kekarainen T, Seppen J, Pognonec P, Maassen JA, et al. Lentiviral vectors efficiently transduce quiescent mature 3T3-L1 adipocytes. *Mol Ther* 2004; **9**:209-217.
33. Barry SC, Harder B, Brzezinski M, Flint LY, Seppen J, Osborne WR. Lentivirus vectors encoding both central polypurine tract and posttranscriptional regulatory element provide enhanced transduction and transgene expression. *Hum Gene Ther* 2001; **12**:1103-1108.
34. Mittereder N, March KL, Trapnell BC. Evaluation of the concentration and bioactivity of adenovirus vectors for gene therapy. *J Virol* 1996; **70**:7498-7509.
35. Zufferey R, Dull T, Mandel RJ, Bukovsky A, Quiroz D, Naldini L, et al. Self-inactivating lentivirus vector for safe and efficient *in vivo* gene delivery. *J Virol* 1998; **72**:9873-9880.
36. Mautino MR, Ramsey WJ, Reiser J, Morgan RA. Modified human immunodeficiency virus-based lentiviral vectors display decreased sensitivity to trans-dominant Rev. *Hum Gene Ther* 2000; **11**:895-908.
37. Sirven A, Pflumio F, Zennou V, Titeux M, Vainchenker W, Coulombel L, et al. The human immunodeficiency virus type-1 central DNA flap is a crucial determinant for lentiviral vector nuclear import and gene transduction of human hematopoietic stem cells. *Blood* 2000; **96**:4103-4110.
38. Follenzi A, Ailles LE, Bakovic S, Geuna M, Naldini L. Gene transfer by lentiviral vectors is limited by nuclear translocation and rescued by HIV-1 pol sequences. *Nat Genet* 2000; **25**:217-222.
39. Swick AG, Janicot M, Cheneval-Kastelic T, McLenithan JC, Lane MD. Promoter-cDNA-directed heterologous protein expression in *Xenopus laevis* oocytes. *Proc Natl Acad Sci U S A* 1992; **89**:1812-1816.



CHAPTER 4

ADENOVIRUS TARGETING TO HLA-A1/MAGE-A1- POSITIVE TUMOR CELLS BY FUSING A SINGLE-CHAIN T-CELL RECEPTOR WITH MINOR CAPSID PROTEIN IX

J de Vrij¹, TG Uil¹, SK van den Hengel¹, SJ Cramer¹,
D Koppers-Lalic¹, MC Verweij², EJHJ Wiertz², J Vellinga¹,
RA Willemsen³, and RC Hoeben¹

¹Department of Molecular Cell Biology and ²Department of Medical Microbiology, Leiden University Medical Center, Leiden, The Netherlands and ³Tumor Immunology Group, Unit of Clinical and Tumor Immunology, Department of Medical Oncology, Erasmus MC-Daniel den Hoed, Rotterdam, The Netherlands

Gene Therapy 2008;15:978-989

ABSTRACT

Adenovirus vectors have great potential in cancer gene therapy. Targeting of cancer-testis (CT) antigens, which are specifically presented at the surface of tumor cells by human leukocyte antigen (HLA) class I molecules, is an attractive option. In this study, a single-chain T-cell receptor (scTCR) directed against the CT antigen melanoma-associated antigen (MAGE)-A1 in complex with the HLA class I molecule of haplotype HLA-A1, is fused with the C-terminus of the adenovirus minor capsid protein IX. Propagation of a protein-IX (pIX)-gene-deleted human adenovirus-5 (HAdV-5) vector on cells that constitutively express the pIXscTCR fusion protein yielded viral particles with the pIXscTCR fusion protein incorporated in their capsid. Generated particles specifically transduced melanoma cell lines expressing the HLA-A1/MAGE-A1 target complex with at least ten-fold higher efficiency than control viruses. Whereas loading of HLA-A1 positive cells with MAGE-A1 peptides leads to enhanced transduction of the cells, the efficiency of virus transduction is strongly reduced if the HLA-A1 molecules are not accessible at the target cell. Taken together, these data provide proof-of-principle that pIXscTCR fusions can be used to target HAdV-5 vectors to tumor cells expressing intracellular CT antigens.

INTRODUCTION

Recombinant viral vectors hold great promise in the field of cancer gene therapy. Much effort is devoted to generating vectors that have the ability to specifically transduce tumor cells. In this respect it will be of major interest to develop vectors that are targeted to antigens that are specifically expressed at the surface of tumor cells to prevent transduction of noncancerous cells.

Intriguingly, in many cases cancer cells have been found to induce a tumor cell-specific response of the immune system. Cytotoxic T lymphocytes (CTLs) have been discovered that eradicate tumor cells via the recognition of tumor-specific antigens, while leaving healthy tissue intact. Such tumor-specific antigens might belong to the group of so-called 'cancer-testis' (CT) antigens, which are presented at the tumor cell surface by major histocompatibility complex (MHC) class I molecules that are recognized by CTLs.¹ CT antigens are expressed in a variety of cancerous tissues and are generally silent in normal tissues, except for the testis.² To date, 89 CT genes or isoforms, which are organised into 44 families, have been described. From these, 19 families are testis restricted, 11 show additional expression in one or two somatic tissues, 9 are expressed in three to six tissue types besides testis and 5 are ubiquitously somatically expressed. With the exception of the testis-restricted CT antigens, the others also show expression in the pancreas but at levels as much as 10 times lower than in the testis.² Expression of CT antigens was first shown in melanoma and all the classic CT antigens are expressed in this type of tumor, but since the 1980s, expression in various other tumors has been recognised.² The highly specific expression profiles of the CT antigens make them interesting target molecules for cancer therapies. Importantly, CT antigens belonging to the melanoma-associated antigen (MAGE) A, B and C family seem to be involved in oncogenesis, providing protection against apoptosis in tumor cells.³ The expression of other tumor antigens, such as 'overexpression' antigens p53 and HER-2/neu, or 'differentiation antigens' gp100 and Mart-1, is less restricted to tumor cells and their use for cancer-drug targeting may be associated with negative side effects.

The principle of targeting human MHC class I molecules (human leukocyte antigen, HLA class I), in complex with tumor-specific antigens, has been the subject of many studies on T-cell targeting to tumor cells.⁴ So far, HLA class I/peptide targeting of viral vectors has not been extensively explored. Promising results have been obtained by targeting measles virus particles to a specific HLA class I/peptide complex via fusion of a single-chain T-cell receptor (scTCR) to the attachment protein H of the virus.⁵ Recently, adenovirus has been also retargeted to CT antigens by replacing the knob domain of the fiber protein with a CT antigen-specific scTCR.⁶

Adenoviral vectors are among the most promising viral vectors for cancer gene therapy for several reasons. They can be produced in large quantities, they do not lead to stable genetic modification of the transduced cells and they have a good safety profile.⁷ Genetic modification of adenoviral capsid proteins might lead to the development of vectors that are specifically targeted to tumor cells, thereby improving safety and efficacy. Cell binding of subgroup C-derived human adenovirus (HAdV) vectors (including HAdV-5 and HAdV-2), which are widely used in gene therapy, involves two distinct steps. First, they bind with high affinity to the coxsackie virus

and adenovirus receptor (CAR) at the cell surface. Second, interaction of penton base Arg-Gly-Asp (RGD) motifs with cellular integrins, including $\alpha\beta3$ and $\alpha\beta5$ leads to endocytosis.⁸ Many tumor cells are relatively refractory to infection by subgroup C-derived HAdV vectors due to the paucity of CAR receptors.⁹ Development of genetically modified vectors that can infect CAR-negative cells has mainly focused on incorporation of heterologous ligands in the fiber knob, or on replacement of the entire knob domain by a heterologous ligand.⁷ The complexity of incorporating ligands into the adenovirus fiber locale has prompted the identification of other capsid proteins amendable for ligand incorporation. These approaches have the potential to incorporate an increased number of complex ligands per virion. To date, the capsid proteins hexon,^{10,11} penton base,¹² minor capsid protein IX (pIX),¹³⁻¹⁸ and protein pIIIa¹⁹ have been explored as platforms for the incorporation of heterologous peptides (reviewed by Vellinga *et al.*²⁰).

We have been exploiting the adenovirus minor capsid pIX as an anchor to genetically incorporate large proteins.^{17,18} Protein IX is a small (14.3 kDa) protein of unknown structure that acts as capsid cement, stabilizing the interactions between hexon trimers on each facet of the virion.²¹ Twelve molecules of pIX are associated with each facet of the icosahedron, with an overall stoichiometry of 240 pIX monomers per virion.²² Although the main mass of pIX is thought to be located in the cavities between the so-called group-of-nine hexon capsomers, the postulated position of pIX in the capsid is being challenged.²³⁻²⁶

Nevertheless, we have recently demonstrated efficient and functional incorporation of the hyperstable single-chain antibody fragment 13R4 that was fused with pIX via a 75-Angstrom spacer.¹⁸ The 13R4 was functional in the capsid as was evidenced by its capacity to bind *Escherichia coli* β -galactosidase.

Here we report the production of an adenoviral vector which is targeted to tumor cells presenting peptides of the CT antigen MAGE-A1 on HLA class I molecules of haplotype HLA-A1, via a scTCR (TCR^{A1M1}) fused with adenovirus minor capsid pIX. To ensure enhanced protrusion of the scTCR at the virus surface, a 75-Angstrom α -helical spacer was included between pIX and the TCR.¹⁷ We produced virus particles that were efficiently loaded with the pIX_TCR^{A1M1} fusion protein. The transduction efficiency of the HLA-A1/MAGE-A1-positive melanoma cell lines MZ2-MEL3.0 and MZ2-MEL43 was strongly increased upon incorporation of the fusion protein. These findings represent (1) the first demonstration of a pIXscTCR-mediated adenovirus targeting of a cell type that is normally refractory to HAdV-5, and (2) further proof-of-principle of targeting the highly tumor-specific CT antigen/HLA class I complexes at the surface of human tumor cell lines.

RESULTS

Establishment and characterization of the pIX_TCR^{A1M1} producing helper cell line

To establish a helper cell line stably expressing the pIX_TCR^{A1M1} fusion protein, 911 cells were transduced with the recombinant lentivirus LV.pIX_TCR^{A1M1}. A schematic

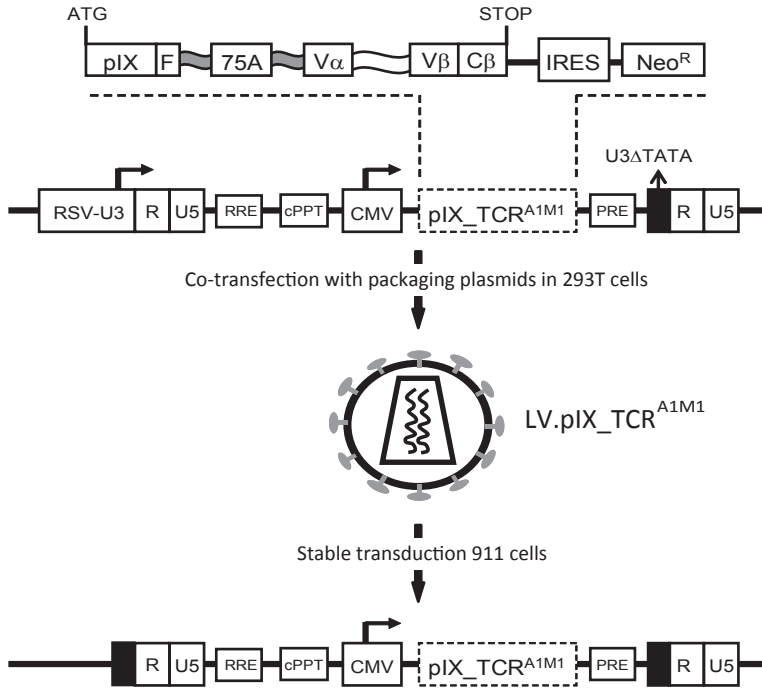


Figure 1. Schematic representation of the lentivirus system, used to establish the 911 helper cell line stably expressing pIX_TCR^{A1M1}. The vector used in this study is a third-generation, self-inactivating (SIN) vector, with major part of the 3' U3 region deleted, including the TATA box.²⁷ The Rev-responsive element (RRE),²⁸ the central polypurine tract (cPPT)²⁹⁻³¹ and the human hepatitis B virus-derived posttranscriptional regulatory element (PRE) are indicated. The encephalomyocardin virus internal ribosomal entry site (IRES) was obtained from pTM3.³² The NPTII coding region (Neo^R), which mediates resistance to G418, was isolated from pEGFPn2 (Clontech, Leusden, the Netherlands).

overview of the pro-lentiviral DNA construct and the sequence eventually incorporated in the 911 genome is provided in **Fig. 1**.

After growing the cells for several weeks in selection medium (containing 200 $\mu\text{g ml}^{-1}$ G418), western analysis on cell lysate was performed. This revealed pIX_TCR^{A1M1} protein amounts that were similar to the pIX level in 911 cells infected with HAdV-5. LUC virus (**Fig. 2a**). The protein size of pIX_TCR^{A1M1} was as expected (65.8 kDa). The percentage of pIX_TCR^{A1M1}-positive cells was determined by immunohistochemistry analysis (**Fig. 2b**). This showed more than 90% of the cells to be positive for pIX_TCR^{A1M1}. The pIX fusion protein appeared to be located mainly in the cytoplasm. Surprisingly, visualizing pIX_TCR^{A1M1} protein in the cells by using a conformation-dependent antibody recognizing the variable domain of the scTCR (V α 12.1) was dependent on adenovirus infection of the cells (**Fig. 2c**). At 24 h post infection, a V α 12.1-mediated signal could be observed. Cells were infected with the viral vector HAdV-5.CMVLUC Δ E1 Δ E3 Δ pIX (see next paragraph). Detection of pIX_scTCR^{A1M1} by V α 12.1 antibody was absent at earlier time points of infection and in pIX_TCR^{A1M1}-

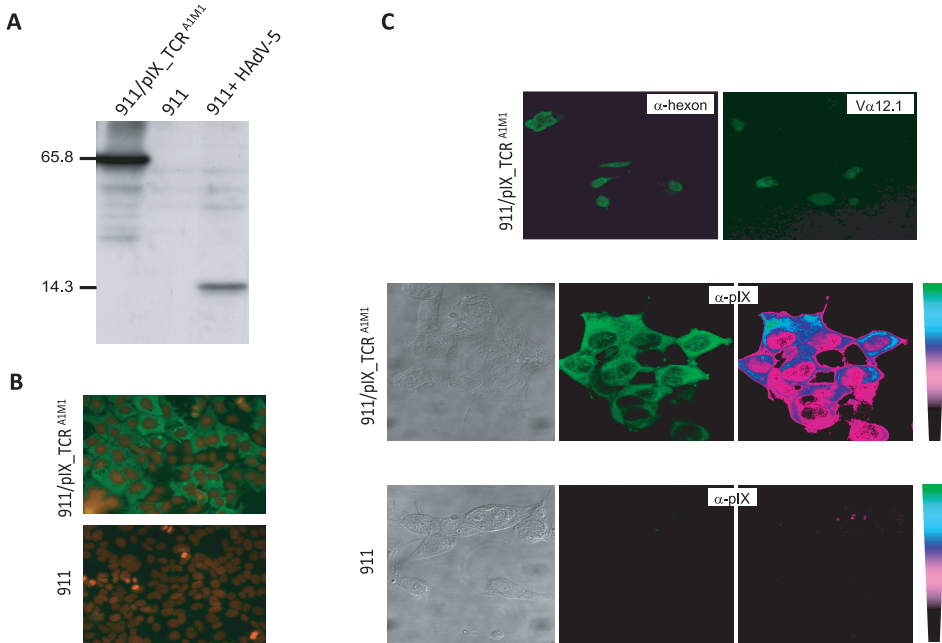


Figure 2. Characterization of the 911/pIX_TCR^{A1M1} helper cell line. (a) Western analysis on lysates of the 911/pIX_TCR^{A1M1} cells. Production of pIX_TCR^{A1M1} was compared to the production of wild-type (wt) pIX in 911 cells infected with HAΔV-5. Used antibodies were anti-pIX and horseradish peroxidase (HRP)-conjugated secondary antibody. The predicted size of 14.3 kDa for wt pIX and 65.8 kDa for pIX_scTCR^{A1M1} was confirmed by the SDS-polyacrylamide gel electrophoresis (PAGE), as indicated in the figure. (b) Immunohistochemistry assay on 911/pIX_TCR^{A1M1} cells. The pIX_TCR^{A1M1} was visualized by using anti-pIX antibody. The nuclei were stained with propidium iodide. (c) Immunohistochemistry assays on 911/pIX_TCR^{A1M1} cells, infected with HAΔV-5ΔpIX. Fixation was performed at 24 h postinfection. The upper panel shows wide-field microscopy images of anti-hexon and Vα12.1-stained cells. The lower panel shows confocal microscopy images of anti-pIX-stained 911/pIX_TCR^{A1M1}. Infected 911 cells were included as negative control. To illustrate the presence of fluorescence signal in the nuclei more clearly, pseudocolor images of the cells are shown. Fluorescent intensities range from purple (low) to green (high).

negative 911 cells (result not shown). Confocal laser scanning microscopy was used to analyze the subcellular localization of the pIX_scTCR^{A1M1} protein after virus infection (Fig. 2c). Although the majority of the pIX_TCR^{A1M1} protein was observed in the cytoplasm, significant amounts were present in the nuclei of infected cells. In >90% of the infected cells the pIX_TCR^{A1M1} fusion protein was readily detectable in the nucleus.

Efficient incorporation of pIX_TCR^{A1M1} in the virus capsid

Next, we tested the incorporation of pIX_TCR^{A1M1} into the capsid of the vector HAΔV-5.CMV_{LUC}ΔE1ΔE3ΔpIX. This vector lacks a functional pIX gene and carries the firefly luciferase reporter gene under control of the cytomegalovirus (CMV) promoter. After transduction of the 911/pIX_TCR^{A1M1} cells with the ΔpIX virus, the offspring virus particles were harvested and purified via the conventional cesium chloride

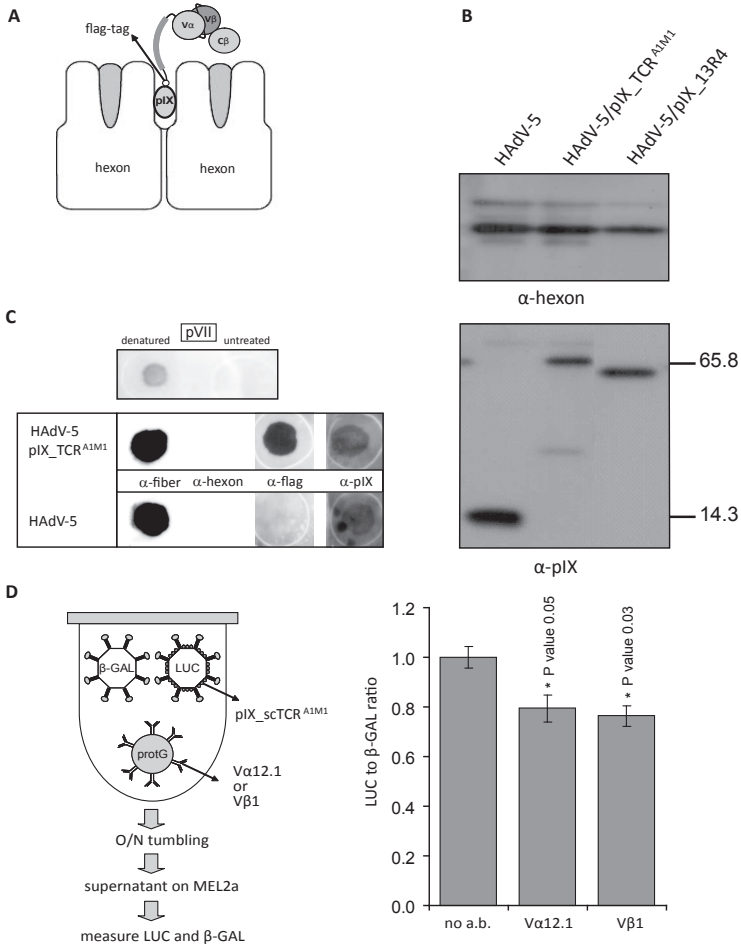


Figure 3. Analysis of pIX_TCR^{A1M1} incorporation in the virus capsid. **(a)** Schematic representation of the pIX_TCR^{A1M1} fusion protein exposing the single-chain TCR^{A1M1} above the hexon capsomers. A spacer of 75 Angstrom is included to improve presentation of the single-chain T-cell receptor (scTCR). A flag tag is present in between the C terminus of pIX and the 75-Angstrom spacer. Additional linkers flank the 75-Angstrom spacer (with amino-acid sequence ‘ser-gly-gly-gly’) to enhance the flexibility of the scTCR. **(b)** Western analysis on virus lysates of cesium chloride (CsCl)-purified viruses to analyze incorporation of pIX_TCR^{A1M1} in the particles. To compare incorporation efficiencies, virus lysates of HAdV-5 and HAdV-5/pIX_13R4 were included. The anti-hexon antibody was included as a virus particle loading control. The predicted size of 14.3 kDa for wild-type pIX and 65.8 kDa for pIX_scTCR^{A1M1} was confirmed by the SDS-PAGE, as indicated in the figure. **(c)** Spot-blot analysis to detect the presence of pIX_TCR^{A1M1} in intact virus particles. Virus was spotted onto a membrane followed by incubation with multiple antibodies. As a control to show integrity of the particles upon the spot-blot treatments, incubation with anti-pVII was included, directed against the core protein VII. Only after denaturation pVII could be detected. **(d)** Binding of pIX_TCR^{A1M1}-loaded virus particles on beads containing anti-TCR antibodies (Vα12.1 or Vβ1). After incubation of beads with the pIX_TCR^{A1M1} virus (containing the luciferase reporter as a transgene) plus a control virus (containing the *Escherichia coli* β-galactosidase gene as a transgene), the supernatant was applied to MEL2A cells. The ratio of luciferase to β-galactosidase expression in the cells was subsequently measured, and was normalized to the ratio obtained on mock beads (beads without antibody).

(CsCl) purification method. This resulted in the virus HAdV-5/pIX_TCR^{A1M1}. During purification, particle-associated pIX molecules were separated from the nonassociated pIX molecules, as nonassociated variants do not co-purify with the virus particles in the CsCl gradient.^{17,33} A schematic representation of the pIX_TCR^{A1M1} fusion protein, with its exposed single-chain TCR^{A1M1} positioned above the hexon capsomers, is depicted in **Fig. 3a**.

The presence of pIX_TCR^{A1M1} in the virus particles was detected by western assay (**Fig. 3b**). The amount of pIX_TCR^{A1M1} in the HAdV-5/pIX_TCR^{A1M1} particles is slightly lower than the amounts of pIX in wild-type (wt) HAdV-5 particles. Loading was similar to the loading of pIX_13R4 in the previously produced virus HAdV-5/pIX_13R4.¹⁸ The 13R4 is a single-chain antibody fragment directed against β -galactosidase, which is approximately 14 kDa smaller than the scTCR^{A1M1}.

Incorporation of pIX_TCR^{A1M1} in the virus capsid was also shown by spot-blot analyses (**Fig. 3c**). Virus particles were spotted on a nitrocellulose membrane, followed by incubation with various antibodies. Upon spotting, the virus particles remain intact, indicated by the inability to detect the adenovirus core protein VII (pVII). Only after denaturation of the virus particles the pVII could be detected. From the appearance of the anti-flag signal it can be concluded that flag epitopes of the pIX_TCR^{A1M1} fusion protein were accessible to immunoglobulins in the context of intact virus particles. For the anti-flag and the anti-pIX detection longer exposure times were used, resulting in increased background signals.

To further investigate the accessibility of the single-chain TCR^{A1M1} at the surface of the virus particles we performed an immunoprecipitation assay, in which the ability of the pIX_TCR^{A1M1} virus to bind to anti-TCR antibody-coated beads was analyzed (**Fig. 3d**). The pIX_TCR^{A1M1} virus was mixed with a control virus and subsequently incubated with V α 12.1 or V β 1 antibody precoated beads. Both antibodies specifically recognize the variable (V) domain of the TCR^{A1M1}. After incubation, supernatant fraction, containing virus particles that were not bound to the beads, was applied to MEL2a cells, and the infection ratio of pIX_TCR^{A1M1} virus (containing the luciferase transgene) to control virus (containing the β -galactosidase transgene) was determined. As a result, significantly lower ratio for the V α 12.1- or V β 1-treated samples was observed when compared to the ratio obtained from the samples without antibody treatment. This shows the binding of intact pIX_TCR^{A1M1} virus particles to the V α 12.1 and V β 1 antibodies. Thus, it can be concluded that the V domains of the TCR^{A1M1} at the surface of the virus particles are accessible, suggesting that the scTCR may be free to interact with the HLA-A1/MAGE-A1 complex at the cell surface.

Targeting of the pIXscTCR-containing virus to HLA-A1/MAGE-A1 positive MZ2-MEL3.0 tumor cells

To test the targeting potential of the HAdV-5/pIX_TCR^{A1M1} virus to HLA-A1/MAGE-A1 expressing cells, transduction of MZ2-MEL3.0 melanoma cells (CAR^{neg}, HLA-A1^{pos}, MAGE-A1^{pos}) was analyzed and compared to control virus transduction. The absence of CAR expression is an important aspect to test the targeting potential of the pIX_TCR^{A1M1} containing virus, since the virus is not ablated for its natural CAR-binding ability, which occurs via the fiber attachment protein. In parallel to the infection of MZ2-MEL3.0, the CAR-positive melanoma cell line MEL2a (CAR^{pos}, HLA-A1^{pos},

MAGE-A1^{neg}) was infected with the viruses to analyze CAR-mediated transduction. Transduction efficiencies of the viruses were determined by measuring luciferase production 24 h after transduction. As represented in **Fig. 4**, presence of the pIX_TCR^{A1M1} fusion protein in the virus capsid results in a highly increased transduction of the target cell line MZ2-MEL3.0. Whereas CAR-mediated transduction on the MEL2a cell line was highest for the pIXscTCR-lacking virus (indicated by a twofold higher luciferase activity), the opposite pattern was obtained for the target cell line MZ2-MEL3.0, which was approximately fourfold better transduced by the pIXscTCR loaded virions. When setting the targeting ratio (MZ2-MEL3.0 / MEL2a) for HAdV-5 at one, the normalized targeting effect for HAdV-5/pIX_TCR^{A1M1} on the MZ2-MEL3.0 cell line is 9.5. The approximate 10-fold increase in transduction specificity on the target cell line did not significantly change by increasing (multiplicity of infection (MOI) = 10,000) or decreasing (MOI = 100) the MOI (results not shown).

Downmodulation of HLA-A1/MAGE-A1 availability results in decreased targeting by HAdV-5/pIX_TCR^{A1M1}

To demonstrate that HAdV-5/pIX_TCR^{A1M1} mediates transduction through binding to HLA molecules at the cell surface, MZ2-MEL3.0 cells were incubated with anti-HLA-ABC antibodies, prior to adding the virus. This resulted in a significant decrease in transduction with the pIXscTCR virus, whereas no decrease was observed for the control virus (**Fig. 5a**). This observation indicates that transduction of the MZ2-MEL3.0 cells is inhibited by the binding of immunoglobulins to HLA molecules.

As an alternative blocking strategy, HLA class I presentation at the surface of MZ2-MEL3.0 was downmodulated by the expression of the human cytomegalovirus (HCMV) US11 protein. The US11 protein causes rapid degradation of newly synthesized HLA class I heavy chains by mediating their retrograde transport or 'dislocation' from the endoplasmic reticulum (ER) into the cytosol, where they are degraded by proteasomes.³⁴ MZ2-MEL3.0 cells were transduced using retroviruses encoding US11 or a control vector and surface HLA class I levels were analyzed by flow cytometry (**Fig.**

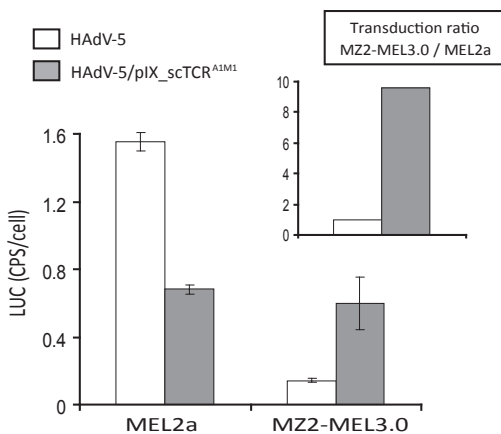


Figure 4. Targeting of HAdV-5/pIX_TCR^{A1M1} to HLA-A1/MAGE-A1-presenting MZ2-MEL3.0 cells. The target cell line MZ2-MEL3.0 (HLA-A1^{pos}/MAGE-A1^{pos}, CAR^{neg}) was transduced with HAdV-5 and HAdV-5/pIX_TCR^{A1M1}. In parallel, transduction of the MEL2a cell line was performed to determine fiber-CAR-mediated transduction of both vectors. As transduction readout, luciferase production was determined 24 h after transduction. Multiplicity of infection was 1000 virus particles per cell. The insert graph shows the ratio of MZ2-MEL3.0 to MEL2a transduction for the targeted virus HAdV-5/pIX_TCR^{A1M1}, which is normalized to the ratio for the control virus. The presence of pIX_TCR^{A1M1} results in a 10-fold improved transduction of the MZ2-MEL3.0 cell line.

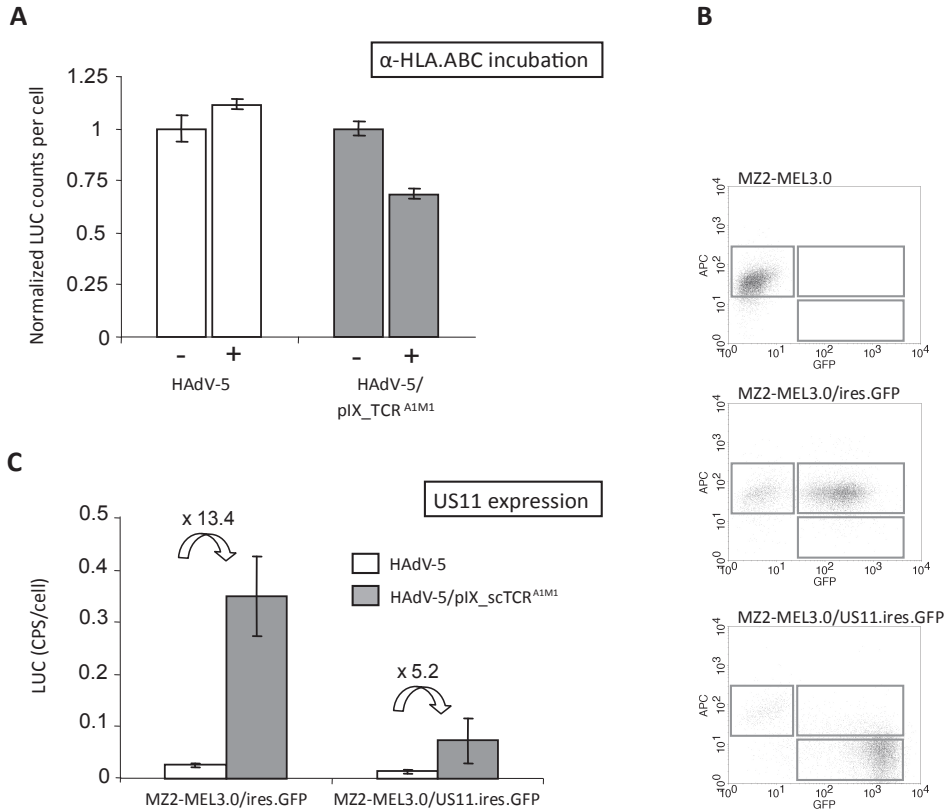


Figure 5. Downmodulation of human leukocyte antigen (HLA) availability results in decreased targeting. **(a)** Incubation of MZ2-MEL3.0 with anti-HLA-ABC antibody results in a significant decrease in HAdV-5/pIX_TCR^{A1M1} transduction. Transduction of the control virus is not downregulated after anti-HLA-ABC loading. **(b)** Flowcytometric analysis shows downregulation of HLA class I presentation at the cell surface of MZ2-MEL3.0 cells after infection with the retroviral vector pLZRS.US11.ires.GFP or the control vector pLZRS.ires.GFP. The dot plots show for both transductions the presence of green fluorescent protein (GFP)-positive cells (shift to the right). The downshift in case of the pLZRS.US11.ires.GFP transduction indicates the downregulation of HLA class I presentation (detection via B9.12.1 antibody plus allophycocyanin (APC)-conjugated secondary antibody). **(c)** Decrease in HAdV-5/pIX_TCR^{A1M1} targeting after US11-mediated downregulation of HLA class I molecules. Compared to the control cell line, the ratio HAdV-5/pIX_TCR^{A1M1} to HAdV-5 transduction is lower for the US11-expressing cell line (ratios of respectively 13.2 and 5.2). Multiplicity of infection was 1000 virus particles per cell. Luciferase production was measured 24 h after transduction.

5b). The MZ2-MEL3.0 cells were efficiently transduced with the retroviruses, since the majority of the cells was positive for the vector-mediated green fluorescent protein (GFP) expression. The downshift of the US11-expressing cells in the dotplots indicates the downregulation of HLA class I presentation. Next, luciferase production after HAdV-5/pIX_TCR^{A1M1} and HAdV-5 transduction was measured in the cell lines MZ2-MEL3.0/US11.ires.GFP and MZ2-MEL3.0/ires.GFP (**Fig. 5c**). This revealed a decrease in pIX_TCR^{A1M1} mediated targeting for the US11 expressing cells. Complete blocking

of targeting did not occur, probably as a result of incomplete downregulation of HLA class I expression.

Further analysis on different cell lines to confirm specificity of targeting to HLA-A1/MAGE-A1

During the time course of our study, the cell line MZ2-MEL43 became available. This line is CAR^{neg}, HLA-A1^{pos}, and MAGE-A1^{pos}. Since the level of HLA-A1 expression

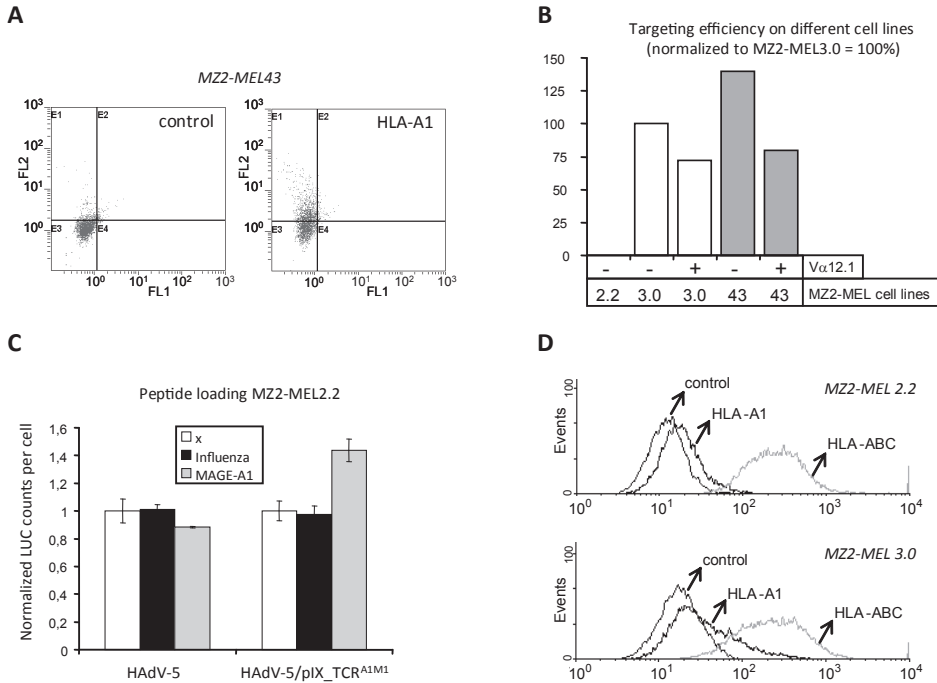


Figure 6. Comparison of the targeting on multiple cell lines to further confirm HLA-A1/MAGE-A1 specificity. **(a)** Flow cytometry analysis of human leukocyte antigen (HLA)-A1 expression at the surface of MZ2-MEL43 cells. The control plot represents incubation with secondary antibody only. **(b)** The targeting efficiency of the HAdV-5/pIX_TCR^{A1M1} virus on three different cell lines was determined, and normalized to the targeting on MZ2-MEL3.0 cells equal to 100%. Enhanced transduction of the pIXscTCR virus compared to the control virus was observed for the cell line MZ2-MEL43. This cell line was more efficiently targeted than the MZ2-MEL3.0 cells. No specific targeting was obtained on the melanoma-associated antigen (MAGE)-A1-negative cell line MZ2-MEL2.2. A decrease in targeting was obtained after incubation of the pIXscTCR virus with Vα12.1 antibody. **(c)** Improved transduction of MZ2-MEL2.2 cells after loading with MAGE-A1 peptide. MAGE-A1 peptide or an irrelevant peptide derived from influenza virus A nucleoprotein antigen was added to the wells 2 h before transduction with HAdV-5/pIX_TCR^{A1M1}. Luciferase production was measured 24 h after transduction and was normalized to transduction on nonpeptide-loaded cells. **(d)** Flow cytometry analysis to compare the presentation of HLA-A1 and HLA-ABC at the cell surface of MZ2-MEL2.2 and MZ2-MEL3.0 cells. The control graphs represent incubation with secondary antibody only. The MZ2-MEL3.0 cell line had significantly more anti-HLA-A1 events in the higher phycoerythrin (PE) range, indicating a higher number of HLA-A1 molecules per cell.

appeared to be at least equal to the HLA-A1 level of the target cell line MZ2-MEL3.0 (**Fig. 6a**), the targeting efficiency of HAdV-5/pIX_TCR^{A1M1} to MZ2-MEL43 and MZ2-MEL3.0 was analyzed in parallel (**Fig. 6b**). A third cell line, MZ2-MEL2.2, which is a derivative from MZ2-MEL3.0 but does not express MAGE-A1, was included as well. As expected, transduction with the pIXscTCR virus was enhanced in cell line MZ2-MEL43. Interestingly, the targeting efficiency was 45% higher to MZ2-MEL43 than to MZ2-MEL3.0. As expected, no targeting was obtained on the MAGE-A1-negative cell line MZ2-MEL2.2, demonstrating the absolute requirement for MAGE-A1 presentation. The enhanced transduction in the two HLA-A1/MAGE-A1-positive cell lines was blocked by incubation of the pIXscTCR virus with the antibody V α 12.1 (**Fig. 6b**), confirming that the targeting is dependent on the scTCR in the capsid.

To further analyze the specificity of targeting, MZ2-MEL2.2 cells (CAR^{neg}, HLA-A1^{pos}, MAGE-A1^{neg}) were loaded either with a control peptide (an irrelevant peptide derived from influenza virus A nucleoprotein), a MAGE-A1 peptide, or were mock treated, and were subsequently exposed to the pIXscTCR virus (**Fig. 6c**). Incubation of the cells with MAGE-A1 peptide, but not with the control peptide, resulted in a significant increase in transduction by HAdV-5/pIX_TCR^{A1M1}. This effect did not occur in HAdV-5 transduction, confirming the dependency of HAdV-5/pIX_TCR^{A1M1} transduction on the presentation of the MAGE-A1 on HLA-A1. Compared to the MZ2-MEL3.0 cell line, the targeting efficiency to MAGE-A1-loaded MZ2-MEL2.2 cells was rather low. This can be explained by the significantly lower number of HLA-A1 molecules at the cell surface (**Fig. 6d**).

DISCUSSION

We demonstrate successful targeting of HAdV-5 vectors to HLA-A1/MAGE-A1-presenting tumor cells using an scTCR incorporated in the capsid as a genetic fusion with pIX. The pIX_TCR^{A1M1}-loaded virions transduced HLA-A1/MAGE-A1-expressing cells and HLA-A1-expressing cells loaded with MAGE-A1 peptides. These findings warrant further exploration of minor capsid pIX as an anchor for the insertion of targeting moieties.

The fusion of targeting proteins to pIX has some potential advantages. The use of pIX allows the incorporation of larger numbers of targeting molecules since it is present in 240 copies whereas 36 fiber molecules are present per virion. Furthermore, incorporation of large targeting ligands in the fiber, such as scTCRs or scFv's, may lead to a reduced number of fiber molecules per virion.³⁵ Intriguingly, pIX fusion proteins with sizes of up to 120 kDa can be accommodated in the capsid, although incorporation efficiency of the modified pIX (linked to an HSV1-TK/luciferase fusion protein) was slightly decreased.³⁶ However, this may be improved by the use of α -helical spacers.¹⁷

To produce our targeting virus, with pIX_TCR^{A1M1} incorporated in the capsid, we used pIX-producing helper cell lines generated via lentiviral transduction.³⁷ By using this strategy of incorporation of pIX in a Δ pIX virus, the time-consuming process of making viruses with pIX modifications in the genome can be avoided. Efficient incorporation of modified pIX, for example, linked to single-chain antibody fragments, can be obtained.¹⁸ After transduction of 911 helper cells that produce the pIX_TCR^{A1M1} protein, production of pIX_TCR^{A1M1} in the cells was verified by immunohistochemistry.

Infection of the transduced helper cells with Δ pIX virus resulted in the production of virus particles with close to wt level of the pIX_TCR^{A1M1} protein incorporated in their capsid, demonstrating the usefulness of this approach.

Interestingly, pIX_TCR^{A1M1} was detected predominantly in the cytoplasm of the LV.pIX_TCR^{A1M1}-transduced 911 helper cells. This is in contrast to the location of the wt pIX, which is mainly nuclear.³⁸ As can be concluded from our results, the aberrant subcellular localization of pIX_TCR^{A1M1} does not hamper incorporation in the virus capsid. Since adenovirus particles are assembled in the nucleus, these results imply that a sufficient amount of pIX_TCR^{A1M1} was present in the nuclei during formation of the HAdV-5/pIX_TCR^{A1M1} virus. Indeed, we could confirm by confocal microscopy that during the adenovirus infection significant amounts of pIX_TCR^{A1M1} are localized in the nucleus.

The targeting specificity to tumor cells expressing the MAGE-A1-derived epitope in the context of HLA-A1 was demonstrated via different approaches. First, transduction of the HLA-A1/MAGE-A1-positive MZ2-MEL3.0 cells was increased up to 10-fold by the incorporation of pIX_TCR^{A1M1} in the virus capsid. The targeting efficiency in another HLA-A1/MAGE-A1-positive cell line, MZ2-MEL43, appeared to be higher. Specificity was also evident from experiments in which HLA-A1-positive/MAGE-A1-negative MZ2-MEL2.2 cells were loaded with MAGE-A1 peptides. This resulted in a significant increase in transduction efficiency. The targeting specificity was lower than achieved on MZ2-MEL3.0 cells. This may be due to distinct presentation of synthetic peptides when compared to endogenously processed and presented peptides at the cell surface. Also, MZ2-MEL2.2 cells express fewer HLA-A1 molecules at their cell surface than MZ2-MEL3.0 cells (**Fig. 6d**). Furthermore, the targeting efficiency to MZ2-MEL3.0 could be reduced by blocking HLA, either via incubation of the cells with anti-HLA-ABC antibody, or alternatively, via the expression of the HCMV US11 gene. The US11 causes degradation of newly synthesized MHC class I heavy chains by mediating their dislocation from the ER into the cytosol.³⁴ For the antibody incubation, as well as the US11-mediated downregulation, the blocking of targeting was not 100%. Apparently, the incubation of cells with anti-HLA-ABC antibody was not sufficient to block all HLA-A1 molecules. In case of the US11-mediated downmodulation, flow cytometry analysis showed that a small but detectable fraction of the cell population had not been transduced (GFP negative), and thus did not downregulate HLA class I presentation, which probably explains the incomplete block of targeting.

We report successful targeting of HAdV-5 via fusion of a specific targeting moiety to capsid pIX. It has been speculated that targeting via pIX results in entrapment of the virions in the endosomes, caused by high-affinity interaction between the pIX fusion protein and the cellular receptor.¹⁶ However, binding of T-cell receptors to their target MHC/peptide complex is known to have low affinity.³⁹ This may allow the scTCR-containing virions to escape from the endosome. Alternatively, binding of the virus particles to the HLA-A1/MAGE-A1 complex may have resulted in a distinct internalization, that is, differing from the normal HAdV-5 internalization via clathrin-coated vesicles. Cellular internalization mediated by binding to MHC molecules is exploited by Simian virus 40, which enters the cell via a unique pathway that involves caveolae, rather than clathrin-coated pits.⁴⁰ Interestingly, HLA class I has been suggested as an alternative receptor for HAdV-5.⁴¹

The fact that the scTCR used in this study is biologically active at the surface of the adenovirus supports the feasibility of targeting adenovirus vectors by fusing complex polypeptide molecules, such as scTCRs or scFv fragments, to capsid pIX. Normally, such complex polypeptides are routed via the protein secretory pathway. This aspect might hamper functional incorporation in the capsid of adenovirus particles, which are assembled in the nucleus. The reducing environment in the cell prevents the formation of disulfide bridges, which may result in improper folding of these proteins.⁴² Another obstacle for the implementation of scTCRs in adenoviral vectors might be that the relatively large scTCRs hamper correct virion formation or might interfere with crucial processes necessary for virus propagation. Initial attempts to produce adenovirus vectors with an scTCR fragment genetically fused to a knobless fiber protein were unsuccessful.⁴³ Incorrect folding and/or trimer formation of the fiber protein due to the presence of the scTCR fragment was reported to be the most likely explanation. The incorrect fiber formation might have caused the inability to rescue the virus, even though the mutated viral DNA was introduced into the target cell line. However, more recently the successful development of an scTCR-containing adenovirus has been reported.⁶ Our results, with an scTCR bound to the minor capsid pIX, emphasize the potential of scTCRs for obtaining transductional specificity in adenoviral vectors. The pIX_TCR^{A1M1} fusion protein was incorporated in the capsid with high efficiency. Although it remains to be established whether all scTCRs are functional if fused with pIX, our results clearly demonstrate the functionality of at least part of the scTCRs. The variable domains of the scTCR, which mediate binding to the HLA-A1/MAGE-A1 target complex, were accessible to antibodies in the context of intact virions, which was shown via immunoprecipitation of the virus on V α 12.1- or V β 1-coated beads, and alternatively, via downregulation of transduction as a result of V α 12.1 incubation. The presence of the 75-Angstrom α -helical spacer¹⁷ in between the scTCR and pIX domains might have been crucial to generate sufficient flexibility for proper orientation of the scTCR at the capsid surface. Detailed studies on elucidating the process of scTCR folding during virus infection would be of great interest. Our immunohistochemistry analysis on the 911/pIX_TCR^{A1M1} cell line yielded staining with the conformation-dependent antibody V α 12.1, only after adenovirus infection. It is tempting to speculate that the scTCR only adopts its proper conformation upon change of the intracellular milieu upon induction of adenovirus-induced cell death.

The pIXscTCR-containing virus used in this study was not de-targeted, as the CAR-binding elements, the heparan sulfate proteoglycans-binding elements and the plasma protein-binding elements are still present in the capsid. For the final aim of *in vivo* tumor therapy via delivery of an HAdV-5 vector, these elements should be abolished. Also, it would be interesting to test whether shortening of the fiber shaft or complete removal of the fiber improves targeting efficiency, for instance by reducing steric hindrance of the pIXscTCR molecules by the protruding fiber proteins. Currently, pIXscTCR targeting in the context of fiber mutations is under investigation.

Our approach as described here utilizes the targeting of CT antigen epitopes that are presented at the cell surface of tumor cells by HLA class I molecules. This principle differs from previously reported retargeting approaches of adenovirus-based vectors, which encompass the targeting of 'overexpression' receptors like Her2/neu⁴⁴ or the epidermal growth factor receptor.⁴⁵ The expression profile of the CT antigens

is generally much more specific compared to the expression profile of the 'more conventional' target molecules such as the overexpressed receptors. The fact that HLA class I/CT antigen complexes can elicit a highly specific response of the immune system has prompted many studies on immune cell modifications with the aim to direct the modified cells toward tumor cells.⁴ However, tumor therapies via such approaches may not be feasible since the process of isolating, modifying and expansion of patient immune cells is likely to be difficult and time consuming. Viral vector-based cancer gene therapy might be a more suitable strategy. Genetic modification of adenoviral vectors, which are the most widely used virus vectors in clinical tumor gene therapy studies, is relatively easy. Besides, adenoviruses have a good safety profile and can be produced with high titers.

Our results show that HAdV-5 vectors can be genetically modified to mediate greatly enhanced gene delivery into tumor cells by targeting HLA class I/CT antigen complexes. The successful combination of two aspects with great potential in cancer gene therapy, adenovirus as a vector and CT antigens as a target, clearly warrants further exploration. Follow-up studies are under way, and especially the fusion of other scTCRs to pIX (directed against other HLA class I/CT antigen complexes), and the evaluation of *in vivo* performance of the modified HAdV-5 vectors will be of great interest.

METHODS

DNA constructs

The lentiviral vectors used in this study were described in earlier studies.³⁷ Plasmid pLV. CMV.pIXflag75AscTCR^{A1M1}.bc.neo, abbreviated as pLV.pIX_TCR^{A1M1}, was constructed by standard cloning procedures. The pLV plasmid contained a G418 resistance gene (neo) downstream of the pIX_TCR^{A1M1} sequence, separated by an internal ribosome entry site (bc). In between the pIX and scTCR sequences, sequences are present that encode a flag tag and a 75-Angstrom spacer. Insertion of this spacer has been shown to greatly enhance presentation of pIX-fused proteins at the virus capsid.¹⁷ The gene for pIXflag75 was obtained from the pcDNA3.1-based construct pAd5pIXflag75MYC.¹⁷ The gene encoding scTCR^{A1M1} was subcloned from the retroviral vector pBullet.V α V β C β .⁴⁶ The scTCR^{A1M1} sequence of pBullet.V α V β C β was originally constructed from the V α , V β and C β sequences from an HLA-A1/MAGE-A1-specific CTL clone MZ2-82/30 of patient MZ2.⁴⁷

Cells

All cell lines were maintained at 37 °C in a humidified atmosphere of 5% CO₂ in Dulbecco's modified Eagle's medium (DMEM, Gibco-BRL, Breda, the Netherlands) supplemented with 8% fetal bovine serum (FBS, Gibco-BRL) and penicillin-streptomycin mixture. Cell lines used for the adenovirus targeting experiments were the melanoma cell lines MEL2a, MZ2-MEL2.2, MZ2-MEL3.0 and MZ2-MEL43. Expression status of the CAR and HLA-A1/MAGE-A1 has been described before for the cell lines MEL2a (CAR^{pos}/HLA-A1^{pos}/MAGE-A1^{neg}), MZ2-MEL2.2 (CAR^{neg}/HLA-A1^{pos}/MAGE-A1^{neg}) and MZ2-MEL3.0 (CAR^{neg}/HLA-A1^{pos}/MAGE-A1^{pos}).⁶ The status of the previously uncharacterized cell line MZ2-MEL43 is CAR^{neg}/HLA-A1^{pos}/MAGE-A1^{pos}, as determined by flow cytometry

analysis and shown in **Fig. 6a** in this paper. The HAdV-5 E1-transformed cell line 911 was used to propagate and titer adenovirus vectors.⁴⁸

Lentiviral and retroviral transductions

The recombinant lentivirus LV.pIX_TCR^{A1M1} was produced as described elsewhere.³⁷ The lentivirus titer was determined by p24 enzyme-linked immunosorbent assay, assuming that 1 ng p24 equals 2.5×10^3 transducing units.⁴⁹ To establish a helper cell line stably expressing pIX_TCR^{A1M1}, 911 cells were transduced with the recombinant lentivirus, resulting in the cell line 911/pIX_TCR^{A1M1}. Infection was done with five transducing units per cell. To select for stably transduced cells, the cell line 911/pIX_TCR^{A1M1} was cultured in medium supplemented with 200 mg l^{-1} G418 (Invitrogen, Breda, the Netherlands).

The retroviral vector pLZRS-US11-IRES-EGFP was made by subcloning the HCMV US11 cDNA fragment into the pLZRS-IRES-EGFP vector.⁵⁰ This construct was used, together with the wt enhanced green fluorescent protein (EGFP)-expressing retroviral vector, to produce amphotropic retrovirus by transfection of the Phoenix cell line with the calcium phosphate method (www.stanford.edu/group/nolan/retroviral_systems/retsys.html). Transfected cells were grown under puromycin selection ($2 \mu\text{g ml}^{-1}$), which was removed 24 h before collecting the virus. MZ2-MEL3.0 cells, grown on retronectin-coated dishes (Takara, Japan), were transduced with the recombinant viruses to create cells stably expressing US11 and the control construct.

Adenovirus vectors

The 911/pIX_TCR^{A1M1} helper cell line was transduced with the replication-deficient adenoviral vector HAdV-5.CMVLUC Δ E1 Δ E3 Δ pIX. Production and characteristics of this vector are described elsewhere.¹⁷ The vector carries a firefly luciferase transgene under control of the human CMV immediate-early promoter. In this vector the pIX gene had been deleted from the genome. Three days after transduction, the offspring virus was harvested and purified by CsCl banding, resulting in the virus HAdV-5.CMVLUC Δ E1 Δ E3 Δ pIX+pIX_TCR^{A1M1} (indicated in this paper as HAdV-5/pIX_TCR^{A1M1}). Adenovirus particle titers were determined by measuring optical density at 260 nm, using a standard protocol.⁵¹ The control virus used in all retargeting experiments was HAdV-5.CMVLUC Δ E1 Δ E3 (indicated as HAdV-5).

Immunohistochemistry

Immunohistochemistry was performed on the helper cell line 911/pIX_TCR^{A1M1}, with or without HAdV-5.CMVLUC Δ E1 Δ E3 Δ pIX infection. Infection was performed with 1000 virus particles per cell, 24 h before fixation. After washing with phosphate-buffered saline (PBS), the cells were fixed in acetone/methanol (1:1) for 10 min at room temperature. Staining was performed with the antibodies anti-pIX (rabbit polyclonal (1:500), kindly provided by Dr Keith Leppard, University of Warwick, UK),⁵² V α 12.1 (Pierce-Endogen Biotechnology, Rockford, IL, USA) and anti-hexon (clone BOD604, fluorescein isothiocyanate (FITC)-conjugated, Biondesign International, Saco, ME, USA). FITC-labeled antibodies (Jackson ImmunoResearch, France) were used as secondary antibody. Upon analysis of the uninfected cells, the nuclei were stained using propidium iodide. The exact detection procedure has been described previously.¹⁸

Wide-field microscopy was performed with a Leica DM-IRBE microscope. Confocal laser scanning microscopy was performed on a confocal microscope system (model TCS/SP2; Leica). Z-series images (slice spacing 0.45 μm) were acquired with a 63_ NA 1.4 plan Apo objective and were analyzed with Leica confocal software.

Immunoblotting procedures

Western analysis was performed to analyze production of pIX_TCR^{A1M1} in the helper cells and to analyze incorporation efficiency of pIX_TCR^{A1M1} in the virus capsid. Cell lysates were made in radioimmunoprecipitation assay lysis buffer (50mM Tris (pH 7.5), 150mM NaCl, 0.1% SDS, 0.5% DOC, 1% NP40). Protein concentrations were measured with the bicinchoninic acid protein assay (Pierce Biotechnology, Perbio Science BV, Etten-Leur, the Netherlands). Virus lysates were prepared by adding 5×10^9 virus particles directly to western sample buffer. The pIX variants were visualized with rabbit polyclonal anti-pIX serum (1:2000).⁵² Goat polyclonal anti-hexon (1:1000) (Abcam, Cambridge, UK) was used as a virus particle loading control. Secondary antibodies were horseradish peroxidase (HRP)-conjugated goat-anti-rabbit and rabbit-anti-mouse (Santa Cruz Biotechnology, Inc., Santa Cruz, CA, USA). The western blotting and detection procedures have been previously described.^{17, 37}

A spot-blot type analysis was used to detect viral capsid proteins in intact virus particles. Immobilon membrane (Millipore, Etten-Leur, The Netherlands) was activated with methanol, washed for 10 min with PBS and virus (3×10^9 particles) was spotted onto the membrane. Virus was spotted as intact particles (untreated) or as virus lysate (denatured through adding western sample buffer plus 5 min incubation at 98 °C). This was followed up by blocking for 1 h in Soja milk (Alpro soja, Breda, The Netherlands), and washing twice for 10 min with 0.2% Tween 20 in PBS. Thereafter, probing of capsid proteins was performed according to the same protocol as applied for the western analysis. The primary antibodies used were mouse monoclonal anti-fiber knob (1D6.14, 1:1000),⁵³ goat polyclonal anti-hexon (1:2000; Abcam), anti-flag (1:500) (anti-flag M2 Affinity Gel Freezer-Safe; Sigma-Aldrich Chemie, Zwijndrecht, the Netherlands), rabbit polyclonal anti-pIX (1:2000)⁵² and anti-pVII antibody (1:500) (kindly provided by Saw See Hong, Laboratoire de Virologie et Pathogénèse Virale, Lyon, France). Secondary antibodies used were HRP-conjugated goat-anti-rabbit and rabbit-anti-mouse (Santa Cruz Biotechnology).

Binding of virus particles to anti-TCR coated beads

The ability of the pIX_TCR^{A1M1} virus to bind to anti-TCR-coated beads was investigated through an immunoprecipitation assay. Protein G Sepharose beads (30 μl ; Pierce Biotechnology) were incubated with 1 μg of antibody (V α 12.1 or V β 1), for 2 h at 4 °C in 600 μl cold PBS. Antibody-coupled beads were added to 1 ml DMEM without serum, containing two types of virus; HAdV-5.CMVLUC Δ E1 Δ E3 Δ pIX (5×10^{10} particles), and HAdV-5.CMVLacZ Δ E1 (5×10^{10} particles). Control samples were incubated with beads only. After incubation for 12 h at 4 °C, 50 μl of the supernatant was added to 450 μl DMEM (containing 8% FBS), which was subsequently applied on MEL2a cells in a 24-well plate. After 24 h, the expression levels of intracellular luciferase and β -galactosidase were determined. To this end, the cells were washed once with PBS, and lysed in 100 μl LUC-lysis mix (25 mM Tris-phosphate (pH 7.8), 2 mM CDTA,

2 mM DTT, 10% glycerol and 1% Triton-X in PBS). After shaking for 15 min at room temperature, lysates were centrifuged (10000 g, 10 min). Luciferase production was determined with Promega Luciferase Assay, and β -galactosidase production was determined with the Tropic Galacto-Light reporter gene assay (Applied Biosystems, Bedford, MA, USA). Light intensity measurement was performed in a Victor Wallac 2 microplate reader (PerkinElmer, Inc., Waltham, MA, USA).

Virus transduction assays

Transduction efficiencies with HAdV-5/pIX_TCR^{A1M1} and HAdV-5 were analyzed by measuring luciferase production. For all virus transduction assays, transduction was performed in a 24-well plate, with 1000 viral particles per cell, in 500 μ l DMEM/8% FBS. After 24 h, luciferase production was measured as described above (25 μ l luciferase assay reagent was added to 10 μ l lysate).

Incubation of cells with anti-HLA-ABC antibody (ascites) was performed to test downmodulation of targeting. The cells were incubated for 12 h with 20 μ g ml⁻¹ anti-HLA-ABC (in medium), which was removed from the cells before adding the virus. TCR blocking analysis was performed by incubating the virus (10⁸ particles) for 12 h (4 °C) with 150 ng V α 12.1 antibody in 100 μ l PBS supplemented with 2% horse serum. After adding 400 μ l medium, the virus was added to 10⁵ cells (resulting in a titer of 1000 particles per cell).

For peptide loading of the MZ2-MEL2.2 cells, 500 ng MAGE-A1 peptide, or 500 ng of an irrelevant peptide derived from influenza virus A nucleoprotein antigen⁵⁴ was added per well 2 h prior to adding the virus.

Flow cytometry

To perform flow cytometry analysis on the different cell lines, the cells were trypsinized, resuspended in PBS (containing 0.5% bovine serum albumin and 0.02% sodium azide), and were incubated with antibodies. The cells were incubated with saturating conditions of anti-CAR antibody,⁵⁵ anti-HLA-ABC antibody (W6/32, Cedarlane, ON, Canada) or anti-HLA-A1 antibody (One Lambda, CA, USA) for 30 min on ice, followed by incubation with phycoerythrin (PE)-labeled secondary antibody (Caltac Laboratories, Burlingame, CA, USA) for 30 min on ice. The status of HLA-ABCGE expression at the cell surface of the US11-expressing MZ2-MEL3.0 cell line and the control lines was performed by using anti-HLA-ABCGE (B9.12.1, Immunotech, Marseille, France) as primary antibody and allophycocyanin (APC)-conjugated goat-anti-mouse immunoglobulin G (Jackson ImmunoResearch) as secondary antibody. Flow cytometry data were analyzed with CellQuest software (Becton Dickinson).

ACKNOWLEDGEMENTS

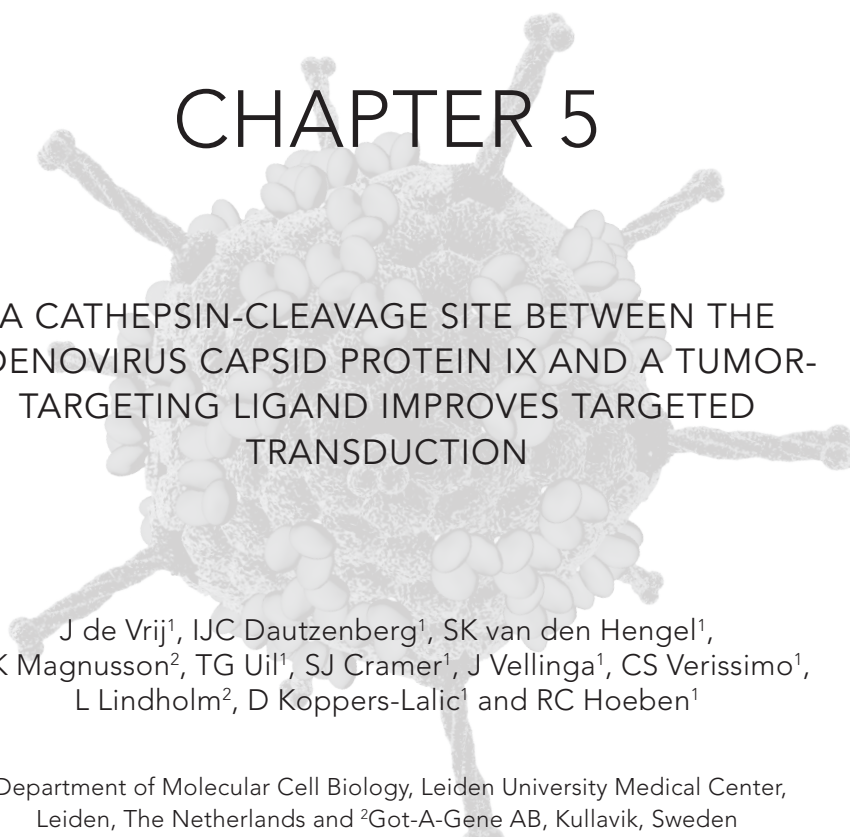
We thank Karien Wiesmeijer (Molecular Cell Biology, LUMC, Leiden) for performing the confocal microscopy, and Saw See Hong (Laboratoire de Virologie et Pathogénèse Virale, Lyon, France) for providing us with the anti-pVII antibody. This work was supported by the European Union through the 6th Framework Program GIANT (contract no. 512087).

REFERENCES

1. Van den Eynde BJ, Mandruzzato S, Gueguen M, van der Bruggen P, Marchand M, Coulie PG, et al. Tumor antigens recognized by cytolytic T lymphocytes. *Cancer Gene Ther* 1997; **4**: 308.
2. Scanlan MJ, Simpson AJ, Old LJ. The cancer/testis genes: review, standardization, and commentary. *Cancer Immun* 2004; **4**: 1.
3. Yang B, O'Herrin SM, Wu J, Reagan-Shaw S, Ma Y, Bhat KMR, et al. MAGE-A, mMage-b, and MAGE-C proteins form complexes with KAP1 and suppress p53-dependent apoptosis in MAGE-positive cell lines. *Cancer Res* 2007; **67**: 9954-9962.
4. Willemsen RA, Debets R, Chames P, Bolhuis RLH. Genetic engineering of T cell specificity for immunotherapy of cancer. *Hum Immunol* 2003; **64**: 56-68.
5. Peng KW, Holler PD, Orr BA, Kranz DM, Russell SJ. Targeting virus entry and membrane fusion through specific peptide/MHC complexes using a high-affinity T-cell receptor. *Gene Ther* 2004; **11**: 1234-1239.
6. Sebestyen Z, de Vrij J, Magnusson M, Debets R, Willemsen R. An oncolytic adenovirus redirected with a tumor-specific T-Cell receptor. *Cancer Res* 2007; **67**: 11309-11316.
7. Glasgow JN, Everts M, Curiel DT. Transductional targeting of adenovirus vectors for gene therapy. *Cancer Gene Ther* 2006; **13**: 830-844.
8. Wickham TJ, Mathias P, Cheres DA, Nemerow GR. Integrin-alpha-V-beta-3 and integrin-alpha-V-beta-5 promote adenovirus internalization but not virus attachment. *Cell* 1993; **73**: 309-319.
9. Cohen CJ, Shieh JT, Pickles RJ, Okegawa T, Hsieh JT, Bergelson JM. The coxsackievirus and adenovirus receptor is a transmembrane component of the tight junction. *Proc Natl Acad Sci U S A* 2001; **98**: 15191-15196.
10. Vigne E, Mahfouz I, Dedieu JF, Brie A, Perricaudet M, Yeh P. RGD inclusion in the hexon monomer provides adenovirus type 5-based vectors with a fiber knob-independent pathway for infection. *J Virol* 1999; **73**: 5156-5161.
11. Wu HJ, Han T, Belousova N, Krasnykh V, Kashentseva E, Dmitriev I, et al. Identification of sites in adenovirus hexon for foreign peptide incorporation. *J Virol* 2005; **79**: 3382-3390.
12. Einfeld DA, Brough DE, Roelvink PW, Kovesdi I, Wickham TJ. Construction of a pseudoreceptor that mediates transduction by adenoviruses expressing a ligand in fiber or penton base. *J Virol* 1999; **73**: 9130-9136.
13. Dmitriev IP, Kashentseva EA, Curiel DT. Engineering of adenovirus vectors containing heterologous peptide sequences in the C terminus of capsid protein IX. *J Virol* 2002; **76**: 6893-6899.
14. Le LP, Everts M, Dmitriev IP, Davydova JG, Yamamoto M, Curiel DT. Fluorescently labeled adenovirus with pIX-EGFP for vector detection. *Mol Imaging* 2004; **3**: 105-116.
15. Meulenbroek RA, Sargent KL, Lunde J, Jasmin BJ, Parks RJ. Use of adenovirus protein IX (pIX) to display large polypeptides on the virion-generation of fluorescent virus through the incorporation of pIX-GFP. *Mol Ther* 2004; **9**: 617-624.
16. Campos SK, Parrott MB, Barry MA. Avidin-based targeting and purification of a protein IX-modified, metabolically biotinylated adenoviral vector. *Mol Ther* 2004; **9**: 942-954.
17. Vellinga J, Rabelink MJWE, Cramer SJ, van den Wollenberg DJM, Van der Meulen H, Leppard KN, et al. Spacers increase the accessibility of peptide ligands linked to the carboxyl terminus of adenovirus minor capsid protein IX. *J Virol* 2004; **78**: 1-10.
18. Vellinga J, de Vrij J, Myhre S, Uil T, Martineau P, Lindholm L, et al. Efficient incorporation of a functional hyperstable single-chain antibody fragment protein-IX fusion in the adenovirus capsid. *Gene Ther* 2007; **14**: 664-670.
19. Glasgow JN, Kashentseva E, Dmitriev IP, Curiel DT. Adenovirus polypeptide IIIa as a novel locale for incorporation of heterologous peptides. *Mol Ther* 2005; **11**: S338.
20. Vellinga J, Van der Heijdt S, Hoebe RC. The adenovirus capsid: major progress

- in minor proteins. *J Gen Virol* 2005; **86**: 1581-1588.
21. Furcinitti PS, Van Oostrum J, Burnett RM. Adenovirus polypeptide-IX revealed as capsid cement by difference images from electron-microscopy and crystallography. *EMBO J* 1989; **8**: 3563-3570.
 22. Van Oostrum J, Burnett RM. Molecular composition of the Adenovirus type-2 virion. *J Virol* 1985; **56**: 439-448.
 23. Saban SD, Nepomuceno RR, Gritton LD, Nemerow GR, Stewart PL. CryoEM structure at 9 angstrom resolution of an adenovirus vector targeted to hematopoietic cells. *J Mol Biol* 2005; **349**: 526-537.
 24. Marsh MP, Campos SK, Baker ML, Chen CY, Chiu W, Barry MA. Cryoelectron microscopy of protein IX-modified adenoviruses suggests a new position for the C terminus of protein IX. *J Virol* 2006; **80**: 11881-11886.
 25. Fabry CMS, Rosa-Calatrava M, Conway JF, Zubieta C, Cusack S, Ruigrok RWH, et al. A quasi-atomic model of human adenovirus type 5 capsid. *EMBO J* 2005; **24**: 1645-1654.
 26. Saban SD, Silvestry M, Nemerow GR, Stewart PL. Visualization of alpha-helices in a 6-angstrom resolution cryoelectron microscopy structure of adenovirus allows refinement of capsid protein assignments. *J Virol* 2006; **80**: 12049-12059.
 27. Zufferey R, Dull T, Mandel RJ, Bukovsky A, Quiroz D, Naldini L, et al. Self-inactivating lentivirus vector for safe and efficient *in vivo* gene delivery. *J Virol* 1998; **72**: 9873-9880.
 28. Mautino MR, Ramsey WJ, Reiser J, Morgan RA. Modified human immunodeficiency virus-based lentiviral vectors display decreased sensitivity to trans-dominant rev. *Hum Gene Ther* 2000; **11**: 895-908.
 29. Barry SC, Harder B, Brzezinski M, Flint LY, Seppen J, Osborne WRA. Lentivirus vectors encoding both central polypurine tract and posttranscriptional regulatory element provide enhanced transduction and transgene expression. *Hum Gene Ther* 2001; **12**: 1103-1108.
 30. Sirven A, Pflumio F, Zennou V, Titeux M, Vainchenker W, Coulombel L, et al. The human immunodeficiency virus type-1 central DNA flap is a crucial determinant for lentiviral vector nuclear import and gene transduction of human hematopoietic stem cells. *Blood* 2000; **96**: 4103-4110.
 31. Follenzi A, Ailles LE, Bakovic S, Geuna M, Naldini L. Gene transfer by lentiviral vectors is limited by nuclear translocation and rescued by HIV-1 pol sequences. *Nat Genet* 2000; **25**: 217-222.
 32. Swick AG, Janicot M, Chenevaskastelic T, Mclenithan JC, Lane MD. Promoter cDNA-directed heterologous protein expression in *Xenopus-laewis* oocytes. *Proc Natl Acad Sci U S A* 1992; **89**: 1812-1816.
 33. Vellinga J, van den Wollenberg DJM, Van der Heijdt S, Rabelink MJWE, Hoeben RC. The coiled-coil domain of the adenovirus type 5 protein IX is dispensable for capsid incorporation and thermostability. *J Virol* 2005; **79**: 3206-3210.
 34. Wiertz EJHJ, Jones TR, Sun L, Bogoy M, Geuze HJ, Ploegh HL. The human cytomegalovirus US11 gene product dislocates MHC class I heavy chains from the endoplasmic reticulum to the cytosol. *Cell* 1996; **84**: 769-779.
 35. Magnusson MK, Hong SS, Henning P, Boulanger P, Lindholm L. Genetic retargeting of adenovirus vectors: functionality of targeting ligands and their influence on virus viability. *J Gene Medicine* 2002; **4**: 356-370.
 36. Matthews QL, Sibley DA, Wu HJ, Li J, Stoff-Khalili MA, Waehler R, et al. Genetic incorporation of a herpes simplex virus type 1 thymidine kinase and firefly luciferase fusion into the adenovirus protein IX for functional display on the virion. *Mol Imaging* 2006; **5**: 510-519.
 37. Vellinga J, Uil TG, de Vrij J, Rabelink MJWE, Lindholm L, Hoeben RC. A system for efficient generation of adenovirus protein IX-producing helper cell lines. *J Gene Medicine* 2006; **8**: 147-154.
 38. Rosa-Calatrava M, Grave L, Puvion-Dutilleul F, Chatton B, Keding C. Functional analysis of adenovirus protein IX identifies domains involved in capsid stability, transcriptional activity, and nuclear reorganization. *J Virol* 2001; **75**: 7131-7141.

39. Davis MM, Boniface JJ, Reich Z, Lyons D, Hampl J, Arden B, et al. Ligand recognition by alpha beta T cell receptors. *Annu Rev Immunol* 1998; **16**: 523-544.
40. Norkin LC. Simian virus 40 infection via MHC class I molecules and caveolae. *Immunol Rev* 1999; **168**: 13-22.
41. Hong SS, Karayan L, Tournier J, Curiel DT, Boulanger PA. Adenovirus type 5 fiber knob binds to MHC class I alpha 2 domain at the surface of human epithelial and B lymphoblastoid cells. *EMBO J* 1997; **16**: 2294-2306.
42. Cattaneo A, Biocca S. The selection of intracellular antibodies. *Trends Biotechnol* 1999; **17**: 115-121.
43. Magnusson MK, Hong SS, Henning P, Boulanger P, Lindholm L. Genetic retargeting of adenovirus vectors: functionality of targeting ligands and their influence on virus viability. *J Gene Medicine* 2002; **4**: 356-370.
44. Magnusson MK, Henning P, Myhre S, Wikman M, Uil TG, Friedman M, et al. Adenovirus 5 vector genetically re-targeted by an affibody molecule with specificity for tumor antigen HER2/neu. *Cancer Gene Ther* 2007; **14**: 468-479.
45. Witlox MA, van Beusechem VW, Grill J, Haisma HJ, Schaap G, Bras J, et al. Epidermal growth factor receptor targeting enhances adenoviral vector based suicide gene therapy of osteosarcoma. *J Gene Medicine* 2002; **4**: 510-516.
46. Willemsen RA, Weijtens MEM, Ronteltap C, Eshhar Z, Gratama JW, Chames P, et al. Grafting primary human T lymphocytes with cancer-specific chimeric single chain and two chain TCR. *Gene Ther* 2000; **7**: 1369-1377.
47. van der Bruggen P, Traversari C, Chomez P, Lurquin C, De Plaen E, Van den Eynde BJ, et al. A gene encoding an antigen recognized by cytolytic T lymphocytes on a human melanoma. *Science* 1991; **254**: 1643-1647.
48. Fallaux FJ, Kranenburg O, Cramer SJ, Houweling A, VanOrmondt H, Hoebe RC, et al. Characterization of 911: A new helper cell line for the titration and propagation of early region 1-deleted adenoviral vectors. *Hum Gene Ther* 1996; **7**: 215-222.
49. Carlotti F, Bazuine M, Kekarainen T, Seppen J, Pognonec P, Maassen JA, et al. Lentiviral vectors efficiently transduce quiescent mature 3T3-L1 adipocytes. *Mol Ther* 2004; **9**: 209-217.
50. Barel MT, Pizzato N, van Leeuwen D, Le Bouteiller P, Wiertz EJHJ, Lenfant F. Amino acid composition of alpha 1/alpha 2 domains and cytoplasmic tail of MHC class I molecules determine their susceptibility to human cytomegalovirus US11-mediated down-regulation. *Eur J Immunol* 2003; **33**: 1707-1716.
51. Mittereder N, March KL, Trapnell BC. Evaluation of the concentration and bioactivity of adenovirus vectors for gene therapy. *J Virol* 1996; **70**: 7498-7509.
52. Caravokyri C, Leppard KN. Constitutive episomal expression of polypeptide-IX (pIX) in a 293-based cell-line complements the deficiency of pIX mutant Adenovirus type-5. *J Virol* 1995; **69**: 6627-6633.
53. Douglas JT, Rogers BE, Rosenfeld ME, Michael SI, Feng MZ, Curiel DT. Targeted gene delivery by tropism-modified adenoviral vectors. *Nat Biotechnol* 1996; **14**: 1574-1578.
54. Willemsen RA, Debets R, Hart E, Hoogenboom HR, Bolhuis RLH, Chames P. A phage display selected Fab fragment with MHC class I-restricted specificity for MAGE-A1 allows for retargeting of primary human T lymphocytes. *Gene Ther* 2001; **8**: 1601-1608.
55. Hsu KHL, Lonbergholm K, Alstein B, Crowell RL. A monoclonal-antibody specific for the cellular receptor for the Group-B Coxsackie-viruses. *J Virol* 1988; **62**: 1647-1652.



CHAPTER 5

A CATHEPSIN-CLEAVAGE SITE BETWEEN THE ADENOVIRUS CAPSID PROTEIN IX AND A TUMOR- TARGETING LIGAND IMPROVES TARGETED TRANSDUCTION

J de Vrij¹, IJC Dautzenberg¹, SK van den Hengel¹,
MK Magnusson², TG Uil¹, SJ Cramer¹, J Vellinga¹, CS Verissimo¹,
L Lindholm², D Koppers-Lalic¹ and RC Hoeben¹

¹Department of Molecular Cell Biology, Leiden University Medical Center,
Leiden, The Netherlands and ²Got-A-Gene AB, Kullavik, Sweden

Gene Therapy 2011; doi:10.1038/gt.2011.162

ABSTRACT

Human adenoviruses have a great potential as anticancer agents. One strategy to improve their tumor-cell specificity and anti-tumor efficacy is to include tumor-specific targeting ligands in the viral capsid. This can be achieved by fusion of polypeptide-targeting ligands with the minor capsid protein IX. Previous research suggested that protein IX-mediated targeting is limited by inefficient release of protein IX-fused ligands from their cognate receptors in the endosome. This thwarts endosomal escape of the virus particles. Here we describe that the targeted transduction of tumor cells is augmented by a cathepsin-cleavage site between the protein IX anchor and the HER2/neu-binding ZH Affibody molecule as ligand. The cathepsin-cleavage site did not interfere with virus production and incorporation of the Affibody molecules in the virus capsid. Virus particles harboring the cleavable protein IX-ligand fusion in their capsid transduced the HER2/neu-positive SKOV-3 ovarian carcinoma cells with increased efficiency in monolayer cultures, three-dimensional spheroid cultures and in SKOV-3 tumors grown on the chorioallantoic membrane of embryonated chicken eggs. These data show that inclusion of a cathepsin-cleavage sequence between protein IX and a high-affinity targeting ligand enhances targeted transduction. This modification further augments the applicability of protein IX as an anchor for coupling tumor-targeting ligands.

INTRODUCTION

Many clinical studies have demonstrated the feasibility and safety of cancer therapy with human adenovirus type 5 (HAdV-5)-derived vectors. However the efficacy of HAdV-5-based therapies still needs further enhancement. Several factors have been identified that limit the anti-tumor efficacy (reviewed in de Vrij *et al.*¹). One of these is the inadequate penetration and spread of the therapeutic virus within the tumor. This might be attributable, at least in part, to the low or heterogeneous expression of the coxsackie and adenovirus receptor (CAR) on the tumor cells.^{2,3} Much effort has been invested in devising strategies to improve the transduction efficiency of tumor cells *in situ*. Such strategies include the replacement of the HAdV-5 fibers with those of non-CAR binding HAdV serotypes, the inclusion of an integrin-binding arginine-glycine-aspartic acid (RGD) motif in the fiber to bypass the CAR dependency, and fusing capsid proteins with tumor-cell-binding polypeptides (reviewed in Bachtarzi *et al.*⁴). In the latter approach, adenovirus capsid proteins, such as fiber, penton-base, hexon and protein IX, have been explored as sites for inclusion of targeting polypeptides.

It has previously been demonstrated that fusion of peptides at the carboxy terminus of protein IX allows incorporation of peptides near the surface of the adenovirus capsid.^{5,6} Incorporation of an α -helical spacer between the targeting peptide and the protein IX anchor increases the accessibility of the protein ligands on the virus surface.⁶ The capsid-exposed domains of protein IX can be modified without negatively interfering with virus stability and infectivity, which is in contrast to fiber modifications.⁷ So far, it has been demonstrated that large and complex proteins, such as single-chain antibodies, single-chain T-cell receptors, fluorescent proteins and herpes simplex virus thymidine kinase, can be fused with protein IX without losing their function.⁸⁻¹⁰

We have shown that enhanced transduction of tumor cells was obtained through fusing protein IX with an RGD domain,⁶ thereby targeting cellular integrins, or through fusing protein IX with a single-chain T-cell receptor directed against MAGE-A1 cancer-testis antigens presented by HLA-A1 molecules.⁹ However, with other ligands targeting efficiency was rather low, which led to the hypothesis that a protein IX-linked ligand requires dissociation from its cellular receptor after cellular uptake, to enable efficient targeted transduction.¹¹ In a normal infection the HAdV-5 particles are taken up in clathrin-coated endosomes after binding of the fiber-knob domains to the CAR receptor, and secondary binding of the penton-base RGD motifs to cellular integrins.¹²⁻¹⁴ Thereafter, the CAR-bound fiber proteins are released from the virus capsid, thereby disconnecting the virus from the endosomal membrane.^{15,16} This allows its release into the cytoplasm. During endosomal escape protein IX remains attached to the capsid without being subject of proteolytic degradation.¹⁶ As a result, high-affinity binding between the protein IX-fused ligand and the receptor may cause inefficient endosomal release of the virus in the endosome.

Here we describe the development and evaluation of a mechanism for dissociation of the protein IX-fused ligand from the virus capsid. To facilitate the release of the vector particles from the cellular receptor, we introduced a cathepsin-cleavage site (ccs) between the protein IX anchor and the targeting ligand. Endosomes contain

high levels of cathepsin proteases, which become active upon acidification of the endosome (reviewed in Kirschke *et al.*¹⁷). The HER2/neu-binding ZH Affibody molecule was chosen as targeting ligand.¹⁸ HER2/neu is overexpressed in many cancers, including cancers from the breast and prostate, and is therefore a potential target for cancer gene therapies.¹⁹ The ZH Affibody molecule has been successfully employed for targeting of HAdV-5 to HER2/neu upon introduction in the fiber.²⁰

Our assays revealed that introducing a ccs between protein IX and a ZH Affibody molecule does not interfere with virus production and incorporation of the ZH Affibody molecules into the virus capsid. The ccs-containing virus demonstrated significantly enhanced transduction of SKOV-3 ovarian carcinoma cells in cell culture models as well as in a chorioallantoic membrane (CAM) tumor model as compared to the non-ccs-containing control virus.

RESULTS

In vitro cleavage analyses on protein IX-ccs-ligand proteins

We first set out to explore the possibility of functionally incorporating a cathepsin-cleavable amino-acid sequence in a protein IX-ligand polypeptide fusion protein. To this end, the fusion proteins pIX.13R4.myc.his, pIX.ccsB.13R4.myc.his and pIX.ccsL.13R4.myc.his were purified and tested for their cathepsin sensitivity. The 13R4.myc.his polypeptide sequence (with 13R4 being a single-chain antibody fragment directed against β -galactosidase) has previously been successfully fused with protein IX.⁸ A schematic overview of the fusion proteins is depicted in **Fig. 1a**.

Lentivirus vectors were used to generate 911 cell lines stably expressing the protein IX fusion proteins. The histidine (his) tag fused to 13R4 enabled the subsequent isolation of the fusion proteins via binding to nickel beads. Thereafter, the proteins were incubated with either cathepsin B or cathepsin L, and the cleavage products were analyzed by sodium dodecyl sulfate-polyacrylamide gel electrophoresis and immunoblotting (**Fig. 1b**). This revealed cleavage of the cathepsin L-cleavage site (ccsL)-containing fusion protein, as indicated by the appearance of the 25 kDa-sized fragment. The cathepsin B-cleavage site (ccsB)-containing protein was not cleaved. Of note, minor adjustments to the protocol (for example, cleavage of pIX.ccsL.13R4.myc.his after elution from the beads) resulted in pIX.ccsL.13R4.myc.his degradation without the appearance of a cleavage product (data not shown). Probably, the cathepsin L preparation (derived from human liver) contains contaminating levels of other proteases, which may degrade the cleavage protein. Cleavage of pIX.ccsL.13R4.myc.his could be blocked by co-incubation with the cathepsin-specific inhibitor Z-FY(t-Bu)-DMK (**Fig. 1b**).

The pIX.13R4.myc.his and pIX.ccsL.13R4.myc.his fusion proteins were incorporated in the capsid of HAdV-5 (**Fig. 1c**). Incorporation efficiency was similar for both fusion proteins, and the presence of the ccsL site did not result in detectable levels of protein cleavage. Importantly, after incorporation of the pIX.ccsL.13R4.myc.his into the HAdV-5 capsid, the fusion protein was still sensitive to cathepsin L (**Fig. 1d**), indicating that the ccsL was functional and accessible in the adenovirus capsid.

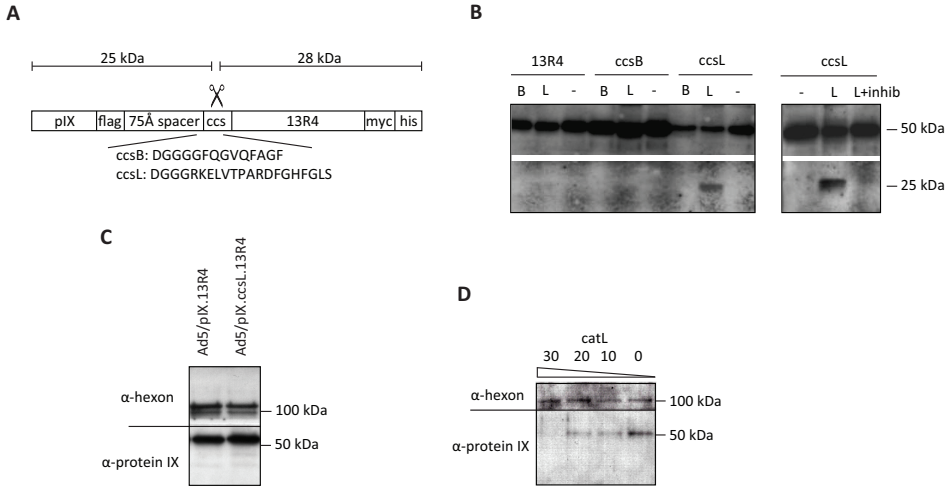


Figure 1. (a) Schematic representation of the pIX.13R4 fusion proteins. All polypeptide components are indicated (protein IX, flag tag, 75-Ångstrom spacer, ccs, 13R4 (single-chain antibody fragment directed against β -galactosidase), myc tag, his tag). (b) Western analyses after cathepsin cleavage of pIX.13R4 fusion proteins bound to nickel beads. The left panel indicates pIX.13R4 (13R4), pIX.ccsB.13R4 (ccsB) and pIX.ccsL.13R4 (ccsL) protein levels after cathepsin B (catB), cathepsin L (catL) or mock incubation. The right panel indicates pIX.ccsL.13R4 protein levels after cathepsin L cleavage in the presence or absence of the cathepsin inhibitor Z-FY(t-Bu)-DMK. Analyses were performed using anti-protein IX antibody. (c) Western analysis of pIX.13R4 and pIX.ccsL.13R4 protein levels after incorporation in the capsid of the protein IX-deleted HAdV mutant dl313 (5×10^9 pp per lane). Detection was carried out with anti-protein IX and anti-hexon antibodies. (d) Western analysis of pIX.ccsL.13R4 incorporated in the dl313 virus after incubation with different concentrations of cathepsin L (0, 10, 20 and 30 $\text{ng } \mu\text{l}^{-1}$) (5×10^9 pp per lane). Detection was carried out with anti-protein IX and anti-hexon antibodies.

5

Binding of Ad5/pIX.ccsL.ZH to the extracellular domain of HER2/neu

We and others have demonstrated that the HER2/neu-binding ZH Affibody molecules can be used for adenovirus targeting by incorporating these ligands in the HI loop of the adenovirus fiber.²⁰ Fusion of these Affibody domains with protein IX was far less efficient in retargeting adenovirus infection to HER2/neu-positive cells (our unpublished data). To study whether protein IX-Affibody-mediated targeting could be improved, we generated adenoviruses with protein IX-ccsL-ZH fusion proteins incorporated in their capsid, with the ccsL site located in between the 75-Ångstrom spacer and the tandem sequence of ZH Affibody molecules. By using standard cloning, recombination, and virus-rescuing procedures, we produced replication-competent HAdV-5 viruses with the sequences for pIX, pIX.ZH, or pIX.ccsL.ZH incorporated in the genome. In the viral genomes, major part of the E3 region was replaced by an enhanced GFP expression cassette.²¹ The incorporation of the modified protein IX genes did not affect the titers (in physical particle (pp) ml^{-1} as well as plaque forming units (PFU) ml^{-1}) of the purified virus preparations (data not shown).

To investigate the functionality of the capsid-incorporated ZH Affibody molecules, a slot-blot-based HER2-ECD binding assay was performed (Fig. 2). Membrane-

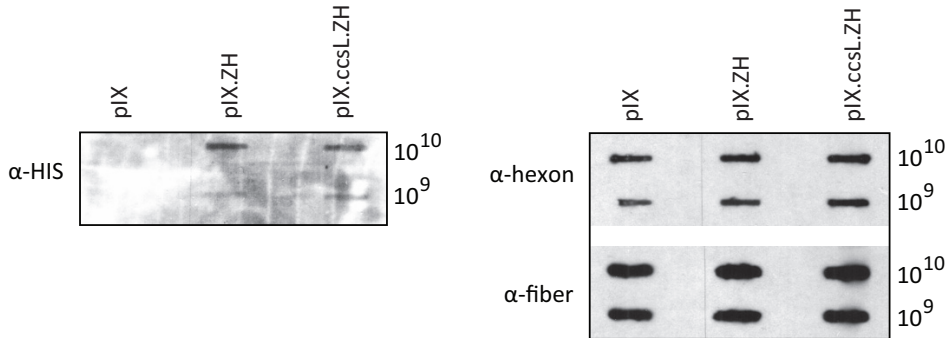


Figure 2. Slot-blot analyses of HER2-ECD binding to intact virus particles. HER2-ECD binding was assayed by subsequent incubation with his-tagged HER2-ECD and anti-HIS antibody. For loading-control purpose, incubation with anti-fiber-knob and anti-hexon antibody was performed. Two virus concentrations (10^{10} and 10^9 pp) were applied to the membrane.

immobilized virus particles were incubated with soluble HER2-ECD, after which virus-bound HER2-ECD was detected by virtue of the his tag, which was fused with the HER2-ECD polypeptide. This experiment demonstrated binding of the HER2-ECD to Ad5/pIX.ZH and Ad5/pIX.ccsL.ZH particles. As expected, all viruses bound equivalent amounts of an antibody recognizing the fiber-knob domain. Also, the amounts of hexon antigen detected were similar, confirming equivalent particle loading in all samples. From these data, we conclude that both viruses with protein IX-Affibody fusions are functionally capable of binding HER2/neu.

Improved transduction of SKOV-3 cell culture by Ad5/pIX.ccsL.ZH

Subsequently, we studied the capacity of the viruses to transduce cultured cells that lack CAR but overexpress HER2/neu. Analyses were performed on the cell lines SKOV-3 (HER2/neu-positive and CAR-negative) and 911 (HER2/neu-negative and CAR-positive). Infection of SKOV-3 cells in an agar-overlaid monolayer culture showed the appearance of larger plaques for Ad5/pIX.ccsL.ZH (mean 2.4 arbitrary surface units (ASU), range 0.5-5.5), as compared to Ad5/pIX (mean 1.4 ASU, range 0.5-2.5) and Ad5/pIX.ZH (mean 0.9 ASU, range 0.5-2.5) (representative plaques are shown in **Fig. 3a**). No differences were observed between Ad5/pIX and Ad5/pIX.ZH, suggesting that the presence of the ccsL site had an effect on the efficiency of transduction of the HER2/neu-positive cells. In contrast, the plaques observed on monolayers of 911 cells had a similar size distribution for all three viruses (mean 1.3 ASU, range 0.5-4.5 for Ad5/pIX, mean 1.3 ASU, range 0.5-3.5 for Ad5/pIX.ZH, mean 1.4 ASU, range 0.5-3.5 for Ad5/pIX.ccsL.ZH). These data suggest that inclusion of the pIX.ccsL.ZH in the capsid enhanced the virus spread in monolayers of CAR-negative, HER2/neu-positive cells.

To test whether the infection is also enhanced in three-dimensional tumor cell cultures, the viruses were applied on SKOV-3 and 911 spheroids (**Fig. 3b**). As in the SKOV-3 monolayer cultures, Ad5/pIX.ccsL.ZH displayed the highest transduction efficiency on SKOV-3 spheroids, with the GFP expression levels being significantly higher than the levels obtained after Ad5/pIX and Ad5/pIX.ZH infection. As expected,

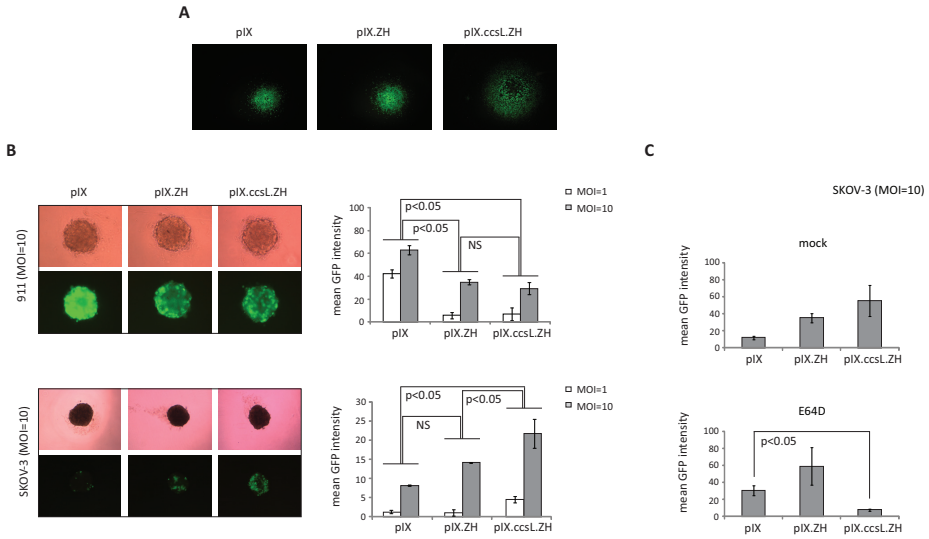


Figure 3. (a) Plaque assay to compare Ad5/pIX, Ad5/pIX.ZH and Ad5/pIX.ccsL.ZH infection of monolayer cell cultures. The microscopy pictures show representative GFP-positive SKOV-3 plaques. (b) Transduction of 911 and SKOV-3 spheroids with Ad5/pIX, Ad5/pIX.ZH and Ad5/pIX.ccsL.ZH. Infection was performed at multiplicities of infection (MOI) of 1 and 10 PFU per cell. The graphs show the mean GFP intensities at 5 days post-transduction. Error bars represent s.d. ($n = 3$). Differences in GFP intensity are considered significant at $P < 0.05$ for both MOIs. Representative pictures (at 5 days post-transduction) are shown on the left. (c) Transduction of SKOV-3 spheroids with Ad5/pIX, Ad5/pIX.ZH and Ad5/pIX.ccsL.ZH in the presence or absence of the cysteine protease inhibitor E64-D. The graphs show the mean GFP intensities at 5 days post-transduction. Error bars represent s.d. ($n = 3$).

no enhanced transgene delivery was observed for the Ad5/pIX.ccsL.ZH virus on the non-target 911 spheroids. Strikingly, the transduction efficiencies for both ZH-containing viruses appeared reduced on the 911 spheroids, as compared with the transduction efficiency for Ad5/pIX. This reduction is in contrast to the results obtained on the 911 monolayers, which showed identical plaque sizes for all three viruses. The cause for this discrepancy between the monolayer and the spheroid model remains to be elucidated. It is conceivable that the growth of the cells in such different conditions affects the cell surface expression or accessibility of the viral receptors CAR and integrins. Irrespective of the mechanism, the reduced transduction of Ad5/pIX.ZH and Ad5/pIX.ccsL.ZH on the non-target 911 spheroids may result from the presence of large targeting ligands fused with protein IX. This warrants further investigation.

The enhanced GFP expression upon Ad5/pIX.ccsL.ZH infection of SKOV-3 spheroids could be inhibited by incubation with the cysteine-protease-specific inhibitor E64-D (**Fig. 3c**). Although the presence of the inhibitor resulted in a modest increase in transduction for Ad5/pIX and Ad5/pIX.ZH, the transduction efficiency for Ad5/pIX.ccsL.ZH was strongly decreased. Of interest, the addition of the cathepsin inhibitor resulted in a general effect on SKOV-3 spheroid morphology, with obvious changes in the cell density on the spheroid surface (results not shown). This effect

probably caused the modest increase in transduction for the Ad5/pIX and Ad5/pIX.ZH viruses.

Analysis of transduction of SKOV-3 tumors on a CAM

To gain insight into the performance of the viruses *in vivo*, the viruses were tested for their transduction efficiencies in human tumors grown on the CAM of embryonated chicken eggs. The engraftment of SKOV-3 cells at embryo development day 7 (EDD7) resulted in the rapid formation of tumors with a size of 4-6 mm at EDD14 (= day of virus injection), with obvious appearance of blood vessel sprouting (**Fig. 4a**). Western analysis was carried out at EDD14 to analyze the expression of cathepsin L in the CAM tumor lysate (**Fig. 4b**). Pro-cathepsin L (42 kDa) as well as the active form of cathepsin L (25 kDa) were detected. At EDD20 (=6 days post virus injection), the tumors were harvested and GFP signals were quantified (**Fig. 4c**). The insertion of the ccsL site significantly enhanced transduction, with the GFP expression level for Ad5/pIX.ccsL.ZH being approximately twice the levels as seen with Ad5/pIX and Ad5/pIX.ZH.

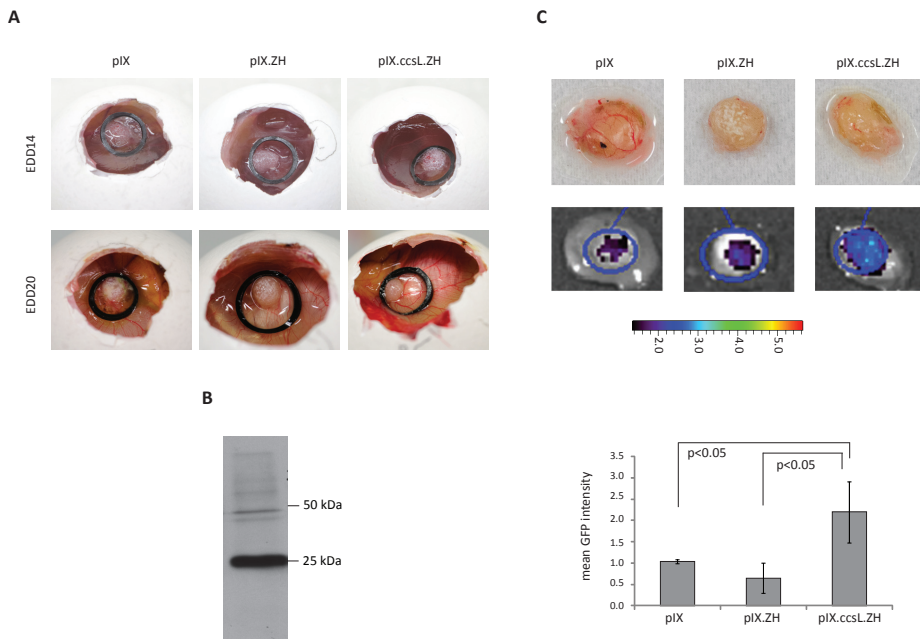


Figure 4. Virus transduction of SKOV-3 cells grown on the CAM. (a) Representative pictures of CAM tumors at EDD 14 (before virus injection) and EDD 20 (before tumor isolation). (b) Western analysis of cathepsin L protein levels in lysates of SKOV-3 cells grown as CAM tumor. Detection was carried out with anti-cathepsin L antibody directed against pro-cathepsin L (42 kDa) as well as the active form of cathepsin L (25 kDa). (c) Biofluorescent imaging with the IVIS system of GFP expression in SKOV-3 tumors retrieved from the CAM (EDD 20). The graph shows the mean GFP intensities. Error bars represent s.d. ($n = 5$). Representative IVIS pictures are included.

DISCUSSION

We studied the usability of cathepsin-cleavage sites in mediating the dissociation of HAdV-5 protein IX from fused tumor-targeting ligands. Inclusion of a ccsL in between protein IX and a HER2/neu-targeted ZH Affibody molecule enhanced the transduction of HER2/neu-positive SKOV-3 tumor cells. The enhanced delivery of an *enhanced* GFP reporter gene was observed in monolayer culture, three-dimensional spheroid culture, as well as in SKOV-3 tumors grown on the CAM of embryonated chicken eggs. These results provide a strategy to enhance the applicability of protein IX as an anchor for coupling high-affinity tumor-targeting ligands.

Varying efficiencies have been reported for protein IX-mediated retargeting approaches, with the targeted transduction efficiency depending on the type of ligand used.^{9,11,22} It was first suggested by Barry *et al.*¹¹ that high-affinity binding between a protein IX-coupled targeting ligand and its receptor may prevent release of the virus particle from the targeted receptor, resulting in inefficient escape of the virus particle from the endosome to the cytoplasm. Such endosomal sequestration is in contrast to fiber-mediated targeting, as the fiber is released from the virus particle upon cellular uptake.^{15,16} To gain more insight into the phenomenon of endosomal entrapment of protein IX targeted HAdV-5 vectors, Corjon *et al.*²² fused protein IX with the RAP (receptor-associated protein) ligand, which is evolutionary designed for dissociation from its target receptor (LRP; LDL-receptor-related protein) at low pH. As intended, this strategy resulted in proper routing of the virus particles in the LDL-expressing target cells (from endosome to the nuclear periphery), and retargeting efficiency appeared to be equal to fiber-RAP-mediated retargeting of HAdV-5.

To prevent the endosomal entrapment of protein IX-targeted HAdV-5, we set out to test whether insertion of a ccs can be used to circumvent this problem, by facilitating endosomal release of the vector. Such mechanism would mimic the strategies adopted by other viruses. Reovirus is disassembled by cathepsins B and L in the endosome. This is a crucial step in its infective pathway.²³ The Ebola virus is dependent on cleavage of glycoprotein GP1 by cathepsins B and L to trigger membrane fusion and cell entry.²⁴ In addition, activation of the Nipah virus fusion protein (responsible for virus entry into the host cell) is mediated by endosomal proteases, presumably cathepsins.²⁵ Ccs incorporation has already been introduced in radioimmunotherapy, which has revealed a decrease in hepatic toxicity when a cathepsin cleavable peptide is attached to the therapeutic-chelated radiometal.²⁶

We first performed an *in vitro* cleavage assay to compare a ccsB and a ccsL site for their cleavage sensitivity if incorporated in between protein IX and a model ligand, that is, the hyper-stable single-chain antibody fragment 13R4.⁸ Cathepsins B and L, which belong to the papain-like family of cysteine proteases, are ubiquitous in the lysosomes of animals.²⁷ The enzymes are endopeptidases, although cathepsin B was found also to be a dipeptidyl carboxypeptidase.²⁸ Among the lysosomal cysteine proteases, cathepsin L was found to be the most active in degradation of protein substrates^{27,29,30} and cathepsin B the most abundant.²⁷ The enzymes are optimally active at slightly acidic pH, that is, pH 6.0 for cathepsin B and pH 5.5 for cathepsin L (reviewed in Kirschke *et al.*¹⁷). This allows full activity within the lysosomal and endosomal compartments. Interestingly, and probably of relevance to our strategy

of using a ccs in HAdV-5 tumor targeting, cathepsins are frequently up regulated in human cancers, and have been implicated in distinct tumorigenic processes such as angiogenesis, proliferation, apoptosis and invasion (reviewed in Gocheva and Joyce³¹).

Our assays demonstrated that the pIX.ccsL.ligand fusion molecule was efficiently inserted in the HAdV-5 capsid. The ccsL site retained its sensitivity for cleavage with cathepsin L. Subsequently, the ccsL site was introduced in the genome of the replication-competent virus Ad5/pIX.ZH, between the protein IX and a tandem pair of ZH Affibody ligands. Binding of the soluble HER2-ECD to the particles was confirmed, demonstrating that the ZH Affibody molecules are located at an assessable location within the virus capsid. Furthermore, Ad5/pIX.ZH and Ad5/pIX.ccsL.ZH bound the HER2-ECD with similar efficiency, demonstrating that during virus production the virus particles were not exposed to active cathepsin L to an extent that leads to proteolytic removal of the targeting ligands.

By quantifying GFP expression levels, we compared the transduction efficiencies of the viruses Ad5/pIX, Ad5/pIX.ZH and Ad5/pIX.ccsL.ZH in different SKOV-3 models. In all models the mere presence of the ZH Affibody molecule was insufficient for significantly improving transduction efficiency. Insertion of the ccsL site, however, resulted in a significantly enhanced transduction in all SKOV-3 models tested. The targeted transduction efficacy was moderately but significantly enhanced in the spheroid as well as in the CAM tumor model.

Of interest, the transduction efficiencies of the ZH-containing viruses were significantly reduced, as compared to the Ad5/pIX virus, on the non-target (CAR-positive/HER2-negative) 911 cells in the three-dimensional spheroid model. The cause of this reduction, which is in contrast to the equal plaque sizes for all viruses in 911 monolayers, is unknown. One explanation might be that the wild-type HAdV-5 receptors (that is, CAR and/or integrins) are relatively poorly accessible on the cell surface in a 911-cell spheroid. As a consequence, extensive HAdV-5 capsid modification, such as the protein IX-ZH incorporation, might lead to changes in virion composition that restrict virus mobility to their receptors. Fusion of other ligands with protein IX can result in reduced transduction of 911 spheroids as well (our unpublished data), demonstrating that the effect is not specific for ZH Affibody molecules. It will be of interest to further analyze protein IX-ligand-targeted HAdV-5 vectors for their infection efficacy on non-target cells, for example, in human tumor xenografts in mice.

In this particular proof-of-principle study, the incorporation of a cathepsin L-cleavage site resulted in substantial improved transduction of SKOV-3 tumor cells. It remains to be established which ccs is optimally suited for a particular ligand and target combination. Tumor cell lines as well as primary tumors have been shown to strongly vary in their expression profile and expression level of the different types of cathepsins (BioGPS Gene Portal;³² NCI60 cell lines (U133A) data set³³ and Human Primary Tumors (U95) data set³⁴). Depending on the tumor type to target, the optimal ccs for incorporation in a pIX.ccs.ligand-containing HAdV-5 may vary, thereby necessitating preclinical ccs evaluations in oncolytic virus protocol development.

The causal mechanistic for the improved performance of the ccsL containing virus remains to be established. Although enhanced endosomal escape of the targeted viruses seems a plausible hypothesis, further studies are necessary to provide a definite answer. Despite these uncertainties on the mechanism, our results demonstrate the

feasibility of using a ccs for improving transgene delivery with protein IX-ligand-targeted HAdV-5 vectors. Enhanced transduction was observed in a spheroid and CAM tumor model, which are highly suitable models for analysis of transgene delivery in a three-dimensional context. Nevertheless, future experiments, implementing *bona fide* tumor models that allow long-term follow-up, will be necessary to reveal whether incorporation of a ccs leads to enhanced anti-tumor efficacy of protein IX-ligand-targeted viruses.

Our cathepsin-cleavage strategy enhances the potential for protein IX-mediated targeting of HAdV-based oncolytic viruses for cancer therapy. Also, the introduction of a ccs might be efficacy-improving for other (non-protein IX-based) HAdV-5 targeting approaches. It would be highly interesting to analyze the effect of introducing a ccs in fiber-ZH viruses,²⁰ and to perform a side-by-side comparison between pIX.ccs.ZH viruses and fiber-ccs-ZH viruses.

Future research will reveal whether protein IX-based targeting, in combination with other targeting (for example, fiber-ligand-based) and de-targeting approaches (for example, ablating CAR-binding by fiber knob modification or blood-coagulation factor X-binding by hexon modification³⁵), can lead to improved oncolytic HAdV vectors. Such rational design strategies, as well as parallel strategies involving random mutagenesis and bioselection methodologies,³⁶⁻³⁹ will facilitate the derivation of new targeted adenoviruses with improved tumor-cell specificity and anti-tumor efficacy.

MATERIALS AND METHODS

5

Cell lines

The human cell lines SKOV-3 (ovarian adenocarcinoma), A549 (carcinomic alveolar epithelium) and 911 (HAdV-5 E1-transformed embryonic retinoblasts)⁴⁰ were maintained at 37°C in a humidified atmosphere of 5% CO₂ in Dulbecco's Modified Eagle's Medium (Gibco-BRL, Breda, The Netherlands) supplemented with 8% fetal bovine serum (Gibco-BRL, Breda, The Netherlands) and penicillin-streptomycin.

Viruses

Overlap extension-polymerase chain reaction (PCR) (with oligonucleotides 1-4; **Table 1**) was used to fuse a tandem of ZH Affibody sequences derived from the plasmid FibR7-ZHZH,²⁰ with the sequence pIX.flag.75 derived from the plasmid pAd5pIX.flag.75.MYC.⁶ Next, the resulting fusion fragment pIX.flag.75.(ZH)2 was flanked at both ends with a short sequence containing a restriction site (*Mlu*I upstream of the pIX.flag.75.(ZH)2 start codon and *Bst*Z17I downstream of the pIX.flag.75.(ZH)2 stop codon) by PCR. The pIX.flag.75.(ZH)2 sequence was ligated to the *Mlu*I- and *Bst*Z17I-digested plasmid pLV-CMV-IRES-NPTII,⁴¹ resulting in the plasmid pLV-CMV-pIX.flag.75.(ZH)2-IRES-NPTII (pLV-pIX.ZH). Subsequently, a unique *Pac*I restriction site was introduced between the 75-Ångstrom spacer and the (ZH)2 sequence (with oligonucleotides 5 and 6; **Table 1**) by site-directed mutagenesis PCR, resulting in the plasmid pLV-CMV-pIX.flag.75.*Pac*I.(ZH)2-IRES-NPTII. The *Pac*I site enabled introduction of a cathepsin L-cleavage site by ligation of the annealed oligonucleotides 7 and 8 (**Table 1**), resulting in pLV-CMV-pIX.flag.75.ccsL.(ZH)2-IRES-NPTII (pLV-pIX.ccsL.ZH). The coding sequences of pIX.flag.75.

Table 1. Oligonucleotide list.

Oligonucleotide	Sequence (5' to 3')
1 FWD Tthii-pIX	TACGAGACCGTGTCTGGAACG
2 REV pIX75Å	GGCGCCGTGTAAGGTTGGGTTGTGGCGTTTGAAGGCGGCTTC
3 FWD pIX75Å-ZH	AACCCAACCTTACACGGCGCCGTAGACAACAAATTCAACAAA
4 REV Dral-ZH	GTTTTAAACTTTCGGCGCCTGAGCATCATT
5 FWD PacI-ZH	CAAACGCCACAACCCAACCTTAATTAAGGCCGTAGACAACAAATTC
6 REV PacI-ZH	GAATTTGTTGTCTACGGCCTTAATTAAGGTTGGGTTGTGGCGTTTG
7 FWD CatL-ZH	CGACGGCGGAGGGAGGAAGGAATTGGTGACGCCAGCACGAGA- CTTCGGTCATTTTGGATTATCCGGAGGCGGGAT
8 REV CatL-ZH	CCCGCCTCCGGATAATCCAAAATGACCGAAGTCTCGTGCTGGCGT- CACCAATTCCTTCTCCCTCCGCCGTCGAT
9 FWD Scal-pIX	CGCGGAAGTACTATGAGCACCAACTCGTTTGATGG
10 REV SpeI-ZH	CGCACTAGTCTAAACTTTCGGCGCCTGAGCAT
11 REV SpeI-pIX	CGCACTAGTTTAAACCGCATTGGGAGGGGAGG
12 FWD PacI-13R4	CAACCCAACCTTAAGCGCCGTCGACGGCTTAATTAACGGCG- GAGGGAGCATGG
13 REV PacI-13R4	CCATGCTCCCTCCGCCGTTAATTAAGCCGTCGACGGCGCTTA- AGTTGGGT
14 FWD CatB-13R4	TCGACGGCGGAGGGGGCTTCCAGGGCGTGCAATTCCGCCG- GCTTCAT
15 REV CatB-13R4	GAAGCCGGCGAACTGCACGCCCTGGAAGCCCCCTCCGCCG
16 FWD CatL-13R4	TCGACGGCGGAGGGAGGAAGGAATTGGTGACGCCAGCACGAGA- CTTCGGTCATTTTGGATTATCCAT
17 REV CatL-13R4	GGATAATCCAAAATGACCGAAGTCTCGTGCTGGCGTCAC- CAATTCCTTCTCCCTCCGCCG

Abbreviations: CatB, cathepsin B; CatL, cathepsin L; FWD, forward; pIX, protein IX; REV, reverse.

(ZH)₂ and pIX.flag.75.ccsL.(ZH)₂ were isolated from, respectively, pLV-pIX.ZH and pLV-pIX.ccsL.ZH by PCR (oligonucleotides 9 and 10; **Table 1**). The sequence for HAdV-5 protein IX was isolated from the plasmid pAd5pIX⁶ by PCR with oligonucleotides 9 and 11 (**Table 1**). The *Scal*-*SpeI*-flanked PCR products were cloned in pShuttle+E1+pIX^{Scal/SpeI}.⁴² The *Scal* restriction site was restored by exchanging the E1B/protein IX sequence containing *MfeI*/*HindIII* region with the corresponding fragment from pTG3602. The resulting plasmids pSh+pIX, pSh+pIX.ZH and pSh+pIX.ccsL.ZH were recombined with the HAdV-5-based backbone plasmid pBB⁴² (containing the *eGFP* gene in the E3 region, based on the previously described pShuttle-ΔE3-ADP-EGFP-F2²¹), followed by virus rescue in A549 cells. Recombination and virus rescue were as described elsewhere.⁴² The viruses (named Ad5/pIX, Ad5/pIX.ZH and Ad5/pIX.ccsL.ZH) were purified by a standard double cesium chloride gradient protocol, dialyzed against sucrose buffer (5% sucrose, 140 mM NaCl, 5 mM Na₂-HPO₄·2H₂O, 1.5 mM KH₂PO₄) and stored at -80 °C. The virus titer was determined by the PicoGreen-DNA binding assay⁴³ (for

pp ml⁻¹ measurement), and a plaque assay on 911 cells (for PFU ml⁻¹ measurement), as described in Fallaux *et al.*⁴⁰ To compare the virus spread in monolayers of 911 and SKOV-3 cells, standard plaque assays were performed, followed by photographing GFP-positive plaques and measuring plaque size with ImageJ software (National Institutes of Health, Bethesda, MD, USA). The plaque surface area of Ad5/pIX.ZH and Ad5/pIX.ccsL.ZH was normalized to the plaque surface area of Ad5/pIX.

Western analyses

Cell lysates were made in radioimmunoprecipitation assay lysis buffer (50 mM Tris-Cl, pH 7.5, 150 mM NaCl, 0.1% sodium dodecyl sulfate, 0.5% DOC, and 1% NP40) supplemented with protease inhibitors. Protein concentrations were determined with a BCA protein assay (Pierce, Etten-Leur, The Netherlands). Cell lysate samples for western analysis were prepared by boiling of 20 µg of total protein in reducing sample buffer (final composition: 33 mM Tris-Cl, pH 6.7, 9% glycerol, 2% sodium dodecyl sulfate and 2.2% β-mercaptoethanol, and 2.2% from a 1:20 dilution of a saturated bromophenol blue solution) for 5 min at 100°C. Virus samples for western analysis were prepared by adding purified viruses directly to the reducing sample buffer, followed by boiling. All samples were subjected to standard sodium dodecyl sulfate-polyacrylamide gel electrophoresis, with 15% polyacrylamide running gels, and subsequent protein transfer to polyvinylidene difluoride (PVDF) membranes (Immobilon-P transfer membrane; Millipore, Amsterdam, The Netherlands) by electroblotting. After immunological probing of the blots, horse radish peroxidase (HRP)-conjugated antibodies were detected by enhanced chemiluminescence. Primary antibodies used were goat polyclonal anti-hexon (1:2000, ab19998; Abcam, Cambridge, UK), rabbit polyclonal anti-protein IX (1:2000)⁴⁴, and mouse monoclonal anti-cathepsin L (1:500, [33/2] ab6314; Abcam). Secondary antibodies used were HRP-conjugated goat-anti-rabbit and mouse-anti-goat (Santa Cruz Biotechnology, Santa Cruz, CA, USA).

5

In vitro cathepsin cleavage assay

To test various protein sequences for their usage as ccs in the context of a protein IX-ligand incorporation, we introduced the sequences in our previously described pIX.13R4.myc.his fusion protein⁸ (**Fig. 1a**). To this end, PCR was carried out (with oligonucleotides 12 and 13; **Table 1**) to introduce a *PacI* site in the plasmid pLV-CMV-pIX.flag.75.13R4.myc.his-IRES-NPTII (pLV-pIX.13R4.myc.his).⁸ Subsequently, oligonucleotides 14 and 15 (**Table 1**) were used for insertion of a ccsB⁴⁵ and oligonucleotides 16 and 17 (**Table 1**) for insertion of a ccsL,²³ resulting in the plasmids pLV-pIX.ccsB.13R4.myc.his and pLV-pIX.ccsL.13R4.myc.his. From the pLV plasmids recombinant lentiviruses were produced, which were subsequently used for transduction of 911 cells to establish the expression of proteins pIX.13R4.myc.his, pIX.ccsB.13R4.myc.his, and pIX.ccsL.13R4.myc.his. Lentivirus production and the transduction of 911 cells were performed as described previously.⁴¹

After lysing the 911 cells with radioimmunoprecipitation assay lysis buffer, the protein IX fusion proteins were bound to nickel beads (IBA, Qiagen, Valencia, CA, USA), enabled by the presence of the his tag fused to the 13R4 ligand. Cell lysates (40 µg) were incubated overnight at 4°C with 20 µl NI-NTA beads and wash buffer (50 mM

$\text{Na}_2\text{H}_2\text{PO}_4$, 300 mM NaCl, 20 mM imidazole, pH 8.0) was added to a final volume of 1 ml. After one washing step with 1 ml wash buffer, the beads were re-suspended in 50 μl cathepsin digestion buffer (50 mM sodium acetate buffer, 2 mM EDTA, 2 mM dithiothreitol, pH 5.0).

Purified virus particles with the protein IX-ligand proteins incorporated in the capsid were prepared by using our previously described strategy involving the infection of protein IX-producing cell lines with a protein IX gene lacking HAdV-5.⁴¹ Briefly, the virus was prepared by infecting the protein IX-ligand-expressing 911 cell lines with the HAdV-5 dl313 mutant, followed by harvesting, purification, and storage of the offspring virus. The sucrose-based storage buffer of the virus preparation was exchanged for cathepsin cleavage buffer by filter centrifugation (Amicon Ultra-4 filter tubes; Millipore). Aliquots of 50 μl , containing 5×10^9 pp (as determined by the PicoGreen-DNA binding assay) were prepared for cathepsin cleavage analysis.

Cathepsin cleavage was tested by incubation with cathepsin L (human, liver; Merck KGaA, Darmstadt, Germany) (28,6 ng/ μl) or cathepsin B (human, liver, Merck KGaA) (250 ng/ μl) for 1 h at 37°C. The samples were subjected to western blotting for the analysis of protein cleavage. Cathepsin L cleavage was inhibited with 10 μM specific inhibitor Z-FY(t-Bu)-DMK (Merck KGaA).

Slot-blot-based assay for analysis of HER2-ECD binding to intact virus particles

Binding of purified virions to the HER2/neu ECD (HER2-ECD) was assessed by a slot-blot-based protocol as described by Uil *et al.*⁴⁶ In brief, the virions were diluted in PBS and blotted onto a polyvinylidene difluoride membrane (Millipore) using a slot-blot apparatus. Blocking was carried out with 2.5% bovine serum albumin, 2.5% protifar (Nutricia, Zoetermeer, The Netherlands) in PBS for 2 h. Functional presentation of HER2/neu on the virion surface was analyzed by overnight incubation with HER2-ECD (300 ng/ml) (Fox Chase Cancer Centre, Philadelphia, PA, USA). The presence of a his tag fused to HER2-ECD allowed the subsequent immunological staining with HRP-conjugated goat polyclonal anti-his tag antibody (ab1269; Abcam). In parallel, staining was performed with mouse anti-fiber-knob (1D6.14 (1:250))⁴⁷ and goat anti-hexon antibody (1:2000, ab19998; Abcam), followed by incubation with HRP-conjugated secondary antibodies.

Spheroid analysis

Semiconfluent 911 cells and SKOV-3 cells were trypsinized, counted, and re-suspended in medium containing 2.4 mg/ml methylcellulose (Sigma Aldrich Chemie, Zwijndrecht, The Netherlands) at the concentration of 10^4 cells/ml. Cell suspension (100 μl) was added into each well of a U-bottom 96-well-plate allowing the formation of one spheroid (consisting of 10^3 cells) per well. Viral infection was initiated at two days after plating by exchanging the medium with infectious medium (multiplicity of infection = 1 or 10 PFU per cell). After 2 h, the infectious medium was replaced with normal medium. To test the dependency of transduction on cathepsin L activity, the cysteine protease inhibitor E64-D (Sigma Aldrich) was added to the infectious medium at a concentration of 5 $\mu\text{g/ml}$. Pictures were taken at 5 days after infection (Olympus Camedia Digital Camera C-3030, installed on an Olympus CK40 microscope) and transduction was quantified by measuring the mean GFP intensity using ImageJ software.

Chicken CAM assay

Human tumors were grown on the chicken CAM as described in detail by Durupt *et al.*⁴⁸ Briefly, fertilized chicken eggs (*Gallus domesticus*) were placed in a humidified incubator at 37°C without CO₂ to induce embryogenesis (EDD 0). On EDD 4, a small hole was made with a 19G needle in the air sack and a window was cut using a forceps under sterile conditions. The shell membrane was humidified with sterile PBS and carefully removed. This window was then sealed with a 3 cm Petri dish and eggs were placed back to the incubator. At day 7 (EDD 7), viability of the embryos and the vasculature of the CAM were visually inspected and the CAM was gently lacerated with a sterile cotton swab to create a blood spot to facilitate engraftment of tumor cells. Tumor cells were collected by trypsinization, washed with culture medium and pelleted by gentle centrifugation. After removing the medium, 10⁷ SKOV-3 cells were resuspended in 50 µL matrigel (Growth-Factor Reduced Matrigel; Becton-Dickinson, Breda, The Netherlands) and inoculated on the CAM. Eggs were sealed, placed back into the incubator, and tumor growth was inspected on a daily basis. Purified virus (1 µl, 10⁴ PFU) was injected at EDD 14 in the center of each tumor mass using a 30G syringe. At EDD 20, the eggs were placed on ice for at least 2 h to euthanize the chick embryos by hypothermia and tumors were isolated and collected in a Petri dish for immediate analyses of GFP expression with a Xenogen IVIS 100 biofluorescence imaging system (Xenogen, Alameda, CA, USA). For the analysis of cathepsin L expression, three tumors (not infected with virus) were transferred at EDD14 to a tube with 2 ml radioimmunoprecipitation assay lysis buffer, followed by sonication at 4°C. The cell debris was removed by centrifugation, and the supernatants were stored at -20°C for western analysis.

ACKNOWLEDGEMENTS

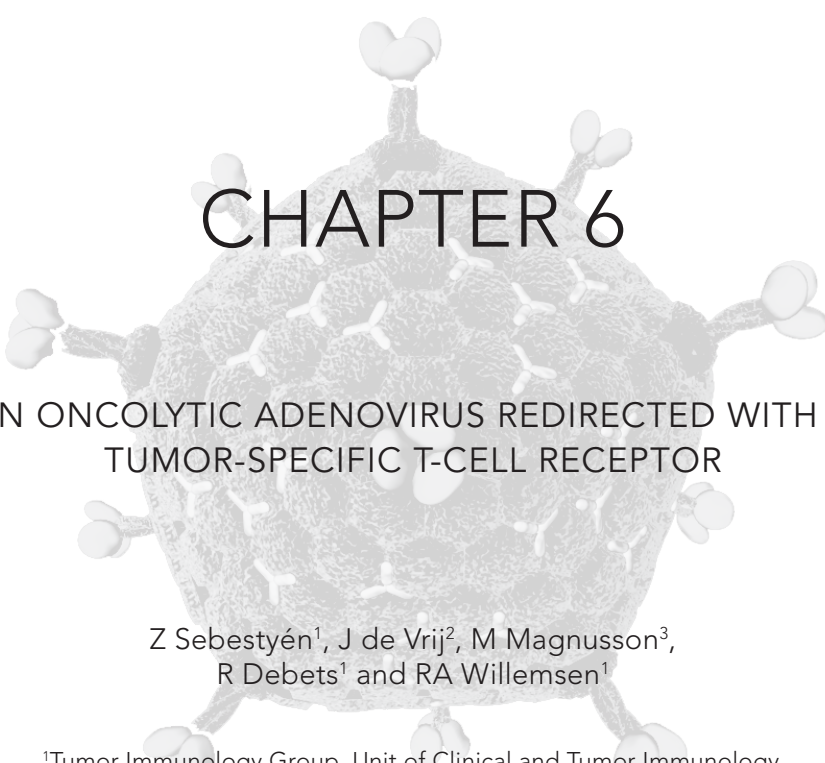
We thank Masato Yamamoto (Department of Surgery, University of Minnesota, MN, USA) for providing us with the plasmid pShuttle-ΔE3-ADP-EGFP-F2. In addition, Ivo Que (Department of Endocrinology, Leiden University Medical Center, Leiden, The Netherlands) is gratefully acknowledged for precious technical assistance in the biofluorescence experiments. This work was supported by the European Union through the 6th Framework Program GIANT (Contract No. 512087).

REFERENCES

1. de Vrij J, Willemsen RA, Lindholm L, Hoeben RC, Bangma CH, Barber C *et al*. Adenovirus-derived vectors for prostate cancer gene therapy. *Hum Gene Ther* 2010; **21**: 795-805.
2. Li D, Duan L, Freimuth P, O'Malley BW, Jr. Variability of adenovirus receptor density influences gene transfer efficiency and therapeutic response in head and neck cancer. *Clin Cancer Res* 1999; **5**: 4175-4181.
3. Hemmi S, Geertsen R, Mezzacasa A, Peter I, Dummer R. The presence of human coxsackievirus and adenovirus receptor is associated with efficient adenovirus-mediated transgene expression in human melanoma cell cultures. *Hum Gene Ther* 1998; **9**: 2363-2373.
4. Bachtarzi H, Stevenson M, Fisher K. Cancer gene therapy with targeted adenoviruses. *Expert Opin Drug Deliv* 2008; **5**: 1231-1240.
5. Dmitriev IP, Kashentseva EA, Curiel DT. Engineering of adenovirus vectors containing heterologous peptide sequences in the C terminus of capsid protein IX. *J Virol* 2002; **76**: 6893-6899.
6. Vellinga J, Rabelink MJ, Cramer SJ, van den Wollenberg DJ, Van der Meulen H, Leppard KN *et al*. Spacers increase the accessibility of peptide ligands linked to the carboxyl terminus of adenovirus minor capsid protein IX. *J Virol* 2004; **78**: 3470-3479.
7. Vellinga J, van den Wollenberg DJ, van der Heijdt S, Rabelink MJ, Hoeben RC. The coiled-coil domain of the adenovirus type 5 protein IX is dispensable for capsid incorporation and thermostability. *J Virol* 2005; **79**: 3206-3210.
8. Vellinga J, de Vrij J, Myhre S, Uil T, Martineau P, Lindholm L *et al*. Efficient incorporation of a functional hyperstable single-chain antibody fragment protein-IX fusion in the adenovirus capsid. *Gene Ther* 2007; **14**: 664-670.
9. de Vrij J, Uil TG, van den Hengel SK, Cramer SJ, Koppers-Lalic D, Verweij MC *et al*. Adenovirus targeting to HLA-A1/MAGE-A1-positive tumor cells by fusing a single-chain T-cell receptor with minor capsid protein IX. *Gene Ther* 2008; **15**: 978-989.
10. Tang Y, Wu H, Ugai H, Matthews QL, Curiel DT. Derivation of a triple mosaic adenovirus for cancer gene therapy. *PLoS One* 2009; **4**: e8526.
11. Campos SK, Barry MA. Comparison of adenovirus fiber, protein IX, and hexon capsomeres as scaffolds for vector purification and cell targeting. *Virology* 2006; **349**: 453-462.
12. Bergelson JM, Cunningham JA, Droguett G, Kurt-Jones EA, Krithivas A, Hong JS *et al*. Isolation of a common receptor for Coxsackie B viruses and adenoviruses 2 and 5. *Science* 1997; **275**: 1320-1323.
13. Nemerow GR, Stewart PL. Role of alpha(v) integrins in adenovirus cell entry and gene delivery. *Microbiol Mol Biol Rev* 1999; **63**: 725-734.
14. Wickham TJ, Mathias P, Cheresch DA, Nemerow GR. Integrins alpha v beta 3 and alpha v beta 5 promote adenovirus internalization but not virus attachment. *Cell* 1993; **73**: 309-319.
15. Sussenbach JS. Early events in the infection process of adenovirus type 5 in HeLa cells. *Virology* 1967; **33**: 567-574.
16. Greber UF, Willetts M, Webster P, Helenius A. Stepwise dismantling of adenovirus 2 during entry into cells. *Cell* 1993; **75**: 477-486.
17. Kirschke H, Barrett AJ, Rawlings ND. Proteinases 1: lysosomal cysteine proteinases. *Protein Profile* 1995; **2**: 1581-1643.
18. Wikman M, Steffen AC, Gunneriusson E, Tolmachev V, Adams GP, Carlsson J *et al*. Selection and characterization of HER2/neu-binding affibody ligands. *Protein Eng Des Sel* 2004; **17**: 455-462.
19. Wang SC, Hung MC. HER2 overexpression and cancer targeting. *Semin Oncol* 2001; **28**: 115-124.
20. Magnusson MK, Henning P, Myhre S, Wikman M, Uil TG, Friedman M *et al*. Adenovirus 5 vector genetically re-targeted by an Affibody molecule with specificity for tumor antigen HER2/neu. *Cancer Gene Ther* 2007; **14**: 468-479.
21. Ono HA, Le LP, Davydova JG, Gavrikova T, Yamamoto M. Noninvasive visualization of adenovirus replication with a fluorescent reporter in the E3

- region. *Cancer Res* 2005; **65**: 10154-10158.
22. Corjon S, Wortmann A, Engler T, van Rooijen N, Kochanek S, Kreppel F. Targeting of adenovirus vectors to the LRP receptor family with the high-affinity ligand RAP via combined genetic and chemical modification of the pIX capsomere. *Mol Ther* 2008; **16**: 1813-1824.
 23. Ebert DH, Deussing J, Peters C, Dermody TS. Cathepsin L and cathepsin B mediate reovirus disassembly in murine fibroblast cells. *J Biol Chem* 2002; **277**: 24609-24617.
 24. Schornberg K, Matsuyama S, Kabsch K, Delos S, Bouton A, White J. Role of endosomal cathepsins in entry mediated by the Ebola virus glycoprotein. *J Virol* 2006; **80**: 4174-4178.
 25. Diederich S, Moll M, Klenk HD, Maisner A. The nipah virus fusion protein is cleaved within the endosomal compartment. *J Biol Chem* 2005; **280**: 29899-29903.
 26. DeNardo GL, DeNardo SJ. Evaluation of a cathepsin-cleavable peptide linked radioimmunoconjugate of a panadenocarcinoma MAb, m170, in mice and patients. *Cancer Biother Radiopharm* 2004; **19**: 85-92.
 27. Barrett AJ, Kirschke H. Cathepsin B, Cathepsin H, and cathepsin L. *Methods Enzymol* 1981; **80 Pt C**: 535-561.
 28. Aronson NN, Jr., Barrett AJ. The specificity of cathepsin B. Hydrolysis of glucagon at the C-terminus by a peptidyl dipeptidase mechanism. *Biochem J* 1978; **171**: 759-765.
 29. Maciewicz RA, Etherington DJ, Kos J, Turk V. Collagenolytic cathepsins of rabbit spleen: a kinetic analysis of collagen degradation and inhibition by chicken cystatin. *Coll Relat Res* 1987; **7**: 295-304.
 30. Mason RW. Interaction of lysosomal cysteine proteinases with alpha 2-macroglobulin: conclusive evidence for the endopeptidase activities of cathepsins B and H. *Arch Biochem Biophys* 1989; **273**: 367-374.
 31. Gocheva V, Joyce JA. Cysteine cathepsins and the cutting edge of cancer invasion. *Cell Cycle* 2007; **6**: 60-64.
 32. Wu C, Orozco C, Boyer J, Leglise M, Goodale J, Batalov S et al. BioGPS: an extensible and customizable portal for querying and organizing gene annotation resources. *Genome Biol* 2009; **10**: R130.
 33. Su AI, Wiltshire T, Batalov S, Lapp H, Ching KA, Block D et al. A gene atlas of the mouse and human protein-encoding transcriptomes. *Proc Natl Acad Sci U S A* 2004; **101**: 6062-6067.
 34. Su AI, Welsh JB, Sapinoso LM, Kern SG, Dimitrov P, Lapp H et al. Molecular classification of human carcinomas by use of gene expression signatures. *Cancer Res* 2001; **61**: 7388-7393.
 35. Pesonen S, Kangasniemi L, Hemminki A. Oncolytic adenoviruses for the treatment of human cancer: focus on translational and clinical data. *Mol Pharm* 2011; **8**: 12-28.
 36. Yan W, Kitzes G, Dormishian F, Hawkins L, Sampson-Johannes A, Watanabe J et al. Developing novel oncolytic adenoviruses through bioselection. *J Virol* 2003; **77**: 2640-2650.
 37. Gros A, Martinez-Quintanilla J, Puig C, Guedan S, Mollevi DG, Alemany R et al. Bioselection of a gain of function mutation that enhances adenovirus 5 release and improves its antitumoral potency. *Cancer Res* 2008; **68**: 8928-8937.
 38. Kuhn I, Harden P, Bauzon M, Chartier C, Nye J, Thorne S et al. Directed evolution generates a novel oncolytic virus for the treatment of colon cancer. *PLoS One* 2008; **3**: e2409.
 39. Uil TG, Vellinga J, de Vrij J, van den Hengel SK, Rabelink MJ, Cramer SJ et al. Directed adenovirus evolution using engineered mutator viral polymerases. *Nucleic Acids Res* 2010.
 40. Fallaux FJ, Kranenburg O, Cramer SJ, Houweling A, Van Ormondt H, Hoeben RC et al. Characterization of 911: a new helper cell line for the titration and propagation of early region 1-deleted adenoviral vectors. *Hum Gene Ther* 1996; **7**: 215-222.
 41. Vellinga J, Uil TG, de Vrij J, Rabelink MJ, Lindholm L, Hoeben RC. A system for efficient generation of adenovirus protein IX-producing helper cell lines. *J Gene Med* 2006; **8**: 147-154.
 42. de Vrij J, van den Hengel SK, Uil TG, Koppers-Lalic D, Dautzenberg IJ, Stassen OM et al. Enhanced transduction of CAR-negative cells by protein IX-gene

- deleted adenovirus 5 vectors. *Virology* 2010.
43. Murakami P, McCaman MT. Quantitation of adenovirus DNA and virus particles with the PicoGreen fluorescent Dye. *Anal Biochem* 1999; **274**: 283-288.
 44. Caravokyri C, Leppard KN. Constitutive episomal expression of polypeptide IX (pIX) in a 293-based cell line complements the deficiency of pIX mutant adenovirus type 5. *J Virol* 1995; **69**: 6627-6633.
 45. DeNardo GL, DeNardo SJ, Peterson JJ, Miers LA, Lam KS, Hartmann-Siantar C et al. Preclinical evaluation of cathepsin-degradable peptide linkers for radioimmunoconjugates. *Clin Cancer Res* 2003; **9**: 3865S-3872S.
 46. Uil TG, de Vrij J, Vellinga J, Rabelink MJ, Cramer SJ, Chan OY et al. A lentiviral vector-based adenovirus fiber-pseudotyping approach for expedited functional assessment of candidate retargeted fibers. *J Gene Med* 2009; **11**: 990-1004.
 47. Douglas JT, Rogers BE, Rosenfeld ME, Michael SI, Feng M, Curiel DT. Targeted gene delivery by tropism-modified adenoviral vectors. *Nat Biotechnol* 1996; **14**: 1574-1578.
 48. Durupt F, Koppers-Lalic D, Balme B, Budel L, Terrier O, Lina B et al. The chicken chorioallantoic membrane tumor assay as model for qualitative testing of oncolytic adenoviruses. *Cancer Gene Ther* 2011; doi:10.1038/cgt.2011.68.



CHAPTER 6

AN ONCOLYTIC ADENOVIRUS REDIRECTED WITH A TUMOR-SPECIFIC T-CELL RECEPTOR

Z Sebestyén¹, J de Vrij², M Magnusson³,
R Debets¹ and RA Willemsen¹

¹Tumor Immunology Group, Unit of Clinical and Tumor Immunology,
Department of Medical Oncology, Erasmus Medical Center-Daniel den Hoed
Cancer Center, Rotterdam, the Netherlands; ²Virus and Stem Cell Biology
Laboratory, Department of Molecular Cell Biology, Leiden University Medical
Center, Leiden, the Netherlands and ³Got-A-Gene AB, Kullavik, Sweden

Cancer Research 2007;67:11309-11316

ABSTRACT

To improve safety and specificity of oncolytic adenoviruses, we introduced T-cell receptors (TCR) specific for a unique class of truly tumor-specific antigens into the adenoviral fiber protein. The adenoviral fiber knob responsible for attachment to the coxsackie-adenoviral receptor (CAR) on target cells was replaced by a single-chain TCR (scTCR) molecule with specificity for the melanoma-associated cancer-testis antigen MAGE-A1, presented by HLA-A1, and an extrinsic trimerization motif in a replicating Ad5 vector (Ad5.R1-scTCR). The production of the recombinant virus was initiated in a novel producer cell line that expressed an antibody-based hexon-specific receptor (293T-AdR) in the cell membrane. This new production system allowed CAR-independent and target antigen-independent propagation of Ad5.R1-scTCR. Infection with adenovirus bearing the scTCR-based fiber resulted in an efficient killing of target tumor cells. The infection was cell type specific because only HLA-A1⁺/MAGE-A1⁺ melanoma cells were killed, and thus, this retargeting strategy provides a versatile tool for future clinical application.

INTRODUCTION

A prerequisite for the safe and effective application of therapies that are based on antigen-driven tumor eradication is the nature of the target antigen, which has to be truly tumor specific. Studying tumor cell eradication by CTL immunologists identified such tumor-specific antigens that were targets for CTL while leaving healthy tissue intact.^{1,2} Tumor cells may express a group of antigens termed “cancer-testis antigens” that are presented as antigenic peptides by MHC molecules to CTL.³ In fact, cancer-testis antigens are immunogenic in cancer patients as they may elicit an anticancer response.⁴⁻⁶ They exhibit highly tissue-restricted expression and are considered promising target molecules for immunotherapies. To date, 44 cancer-testis antigen gene families have been identified and their expression has been studied in numerous cancer types.⁷ For example, bladder cancer, non-small lung cancer, and melanoma are high cancer-testis antigen gene expressers, with 55%, 51%, and 53% of the cancer-testis antigen transcripts examined by reverse transcription-PCR detected in 20% or more of the specimens examined, respectively. With the exception of testis-restricted cancer-testis antigen transcripts, all remaining cancer-testis antigen transcripts were expressed in normal pancreas. Other antigens that were shown to elicit potent antitumor responses in cancer patients include differentiation antigens, such as the melanoma antigens gp100, Mart-1, and tyrosinase, or antigens that are overexpressed on tumor cells, such as p53, Her-2/neu, and WT-1.^{7,8} Both groups of antigens are also expressed in healthy tissue and may therefore elicit autoimmune disease when targeted.

Oncolytic adenoviral vectors hold great promise for cancer gene therapy because they potently eradicate tumor cells.⁹ Therefore, efforts are currently invested in improving replication-competent adenoviruses with respect to safety and specificity to fulfill criteria for clinical application.¹⁰ Among several strategies, genetic modification of the adenoviral fiber, which is responsible for cell binding, may result in a logical and preferable site to carry structures that specifically bind to target antigens of choice, thereby changing viral tropism.

Application of adenoviruses in a tumor cell-specific fashion is highly hampered because the natural cellular receptor of adenovirus is widely expressed on normal tissues and, on the other hand, often reported to be down-regulated or even absent on tumor cells.¹¹ To address this issue, one needs strategies to alter the tropism of adenoviral vectors and retarget them against tumor-specific antigens.

Recent developments to change the natural tropism of adenoviral vectors into tumor-specific recognition are based on the genetic engineering of capsid proteins, such as pIX,^{12,13} hexon, and fiber.¹⁴⁻¹⁹

Genetic modification of the fiber protein has been achieved either through exchange of the Ad5 fiber knob with the Ad3 knob,^{20,21} knob mutagenesis,^{22,23} or incorporation of small ligands into the knob domain.^{21,24} However, it should be noted that an effective and safe retargeting strategy should include complete ablation of the natural tropism, which is not guaranteed by the above-mentioned modifications, and preferably include deletion of the fiber knob. This can be accomplished by replacing the fiber knob by new antigen-binding structures and an extrinsic trimerization signal.^{18,21} Antibody or T-cell receptor (TCR) fragments [e.g., single-chain Fv (scFv)

and single-chain TCR (scTCR)] mediate tumor cell recognition and are able to redirect T cells²⁵ and viruses²⁶ and, as such, are candidate structures to genetically redirect adenoviruses to tumor cells. Previous attempts to produce adenoviruses with fibers that include scFv have failed, most likely as a consequence of improper folding of the chimeric fiber in the cellular cytoplasm.¹⁸

Here, we show that an oncolytic adenovirus bearing chimeric fibers, comprising an extrinsic trimerization signal and scTCR with HLA-A1–restricted MAGE-A1 specificity, can be produced. To this end, we generated a novel producer cell line expressing an anti-hexon receptor, which was needed to initiate production of virus that specifically infects HLA-A1/MAGE-A1⁺ melanoma cells but not MAGE-A1⁻ or HLA-A1⁻ target cells. The presented strategy to produce genetically retargeted oncolytic adenoviruses holds great promise to develop clinically applicable anticancer agents.

RESULTS

Construction of a replication-competent adenovirus with HLA-A1/MAGE-A1 specificity

A knobless fiber containing fiber tail plus NH₂-terminal first shaft repeat (R1, 61 amino acids), an extrinsic trimerization motif (NRP, 36 amino acids) from lung surfactant protein D, a linker derived from *Staphylococcus* protein A (13 amino acids), and scTCR V α V β C β (377 amino acids), specific for the melanoma antigen MAGE-A1, presented by HLA-A1 (which replaced the natural fiber knob), was constructed (**Fig. 1**) and introduced into replication-competent adenovirus serotype 5 essentially as described.^{17,18} To construct the scTCR, TCR α and β chains were cloned from an HLA-A1–restricted, MAGE-A1–specific CTL clone, MZ2-82/30, and reformatted into the scTCR V α V β C β as described.²⁷ Specific binding of the scTCR was verified by expression on primary human T lymphocytes, which showed scTCR-directed immune functions such as specific tumor cell kill and cytokine production. The apparent molecular weight of the R1-scTCR fiber (54 kDa) is similar to that of the WT Ad5 fiber (59 kDa).

Generation of 293T-AdR cells to propagate fiber-modified adenoviruses

As a consequence of ablating the natural tropism, we expected that recombinant Ad5-scTCR virus would require the presence of its target antigen, HLA-A1/MAGE-A1, on the surface of the producer cell line for the primary attachment and entry. Therefore, we generated 293T cells expressing the HLA-A1/MAGE-A1 antigen. 293T cells were infected with retroviral vectors pBullet HLA-A1 and pBullet MAGE-A1 (full-length cDNA and minigene). Next to these antigen⁺ 293T cells, we also used MZ2-mel 3.0 melanoma cells, which naturally present MAGE-A1 in the context of HLA-A1. Neither the antigen-transduced 293T cells nor MZ2-mel 3.0 cells were able to initiate production of the recombinant virus starting with transfection of the adenoviral DNA (data not shown). To support initiation of viral production and propagation of fiber-modified adenoviruses that depend neither on CAR nor on MAGE-A1/HLA-A1 antigen (or any ligands of interest for that matter), we generated a novel producer cell line based on the introduction of an adenovirus-binding antibody into 293T cells.

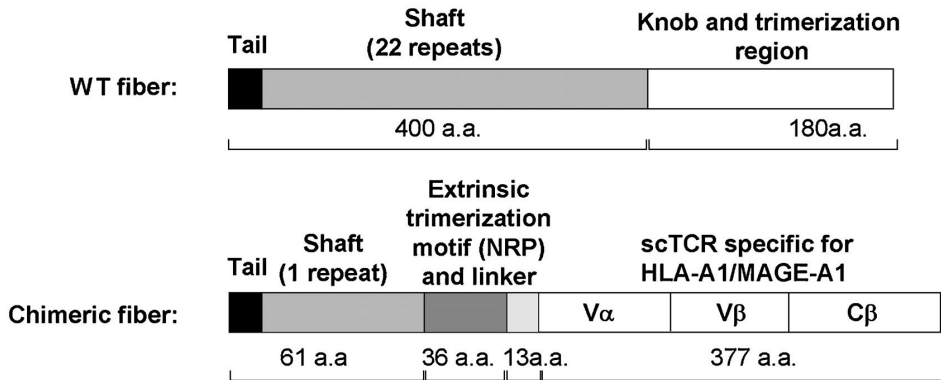


Figure 1. Diagram of WT Ad5 fiber and R1-scTCR fiber. Distinct domains of the Ad5 WT fiber and R1-scTCR fiber as well as the amino acid (a.a.) composition of the distinct domains. V α , variable domain of TCR α chain; V β , variable domain of TCR β chain; C β , constant domain of TCR β chain.

To this end, we constructed two membrane-anchored anti-adenovirus receptors, AdR and AdR-cMyc/ ζ , from hybridoma cells producing a hexon-specific antibody (**Fig. 2a**) that cross-reacts with many adenovirus subtypes and introduced it via retroviral transduction into 293T cells. Due to a lack of antibodies binding to the scFv directly, demonstration of cell surface expression of the anti-adenovirus receptors on 293T cells was only possible for AdR-cMyc/ ζ using anti-c-Myc mAb (**Fig. 2b**).

The ability of AdR and AdR-cMyc/ ζ to serve as universal receptors for Ad5 was analyzed in 293T cells. 293T cells with AdR, termed 293T-AdR, 293T cells with AdR-cMyc/ ζ , termed 293T-AdR-cMyc/ ζ , or parental 293T cells were transfected with a fiberless Ad5 vector encoding the EGFP gene. We observed a severely impaired propagation of fiberless adenovirus in 293T cells in line with previous reports and most likely due to a lack of CAR-fiber knob interactions.^{21,28} We hypothesized that the presence of the AdR receptor would at least in part restore the ability of 293T cells to produce fiber-deleted viruses. As shown in **Fig. 2c**, on day 1 following transfection, the expression of EGFP was comparable in both 293T and 293T-AdR cells. The ratio of EGFP in normal 293T cells did not improve on day 2 or 3. However, in 293T-AdR cells, we observed a robust spread of the reporter gene together with comet-like formation that was most significant on day 3 after transfection. Production of virus particles in culture supernatant was confirmed by an adenovirus-specific ELISA (data not shown). When 293T cells were stably expressing the AdR-cMyc/ ζ receptor, we also observed an increase in reporter gene expression and release of viral particles. However, the ability of 293T-AdR-cMyc/ ζ to induce adenovirus production was significantly less than that of 293T-AdR cells (data not shown).

We then introduced the Ad5.R1-scTCR construct into 293T-AdR cells and showed that, 3 days following transfection, virus was produced at a titer of 6×10^7 particles/mL (= physical particles, determined by ELISA), starting from 3×10^6 293T-AdR cells.

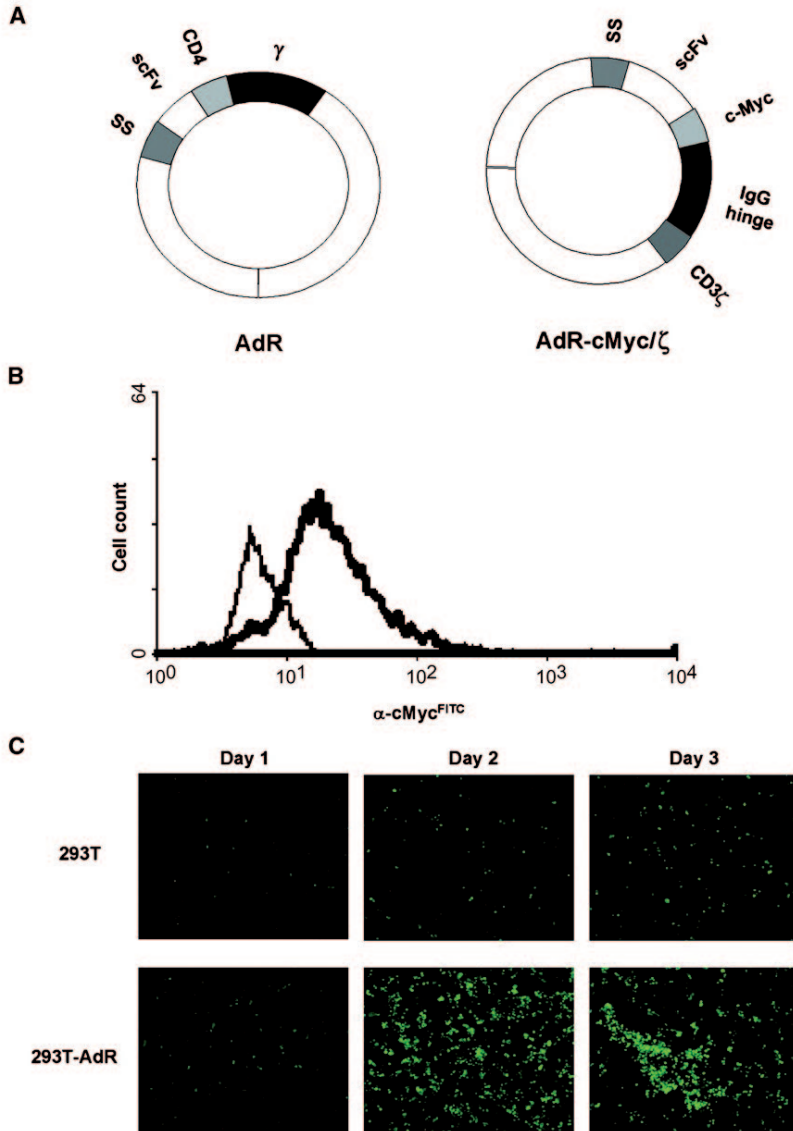


Figure 2. (a) Diagram of expression vectors encoding the “adenoreceptor.” SS, Igk signal sequence; γ , intracellular domain of Fc ϵ R1- γ chain. (b) Surface expression of AdR-cMyc/ ζ on 293T cells. 293T cells were retrovirally transduced with the adenoreceptor fused to a c-Myc tag (AdR-cMyc/ ζ). Cells were stained with FITC-conjugated c-Myc-specific mAb (9E10) and samples were measured by flow cytometry. Histograms represent nontransduced 293T cells (*thin line*) and receptor-positive 293T cells (*thick line*). (c) Infection of 293T cells by fiberless adenovirus requires the expression of AdR on the cell surface. 293T and 293T-AdR cells were seeded and transfected with fiberless pAdeasy EGFP construct. Kinetics of green fluorescent protein expression was monitored by fluorescence microscopy at days 1, 2, and 3 after transfection. Representative images ($\times 10$ magnification) from one of three experiments.

Ad5.R1-scTCR virus is produced, specifically binds to HLA-A1/MAGE-A1 complexes, and replicates in HLA-A1⁺/MAGE-A1⁺ tumor cells

To show production, specific binding to peptide/MHC complexes, and fiber incorporation of adenoviral particles that incorporate the chimeric R1-scTCR fiber, we did the following experiments: (a) electron microscopy, to show presence of viral particles in MZ2-mel 3.0 cells (**Fig. 3a**); (b) flow cytometry analysis of HLA-A1/MAGE-A1-specific binding of Ad5-R1-scTCR (**Fig. 3b**); (c) Western blot analysis, to show incorporation of the R1-scTCR fiber (**Fig. 3c**); and (d) ELISA, to show production of Ad5.R1-scTCR in 293T AdR and MZ2-mel 3.0 cells.

To show production of Ad5.R1-scTCR particles, MZ2-mel 3.0 cells were infected with viral supernatant and analyzed by electron microscopy. **Fig. 3a** shows the presence of viral particles in the nucleus of MZ2-mel 3.0 cells 72 h after infection.

To show specific binding to HLA-A1/MAGE-A1, supernatant from 293T-AdR cells producing Ad5-R1-scTCR was incubated with magnetic beads that were loaded with HLA-A1/MAGE-A1 complexes or HLA-A1 complexes that present an irrelevant peptide derived from influenza virus A nucleoprotein.

As shown, Ad5.R1-scTCR virus only bound to HLA-A1/MAGE-A1 complexes and not to HLA-A1 complexes presenting an irrelevant influenza virus peptide (**Fig. 3b**).

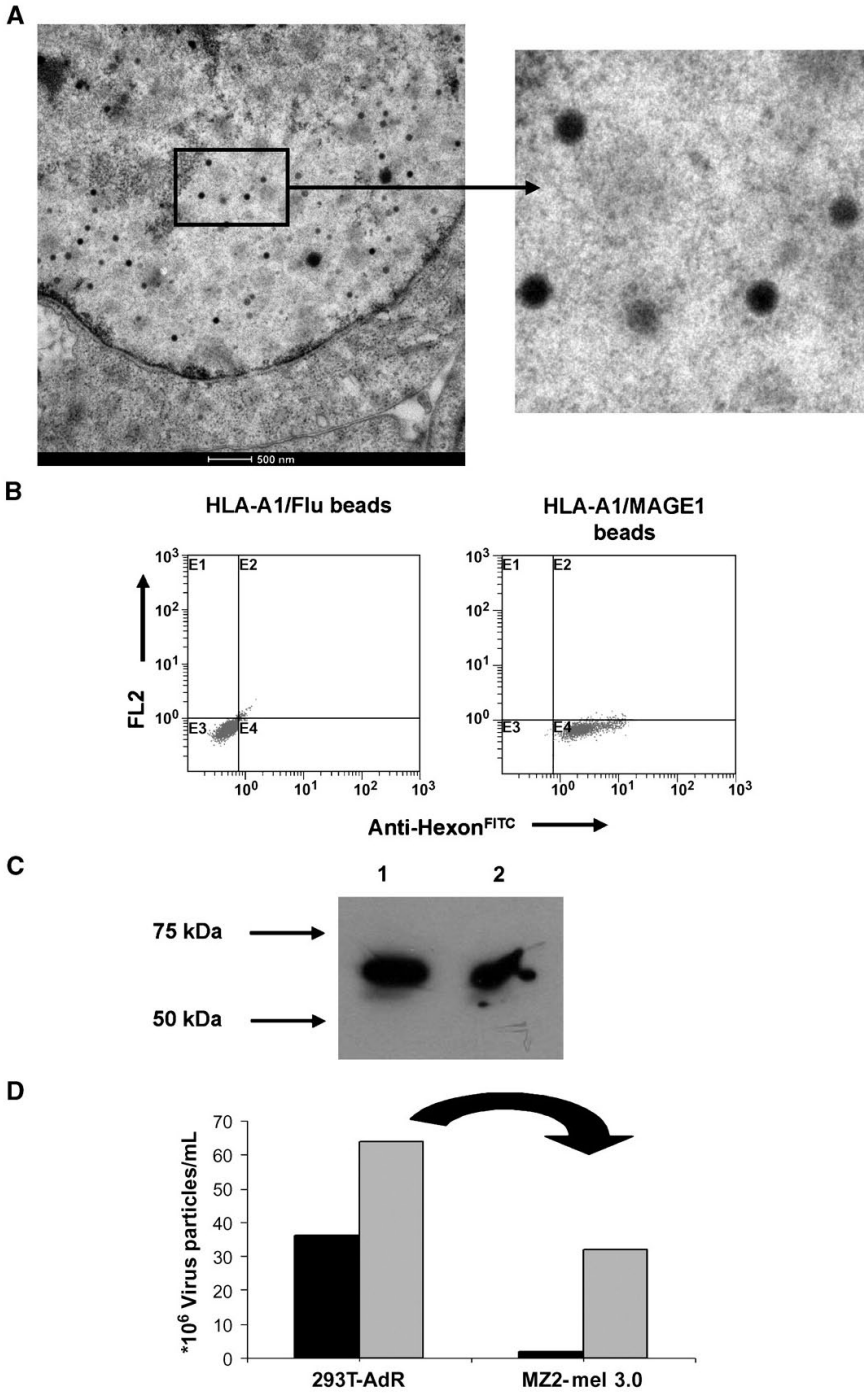
Ad5.R1-scTCR virus bound to HLA-A1/MAGE-A1-coated magnetic beads was then analyzed by Western blotting using fiber tail-specific mAb 4D2. As shown in **Fig. 3c**, chimeric scTCR fibers were incorporated into adenoviral particles.

To determine whether Ad5.R1-scTCR virus is able to infect HLA-A1⁺/MAGE-A1⁺ tumor cells, we incubated MZ2-mel 3.0 melanoma cells with supernatant obtained from 293T AdR cells transfected with either Ad5.WT or Ad5.R1-scTCR DNA. MZ2-mel 3.0 cells lack CAR expression (**Table 1**), making them refractory to infection by WT virus. As shown in **Fig. 3d**, Ad5.R1-scTCR virus produced by 293T AdR cells infected MZ2-mel 3.0 cells and was able to replicate in these cells, shown by the presence of viral particles in the tissue culture supernatant 3 days after infection. In contrast, WT virus at comparable virus particle-to-cell ratio did not result in adenoviral infection.

6

Cellular localization of Ad5.R1-scTCR epitopes during replication

It has been suggested that only those recombinant fibers that assemble correctly in the nucleus may be incorporated into an infectious adenoviral particle.²⁴ To analyze intracellular localization of adenoviral proteins, we infected MZ2-mel 3.0 cells with Ad5.R1-scTCR and did intracellular immunofluorescent staining with mAbs specific for hexon, fiber tail, and scTCR. Hexon and fiber tail molecules showed a comparable cellular distribution, localized almost exclusively to the nucleus 24 h after infection (**Fig. 4, top**). Interestingly, at that time point, hexon molecules were detected in the cytoplasm to some extent, whereas fiber molecules were not. In control experiments, we observed that adenoviruses displaying WT fiber showed similar cellular localization of hexon and fiber tail (data not shown). In contrast, staining for the R1-scTCR fiber with the anti-TCR-specific antibody did not result in any detectable fluorescent signal at 24 h after infection (**Fig. 4, top**).



- ◀ **Figure 3.** Characterization of Ad5.R1-scTCR particles. **(a)** Electron microscopic image of Ad5.R1-scTCR in MZ2-mel 3.0 cells. Presence of Ad5.R1-scTCR particles in the nucleus of MZ2-mel 3.0 cells was shown by electron microscopy 72 h after incubation of MZ2-mel 3.0 cells with viral supernatant. Right, a five times enlargement of a region of the left. **(b)** Ad5.R1-scTCR particles from 293T-AdR supernatant specifically bind to HLA-A1/MAGE-A1 complexes only. Tissue culture supernatants derived from 293T-AdR cells producing Ad5.R1-scTCR particles were incubated with HLA-A1/MAGE-A1 or irrelevant HLA-A1/Flu complex-coated magnetic beads. Ad5.R1-scTCR particles were detected by flow cytometric analysis using anti-hexonFITC mAb. **(c)** Ad5.R1-scTCR viral particles incorporate the R1-scTCR fiber. Ad5.R1-scTCR virus bound to HLA-A1/MAGE-A1 complex-coated beads and cesium chloride-purified WT Ad5 were loaded on 7% SDS-PAGE, transferred to nitrocellulose membrane, and detected with anti-fiber tail antibody 4D2. Lane 1, Ad5.WT; lane 2, Ad5.R1-scTCR. **(d)** Adenovirus expressing the scTCR fiber infects and replicates in HLA-A1/MAGE-A1+ melanoma cells. MZ2-mel 3.0 cells were incubated with viral supernatant obtained from 293T AdR cells transfected with either Ad5.R1-scTCR or Ad5.WT DNA. Adenoviral titer in tissue culture medium was detected by ELISA after (a) transfection of the producer cell 293T-AdR with Ad5.WT (black columns) or Ad5.R1-scTCR (gray columns) and (b) 3 d after infection of MZ2-mel 3.0 cells by crude lysates from a.

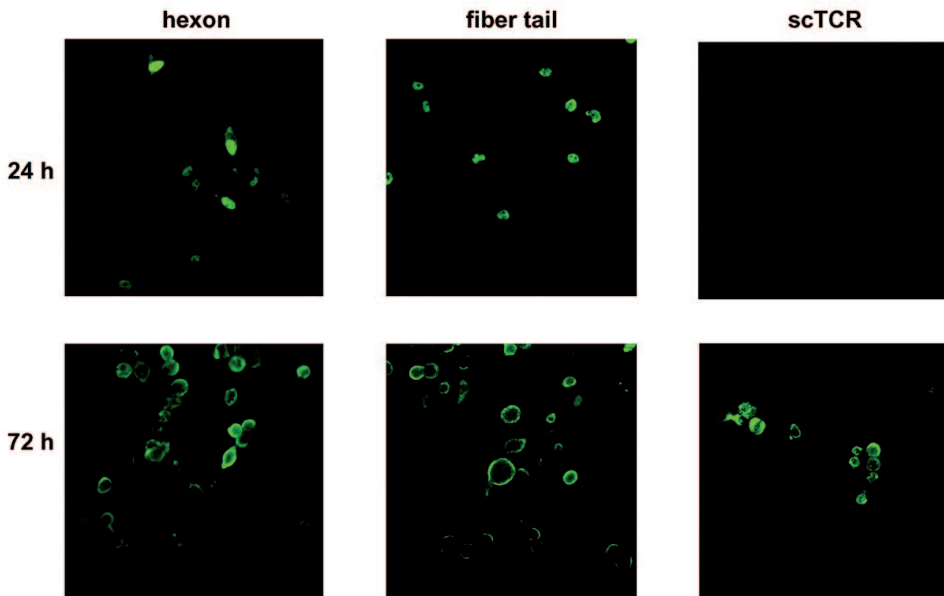


Figure 4. Localization of adenoviral proteins during replication. MZ2-mel 3.0 cells were infected with Ad5.R1-scTCR at a virus particle-to-cell ratio of 50, and cell-associated adenoviral proteins were stained with mAbs against hexon (α -hexon), fiber tail (4D2.5), and scTCR V α domain (V α 12.1) at 24 and 72 h after infection. Images were collected with a fluorescent microscope.

Localization of both hexon and fiber proteins changed at 72 h after infection from a prominent nuclear localization to accumulation at the cell periphery, most likely at the plasma membrane. At this stage of replication, presumably on virus release, R1-scTCR could be detected with anti-TCR antibody and also located to the plasma membrane or to its proximity, indicating an identical cellular compartmentalization of hexon, fiber tail, and scTCR (**Fig. 4, bottom**).

Infection by Ad5.R1-scTCR is epitope specific

Specificity of infection of Ad5.R1-scTCR was analyzed by infecting the melanoma cells: MZ2-mel 3.0 (HLA-A1⁺/MAGE-A1⁺) and MEL.2A (HLA-A1⁺/MAGE-A1⁻). Also included were 293T and 293T-AdR cells. Target cells were infected at different virus particle-to-cell ratios and monitoring the production of hexon protein at 2 days after infection. In this assay, cells expressing the hexon molecule represent infected cells and constitute an indirect readout for viral titers as an alternative to plaque assay. As shown in **Fig. 5**, Ad5.R1-scTCR virus reached maximum infectivity at ~20 virus particle-to-cell ratio when infecting antigen⁺ MZ2-mel 3.0 cells and 293T-AdR, approximately corresponding to a MOI of 4. When using antigen⁻ MZ2-mel 2.2 cells, Ad5.R1-scTCR infectivity remained low even at high virus particle-to-cell ratio and showed a similar titration curve when using 293T cells.

Specificity studies were expanded by the use of a larger panel of target cells, including the following melanoma cell lines: MZ2-mel 3.0; 9303-A; 518-A2; MZ2-mel 2.2, a MAGE-A1 antigen lost mutant obtained from MZ2-mel 3.0; MEL.2A; and FM-3. We also included Nemeth renal cell carcinoma cell lines and the 293T cells. Five days after infection, surviving tumor cells were stained with methylene blue. HLA-A1/MAGE-A1 expression as well as infectivity data of all target cells are summarized in **Table 1**. As shown in **Table 1** only HLA-A1⁺/MAGE-A1⁺ melanoma cells were infected.

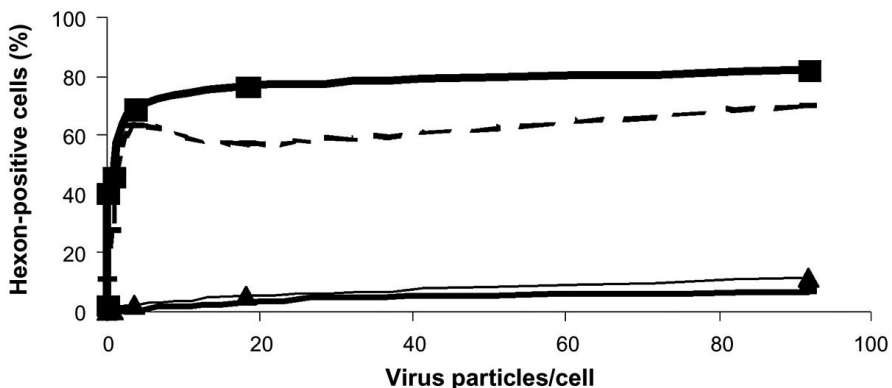


Figure 5. Ad5.R1-scTCR specifically infects melanoma cells expressing the HLA-A1/MAGE-A1 epitope at a low virus particle-to-cell ratio. Cells (5×10^5) of MZ2-mel 3.0 (solid line with black box), MEL.2A (solid thin line), 293T (solid line with triangle), and 293T-AdR (dashed line) were infected at various virus particle-to-cell ratios of Ad5.R1-scTCR. Cells were harvested 2 d after infection and stained with FITC-labeled mAb against hexon molecule. Percentage of hexon-expressing cells analyzed by flow cytometry.

Table 1. Antigen expression and infection of melanoma and renal cell carcinoma cell lines by Ad5.R1-scTCR.

Target cell	HLA-A1	MAGE-A1	CAR	Infection by Ad5.R1-scTCR*
MZ2-mel 3.0	+	+	–	+
9303-A	+	+	+	+
518-A1	+	+	+	+
MZ2-mel 2.2	+	–	–	–
MEL2A	+	–	+	–
FM-3	–	–	+	–
Nemeth	–	–	+	–
293T	–	–	+	–

* Represents infection of target cells analyzed by methylene blue staining. + or – is based on qualitative comparison with noninfected control cells.

DISCUSSION

Our aim of this study was to provide oncolytic adenoviral vectors with a truly tumor cell specificity to improve safety and efficacy, which are major criteria for the clinical use of replicating vectors. TCR recognizing MHC-restricted cancer-testis antigens, such as MAGE-A1, which are distributed in a highly tumor tissue-specific manner, may constitute promising molecules to retarget adenoviruses. This study shows for the first time that even complex molecules such as TCR can genetically replace the fiber knob and be expressed on the adenoviral fiber, thereby ablating its natural tropism. The Ad5 fiber knob was replaced by an extrinsic trimerization motif and an HLA-A1/MAGE-A1-specific scTCR. Critical to the experimental use of this recombinant adenovirus was the generation of a novel producer cell line, 293T-AdR, which was successfully used to initiate production, starting by transfection with adenoviral DNA, and supported propagation of adenovirus, which depended neither on CAR nor on HLA-A1/MAGE-A1. Our failure to use 293T expressing the HLA-A1 and MAGE-A1 cDNA for the initiation of adenovirus production was most likely attributed to unstable expression of the *HLA-A1* gene. Within 3 days after infection with retrovirus encoding the *HLA-A1* gene, HLA-A1 molecules disappeared from the cell surface, resulting in lack of MAGE-A1 antigen presentation to the chimeric fibers (data not shown). There may be more reasons why we were unable to initiate adenovirus production in MZ2-mel 3.0 cells. In general, the production of adenovirus after DNA transfection is inefficient because plasmid DNA does not contain the protein binding to the viral inverted terminal repeats and therefore requires several rounds of amplification.²⁹ When DNA transfection efficiencies become limiting, as might be the case when using MZ2-mel 3.0 cells, low numbers of virus-producing cells may result in undetectable levels of virus even after serial amplification. In addition, MZ2-mel 3.0 cells may produce lower numbers of viral particles than, for example, 293 cells.

Importantly, the retargeted viruses specifically bound to relevant HLA-A1/MAGE-A1 complexes only (Fig. 3b), specifically infected target cells expressing HLA-A1-restricted MAGE-A1 antigen (Fig. 5; Table 1), and killed these melanoma cells.

The initiation of production when starting from recombinant Ad5 DNA seemed to be a critical step during propagation. As a consequence of ablation of native Ad5 tropism, the recombinant Ad5.R1-scTCR is not able to use the natural CAR-mediated cellular entry pathway during propagation in conventional packaging cell lines, such as 293 or 911. Although there are reports on possible solutions to overcome the limitations of fiber-modified adenoviral vector production,^{28,30} there is no precedent on virus retargeting via complex molecules, such as TCR or Igs, and an alternative strategy had to be developed. A major factor that can hamper genetic retargeting of adenoviral vectors, especially when including complex molecules into the viral genome, is the proper folding of these new molecules in the nucleus. According to Pecorari *et al.*,³¹ the formation of intrachain disulfide bridges, which are crucial for the correct folding and stability of IgG or TCR, is suboptimal in the reducing environment of the cytoplasm and nucleus. One could address this issue by using small molecules, such as affibodies, which possess the binding properties of an antibody but do not require intrachain disulfide bonds.¹⁶ Magnusson *et al.*¹⁸ reported that, although the scTCR fiber was able to form homotrimers and bound its ligand, the recombinant fiber protein misfolded, thereby possibly explaining the unsuccessful propagation of Ad5.R1-scTCR in MZ2-mel 3.0 melanoma cells. However, our studies on scTCR fiber expression suggest that at the proximity to the cell membrane (**Fig. 4, bottom**) proper folding of the scTCR fiber occurs, resulting in exposure of a fully functional scTCR fiber on the virus particle. We assume that at this stage of virus assembly restricting intracellular conditions no longer limits the formation of sulfide bridges. Furthermore, we now also succeeded in the initiation of production of two other recombinant viruses, one with a scTCR fiber and a virus equipped with an affibody fiber (data not shown), which shows the universal applicability of this production system.

These findings open new and safer strategies for cell-specific retargeting of oncolytic adenoviruses, providing a versatile tool for future clinical application.

MATERIALS AND METHODS

Cells and antibodies

Target cell lines used in this study are the melanoma cell line MZ2-mel 3.0, MZ2-mel 2.2, and MEL.2A (kindly provided by T. Boon and P. Coulie, Ludwig Institute for Cancer Research, Brussels, Belgium). The melanoma cell lines 9303-A, 518-A1, and FM-3; the renal cell carcinoma cell line Nemeth (kindly provided by Dr. E. Oosterwijk, University Medical Center Nijmegen, Nijmegen, the Netherlands); and the human embryonic kidney cell line 293T and its derivative 293T-AdR (further described in the Results section) were grown in DMEM (Life Technologies) supplemented with 10% fetal bovine serum (FBS; Hyclone). HLA-A1/MAGE-A1 and coxsackie-adenovirus receptor (CAR) expression status of the target cell lines is further described in **Table 1** (see Results).

Antibodies used in this study were against fiber tail (4D2.5; NeoMarkers), hexon (clone BOD604, FITC conjugated; Biondesign), rabbit polyclonal anti-Ad5 (Abcam), TCR V α 12.1 (FITC or nonconjugated; Endogen), CAR (USBiological), and c-Myc (9E10, FITC conjugated; Convance). FITC-conjugated rabbit anti-mouse IgG Fab fragment

(Jackson ImmunoResearch) or horseradish peroxidase–conjugated goat anti-rabbit IgG (Becton Dickinson Biosciences) was used as secondary antibodies.

Infectivity assay with fiberless virus

293T and 293T-AdR cells were transfected with a fiberless pAdeasy-EGFP construct (a kind gift of Wim Jongmans, University Medical Center, Nijmegen, the Netherlands) using the CellPfect Transfection kit (Amersham Biosciences). The expression of the reporter gene *EGFP* was monitored using a Leica DMIL inverted fluorescence microscope (Leica Microsystems). At time points indicated, culture supernatant was collected and virus release (particle count) was analyzed using the IDEIA Adenovirus ELISA kit (DakoCytomation).

DNA constructs

Ad5.R1-scTCR adenoviral DNA was generated as described.¹⁸ Briefly, recombinant fiber genes were constructed using methods based on ligation, PCR, and splicing by overlap extension. The gene encoding the Ad5 wild-type (WT) fiber was obtained from pAB26 (Microbix, Inc.) by PCR introducing an upstream *Bam*HI and downstream *Xho*I site, respectively. The knob domain in recombinant fibers was deleted and replaced by a 36-amino acid extrinsic trimerization motif derived from the neck region peptide (NRP) of human lung surfactant protein D.¹⁸ The NRP sequence followed by a linker sequence from *Staphylococcus* protein A was ligated to the COOH-terminal end of fiber shaft with one repeat and named R1, and the scTCR V α V β C β was added to the COOH-terminal end of the Staph-A linker. The resulting R1-scTCR fiber was then cloned into a fiberless Ad5 genome as described.¹⁸

Retroviral vectors encoding the *HLA-A1* gene, *MAGE-A1* complete cDNA, or *MAGE-A1* minigene (encoding the 9-amino acid antigenic epitope EADPTGHSY) were generated as follows: *HLA-A1* and *MAGE-A1* cDNA cloned in pCDNA-3 (a kind gift from Pierre van der Bruggen, Ludwig Institute for Cancer Research, Brussels, Belgium) were reamplified to introduce *Nco*I and *Xho*I sites and cloned into the retroviral vector pBullet. The *MAGE-A1* minigene was introduced into a version of pBullet that contains a signal sequence from the G250 antibody heavy chain³² by ligation of a small linker encoding the *MAGE-A1* minigene next to the signal sequence.

To construct the membrane-bound adenovirus-specific receptor (AdR), first an scFv was generated from the hexon-specific hybridoma 2Hx-2 (American Type Culture Collection). In short, RNA isolated from the 2Hx-2 hybridoma was reverse transcribed using SuperScript II (Invitrogen) and amplified using Ig variable heavy and variable light chain primers (Amersham scFv module, Amersham Biotech). The variable heavy and variable light chain DNA fragments were then reamplified to fuse them together by introducing a linker sequence between the two fragments and to introduce *Sfi*I and *Not*I restriction sites. The resulting scFv was then introduced into the retroviral expression cassette pBullet-CD4 γ , and pBullet-cMyc/ ζ , which allows for membrane expression of the scFv.^{32,33}

Generation of the recombinant virus

293T-AdR cells were transfected with *Pac*I-digested recombinant adenovirus plasmid (Ad5.R1-scTCR), and after 3 days, culture supernatant was harvested and used

immediately for infection or further analysis. Adenovirus particle count (semiquantitative) was determined by IDEIA Adenovirus ELISA kit. Infectious adenovirus particle number [multiplicity of infection (MOI)] was determined by the Adeno-X Rapid titer kit (BD Clontech) on 293T-AdR cells.

Analysis of adenoviral particles

Electron microscopy

For electron microscopy, MZ2-mel 3.0 cells were fixed in 1.5% glutaraldehyde in 0.1 mol/L cacodylate buffer for 1 h at room temperature, postfixed in 1% OsO₄ in the same buffer for 1 h at 4°C, dehydrated in a graded ethanol series, and embedded in epon. Ultrathin sections were poststained with uranyl acetate and lead citrate and viewed with a Tecnai 12 electron microscope at 80 kV (FEI).

Flow cytometry

Supernatant derived from Ad5.R1-scTCR-producing 293T-AdR cells (12.5 mL containing 10⁸ particles/mL) was incubated overnight with magnetic beads (DynaL Biotech ASA) that were loaded with *in vitro*-generated HLA-A1 complexes (1 µg total) presenting the MAGE-A1 nonapeptide (EADPTGHSY) or an irrelevant peptide derived from influenza virus A nucleoprotein (CTELKLSDY). After three wash steps with PBS, the beads were incubated with a saturating concentration of anti-hexon^{FITC} monoclonal antibody (mAb) and incubated for 30 min at 4°C. Specific binding of Ad5.R1-scTCR virus to the beads was then analyzed by flow cytometry on a Cytomics FC-500 flow cytometer (Beckman Coulter).

Western blotting

Ad5.R1-scTCR virus bound to the HLA-A1/MAGE-A1-coated magnetic beads was eluted from the beads by addition of high-affinity Fab fragments that specifically bind to HLA-A1/MAGE-A1 (15 min at room temperature, 39 µg total in 1 mL PBS).³⁴ Excess high-affinity Fab fragments were then removed by addition of Ni-NTA agarose (Qiagen) that binds to the 6× His tag present in the Fab fragment. Purified Ad5.R1-scTCR virus was then separated on SDS-PAGE, immobilized on a nitrocellulose membrane, and detected with fiber tail-specific mAb (4D2).

Detection of adenoviral infection

Flow cytometry of infected cells

One million cells were infected at indicated virus particle-to-cell ratios using virus supernatant diluted in DMEM supplemented with 10% FBS for 2 h at 37°C/5% CO₂. After infection, cells were seeded in six-well plates. Cells were harvested 2 days after infection by scraping, after which they were spun and permeabilized in FACSPerm2 solution (Becton Dickinson). Following a PBS wash, cells were incubated in the presence of FITC-hexon mAb (1:10 dilution) for 30 min at room temperature in the dark, washed again, and analyzed on a Cytomics FC-500 flow cytometer.

Methylene blue staining of infected cells

Half a million cells were infected using virus supernatant as described above. After infection, cells were seeded in gelatin-coated (0.1% gelatin in PBS) six-well plates in the presence of 2 mL 1.25% agar in DMEM culture medium. Cells were stained

with methylene blue 5 days (after infection) and photographed (LEICA DMIL inverted microscope).

Expression and localization of adenoviral proteins

A quarter of a million cells were infected using virus supernatant (at virus particle-to-cell ratio of 50) as described above. After infection, cells were seeded in 24-well plates and cultured for the indicated times. Cells were carefully washed with PBS and fixed with a 1:1 solution of ice-cold methanol and acetone for 10 min on ice. After repeated washing steps with PBS, cells were blocked using 1% bovine serum albumin in PBS for 30 min at room temperature. Cells were then shortly air dried and stained with primary and secondary antibodies (diluted in blocking buffer). Kinetics of expression and cellular localization of fluorescently labeled adenoviral proteins were monitored (LEICA DMIL inverted fluorescence microscope).

ACKNOWLEDGEMENTS

Grant support: European Union grant QLK3-1999-01262.

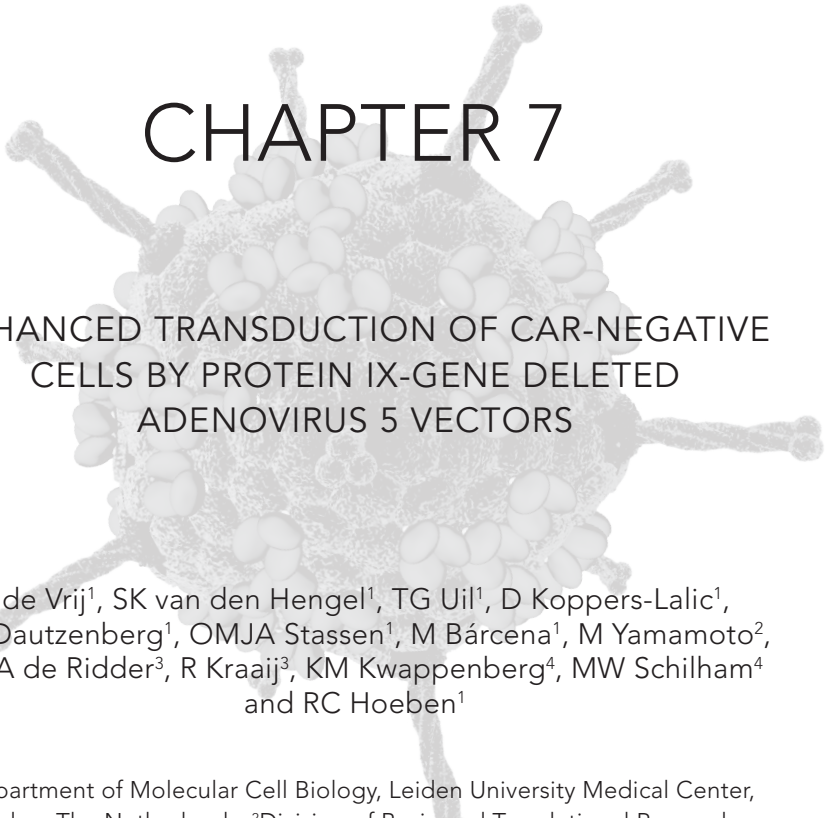
We thank Prof. Rob Hoeben (Virus and Stem Cell Biology Laboratory, Department of Molecular Cell Biology, Leiden University Medical Center, Leiden, the Netherlands) for helpful suggestions and critical reading of the manuscript, Mirjam Heuveling for technical assistance, and Ronald Limpens and Mieke Mommaas-Kienhuis for doing the electron microscopic analysis (Section Electron Microscopy, Leiden University Medical Center).

REFERENCES

1. Zinkernagel RM, Doherty PC. The discovery of MHC restriction. *Immunol Today* 1997; **18**: 14-17.
2. van der BP, Traversari C, Chomez P, et al. A gene encoding an antigen recognized by cytolytic T lymphocytes on a human melanoma. *Science* 1991; **254**: 1643-1647.
3. Boon T, Coulie PG, Van den Eynde B. Tumor antigens recognized by T cells. *Immunol Today* 1997; **18**: 267-268.
4. Schultz ES, Schuler-Thurner B, Stroobant V, et al. Functional analysis of tumor-specific Th cell responses detected in melanoma patients after dendritic cell-based immunotherapy. *J Immunol* 2004; **172**: 1304-1310.
5. Couly G, Creuzet S, Bennaceur S, Vincent C, Le Douarin NM. Interactions between Hox-negative cephalic neural crest cells and the foregut endoderm in patterning the facial skeleton in the vertebrate head. *Development* 2002; **129**: 1061-1073.
6. Lonchay C, van der Bruggen P, Connerotte T, et al. Correlation between tumor regression and T cell responses in melanoma patients vaccinated with a MAGE antigen. *Proc Natl Acad Sci USA* 2004; **101** Suppl 2: 14631-14638.
7. Scanlan MJ, Simpson AJ, Old LJ. The cancer/testis genes: review, standardization, and commentary. *Cancer Immunol* 2004; **4**: 1.
8. Renkvist N, Castelli C, Robbins PF, Parmiani G. A listing of human tumor antigens recognized by T cells. *Cancer Immunol Immunother* 2001; **50**: 3-15.
9. Nemunaitis J, Khuri F, Ganly I, et al. Phase II trial of intratumoral administration of ONYX-015, a replication-selective adenovirus, in patients with refractory head and neck cancer. *J Clin Oncol* 2001; **19**: 289-298.

10. Kanerva A, Hemminki A. Modified adenoviruses for cancer gene therapy. *Int J Cancer* 2004; **110**: 475-480.
11. Kanerva A, Wang M, Bauerschmitz GJ, et al. Gene transfer to ovarian cancer versus normal tissues with fiber-modified adenoviruses. *Mol Ther* 2002; **5**: 695-704.
12. Vellinga J, Rabelink MJWE, Cramer SJ, et al. Spacers increase the accessibility of peptide ligands linked to the carboxyl terminus of adenovirus minor capsid protein IX. *J Virol* 2004; **78**: 3470-3479.
13. Dmitriev IP, Kashentseva EA, Curiel DT. Engineering of adenovirus vectors containing heterologous peptide sequences in the C terminus of capsid protein IX. *J Virol* 2002; **76**: 6893-6899.
14. Gaden F, Franqueville L, Magnusson MK, et al. Gene transduction and cell entry pathway of fiber-modified adenovirus type 5 vectors carrying novel endocytic peptide ligands selected on human tracheal glandular cells. *J Virol* 2004; **78**: 7227-7247.
15. Henning P, Andersson KME, Frykholm K, et al. Tumor cell targeted gene delivery by adenovirus 5 vectors carrying knobless fibers with antibody-binding domains. *Gene Ther* 2005; **12**: 211-224.
16. Hong SS, Magnusson MK, Henning P, Lindholm L, Boulanger PA. Adenovirus stripping: a versatile method to generate adenovirus vectors with new cell target specificity. *Mol Ther* 2003; **7**: 692-699.
17. Magnusson MK, Hong SS, Boulanger P, Lindholm L. Genetic retargeting of adenovirus: novel strategy employing "deknobbing" of the fiber. *J Virol* 2001; **75**: 7280-7289.
18. Magnusson MK, Hong SS, Henning P, Boulanger P, Lindholm L. Genetic retargeting of adenovirus vectors: functionality of targeting ligands and their influence on virus viability. *J Gene Med* 2002; **4**: 356-370.
19. Nilsson M, Ljungberg J, Richter J, et al. Development of an adenoviral vector system with adenovirus serotype 35 tropism; efficient transient gene transfer into primary malignant hematopoietic cells. *J Gene Med* 2004; **6**: 631-641.
20. Krasnykh VN, Mikheeva GV, Douglas JT, Curiel DT. Generation of recombinant adenovirus vectors with modified fibers for altering viral tropism. *J Virol* 1996; **70**: 6839-6846.
21. Wickham TJ, Tzeng E, Shears LL, et al. Increased *in vitro* and *in vivo* gene transfer by adenovirus vectors containing chimeric fiber proteins. *J Virol* 1997; **71**: 8221-8229.
22. Jakubczak JL, Rollence ML, Stewart DA, et al. Adenovirus type 5 viral particles pseudotyped with mutagenized fiber proteins show diminished infectivity of coxsackie B-adenovirus receptor-bearing cells. *J Virol* 2001; **75**: 2972-2981.
23. Kirby I, Davison E, Beavil AJ, et al. Mutations in the DG loop of adenovirus type 5 fiber knob protein abolish high-affinity binding to its cellular receptor CAR. *J Virol* 1999; **73**: 9508-9514.
24. Borovjagin AV, Krendelchchikov A, Ramesh N, Yu DC, Douglas JT, Curiel DT. Complex mosaicism is a novel approach to infectivity enhancement of adenovirus type 5-based vectors. *Cancer Gene Ther* 2005; **12**: 475-486.
25. Willemsen RA, Debets R, Chames P, Bolhuis RLH. Genetic engineering of T cell specificity for immunotherapy of cancer. *Hum Immunol* 2003; **64**: 56-68.
26. Peng KW, Holler PD, Orr BA, Kranz DM, Russell SJ. Targeting virus entry and membrane fusion through specific peptide/MHC complexes using a high-affinity T-cell receptor. *Gene Ther* 2004; **11**: 1234-1239.
27. Willemsen RA, Weijtens ME, Ronteltap C, et al. Grafting primary human T lymphocytes with cancer-specific chimeric single chain and two chain TCR. *Gene Ther* 2000; **7**: 1369-1377.
28. Von Seggern DJ, Kehler J, Endo RI, Nemerow GR. Complementation of a fibre mutant adenovirus by packaging cell lines stably expressing the adenovirus type 5 fibre protein. *J Gen Virol* 1998; **79**: 1461-1468.
29. van Bergen BG, van der Ley PA, van Driel W, van Mansfeld AD, van der Vliet PC. Replication of origin containing adenovirus DNA fragments that do not carry the terminal protein. *Nucleic Acids Res* 1983; **11**: 1975-1989.
30. Douglas JT, Miller CR, Kim M, et al. A system for the propagation of adenoviral vectors with genetically modified

- receptor specificities. *Nat Biotechnol* 1999; **17**: 470-475.
31. Pecorari F, Tissot AC, Pluckthun A. Folding, heterodimeric association and specific peptide recognition of a murine $\alpha\beta$ T-cell receptor expressed in *Escherichia coli*. *J Mol Biol* 1999; **285**: 1831-1843.
 32. Willemsen RA, Debets R, Hart E, Hoogenboom HR, Bolhuis RL, Chames P. A phage display selected fab fragment with MHC class I-restricted specificity for MAGE-A1 allows for retargeting of primary human T lymphocytes. *Gene Ther* 2001; **8**: 1601-1608.
 33. Turatti F, Figini M, Alberti P, Willemsen RA, Canevari S, Mezzanica D. Highly efficient redirected anti-tumor activity of human lymphocytes transduced with a completely human chimeric immune receptor. *J Gene Med* 2005; **7**: 158-170.
 34. Chames P, Willemsen RA, Rojas G, et al. TCR-like human antibodies expressed on human CTLs mediate antibody affinity-dependent cytolytic activity. *J Immunol* 2002; **169**: 1110-1118.



CHAPTER 7

ENHANCED TRANSDUCTION OF CAR-NEGATIVE CELLS BY PROTEIN IX-GENE DELETED ADENOVIRUS 5 VECTORS

J de Vrij¹, SK van den Hengel¹, TG Uil¹, D Koppers-Lalic¹,
IJC Dautzenberg¹, OMJA Stassen¹, M Bárcena¹, M Yamamoto²,
CMA de Ridder³, R Kraaij³, KM Kwappenberg⁴, MW Schilham⁴
and RC Hoeben¹

¹Department of Molecular Cell Biology, Leiden University Medical Center,
Leiden, The Netherlands; ²Division of Basic and Translational Research,
Department of Surgery, University of Minnesota, Minneapolis, Minnesota, USA;
³Department of Urology, Erasmus Medical Center, Rotterdam, The Netherlands
and ⁴Department of Paediatrics, Leiden University Medical Center, Leiden,
The Netherlands

Virology 2011; 410:192-200

ABSTRACT

In human adenoviruses (HAdV), 240 copies of the 14.3-kDa minor capsid protein IX stabilize the capsid. Three N-terminal domains of protein IX form triskelions between hexon capsomers. The C-terminal domains of four protein IX monomers associate near the facet periphery. The precise biological role of protein IX remains enigmatic. Here we show that deletion of the protein IX gene from a HAdV-5 vector enhanced the reporter gene delivery 5 to 25-fold, specifically to Cocksackie and Adenovirus Receptor (CAR)-negative cell lines. Deletion of the protein IX gene also resulted in enhanced activation of peripheral blood mononuclear cells. The mechanism for the enhanced transduction is obscure. No differences in fiber loading, integrin-dependency of transduction, or factor-X binding could be established between protein IX-containing and protein IX-deficient particles. Our data suggest that protein IX can affect the cell tropism of HAdV-5, and may function to dampen the innate immune responses against HAdV particles.

INTRODUCTION

Protein IX is a non-essential protein in the capsid of human adenoviruses (HAdV). The protein has a size of 14.3 kDa, is present at 240 copies per virion, and has three highly conserved regions present in the amino (N) terminus, the central part (alanine-rich), and the carboxy (C) terminus (leucine-rich). The location and function of protein IX in the virus capsid has been the subject of investigation and debate for many years.¹ Recent work by different groups has brought consensus on its location and topology in the capsid.^{2,3} The N-terminus of the protein is located in between hexon cavities of the groups of nine (GON) hexons, presumably stabilizing the GONs. The C-terminus of the protein forms an alpha helix and is exposed on the capsid surface in close contact with hexon hypervariable region 4 (HVR4).³ C-terminal domains of three protein IX molecules associate in a parallel orientation, whereas a fourth domain binds in an antiparallel orientation.² The role of protein IX in the capsid remains enigmatic. *In vitro* analysis revealed the N-terminus of protein IX to confer a thermostable phenotype on HAdV-5 capsids.⁴ Propagation of protein IX gene deleted HAdV-5 in cell culture yields wild-type like virus titers, demonstrating that protein IX is dispensable for virus replication *in vitro*.

Protein IX has potential as an anchor for the attachment of different types of polypeptides to the viral capsid. Targeting of HAdV-5 to tumor cells has been achieved by genetically fusing protein IX to a single-chain T cell receptor directed against MHC class I in complex with MAGE-A1 peptides.⁵ Similarly, integrin-binding arginine-glycine-aspartate (RGD) peptides, as well as single-chain antibody fragments have been incorporated in this way.^{6,7} Alternatively, targeting ligands can be coupled to protein IX via the genetic inclusion of cysteine residues and subsequent chemical coupling of ligands to the reactive thiol groups.⁸ Multiple polypeptides can be incorporated simultaneously.⁹ A triple-mosaic HAdV-5 vector was developed with a poly-lysine motif, the herpes simplex virus type 1 (HSV-1) thymidine kinase, and the monomeric red fluorescent protein fused with protein IX, thereby combining targeting, therapeutic, and imaging modalities. Recently, it was demonstrated that HAdV-5 vaccine vectors with pathogen-specific antigens fused to pIX can stimulate robust protective immune responses in animals, suggesting a new route for the development of improved HAdV-5 based recombinant vaccines.^{10,11}

Here we report on the enhanced delivery of transgenes into CAR-negative cell lines as a result of protein IX-gene deletion from a HAdV-5-based vector. Furthermore, the protein IX-deficient particles demonstrated enhanced activation of peripheral blood mononuclear cells (PBMCs), and had a different *in vivo* distribution after intravenous delivery in a mouse model. The exact molecular mechanism behind this ' Δ pIX effect' remains to be delineated. Our data suggest that protein IX can affect the cell tropism of HAdV-5, and may function to dampen the innate immune responses against HAdV particles.

RESULTS

Enhanced transgene expression in CAR-negative cells with Ad5ΔE1ΔpIX

To study the role of protein IX in the HAdV-5 transduction of cells, we compared the vectors Ad5ΔE1+pIX and Ad5ΔE1ΔpIX for luciferase transgene expression in a panel of cell lines (**Fig. 1a**). Cell lines with varying expression levels of CAR were included (**Fig. 1b**). Whereas similar expression levels were obtained with both vectors in the CAR-positive cell lines HeLa, A549, and MEL2A, the vector Ad5ΔE1ΔpIX yielded higher levels than Ad5ΔE1+pIX in the CAR-negative cell lines MZ2-MEL3.0 and VH10. Since these results suggested a specific role of the protein IX lacking vector in mediating relatively higher transduction in the absence of CAR, Ad5ΔE1+pIX and Ad5ΔE1ΔpIX were analyzed for reporter gene expression in MZ2-MEL3.0 cells versus MZ2-MEL3.0/CAR cells (**Fig. 2B**). MZ2-MEL3.0/CAR cells stably expressed CAR via transduction with a recombinant lentivirus, which was confirmed by flow cytometry and immunofluorescence staining (**Fig. 2A**). In MZ2-MEL3.0 cells the reporter gene expression upon infection with Ad5ΔE1ΔpIX was found to be ten-fold increased compared to infection with Ad5ΔE1+pIX, while in MZ2-MEL3.0/CAR cells the difference was a mere two-fold (**Fig. 2b**). The enhanced transgene expression for Ad5ΔE1ΔpIX on the CAR-negative cell line MZ2-MEL3.0 appeared to be not affected by the establishment of protein IX expression in the cells (by using the recombinant lentivirus LV-CMV-pIX-IRES-NPTII¹²) prior to the transduction) (result not shown).

As a next step, the involvement of the C-terminal region of protein IX in the observed phenomenon was investigated. This domain, which is rich in leucine amino acids and is exposed on the HAdV-5 capsid as an alpha-helical structure,^{2,3} is highly conserved in human adenoviruses. The biological function of this conserved domain of protein IX is unknown. We analyzed the vector Ad5ΔE1pIX^{ΔLEU}, which lacks a major part of the C-terminal region of protein IX (amino acids 100 to 114) for reporter gene expression in MZ2-MEL3.0 and MZ2-MEL3.0/CAR. Ad5ΔE1pIX^{ΔLEU} demonstrated enhanced transduction of the CAR-negative cell line, very similar to the Ad5ΔE1ΔpIX vector (**Fig. 2c**).

To assess the appearance of the vector particles and to check for the absence of microaggregation, electron microscopy was performed on Ad5ΔE1+pIX and Ad5ΔE1ΔpIX vector batches. This showed identically shaped virus particles (**Fig. 3a**). No signs of microaggregation were observed. The Ad5ΔE1ΔpIX stock appeared to contain more small particulate matter, possibly virus debris. As previously described, pIX-deficient HAdV-5 particles have an enhanced tendency to partly dissociate into fiber- and penton base- lacking particles.¹³ However, our vectors had similar capsid incorporation levels of fiber and hexon proteins, as evident from immunoblot analyses (**Fig. 3b**), thus ruling out differences in particle dissociation for the vector preparations.

Transduction with Ad5ΔE1ΔpIX is integrin-dependent

Wild-type HAdV-5 enters cells via high affinity binding of the fiber knob domain to CAR.¹⁴ Subsequently low affinity interaction of the penton base with cellular integrins $\alpha_v\beta_3$ and $\alpha_v\beta_5$ promotes virus internalization in clathrin coated pits.^{15,16} To answer the question if Ad5ΔE1ΔpIX still uses integrins for cellular uptake, we analyzed

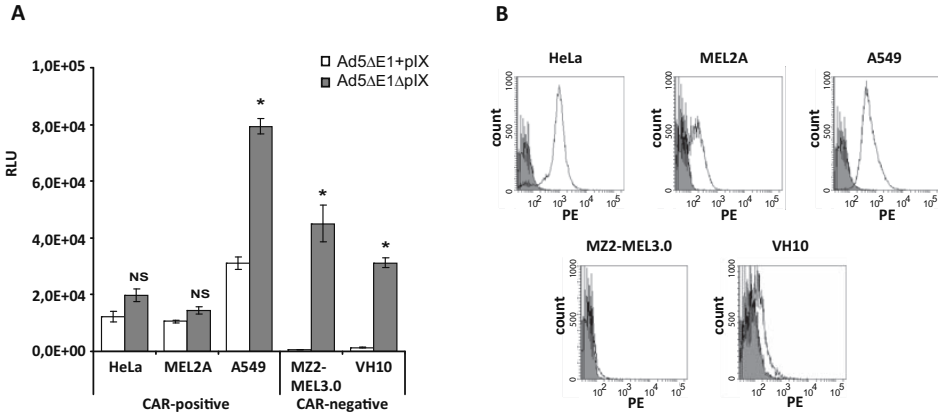


Figure 1. (a) Transduction of CAR-positive and CAR-negative cells with the replication deficient vectors Ad5ΔE1+pIX and Ad5ΔE1ΔpIX. At 24 hours post transduction (at 10 pp/cell) the luciferase expression was measured as indicated by the relative luciferase units (RLU) (NS signifies Not Significant, * $p < 0.02$ versus Ad5ΔE1+pIX). Error bars represent S.D. ($n=3$). (b) Flow cytometry with anti-CAR antibody and PE-labeled secondary antibody to analyze cell surface expression level of CAR (white histograms). The gray histograms represent incubation with secondary antibody only.

Ad5ΔE1+pIX and Ad5ΔE1ΔpIX for transgene expression (GFP) in the presence or absence of bivalent cations, which are necessary for integrin-mediated uptake of wild-type HAdV-5 into cells¹⁶ (**Fig. 4a**). This experiment again displayed a stronger reporter gene expression of Ad5ΔE1ΔpIX in MZ2-MEL3.0 cells compared to Ad5ΔE1+pIX. For both vectors the transduction appeared to be totally dependent on the presence of bivalent cations, with a complete reduction to background GFP levels for the cation-negative incubation. This is consistent with integrin-mediated uptake for both vectors. More specifically, the integrin-dependency of Ad5ΔE1ΔpIX was confirmed by a small but significant (approximately two-fold) decrease in transduction after incubation of MZ2-MEL3.0 cells with antibodies directed against $\alpha_v\beta_3$ and $\alpha_v\beta_5$ integrins (**Fig. 4b**). Similar antibody-blocking (1.5-fold reduced transduction for anti- $\alpha_v\beta_3$ and anti- $\alpha_v\beta_5$) was observed for Ad5ΔE1+pIX. Incubating the cells with higher concentrations of antibodies did not result in further reductions in transduction levels (data not shown). Anti-integrin mediated blocking of transduction was also observed on A549 cells (**Fig. 4b**). From these data we conclude that the vector Ad5ΔE1ΔpIX still uses integrins for cell internalization in CAR-deficient cells.

Reduced virus spread of the replication competent virus Ad5ΔpIX

Our data from the comparative transduction analysis suggest an alternative interaction of HAdV-5 particles lacking protein IX with the cell surface. In parallel to cell tropism extending capsid modifications described for other viruses¹⁷, it is likely that protein IX deletion from a replication competent HAdV-5 virus would result in a modified ability to spread in monolayer cell cultures. To investigate this, we constructed the replication-competent HAdV-5 viruses Ad5+pIX and Ad5ΔpIX. Both viruses expressed GFP, allowing accurate measurement of plaque size. On A549 cells the plaque size for

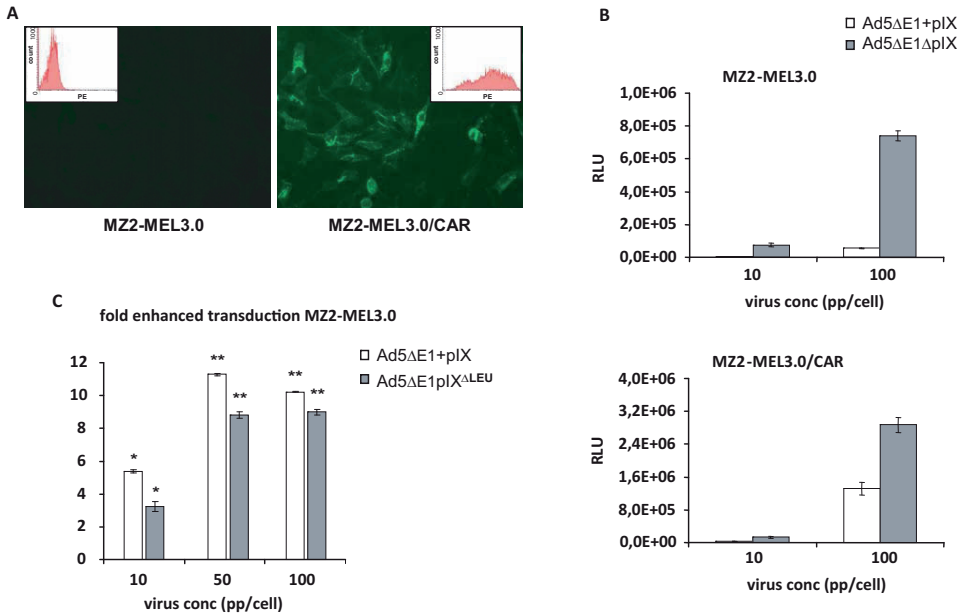


Figure 2. Transduction assays on MZ2-MEL3.0 and MZ2-MEL3.0/CAR (a) Detection of CAR expression in MZ2-MEL3.0 cells by immune-fluorescence staining with anti-CAR antibody and FITC-labeled secondary antibody. The insets represent flow cytometry histograms after staining with anti-CAR antibody and PE-labeled secondary antibody. (b) Luciferase expression in MZ2-MEL3.0 and MZ2-MEL3.0/CAR after Ad5ΔE1+pIX and Ad5ΔE1ΔpIX transduction. Error bars represent S.D. ($n=3$). (c) Fold enhancement of MZ2-MEL3.0 transduction with Ad5ΔE1ΔpIX and Ad5ΔE1ΔpIX^{ΔLEU} as compared to the transduction with Ad5ΔE1+pIX. The fold enhancements are normalized to the vector transduction ratios on MZ2-MEL3.0/CAR (* $p<0.05$, ** $p<0.005$ versus Ad5ΔE1+pIX). Errors bars represent S.D. ($n=3$).

the Ad5ΔpIX virus (median 30 arbitrary surface units (ASU), range 20-170) appeared to be significantly smaller than the plaque size for Ad5+pIX (median 100 ASU, range 30-290). A similar difference in plaque size was observed on the CAR-negative cell line VH10, with Ad5ΔpIX (median 50 ASU, range 30-150) yielding much smaller plaques compared to Ad5+pIX (median 100 ASU, range 75-280). From these analyses we conclude that protein IX-gene deletion from the genome of the replication competent virus results in a decrease in virus spread in CAR-positive (A549) as well as CAR-negative (VH10) monolayer cell cultures.

Enhanced activation of peripheral blood mononuclear cells by Ad5ΔE1ΔpIX

Our findings on the modified transduction characteristics of protein IX-deficient HAdV-5 vectors are of relevance for: (1) fundamental adeno-virology (as the findings point towards a novel biological function of protein IX), and (2) the development of protein IX-modified HAdV-5 vectors for gene therapies. For both these aspects, it will be highly interesting to determine the effect of protein IX-deletion on the interaction of HAdV-5 vectors with white blood cells. Therefore, we incubated freshly isolated

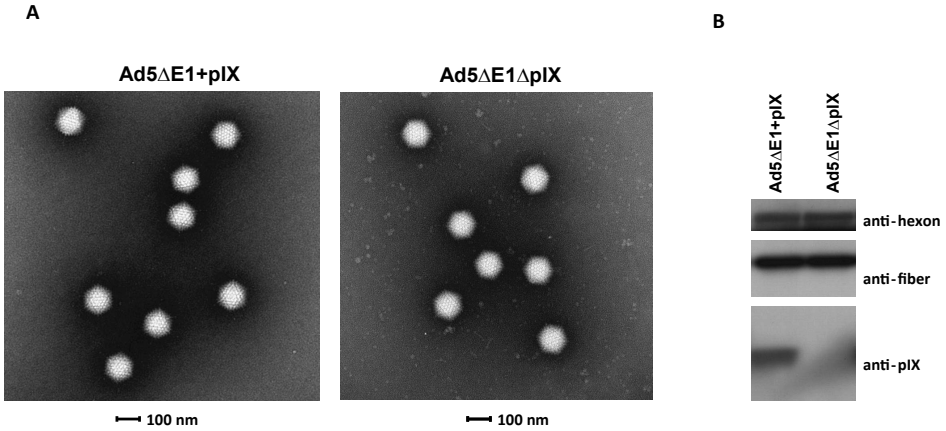


Figure 3. (a) Electron microscopy on Ad5ΔE1+pIX and Ad5ΔE1ΔpIX samples with negative staining of the vector particles in phosphotungstic acid. (b) Immunoblot detection on Ad5ΔE1+pIX and Ad5ΔE1ΔpIX lysates to analyze capsid incorporation levels of protein IX, hexon, and fiber proteins.

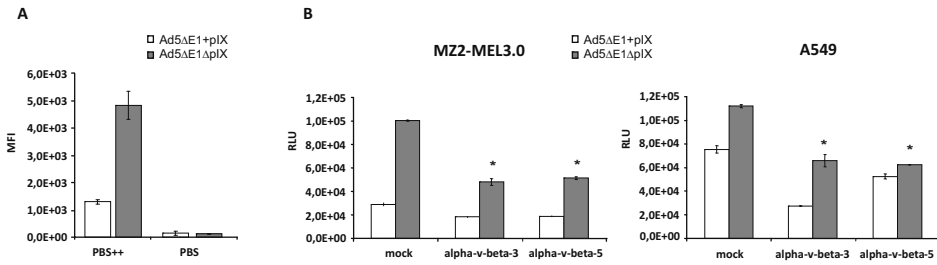


Figure 4. The effect of integrin blocking on transduction of cells with Ad5ΔE1+pIX and Ad5ΔE1ΔpIX. (a) MZ2-MEL3.0 cells were treated with EDTA to remove bivalent cations necessary for HAdV-5 interaction with integrins. Subsequent transduction was performed in the presence (PBS++) or absence (PBS) of bivalent cations and GFP expression was measured, as indicated by the mean fluorescence intensity (MFI). Error bars represent S.D. (n=3). (b) Vector mediated luciferase expression in MZ2-MEL3.0 and A549 cells in the presence or absence of antibodies directed against α V β 3 or α V β 5 integrins in the infection medium (*p<0.05 versus control treatment). Error bars represent S.D. (n=3).

human peripheral blood mononuclear cells with Ad5ΔE1+pIX and Ad5ΔE1ΔpIX, and analyzed GFP expression and the expression of cellular activation markers. This revealed relatively high levels of GFP expression in the monocyte population. The percentage of GFP-positive monocytes was similar for both vectors, varying between 10% and 30% at 100 pp/cell, depending on the donor (data not shown). For both vectors, the GFP expression in the T cell, B cell, and NK cell populations was very low (<1% GFP-positive cells). Although Ad5ΔE1+pIX and Ad5ΔE1ΔpIX showed identical GFP expression levels in the monocytes, the incubation with Ad5ΔE1ΔpIX resulted in a remarkably higher level of monocyte activation, as indicated by enhanced CD86 expression (Fig. 5a). The percentage of CD86 positive monocytes as well as the mean

fluorescence intensity for CD86 was significantly higher for the protein IX-lacking vector. This enhancement in monocyte activation was observed for monocytes derived from PBMCs of three different donors and with different virus batches. The up-regulated CD86 level involved the entire Ad5 Δ E1 Δ pIX-incubated monocyte population, not only the GFP-positive cells (**Fig. 5a**). Incubation with Ad5 Δ E1 Δ pIX also resulted in enhanced activation of NK cells, as demonstrated by an increase in CD69 expression (**Fig. 5b**). Interferon-gamma (IFN- γ) ELISA of PBMC supernatants revealed higher levels of IFN- γ production after incubation with Ad5 Δ E1 Δ pIX at the higher input virus levels (**Fig. 5c**).

Enhanced liver transduction upon intravenous administration of Ad5 Δ E1 Δ pIX

To study the functional consequences of protein IX gene deletion on biodistribution in mice, Ad5 Δ E1+pIX and Ad5 Δ E1 Δ pIX viruses were administered via tail vein injection. Luciferase expression in multiple organs was determined at 3 days post injection.

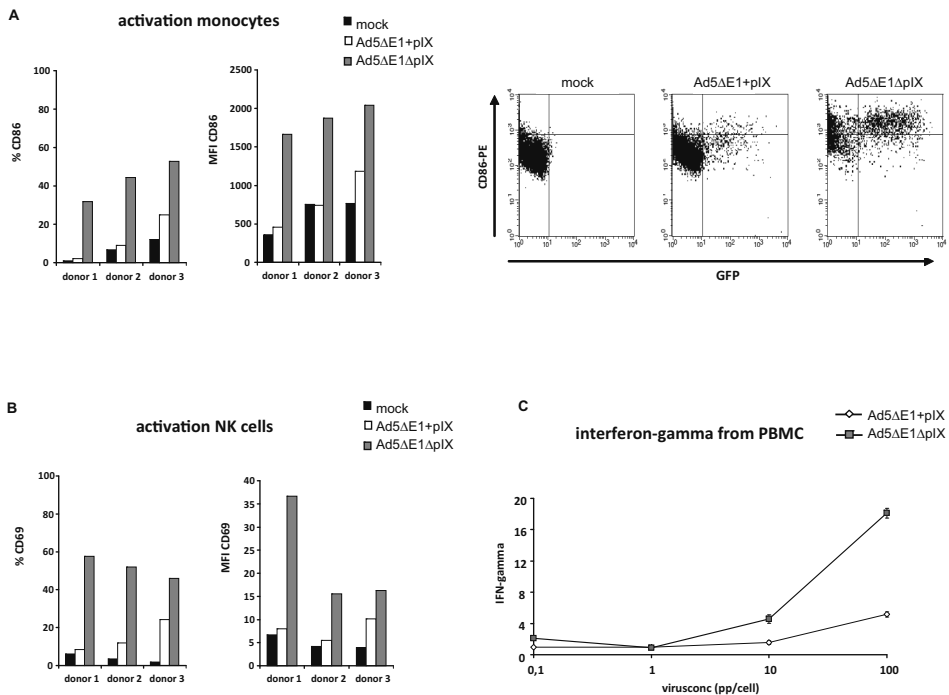


Figure 5. Activation of peripheral blood mononuclear cells (PBMCs) after incubation with Ad5 Δ E1+pIX and Ad5 Δ E1 Δ pIX for two days. **(a)** Activation of the monocyte population. The graphs on the left show the percentage of CD86 positive cells and the mean CD86 expression levels (MFI) for three different donors. The flow cytometry figures on the right illustrate the CD86 up-regulation for transduced (GFP-positive) monocytes and non-transduced (GFP-negative) monocytes (from donor 1). **(b)** Activation of the NK cell population. The percentage of CD69 positive cells and the mean CD69 expression levels (MFI) are shown for three different donors. **(c)** Measurement of IFN- γ levels in PBMC supernatant (from a single donor) after incubation with Ad5 Δ E1+pIX and Ad5 Δ E1 Δ pIX. The data represent mean values of two independent measurements.

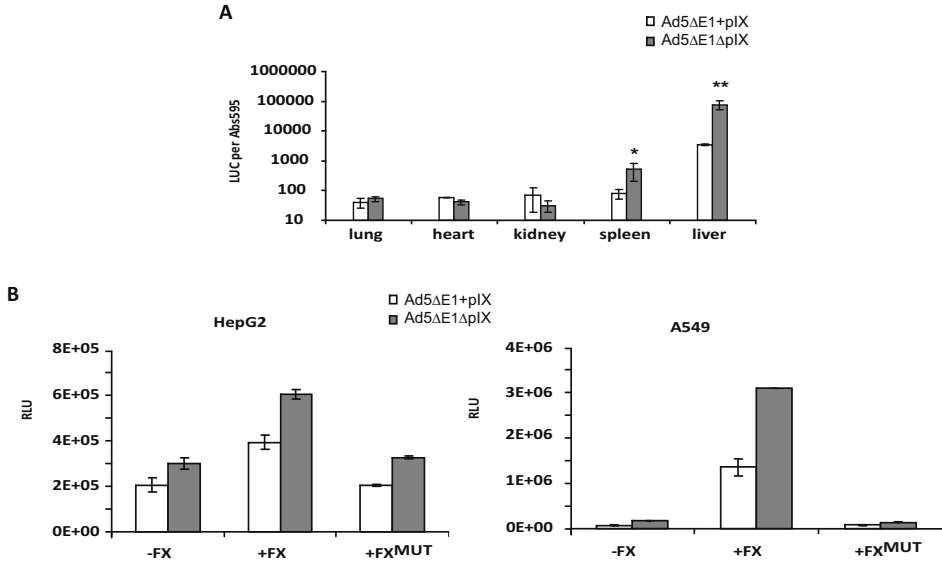


Figure 6. (a) Distribution of Ad5ΔE1+pIX and Ad5ΔE1ΔpIX in mice after tail vein injection of 10^9 vector particles. Prior to vector injection, pre-dosing was performed with the vector HAdV-5.CMV to saturate Kupffer cell macrophages. Organs were harvested three days post injection and the luciferase expression per total protein was measured (* $p=0.057$, ** $p=0.006$ versus Ad5ΔE1+pIX). Error bars represent S.D. ($n=2$). (b) Luciferase expression in HepG2 and A549 cells after transduction with Ad5ΔE1+pIX and Ad5ΔE1ΔpIX in the presence of coagulation factor X (FX), Gla-domainless mutant factor X (FX^{MUT}), or no coagulation factors (mock). Error bars represent S.D. ($n=3$).

The vector lacking protein IX yielded a more than ten-fold higher luciferase activity in the liver (**Fig. 6a**). These data show that the absence of protein IX in the viral capsid strongly affected the biodistribution of HAdV-5 particles.

Recent reports have described the involvement of plasma proteins, such as the blood coagulation factor X (FX), in HAdV-5 transduction of the liver.^{18,19} To study whether removal of protein IX influences the effects of clotting-factor binding, we compared the FX-mediated transduction for Ad5ΔE1+pIX and Ad5ΔE1ΔpIX (**Fig. 6b**). *In vitro* incubation of A549 cells and HepG2 cells with FX resulted in a similar enhancement in transduction for Ad5+pIX and Ad5ΔpIX. As expected, no effect on transduction was observed after incubation with the mutant FX (FX^{MUT}), which lacks the domain necessary for binding to the HAdV-5 capsid.¹⁹ From these data we conclude that the absence of protein IX does not affect the binding of coagulation factor X.

DISCUSSION

From our data we conclude that the omission of protein IX from HAdV-5 vectors enhances viral transduction of cell lines that are low in expression of the adenovirus receptor CAR. This finding is of relevance for the development and implementation of protein IX-gene modified HAdV-5 vectors. Also, the findings enhance our knowledge

on HAdV-5 biology and evolution, which especially becomes clear if stating our conclusion in a 'backwards' manner: the introduction of protein IX in HAdV-5 (making it wild-type HAdV-5) decreases viral transduction of cell lines that are low in CAR expression. Although speculative, it is very well possible that the presence of protein IX in the HAdV-5 capsid negatively interferes with non-specific cell transduction, and thereby plays a role in determining the virus tropism. Noteworthy, the extended cell tropism of the Ad5ΔE1ΔpIX vector, as presented by its enhanced transduction of CAR-negative cells, did not come with a loss in ability of CAR-mediated transduction of cells. This is clear from the comparison on MZ2-MEL3.0 and MZ2-MEL3.0/CAR. Introduction of CAR in the CAR-negative cells significantly increased transduction levels with Ad5ΔE1ΔpIX. It is conceivable that in CAR-expressing cells the protein IX-deficient particles can use either the CAR/fiber-dependent mechanism, or the CAR-independent pIX-dependent mechanism. Quantifying the relative contribution of each of these mechanisms to the total transduction requires tools for specifically blocking the new pathway. Such inhibitors remain to be identified.

Interestingly, the vector Ad5ΔE1pIX^{ALEU} had Ad5ΔE1ΔpIX-like properties, implicating the importance of the C-terminal domain of protein IX in inhibiting transgene expression in CAR-negative cell lines. The specificity for the C-terminal domain of protein IX excludes differences in viral capsid stability as a cause for the observed phenomenon, since deletion of this domain does not result in reduced capsid stability.⁴

Wild-type HAdV-5 enters cells via high affinity binding of the fiber knob domain to CAR,¹⁴ followed by interaction of the RGD motif of the penton base with cellular integrins $\alpha_v\beta_3$ and $\alpha_v\beta_5$ promoting rapid adenovirus cell entry into clathrin-coated vesicles.^{15,16} Similar to the Ad5ΔE1+pIX control virus, Ad5ΔE1ΔpIX requires the presence of bivalent cations for its transgene delivery, indicating the usage of cellular integrins for cell internalization.¹⁶ More specifically, blocking cells with anti-integrin antibodies resulted in a decrease in transduction for Ad5ΔE1ΔpIX, thereby confirming the integrin-dependency. Unfortunately, our efforts to compare the vectors for a general difference in cell binding affinity, using Alexa488-TFP (tetrafluorophenyl) labeled vector particles, were not conclusive as a result of strong and reproducible negative effects of the labeling procedure on the pIX-deficient vector particles. The effects were not identical for protein IX-positive and protein IX-negative particles, making the results obtained with these particles in comparative binding assays unreliable. Alternative protocols for fluorescent- or radio-labeling of vector particles might be more suitable for comparing the cell-binding affinity. Labeled vector particles might also be used for analysing differences in cell surface motility between protein IX-containing and protein IX-lacking vectors. Through largely unknown mechanisms HAdV-5 particles migrate on the cell surface and alterations in viral movement can result in modified transduction.²⁰

The removal of the protein IX gene from a replication competent HAdV-5 virus results in a small-plaque phenotype on CAR-positive as well as CAR-negative cell lines. This suggests the tropism modifying mutation affects the virus's capacity to spread from cell to cell. Such small-plaque phenotypes of extended tropism mutants is not unprecedented: similar phenotypes have been described for murine corona virus mutants that acquired the capacity to bind heparin.¹⁷

To investigate the effect of protein IX-gene deletion on the interaction of HAdV-5 with human mononuclear leukocytes, we compared the vectors Ad5ΔE1+pIX and Ad5ΔE1ΔpIX for GFP expression in PBMCs. Flow cytometry analyses demonstrated GFP expression almost exclusively in monocytes, with similar expression levels for both vectors. However, increased activation of the entire monocyte population (so not exclusively restricted to the GFP-positive population) was observed for Ad5ΔE1ΔpIX, as demonstrated by an enhancement in CD86 expression. CD86 is an activation marker on antigen-presenting cells such as monocytes, macrophages, dendritic cells, and B cells, and is important for co-stimulation of T cells.²¹ The increased activation of monocytes despite similar levels of transduction (GFP expression) could be due to a direct effect on the monocytes themselves or indirectly via a more efficient stimulation of T cells or NK cells. Uptake of the protein IX-deleted vector may be increased and/or may follow different intracellular trafficking routes.^{22,23} As a consequence, more efficient viral antigen loading onto human leukocyte antigen (HLA) molecules, or an increase in CD86 expression, could lead to more T cell activation, and e.g. IFN-γ secretion. Of note, most healthy adult donors have HAdV specific T cells.²⁴ Indeed, Ad5ΔE1ΔpIX incubation resulted in enhanced production of IFN-γ. Protein IX-gene deletion appeared to affect NK cell activation as well, resulting in increased expression levels of CD69, which is an activation marker for lymphocytes including NK cells.²⁵ Increased T cell activation could have been accompanied by increased levels of other T cell cytokines like interleukin-2 (IL-2). IL-2 is a known activating cytokine of NK cells.^{26,27} Alternatively, the increased production of IFN-γ in the supernatant would also be consistent with increased activation of NK cells by the vector lacking protein IX, without the involvement of T cells.

Irrespective of the mechanism, the increased activation of monocytes and NK cells as a result of protein IX deletion is likely to have important consequences for the *in vivo* implementation of protein IX modified HAdV-5 vectors, since monocytes (after differentiation to Kupffer macrophages in the liver) as well as NK cells are important players in the sequestration of HAdV-5 vectors from the blood after systemic delivery (reviewed by Muruve²⁸). Furthermore, the observed differences in PBMC activation between Ad5ΔE1+pIX and Ad5ΔE1ΔpIX suggest a biological function of protein IX in diminishing the immune response against HAdV-5. Further studies will be necessary to fully determine the effects of protein IX deletion from HAdV-5 on the activation of immune cells.

Omission of protein IX from the capsid resulted in a remarkable difference between Ad5ΔE1+pIX and Ad5ΔE1ΔpIX upon intravenous administration in mice. Administration of Ad5ΔE1ΔpIX yielded more than ten-fold higher luciferase activity in the liver, for reasons that remain to be clarified. Extensive research has been devoted to defining the molecular mechanisms behind the sequestration of intravenously administered HAdV-5 in the human liver, with the aim to eventually improve the therapeutic efficacy of intravenously delivered HAdV-5 vectors (reviewed by Di Paolo and Shayakhmetov²⁹). The uptake of HAdV-5 in the liver has been found to occur in a CAR-independent manner and involves binding of the virus particles in the blood to complement factors and immunoglobulins (mediating uptake in Kupffer cell macrophages),^{18,30} and coagulation factors (resulting in hepatocyte transduction).^{18,19} The enhanced transduction of the liver with Ad5ΔE1ΔpIX observed in our mouse

model seems not to be a result of more efficient binding of the vector to coagulation factor X (FX), as can be concluded from our *in vitro* FX-binding assay. An alternative explanation might be that the absence of protein IX extends the HAdV-5 tropism, enabling the transduction of cells in the liver that do not present CAR. Of interest, primary human hepatocytes were recently found to have CAR localized at cellular junctions that are inaccessible to the hepatic blood flow.³¹ This localization is in contrast to the CAR molecules on hepatocellular carcinoma cells (like HepG2), being highly available for HAdV-5 binding.^{31,32}

Protein IX is strongly conserved in all primate adenoviruses indicating the importance of the protein. A biological role for protein IX in HAdV-5 capsid stabilization has been proposed, based on *in vitro* heat-stability assays.⁴ Our findings point toward other biological functions of protein IX in (i) determining the cell tropism of HAdV-5, and (ii) negatively interfering with the innate immune response against HAdV-5. More insight into the mechanisms by which the presence of protein IX affects gene transfer and activation of immune cells may be of use for enhancing the efficiency of current (e.g.³³) and future gene therapies involving protein IX modified HAdV-5 vectors.

MATERIALS AND METHODS

Cell lines

All cell lines were maintained as monolayers at 37°C in a humidified atmosphere of 5% CO₂. The human cell lines HeLa (cervical cancer), A549 (carcinomic alveolar epithelium), MEL2A (melanoma), MZ2-MEL3.0 (melanoma),⁵ VH10 (primary foreskin fibroblasts),³⁴ HepG2 (hepatocellular carcinoma), and 911 cells (HAdV-5 E1-transformed human embryonic retinoblasts)³⁵ were maintained in Dulbecco's Modified Eagle's Medium (DMEM) (Gibco-BRL, Breda, The Netherlands) supplemented with 8% fetal bovine serum (FBS) (Gibco-BRL, Breda, The Netherlands) and penicillin-streptomycin mixture.

Lentivirus transduction was used to create a MZ2-MEL3.0 cell line stably expressing human CAR. To this end, the CAR gene was PCR-amplified by using primers 1 and 2 (**Table 1**) from plasmid pCMV_hCAR (kindly provided by Dr. J.M. Bergelson¹⁴). The *Pst*I+*Nhe*I digested PCR product was ligated in between the corresponding restriction sites of pLV.CMV.IRES.PURO³⁶, resulting in pLV.CMV.CAR.IRES.PURO. The virus LV.CMV.CAR.IRES.PURO was produced by a previously described procedure involving cotransfection of pLV.CMV.CAR.IRES.PURO together with helper plasmids encoding HIV-1 gag-pol, HIV-1 rev, and the VSV-G envelope³⁷. The methods for determining the titer of the LV.CMV.CAR.IRES.PURO vector stock and the procedures for transduction of the MZ2-MEL3.0 cells have been described before³⁶. Selection for antibiotic resistance was achieved by seeding the cells in medium with 0.6 µg/ml puromycin (MP Biomedicals, Amsterdam, The Netherlands).

Viruses

The vectors HAdV-5.CMV.GFP/LUC¹² (Ad5ΔE1+pIX) and HAdV-5ΔpIX.CMV.GFP/LUC¹² (Ad5ΔE1ΔpIX) contain a green fluorescent protein (GFP) gene as well as a firefly luciferase (LUC) gene, which are both driven by a human cytomegalovirus (CMV) promoter. The vector HAdV-5pIXΔ100-114.CMV.LUC (Ad5ΔE1pIX^{ΔLEU}), encoding LUC

only, was described previously as well.⁴ Titration of the vector stocks was performed by a PicoGreen-DNA binding assay to determine the concentration in physical vector particles per ml (pp/ml).³⁸ A standard agar overlay plaque assay on 911 cells was used to determine the infectious virus concentration in plaque forming units per ml (pfu/ml).³⁵ The pp/pfu ratios of the three vectors were very similar, within the range of 10 to 12.

The replication-competent viruses HAdV-5.ΔE3.ADP.eGFP (Ad5+pIX) and HAdV-5.ΔE3.ADP.eGFP.ΔpIX (Ad5ΔpIX) were constructed by recombination of the shuttle plasmids pShuttle+E1+pIX (pSh+pIX) and pShuttle+E1ΔpIX (pShΔpIX) with a HAdV-5 backbone plasmid containing the eGFP gene in the E3 region (pBB). The plasmids pSh+pIX, pShΔpIX and pBB were constructed as follows. The wild-type HAdV-5 *BsrGI-MfeI* fragment containing the E1 genes (nucleotides 193-3925) was isolated from pTG3602 (kindly provided by Dr. M. Luski, Transgene, Strasbourg, France), and cloned into the *BsrGI-MfeI* digested pTrackCMV-GFP/LUC,¹² thereby replacing the GFP/LUC genes with the HAdV-5 E1 region. By using site-directed mutagenesis (QuikChange site-directed mutagenesis kit; Stratagene) (primers 3, 4, 5, 6 (**Table 1**)) two restriction sites were introduced in the protein IX gene; a *Scal* site at the start codon of protein IX and a *SpeI* site upstream of the protein IX stop codon, thereby creating pShuttle+E1+pIX^{Scal/SpeI}. Next, the pShΔpIX plasmid was constructed by *Scal/SpeI* digestion and re-ligation of the protein IX gene-deleted fragment. The pSh+pIX plasmid was created by introducing the protein IX sequence (amplified from pAd5pIX⁷ by using primers 7 and 8 (**Table 1**)) into the *Scal/SpeI* linearized pShuttleE1+pIX^{Scal/SpeI}. The *Scal*-site was restored to the wild-type HAdV-5 sequence by exchanging the *Scal*-overlapping *MfeI/HindIII* fragment with the corresponding fragment from pTG3602. The *SpeI* site and the downstream 'pIX-remainder sequence' were left intact, since part of this sequence forms a hairpin-loop structure situated over the polyA site of the E1B transcript, which might be essential for efficient polymerase slippage needed for polyadenylation.³⁹

The pBB backbone plasmid was constructed by replacing the E3-lacking *SpeI-PacI* fragment (nucleotides 27238-33443) of pAdEasy-1⁴⁰ with the corresponding *SpeI-PacI* fragment of pShuttle-ΔE3-ADP-EGFP-F2⁴¹, thereby introducing eGFP in the E3 region under control of the viral major late promoter. The coding sequence for the E3 Adenovirus Death Protein (ADP) was retained. The kanamycin resistance gene (inserted with the pShuttle-ΔE3-ADP-EGFP-F2 fragment) was removed by *Clal* digestion and re-ligation of the two largest fragments.

Recombination of pBB with pSh+pIX and pShΔpIX in *E.coli* and subsequent virus rescue in A549 cells were performed as described elsewhere.⁴⁰ Virus was purified by a standard double cesium chloride gradient protocol, dialyzed against sucrose buffer (5% sucrose, 140 mM NaCl, 5 mM Na₂HPO₄·2H₂O, 1.5 mM KH₂PO₄) and stored at -80°C. The virus titer was determined by the PicoGreen-DNA binding assay³⁸ (for pp/ml measurement), and a plaque assay on A549 cells³⁵ (for pfu/ml measurement). For analysis of virus spread, GFP positive plaques were photographed (Olympus Camedia Digital Camera C-3030, installed on an Olympus CK40 microscope) and the plaque size was determined in arbitrary units (Olympus DP-soft v.5.0 Soft imaging System software). The median plaque size of Ad5ΔpIX was normalized to the plaque size for Ad5+pIX.

Table 1. Oligonucleotides used in the cloning procedures.

FWD CAR_PstI	5'-GATGTACTGCAGATGGCGCTCCTGCTGTG-3'
REV CAR_NheI	5'-CGACGCTAGCTATACTATAGACCCATCCTTGCTCTG-3'
FWD Scal_correct	5'-TTGCAGCAGCCGCCGCCAGTACTAGCACCAACTCGTTTGATGG-3'
REV Scal_correct	5'-CCATCAAACGAGTTGGTGCTAGTACTGGCGGCGGCGGCTGCTGCAA-3'
FWD SpeI_correct	5'-GGTTTCTGCCCTGAAGGCTTACTAGTCTCCCAATGCGGTTTAAAC-3'
REV SpeI_correct	5'-GTTTTAAACCGCATTGGGAGACTAGTAAGCCTTCAGGGCAGAAACC-3'
FWD pIX_Scal	5'-CGCGGAAGTACTATGAGCACCAACTCGTTTGATGG-3'
REV pIX_SpeI	5'-CGCACTAGTTTAAACCGCATTGGGAGGGGAGG-3'

Analysis of CAR presentation on the cell surface

Flow cytometry was performed to determine the levels of CAR presentation on the cell surface. Cells in suspension (in PBS with 0.5% bovine serum albumin and 0.02% sodium azide) were incubated with mouse monoclonal anti-CAR antibody (clone Rmcb, Upstate Biotechnology, Lake Placid, NY, diluted 1:1000) for 30 min on ice, followed by incubation with phycoerythrin (PE)-conjugated rabbit-anti-mouse secondary antibody (Caltac Laboratories, Burlingame, CA, USA) for 30 min on ice. Flow cytometry data were analyzed with CellQuest software (Becton Dickinson).

Immunohistochemistry was performed on the cell line MZ2-MEL3.0/CAR. After washing with phosphate-buffered saline (PBS), the cells were fixed in acetone/methanol (1:1) for 10 min at room temperature. Staining was performed with the anti-CAR antibody (clone Rmcb, Upstate Biotechnology, Lake Placid, NY, diluted 1:500). Fluorescein isothiocyanate (FITC)-conjugated rabbit-anti-mouse antibody (Jackson ImmunoResearch, France) was used as secondary antibody.

Virus transduction assays

(1) Luciferase expression

The transduction efficiency of CAR-positive (HeLa, A549, MEL2A, MZ2-MEL3.0/CAR) and CAR-negative (MZ2-MEL3.0, VH10) cell lines by Ad5ΔE1+pIX and Ad5ΔE1ΔpIX was compared by measuring luciferase expression. Transduction was performed in triplicate in 24-well plate wells in 500 μl DMEM/8% FBS. After a two-hours incubation the virus-containing medium was replaced with fresh medium without virus. At 24 hours post transduction the cells were washed once with PBS and lysed in 100 μl LUC-lysis mix (25 mM Tris-phosphate (pH 7.8), 2 mM CDTA, 2 mM DTT, 10% glycerol and 1% Triton-X in PBS). Luciferase production was determined with the Promega Luciferase Assay by adding 25 μl luciferase assay reagent to 10 μl lysate. Light intensity measurement was performed in a Victor Wallac 2 microplate reader (PerkinElmer, Inc., Waltham, MA, USA).

(2) Integrin blocking

Indirect blocking of integrin-mediated virus uptake was performed by incubating cells with EDTA. MZ2-MEL3.0 cells were harvested from semi-confluent tissue culture plates, washed three times in PBS with 5 mM EDTA, and resuspended in standard PBS

or PBS supplemented with 0.9 mM CaCl₂ and 0.5 mM MgCl₂ (PBS⁺⁺). The Ad5ΔE1+pIX and Ad5ΔE1ΔpIX stocks were adjusted to equal pp concentrations by adding sucrose buffer and were diluted 1:1 in a 5 mM EDTA solution in PBS. Virus (100 pp/cell) was added to 500,000 cells in 1 ml PBS or PBS⁺⁺ and incubation was performed for 60 min at 37°C under constant agitation. Subsequently, the cells were pelleted by centrifugation, dissolved in 5 ml medium and transferred to 24-well plate wells (500 μl per well). Cells were incubated for 24 hours and analyzed for GFP expression by flow cytometry. Data were analyzed with CellQuest software (Becton Dickinson).

The anti-human CD51/61 monoclonal antibody (MAb LM609), an αVβ3 integrin antagonist, and MAb P1F6, an αVβ5 integrin antagonist (both obtained from Millipore) were used to test the inhibitory effect of anti-integrin antibodies on virus transduction. Cells grown as monolayers were pre-incubated with medium only or with medium containing integrin function-blocking MAbs (10 mg/ml). After 30 min of incubation, the excess antibody was removed by gentle washing followed by virus transduction (100 pp/cell). Reporter gene expression was measured 24 hours post transduction by performing a standard luciferase assay.

(3) *Virus incubation with coagulation factor X (FX)*

HepG2 and A549 cells were plated in 24-well plate wells. After a PBS wash step, Ad5ΔE1+pIX or Ad5ΔE1ΔpIX (100 pp/cell) was added in serum-free medium containing 8 μg/ml Factor X (FX) (HCX-0050, Haemotologic Technologies Inc.), 8 μg/ml Gla-domainless Factor X (FX^{MUT}) (HCX-GD, Haemotologic Technologies Inc.) or no FX/FX^{MUT}. After 2 hours the medium was replaced by normal medium. Luciferase expression was measured 24 hours post transduction.

Immunoblot analysis and electron microscopy

Immunoblot analyses were performed to assess the incorporation of proteins into the capsid of Ad5ΔE1+pIX and Ad5ΔE1ΔpIX. The western blotting and detection procedures were described previously.⁵ Virus lysates were prepared by adding 5×10⁹ virus particles directly to western sample buffer. Capsid proteins were visualized with rabbit polyclonal anti-protein IX serum (1:2000,⁴² goat polyclonal anti-hexon (1:1000, ab19998, Abcam, Cambridge, UK), and mouse monoclonal anti-fiber (1:5000, 4D2, Abcam).⁴³ Secondary antibodies were horseradish peroxidase (HRP)-conjugated goat-anti-rabbit and rabbit-anti-mouse (Santa Cruz Biotechnology, Inc., Santa Cruz, CA, USA).

Electron microscopy was performed on Ad5ΔE1+pIX and Ad5ΔE1ΔpIX samples adsorbed into glow-discharged carbon coated copper grids and negatively stained for 30 seconds with 2% phosphotungstic acid (pH 7). The viruses were examined with a FEI Tecnai Spirit BioTwin transmission electron microscope operating at 120 kV. Images were recorded on a 4k × 4k Eagle CCD camera.

PBMC analysis

Buffy coats were obtained from healthy donors after consent (Sanquin Bloodbank, Leiden, The Netherlands) and centrifuged on a Ficoll gradient to obtain PBMC. PBMC (1 × 10⁶) were added to a well of a 24-well plate in 0.5 ml medium (RPMI/10%FCS) and virus was added at the indicated MOI in 0.5 ml medium. After incubation at 37°C and 5% CO₂ for two days, the supernatants were isolated for interferon gamma (IFN-γ) measurement, and the cells were prepared for flow cytometry analysis. Cells were

washed twice with PBS/0.02% sodium azide, fixed for 10 min in 4% paraformaldehyde, washed twice with PBS/0.5% BSA/0.02 sodium azide, and stained with antibodies. Antibodies used were anti-CD3-PerCP-Cy5.5, anti-CD4-PE, anti-CD14-APC, anti-CD14-PerCP-Cy5.5, anti-CD19-PE, anti-CD19-PerCP-Cy5.5, anti-CD69-PE and anti-CD86-PE (Becton Dickinson, Franklin Lakes, NJ, USA), anti-CD8-APC and anti-CD56-APC (Beckman Coulter, Brea, CA, USA). Activation of NK cells was evaluated as increased CD69 expression on CD3-, CD14-, CD19-, CD56+ cells. Monocyte activation was analyzed as increased CD86 expression on CD3-, CD19-, CD14+ cells. Fluorescence was measured by flow cytometry on a FACS Calibur (Becton Dickinson) and data were analyzed with CellQuest software (Becton Dickinson). IFN- γ in supernatants was measured by ELISA using the PeliPair reagent set for human IFN- γ (Sanquin, Amsterdam, NL).

Viral distribution after intravenous delivery

Ad5 Δ E1+pIX or Ad5 Δ E1 Δ pIX (10^9 pp) was injected in the tail vein of 6-week-old athymic nude mice (NMRI nu/nu; Taconic M&B A/S, Ry, Denmark), followed by sacrificing the animals and harvesting of multiple organs at 3 days post injection. Four hours before Ad5 Δ E1+pIX and Ad5 Δ E1 Δ pIX injection, pre-dosing was performed with the empty vector HAdV-5.CMV (replication-deficient and not encoding a transgene) (5×10^{10} pp) to saturate Kupffer cell macrophages. Tissue samples from each organ were lysed in LUC-lysis mix and the luciferase expression was measured according to the Promega Luciferase Assay. The protein concentration in the lysates was determined by using the bicinchoninic acid protein assay (Pierce, Perbio Science BV, Etten-Leur, The Netherlands), enabling the calculation of luciferase expression per total protein. The experiment was performed under the Dutch Experiments on Animals Act that serves the implementation of "Guidelines on the protection of experimental animals" by the Council of Europe (1986), Directive 86/609/EC, and only after a positive recommendation by the Animal Experiments Committee.

ACKNOWLEDGEMENTS

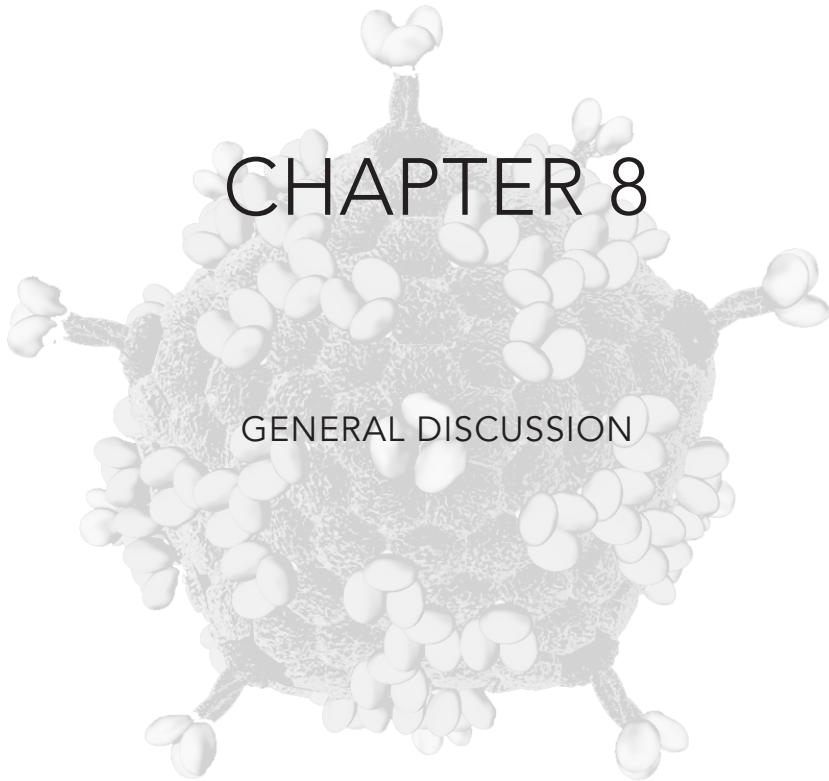
We thank Jort Vellinga and Vivien Mautner for valuable scientific discussions and critically reading the manuscript, Steve Cramer for expert technical support, and Martijn Rabelink for producing the viruses used in these studies. This work was supported by the European Union through the 6th Framework Program GIANT (contract no. 512087).

REFERENCES

1. Vellinga J, Van der Heijdt S, Hoeben RC. The adenovirus capsid: major progress in minor proteins. *J Gen Virol* 2005; **86**: 1581-1588.
2. Fabry CMS, Rosa-Calatrava M, Moriscot C, Ruigrok RWH, Boulanger P, Schoehn G. The C-terminal domains of adenovirus serotype 5 protein IX assemble into an antiparallel structure on the facets of the capsid. *J Virol* 2009; **83**: 1135-1139.
3. Saban SD, Silvestry M, Nemerow GR, Stewart PL. Visualization of alpha-helices in a 6-angstrom resolution cryoelectron microscopy structure of adenovirus allows refinement of capsid protein assignments. *J Virol* 2006; **80**: 12049-12059.
4. Vellinga J, van den Wollenberg DJM, van der Heijdt S, Rabelink MJWE, Hoeben RC. The coiled-coil domain of the adenovirus type 5 protein IX is dispensable for capsid incorporation and thermostability. *J Virol* 2005; **79**: 3206-3210.
5. de Vrij J, Uil TG, van den Hengel SK, Cramer SJ, Koppers-Lalic D, Verweij MC et al. Adenovirus targeting to HLA-A1/MAGE-A1-positive tumor cells by fusing a single-chain T-cell receptor with minor capsid protein IX. *Gene Ther* 2008; **15**: 978-989.
6. Vellinga J, de Vrij J, Myhre S, Uil T, Martineau P, Lindholm L et al. Efficient incorporation of a functional hyperstable single-chain antibody fragment protein-IX fusion in the adenovirus capsid. *Gene Ther* 2007; **14**: 664-670.
7. Vellinga J, Rabelink MJWE, Cramer SJ, van den Wollenberg DJM, Van der Meulen H, Leppard KN et al. Spacers increase the accessibility of peptide ligands linked to the carboxyl terminus of adenovirus minor capsid protein IX. *J Virol* 2004; **78**: 3470-3479.
8. Corjon S, Wortmann A, Engler T, van Rooijen N, Kochanek S, Kreppel F. Targeting of adenovirus vectors to the LRP receptor family with the high-affinity ligand RAP via combined genetic and chemical modification of the pIX capsomere. *Mol Ther* 2008; **16**: 1813-1824.
9. Tang Y, Wu H, Ugai H, Matthews QL, Curiel DT. Derivation of a triple mosaic adenovirus for cancer gene therapy. *PLoS One* 2009; **4**: e8526.
10. Bayer W, Tenbusch M, Lietz R, Johrden L, Schimmer S, Uberla K et al. Vaccination with an adenoviral vector that encodes and displays a retroviral antigen induces improved neutralizing antibody and CD4+ T-cell responses and confers enhanced protection. *J Virol* 2010; **84**: 1967-1976.
11. Boyer J, Sofer-Podesta C, Ang J, Hackett N, Chiuchiolo M, Senina S et al. Protective Immunity Against a Lethal Respiratory Yersinia pestis Challenge Induced by V Antigen or the F1 Capsular Antigen Incorporated into the Adenovirus Capsid. *Hum Gene Ther* 2010; **21**: 891-901.
12. Vellinga J, Uil TG, de Vrij J, Rabelink MJWE, Lindholm L, Hoeben RC. A system for efficient generation of adenovirus protein IX-producing helper cell lines. *J Gene Med* 2006; **8**: 147-154.
13. Fabry CM, Rosa-Calatrava M, Conway JF, Zubieta C, Cusack S, Ruigrok RW et al. A quasi-atomic model of human adenovirus type 5 capsid. *EMBO J* 2005; **24**: 1645-1654.
14. Bergelson JM, Cunningham JA, Droguett G, Kurt-Jones EA, Krithivas A, Hong JS et al. Isolation of a common receptor for Coxsackie B viruses and adenoviruses 2 and 5. *Science (New York, NY)* 1997; **275**: 1320-1323.
15. Nemerow GR, Stewart PL. Role of alpha(v) integrins in adenovirus cell entry and gene delivery. *Microbiol Mol Biol Rev* 1999; **63**: 725-734.
16. Wickham TJ, Mathias P, Cheresch DA, Nemerow GR. Integrins alpha v beta 3 and alpha v beta 5 promote adenovirus internalization but not virus attachment. *Cell* 1993; **73**: 309-319.
17. de Haan CA, Li Z, te Lintelo E, Bosch BJ, Haijema BJ, Rottier PJ. Murine coronavirus with an extended host range uses heparan sulfate as an entry receptor. *J Virol* 2005; **79**: 14451-14456.
18. Kalyuzhnyi O, Di Paolo NC, Silvestry M, Hoffherr SE, Barry MA, Stewart PL et al. Adenovirus serotype 5 hexon is critical for virus infection of hepatocytes *in vivo*. *Proc Natl Acad Sci USA* 2008; **105**: 5483-5488.

19. Waddington SN, McVey JH, Bhella D, Parker AL, Barker K, Atoda H et al. Adenovirus serotype 5 hexon mediates liver gene transfer. *Cell* 2008; **132**: 397-409.
20. Patterson S, Russell WC. Ultrastructural and immunofluorescence studies of early events in adenovirus-HeLa cell interactions. *J Gen Virol* 1983; **64**: 1091-1099.
21. Reiser H, Stadecker MJ. Costimulatory B7 molecules in the pathogenesis of infectious and autoimmune diseases. *N Engl J Med* 1996; **335**: 1369-1377.
22. McNees AL, Mahr JA, Ornelles D, Gooding LR. Postinternalization inhibition of adenovirus gene expression and infectious virus production in human T-cell lines. *J Virol* 2004; **78**: 6955-6966.
23. Drouin M, Cayer MP, Jung D. Adenovirus 5 and chimeric adenovirus 5/F35 employ distinct B-lymphocyte intracellular trafficking routes that are independent of their cognate cell surface receptor. *Virology* 2010; **401**: 305-313.
24. Heemskerk B, Veltrop-Duits LA, van Vreeswijk T, ten Dam MM, Heidt S, Toes RE et al. Extensive cross-reactivity of CD4+ adenovirus-specific T cells: implications for immunotherapy and gene therapy. *J Virol* 2003; **77**: 6562-6566.
25. Cambiaggi C, Scupoli MT, Cestari T, Gerosa F, Carra G, Tridente G et al. Constitutive expression of CD69 in interspecies T-cell hybrids and locus assignment to human chromosome 12. *Immunogenetics* 1992; **36**: 117-120.
26. Trinchieri G, Matsumoto-Kobayashi M, Clark SC, Seehra J, London L, Perussia B. Response of resting human peripheral blood natural killer cells to interleukin 2. *J Exp Med* 1984; **160**: 1147-1169.
27. He XS, Draghi M, Mahmood K, Holmes TH, Kemble GW, Dekker CL et al. T cell-dependent production of IFN-gamma by NK cells in response to influenza A virus. *J Clin Invest* 2004; **114**: 1812-1819.
28. Muruve DA. The innate immune response to adenovirus vectors. *Hum Gene Ther* 2004; **15**: 1157-1166.
29. Di Paolo NC, Shayakhmetov DM. Adenovirus de-targeting from the liver. *Curr Opin Mol Ther* 2009; **11**: 523-531.
30. Xu Z, Tian J, Smith JS, Byrnes AP. Clearance of adenovirus by Kupffer cells is mediated by scavenger receptors, natural antibodies, and complement. *J Virol* 2008; **82**: 11705-11713.
31. Au T, Thorne S, Korn WM, Sze D, Kirn D, Reid TR. Minimal hepatic toxicity of Onyx-015: spatial restriction of coxsackie-adenoviral receptor in normal liver. *Cancer Gene Ther* 2007; **14**: 139-150.
32. Bangari DS, Shukla S, Mittal SK. Comparative transduction efficiencies of human and nonhuman adenoviral vectors in human, murine, bovine, and porcine cells in culture. *Biochem Biophys Res Commun* 2005; **327**: 960-966.
33. Atencio IA, Grace M, Bordens R, Fritz M, Horowitz JA, Hutchins B et al. Biological activities of a recombinant adenovirus p53 (SCH 58500) administered by hepatic arterial infusion in a Phase 1 colorectal cancer trial. *Cancer Gene Ther* 2006; **13**: 169-181.
34. Klein B, Pastink A, Odijk H, Westerveld A, van der Eb AJ. Transformation and immortalization of diploid xeroderma pigmentosum fibroblasts. *Exp Cell Res* 1990; **191**: 256-262.
35. Fallaux FJ, Kranenburg O, Cramer SJ, Houweling A, Van Ormondt H, Hoebe RC et al. Characterization of 911: a new helper cell line for the titration and propagation of early region 1-deleted adenoviral vectors. *Hum Gene Ther* 1996; **7**: 215-222.
36. Uil TG, de Vrij J, Vellinga J, Rabelink MJWE, Cramer SJ, Chan OYA et al. A lentiviral vector-based adenovirus fiber-pseudotyping approach for expedited functional assessment of candidate retargeted fibers. *J Gene Med* 2009; **11**: 990-1004.
37. Carlotti F, Bazuine M, Kekarainen T, Seppen J, Pognonec P, Maassen JA et al. Lentiviral vectors efficiently transduce quiescent mature 3T3-L1 adipocytes. *Mol Ther* 2004; **9**: 209-217.
38. Murakami P, McCaman MT. Quantitation of adenovirus DNA and virus particles with the PicoGreen fluorescent Dye. *Anal Biochem* 1999; **274**: 283-288.
39. Sittler A, Gallinaro H, Jacob M. The secondary structure of the adenovirus-2 L4 polyadenylation domain: evidence for a hairpin structure exposing the

- AAUAAA signal in its loop. *J Mol Biol* 1995; **248**: 525-540.
40. He TC, Zhou S, da Costa LT, Yu J, Kinzler KW, Vogelstein B. A simplified system for generating recombinant adenoviruses. *Proc Natl Acad Sci USA* 1998; **95**: 2509-2514.
 41. Ono HA, Le LP, Davydova JG, Gavrikova T, Yamamoto M. Noninvasive visualization of adenovirus replication with a fluorescent reporter in the E3 region. *Cancer Res* 2005; **65**: 10154-10158.
 42. Caravokyri C, Leppard KN. Constitutive episomal expression of polypeptide IX (pIX) in a 293-based cell line complements the deficiency of pIX mutant adenovirus type 5. *J Virol* 1995; **69**: 6627-6633.
 43. Hong JS, Engler JA. The amino terminus of the adenovirus fiber protein encodes the nuclear localization signal. *Virology* 1991; **185**: 758-767.



CHAPTER 8

GENERAL DISCUSSION

8.1 INTRODUCTION

Human adenovirus type 5 (HAdV-5)-derived vectors are among the most promising viral vectors for cancer gene therapy. Although clinical trials have shown safety for anti-tumor therapy with HAdV-5 vectors, the efficacy in general remains limited. A variety of efficacy-limiting aspects has been identified, as outlined in Chapter 2 of this thesis. A major problem is the poor penetration of the tumor due to the paucity of the coxsackievirus and adenovirus receptor (CAR) on the surface of the tumor cells.^{1,2} Genetic modification of HAdV-5 capsid proteins might lead to the development of vectors that are specifically targeted to tumor cells, thereby improving efficacy as well as safety. Development of genetically modified vectors that can infect CAR-negative cells has mainly focused on the incorporation of heterologous ligands in the fiber knob, or on replacement of the entire knob domain by a heterologous ligand.³ The complexity of incorporating ligands into the adenovirus fiber locale has prompted the identification of other capsid proteins amendable for ligand incorporation.⁴ These approaches have the potential to incorporate an increased number of complex ligands per virion.

Major part of this thesis describes proof-of-principle studies on the usability of the minor capsid protein IX for targeting HAdV-5 to tumor cells (Chapters 3, 4, 5). Different ligands (single-chain antibody fragments (scFv's), single-chain T-cell receptors (scTCRs) and Affibody molecules) were efficiently incorporated in the virus capsid after genetic fusion to the carboxyl terminus of protein IX. This leads to enhanced transgene delivery to the targeted tumor cells. Also, a variety of analyses was performed on HAdV-5 vectors lacking the protein IX gene, motivated by the fact that the biological role of protein IX has not been fully elucidated (Chapter 7). This revealed aberrant characteristics for the protein IX-deficient vectors, such as enhanced transgene expression in CAR-negative cell lines, and enhanced activation of immune cells. Besides the assessment of protein IX-based tumor targeting, Chapter 6 of this thesis involves an alternative tumor-targeting methodology, i.e. through the fusion of ligands (scTCRs) to the fiber protein.

In this section, the major conclusions from the work presented in this thesis are summarized and recommendations for further research are provided. Furthermore, a general perspective is given on the future directions of developing oncolytic adenoviruses.

8.2 CONCLUSIONS

From the work presented in this thesis, we can draw the following major conclusions:

1. Large and complex polypeptide moieties with proven potential for tumor targeting, such as single-chain antibody fragments, single-chain T-cell receptors, or Affibody molecules, can be efficiently incorporated in the capsid of HAdV-5.
2. HAdV-5 can be targeted *in vitro* to cancer-testis (CT) antigens through fusing a single-chain T-cell receptor with protein IX or fiber molecules.
3. HAdV-5 can be targeted *in vitro* to Human Epidermal growth factor Receptor-2 (HER2) expressing tumor cells through fusing ZH-Affibody molecules with protein IX. This methodology requires the introduction of a cathepsin-cleavage site in between protein IX and the Affibody molecule.

4. Deleting the protein IX gene from HAdV-5 vectors results in enhanced delivery of transgenes into CAR-negative cells and enhanced activation of immune cells

8.3 PERSPECTIVES ON PROTEIN IX-LIGAND MEDIATED TUMOR TARGETING OF ADENOVIRUSES

Our studies present novel strategies for targeting HAdV-5 to tumor cells, which may be of great value for the future development of oncolytic adenovirus technology with improved efficacy and/or safety. The applicability of protein IX as an anchor for fusing large and complex polypeptides opens new opportunities for tumor cell targeting, as an alternative or in addition to the currently used fiber modification strategies. Of special interest, our studies also demonstrate the feasibility of targeting HAdV-5 to CT antigens through the fusion of scTCRs to protein IX or fiber. This significantly extends the number of tumor cell-specific molecules that can be targeted. Although these results are highly promising, a variety of further studies is needed to delineate the true clinical potential.

One important aspect will be to introduce the protein IX-ligand modifications in the genome of replication competent adenoviruses. Our studies mainly involved assessments of transduction efficiencies using replication deficient vectors. However, it is currently anticipated that the clinical anti-tumor efficacy of replication deficient vectors remains insufficient, irrespective the type of foreign transgene delivery.⁵ This has led to the ongoing development and clinical testing of different variants of Conditionally-Replicating Adenoviruses (CRAds), such as the HAdV-5.RGD.Δ24 virus that is tested for its anti-tumor efficacy and specificity in ovarian carcinoma and glioma patients.⁶ Future work may include the incorporation of protein IX-attached targeting ligands in CRAds to further improve their efficacy or specificity.

One aspect probably hampering the efficacy of oncolytic adenoviruses, and possibly all other types of oncolytic viruses, is the heterogeneity of tumor cells within a solid tumor mass. As such, highly differentiated tumor cells exist beside (a minor percentage of) tumor stem cells, which differ in the amount and type of cell surface receptor presentation. As a consequence of the heterogeneities, a significant fraction of a tumor might escape from infection with an oncolytic adenovirus. As a solution, 'mosaic' adenovectors might be developed, that are harnessed with multiple tumor targeting ligands. Protein IX offers new potential for the establishment of mosaic HAdV-5 vectors, for example combining fiber- with protein IX-mediated targeting. Also, vectors might be developed that have protein IX fused to different targeting ligands in a single virus particle. Proof-of-principle of creating protein IX-polypeptide mosaic viruses has already been shown through simultaneously incorporating a targeting, imaging, and therapeutic motif in the capsid of HAdV-5.⁷

Alongside our applied studies on the feasibility of using protein IX as an anchor for the attachment of tumor targeting ligands, aberrant characteristics were found for protein IX-gene deleted vectors (Chapter 7). Most strikingly, protein IX-deficient vectors showed increased transgene expression in a variety of cell types, as compared to the control vectors. The highest enhancements were observed on CAR-low/negative cells. Also, protein IX deletion appeared to lead to increased activation of cellular

subsets of peripheral blood mononuclear cells (PBMCs), as demonstrated by changes in cell surface marker expression. Although our experiments ruled out various aspects as causative mechanism, the exact molecular mechanism could not be elucidated. Recently, Strunze *et al.* reported an essential role for protein IX in facilitating access of viral DNA to the cellular nucleus.⁸ Upon infection of a cell, the HAdV-5 particle successively travels towards the nucleus, binds with hexon epitopes to a nuclear pore complex (NPC), uncoats, and inserts its DNA into the nucleus. Protein IX molecules were found to link the virus with microtubule motor kinesin-1 molecules after docking to the NPC. This results in nuclear access of viral genomes through compromising the integrity of the NPC and uncoating of the virus particles. Infection of cells with a protein IX-gene lacking HAdV-5 was shown to be less efficient as compared to wild-type HAdV-5 infection, as demonstrated by the formation of lower levels of progeny virus particles. These findings by Strunze *et al.* do not necessarily contradict our observations. Reduced microtubule motor binding of protein IX-lacking adenoviruses likely causes enhanced innate inflammatory responses, such as the interferon response, as a result of cytoplasmic sequestration and/or altered movement kinetics of the virus particles. In support of this, we observed enhanced activation of PBMCs. The cellular inflammatory responses might have had serious consequences on our protein IX-lacking vector's luciferase and GFP expression levels, since both transgenes were driven by the cytomegalovirus (CMV) promoter. The activity of this promoter is known to be stimulated by the cellular interferon response.⁹ Still, it remains to be investigated why CAR-negative cell lines display the strongest increase in transgene expression for protein IX-gene deleted HAdV-5 vectors.

Obviously, translation of protein IX-mediated tumor targeting towards the clinic requires the performance of studies in models that resemble the eventual application in humans, including animal studies. This will reveal the anti-tumor efficacy of protein IX-ligand viruses in the complex environment of a tumor, which consists of a large variety of cell types and extracellular matrix components. These studies should include careful analyses on the interactions of protein IX-liganded viruses with non-tumor cells, such as immune cells or hepatocytes.

Our studies suggest inefficient protein IX-mediated targeting after the attachment of high-affinity binding ligands. To obtain definite answers, it will be informative to perform a side-by-side comparison between vectors containing protein IX-linked ligands with different affinities for a certain receptor. Also, further studies are necessary to determine the most suitable type of polypeptide ligand to be fused with protein IX, e.g. comparing single-chain antibody fragments with single-chain T cell receptors. Again, it is recommended to use relevant model systems, since the outcome of such experiments probably depends on the tumor (micro)environment.

8.4 GENERAL PERSPECTIVES ON THE FUTURE DEVELOPMENT OF ONCOLYTIC ADENOVIRUSES

Recent years have witnessed the publication of a large variety of preclinical improvements on HAdV-5 vectors. These developments, as summarized in Chapter 2 of this thesis, have been driven by an increased knowledge on oncolytic HAdV-5

performance in humans (through evaluation of clinical trial data), improved insights into tumor biology, and improved vector modification techniques.

Clearly, this plethora of 'next generation oncolytic AdV techniques' needs extensive evaluation in the near future. Performing well-designed studies (for example comparing different vectors) will facilitate translation of the technology to the clinic. Preclinical studies suggest differences in the performance of various oncolytic viruses, with certain viruses outperforming others, depending on the tumor type or the delivery technique.¹⁰ Therefore, it will be important to compare AdV-derived oncolytic viruses with other oncolytic viruses, such as Reovirus,¹¹ Newcastle Disease Virus vectors,¹² and Herpes Simplex Virus vectors.¹³ Also, it will be essential to use testing models that resemble the eventual clinical setting. With this respect, important lessons can be learned from previous studies, which demonstrated remarkable differences in the *in vivo* behavior of HAdV-5 vectors between animals and humans. HAdV-5 binds extensively to human erythrocytes, thereby hampering systemic delivery. This is in contrast to rodents.^{14,15} Important differences occur between animal species as well. It has been found that tissues and cells of mice do not support HAdV-5 replication, whilst other species (e.g. cotton rats and Syrian hamsters) are permissive.¹⁶ For this reason, mouse models are less suitable for studying aspects on the specificity of oncolytic HAdV-5 vectors, such as liver toxicity and immune cell activation.

The existence of 'human versus animal' discrepancies makes human models more suitable to answer certain research questions. Various human models have been developed that are of special interest for the evaluation of oncolytic vectors. Vectors might be tested in *ex vivo* blood circulation models, a model that has already been used with success to compare blood circulation times and binding to blood components between AdV vectors.¹⁷ Also, oncolytic AdV testing is anticipated to benefit from the recent developments of *ex vivo* human tumor models.¹⁸ As an example, novel methodologies enable the *ex vivo* culturing of primary tumor material resected from brain tumors, including tumor stem cell cultures in specialized growth media (either as three-dimensional spheres,¹⁹ or as two-dimensional monolayers²⁰) and organotypic brain slice cultures.²¹ To simulate the heterogeneity of a solid tumor, efforts are undertaken to create spheres that consist of co-cultures of tumor cells with stromal cells, like fibroblasts or endothelial cells.²² These systems require further optimization, mainly to prevent the stromal cells from rapidly losing their viability or phenotype.

Of additional benefit, *ex vivo* culturing of primary tumor material opens opportunities for the design of 'personalized therapeutics'. In theory, therapeutic vector regimens can be screened on patient-derived tumor material before initiating a therapy. Personalizing viral gene therapy might improve the clinical success rate, taking into account that most tumor types consist of a 'family' of tumor subtypes. It is unlikely that all patients suffering from a single tumor type respond similarly to an oncolytic virus therapy.

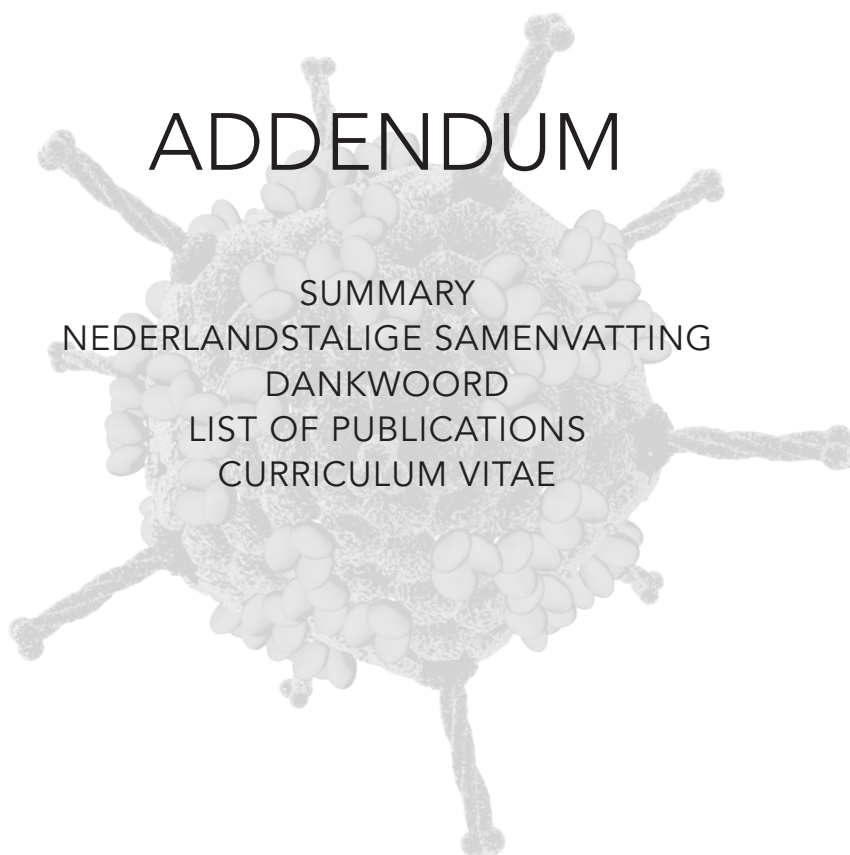
Besides the above mentioned requirements for vector testing in appropriate tumor models, it will be important to investigate the effects of combining oncolytic AdV therapy with other therapies. Combining chemotherapy with oncolytic virus treatment can lead to enhanced or even synergistic therapeutic efficacy, as demonstrated in animal models.^{23,24} Moreover, oncolytic virus treatment might enable the usage of lower concentrations of certain chemotherapeutics, thereby reducing the toxicity.

Taken together, the availability of improved experimental models and improved viral vectors offers great opportunities for the development of 'next generation oncolytic AdV therapies'. As a response on the previous identification of treatment efficacy-limiting aspects, a large plethora of novel vectors and strategies has been developed. Transductional targeting via attachment of ligands to protein IX offers a methodology for further improvements on oncolytic AdV vectors. Future studies in well-designed preclinical and clinical settings will teach whether the regained expectations for oncolytic adenoviruses as therapeutic regimens for cancer treatment will be fulfilled.

REFERENCES

- Hemmi S, Geertsen R, Mezzacasa A, Peter I, Dummer R. The presence of human coxsackievirus and adenovirus receptor is associated with efficient adenovirus-mediated transgene expression in human melanoma cell cultures. *Hum Gene Ther* 1998; **9**: 2363-2373.
- Li D, Duan L, Freimuth P, O'Malley BW, Jr. Variability of adenovirus receptor density influences gene transfer efficiency and therapeutic response in head and neck cancer. *Clin Cancer Res* 1999; **5**: 4175-4181.
- Glasgow JN, Everts M, Curiel DT. Transductional targeting of adenovirus vectors for gene therapy. *Cancer Gene Ther* 2006; **13**: 830-844.
- Vellinga J, Van der Heijdt S, Hoeben RC. The adenovirus capsid: major progress in minor proteins. *J Gen Virol* 2005; **86**: 1581-1588.
- Yamamoto M, Curiel DT. Current issues and future directions of oncolytic adenoviruses. *Mol Ther* 2010; **18**: 243-250.
- Kimball KJ, Preuss MA, Barnes MN, Wang M, Siegal GP, Wan W et al. A phase I study of a tropism-modified conditionally replicative adenovirus for recurrent malignant gynecologic diseases. *Clin Cancer Res* 2010; **16**: 5277-5287.
- Tang Y, Wu H, Ugai H, Matthews QL, Curiel DT. Derivation of a triple mosaic adenovirus for cancer gene therapy. *PLoS One* 2009; **4**: e8526.
- Strunze S, Engelke MF, Wang IH, Puntener D, Boucke K, Schleich S et al. Kinesin-1-mediated capsid disassembly and disruption of the nuclear pore complex promote virus infection. *Cell Host Microbe*; **10**: 210-223.
- Schaack J, Bennett ML, Shapiro GS, DeGregori J, McManaman JL, Moorhead JW. Strong foreign promoters contribute to innate inflammatory responses induced by adenovirus transducing vectors. *Virology* 2011; **412**: 28-35.
- Eager RM, Nemunaitis J. Clinical development directions in oncolytic viral therapy. *Cancer Gene Ther* 2011; **18**: 305-317.
- Van den Wollenberg DJ, Van den Hengel SK, Dautzenberg IJC, Kranenburg O, Hoeben RC. Modification of mammalian reoviruses for use as oncolytic agents. *Expert Opin Biol Ther* 2009; **9**: 1509-1520.
- Schirmmacher V, Fournier P. Newcastle disease virus: a promising vector for viral therapy, immune therapy, and gene therapy of cancer. *Methods Mol Biol* 2009; **542**: 565-605.
- Kaur B, Chiocca EA, Cripe TP. Oncolytic HSV-1 Virotherapy: Clinical Experience and Opportunities for Progress. *Curr Pharm Biotechnol* 2011.
- Carlisle RC, Di Y, Cerny AM, Sonnen AF, Sim RB, Green NK et al. Human erythrocytes bind and inactivate type 5 adenovirus by presenting Coxsackie virus-adenovirus receptor and complement receptor 1. *Blood* 2009; **113**: 1909-1918.
- Seiradake E, Henaff D, Wodrich H, Billet O, Perreau M, Hippert C et al. The cell adhesion molecule "CAR" and sialic acid on human erythrocytes influence adenovirus *in vivo* biodistribution. *PLoS Pathog* 2009; **5**: e1000277.

16. Thomas MA, Spencer JF, Wold WS. Use of the Syrian hamster as an animal model for oncolytic adenovirus vectors. *Methods Mol Med* 2007; **130**: 169-183.
17. Danielsson A, Elgue G, Nilsson BM, Nilsson B, Lambris JD, Totterman TH et al. An ex vivo loop system models the toxicity and efficacy of PEGylated and unmodified adenovirus serotype 5 in whole human blood. *Gene Ther* 2010; **17**: 752-762.
18. Hirschhaeuser F, Menne H, Dittfeld C, West J, Mueller-Klieser W, Kunz-Schughart LA. Multicellular tumor spheroids: an underestimated tool is catching up again. *J Biotechnol* 2010; **148**: 3-15.
19. Lee J, Kotliarova S, Kotliarov Y, Li A, Su Q, Donin NM et al. Tumor stem cells derived from glioblastomas cultured in bFGF and EGF more closely mirror the phenotype and genotype of primary tumors than do serum-cultured cell lines. *Cancer Cell* 2006; **9**: 391-403.
20. Pollard SM, Yoshikawa K, Clarke ID, Danovi D, Stricker S, Russell R et al. Glioma stem cell lines expanded in adherent culture have tumor-specific phenotypes and are suitable for chemical and genetic screens. *Cell Stem Cell* 2009; **4**: 568-580.
21. DeWitt Hamer PC, Van Tilborg AA, Eijk PP, Sminia P, Troost D, Van Noorden CJ et al. The genomic profile of human malignant glioma is altered early in primary cell culture and preserved in spheroids. *Oncogene* 2008; **27**: 2091-2096.
22. Burdett E, Kasper FK, Mikos AG, Ludwig JA. Engineering tumors: a tissue engineering perspective in cancer biology. *Tissue Eng Part B Rev* 2010; **16**: 351-359.
23. Chu RL, Post DE, Khuri FR, Van Meir EG. Use of replicating oncolytic adenoviruses in combination therapy for cancer. *Clin Cancer Res* 2004; **10**: 5299-5312.
24. Jiang G, Xin Y, Zheng JN, Liu YQ. Combining conditionally replicating adenovirus-mediated gene therapy with chemotherapy: a novel antitumor approach. *Int J Cancer* 2011; **129**: 263-274.



ADDENDUM

SUMMARY
NEDERLANDSTALIGE SAMENVATTING
DANKWOORD
LIST OF PUBLICATIONS
CURRICULUM VITAE

SUMMARY

Recombinant viral vectors hold great promise in the field of cancer gene therapy. While a plethora of viruses is being evaluated as oncolytic agents, human adenoviruses of serotype 5 (HAdV-5) are among the most popular of viruses to be developed. Although clinical studies have demonstrated safety of cancer gene therapy with HAdV-5-derived vectors, the efficacy still needs further enhancement. Several factors have been identified that limit the anti-tumor efficacy, as reviewed in **Chapter 2** of this thesis. One major bottleneck is the inadequate penetration and spread of the virus within the tumor. This is attributable, at least in part, to the low or heterogeneous expression of the coxsackie and adenovirus receptor (CAR) on the tumor cells. This thesis describes the development and preclinical evaluation of novel tumor-targeted HAdV-5 vectors, through implementing the genetic fusion of capsid proteins (protein IX and fiber) with a variety of tumor-targeting polypeptides.

Chapters 3, 4, and 5 describe the usability of the HAdV-5 minor capsid protein IX as a locale for genetically fusing tumor targeting ligands. At first, proof-of-principle is described of fusing protein IX with hyper-stable single-chain antibody fragments (scFv's) (**Chapter 3**). Hyper-stable scFv's are anticipated to be highly suitable for incorporation in adenovirus capsids, as a result of their ability to fold correctly in the reducing environment of the cytoplasm. A hyper-stable scFv directed against β -galactosidase (13R4) was fused with protein IX. To ensure enhanced protrusion of the scFv at the virus surface, a 75-Ångstrom α -helical spacer was included between protein IX and the 13R4. The protein IX-13R4 fusion proteins were efficiently incorporated in the HAdV-5 capsid and, importantly, 13R4 appeared to preserve its functionality in terms of β -galactosidase binding.

Next, protein IX also appears to be suitable for fusing tumor cell-directed single-chain T cell receptors (scTCRs) (**Chapter 4**). Tumor cell targeting was established via the fusion of protein IX with a scTCR (scTCR^{HLA-A1/MAGE-A1}) directed against the cancer testis (CT) antigen MAGE-A1, presented on the cell surface in complex with human leukocyte antigens of haplotype A1 (HLA-A1). HAdV-5 vector particles loaded with protein IX-scTCR^{HLA-A1/MAGE-A1} fusion proteins transduced melanoma target cell lines with at least 10-fold higher efficiency than the control particles. Importantly, specificity of targeting could be shown as well. These results underscore the potential of using protein IX for targeting HAdV-5, and demonstrate the feasibility of targeting HAdV-5 vectors to intracellularly-derived CT antigens. The highly specific expression profiles of CT antigens, which are expressed in a variety of cancerous tissues and are generally silent in normal tissues (except for the testis), make them interesting target molecules for cancer therapies.

Chapter 5 describes protein IX-mediated tumor targeting of HAdV-5 through fusing Affibody molecules. Affibody molecules might be valuable moieties for virus targeting, because of their relatively small size and high binding affinity. Previous reports, however, showed limited targeting efficacies after fusing 'high-affinity binders', such as Affibody molecules, to protein IX, which has been suggested to be the result of inefficient release of the virions from their targeted receptors in the endosome. Our studies demonstrate that the transduction of tumor cells is augmented by incorporating a cathepsin-cleavage site (CCS) between protein IX and a 'ZH Affibody molecule',

directed against the Human Epidermal growth factor Receptor 2 (HER2). Virus particles harboring the protein IX-CCS-ZH in their capsid transduced HER2 positive SKOV-3 ovarian carcinoma cells with increased efficiency in monolayer cultures, 3-dimensional spheroid cultures, and in SKOV-3 tumors grown on the chorioallantoic membrane of embryonated chicken eggs. These findings further augment the applicability of protein IX as an anchor for coupling tumor-targeting ligands.

An alternative HAdV-5 targeting strategy is described in **Chapter 6**, concerning the genetic fusion of a scTCR with the fiber capsid protein. In the genome of wild-type HAdV-5, the sequence encoding for the fiber knob domain was replaced by sequences encoding a scTCR (identical to the scTCR molecule as described in Chapter 4) and an artificial trimerization domain. The resulting virus was, as anticipated, detargeted from Coxsackie- and Adenovirus Receptor (CAR) binding, and targeted to HLA-A1/MAGE-A1 molecules on tumor cells. Efficient and specific killing of targeted melanoma cell cultures was observed.

Finally, **Chapter 7** provides information on functional consequences of deleting the protein IX gene from HAdV-5 vectors. Various effects of protein IX deletion are reported, including enhanced reporter gene delivery to CAR-negative cell lines and enhanced activation of peripheral blood mononuclear cells. These findings suggest that protein IX can affect the cell tropism of HAdV-5, and may function to dampen the innate immune responses against HAdV particles. This may be of relevance for future development and clinical implementation of protein IX-modified HAdV-5 vectors.

NEDERLANDSTALIGE SAMENVATTING

Genetisch gemodificeerde virale vectoren hebben potentie voor gebruik als oncolytisch therapeutikum. In het scala aan virussen dat geëvalueerd wordt, neemt humaan adenovirus serotype 5 (HAdV-5) een voornaam plaats in binnen het onderzoek naar oncolytische virustherapie. Uit klinische studies is gebleken dat kankergentherapie met HAdV-5 vectoren veilig is, maar de effectiviteit blijkt voornamelijk beperkt te zijn. Verscheidene factoren belemmeren de effectiviteit, zoals samengevat in **Hoofdstuk 2** van dit proefschrift. Een voornaam probleem wordt gevormd door het onvermogen van het virus om tot de gehele tumor massa door te dringen. Dit wordt onder meer veroorzaakt door de lage en heterogene expressie van de coxsackie- en adenovirus receptor (CAR) op het oppervlak van de tumorcellen. In dit proefschrift wordt de ontwikkeling en preklinische evaluatie beschreven van nieuwe oncolytische HAdV-5 vectoren. Deze vectoren zijn gericht tegen tumorcellen door middel van het koppelen van virale manteleiwitten (IX en fiber) aan verschillende typen polypeptiden.

In de hoofdstukken 3 tot en met 5 wordt de ontwikkeling en evaluatie beschreven van een nieuw HAdV-5 'tumor-targeting' systeem, gebaseerd op het fuseren van polypeptiden aan het kleinste HAdV-5 manteleiwit, eiwit IX. In **Hoofdstuk 3** wordt de haalbaarheid aangetoond van het fuseren van eiwit IX met hyperstabiele enkelstrengs antilichamen (scFv's). In tegenstelling tot normale antilichamen nemen hyperstabiele scFv's een functionele vouwing aan in het reducerende milieu van het cytoplasma, waardoor ze in potentie zeer geschikt zijn om in te bouwen in de mantel van adenovirussen. We beschrijven de fusie van eiwit IX met een hyperstabil scFv gericht tegen β -galactosidase (13R4), waarbij een 75-Ångstrom α -helix is geïncorporeerd om de presentatie van 13R4 op het virusoppervlak te optimaliseren. Het 13R4 polypeptide bleek efficiënt te worden geïncorporeerd in de mantel van HAdV-5, en bleek de juiste vouwing aan te nemen gezien de binding aan β -galactosidase.

In het volgende hoofdstuk (**Hoofdstuk 4**) wordt aangetoond dat eiwit IX tevens geschikt is voor het beladen van HAdV-5 met enkelstrengs T cel receptoren (scTCRs). Infectie van tumorcellen kon worden verbeterd door middel van het koppelen van eiwit IX aan een scTCR (scTCR^{HLA-A1/MAGE-A1}) die gericht is tegen het kanker-testis antigeen MAGE-A1, welke gepresenteerd wordt op het celoppervlak door humaan leukocyt antigeen met haplotype A1 (HLA-A1). Ten opzichte van een controle virus bleken virusdeeltjes geladen met scTCR^{HLA-A1/MAGE-A1} in staat om HLA-A1/MAGE-A1-positieve melanoma cellen te transduceren met een tienmaal hogere efficiëntie. Tevens werd specificiteit van de HLA-A1/MAGE-A1 binding aangetoond. Deze resultaten laten zien dat eiwit IX potentieel heeft voor het richten van HAdV-5 vectoren naar kanker-testis antigeen op tumorcellen. Het principe van kanker-testis antigeen targeting, gericht tegen tumor-specifieke peptides die afkomstig zijn uit het cytoplasma van een cel, wijkt af van de conventionele targeting van oncolytische (adeno)virale vectoren, welke gericht is tegen celoppervlakte-eiwitten die tot overexpressie komen op tumorcellen. Kanker-testis antigeen zijn mogelijk zeer geschikt om als target te dienen voor kankertherapieën, doordat deze moleculen tot expressie komen op het celoppervlak van tumorcellen, maar niet op cellen in gezonde weefsels (met uitzondering van de teelballen).

In **Hoofdstuk 5** wordt uiteengezet hoe eiwit IX gebruikt kan worden voor de koppeling van Affibody eiwitten. Door het relatief kleine formaat en de hoge bindingsaffiniteit aan receptoren worden Affibody eiwitten beschouwd als interessante structuren voor tumortargeting van virussen. Eerdere publicaties duiden echter op een inefficiënte targeting na het fuseren van eiwit IX met 'hoog-affiniteit liganden', zoals Affibody eiwitten, doordat het virus niet kan loskoppelen van de receptor in het endosoom. Onze studies laten zien dat de infectie van tumorcellen verbeterd kan worden door het incorporeren van een cathepsin-knipsequentie (CKS) tussen eiwit IX en het Affibody eiwit 'ZH', welke gericht is tegen de Humane Epidermale groeifactor Receptor 2 (HER2). Het includeren van de CKS bleek noodzakelijk te zijn om tumortargeting te bewerkstelligen van eiwit IX-ZH beladen virusdeeltjes. Verbeterde infectie vond plaats van HER2-positieve targetcellen (SKOV-3 eierstokkankercellen) in verschillende modellen, zijnde monolaagkweken, 3-dimensionale sferoïdekweken en tumorkweken op de chorioallantoïsche membraan van bevruchte kippeneieren. Deze vindingen vergroten het potentieel van eiwit IX voor het koppelen van anti-tumor liganden.

In **Hoofdstuk 6** wordt een alternatieve targetingstrategie beschreven, door middel van het fuseren van een scTCR (scTCR^{HLA-A1/MAGE-A1}) met het fiber manteleiwit. In het genoom van een wildtype HAdV-5 is de sequentie coderende voor het globulaire deel van de fiber vervangen door sequenties coderende voor de scTCR^{HLA-A1/MAGE-A1} en voor een kunstmatig trimerizatie domein. Door de afwezigheid van het globulaire fiberfragment bleek het gemodificeerde virus niet meer in staat tot binding aan de Coxsackie- en Adenovirus Receptor (CAR). In plaats hiervan vond binding plaats aan HLA-A1/MAGE-A1. Als gevolg werd een sterkere en meer specifieke doding van verschillende melanoma targetcellen waargenomen.

Tot slot wordt in **Hoofdstuk 7** een studie beschreven naar de functionele gevolgen van eiwit IX deletie in het genoom van HAdV-5 vectoren. Verschillende effecten vinden plaats, waaronder een verhoogde afgifte van transgenen in CAR-negatieve cellen en een verhoogde activatie van bepaalde typen cellen van het aangeboren immuunsysteem. De bevindingen suggereren dat eiwit IX een rol speelt in de totstandkoming van het cellulair tropisme, en dat het eiwit een functie heeft bij vermindering van de aangeboren immunrespons. Deze aspecten verdienen nader onderzoek bij verdere ontwikkeling van oncolytische HAdV-5 vectoren met eiwit IX modificaties.

DANKWOORD

Nu het proefschrift klaar is, wil ik graag alle mensen bedanken die de afgelopen jaren op de een of andere wijze een steentje hebben bijgedragen. Mijn dank voor jullie hulp is groot!

Rob, ik ben er trots op om onder jouw hoede te mogen promoveren. Van het begin tot het einde heb je vertrouwen getoond en mij de ruimte gegeven voor persoonlijke ontwikkeling als onderzoeker. Hoop ook na mijn promoveren nog bij je aan te kunnen kloppen voor een goed staaltje mentorschap.

Heel veel dank aan mijn collega's van de (voormalige) MCB-virusbiologie groep, met wie ik jarenlang (eerst op het Sylvius Laboratorium, daarna aan de Einthovenweg) een kamer, een lab, en lief-en-leed heb gedeeld (Taco, Steve, Martijn, Diana, Arnaud, Françoise, Jort, Danijela, François). Het was bijzonder gezellig en stimulerend om in jullie bijzijn te zijn, niet alleen op de werkvloer, maar ook daarbuiten. Door jullie was het een feestje om op het lab te zijn, die goede sfeer zal ik nooit vergeten. Iris en Sanne; bedankt dat jullie mijn paranimfen willen zijn. Met jullie aan mijn zijde voel ik me ongetwijfeld vele malen sterker. Ook mijn dank aan alle andere collega's van de MCB-VSB groep, die na de 'grote fusie' opeens ook te doen hadden met mijn perikelen omtrent het adenovirale eiwit IX. Maarten, Gijs, Harald, Jim, Anabel, Manuel, Dirk, Selina, Hester, Letitia, Kim, Ietje, Twan, Sjosh, Dirk v. B.; het was een eer om met jullie te mogen samenwerken.

Aan mijn studenten (Hannah, Payman, Oscar); jullie werk en enthousiasme was van grote waarde voor het onderzoek, duizend maal dank!

Also my acknowledgements to our collaborators of the GIANT consortium (amongst others Leif, Maria, Susanna, Petra, Robert, Ralph, Magnus, Florian, Stefan, Len, Kerry, Ellen, Wytske, Norman): I highly appreciated our meetings, in which we shared our common interests in adenovirus targeting in an extremely relaxed and fruitful way.

Marieke, Martine, Clemens, Sieger; mijn waardering en dank voor jullie positieve houding ten tijde van mijn laatste loodjes voor het schrijfwerk van mijn proefschrift.

Dank aan mijn 'Wageningse', Stolwijkse en Klimmense vrienden en familie, vooral ook voor jullie geduld met mijn drukke labbestaan in het Leidsche. Opa en oma; dank voor jullie eeuwige vertrouwen en interesse.

Pa en ma; zonder jullie had dit boekwerk er niet gelegen. Bedankt voor alle hulp en liefde die jullie mij gegeven hebben.

Lieve Iris, jij bent mijn rots in de branding. Een buiging voor je nimmer aflatende steun, ondanks de vele nachtelijke uurtjes aan typwerk (en de lamme days-after), het regelmatig uitlopen van 'even-snel-naar-het-lab', en het vele geblaas over een klein viraal eiwitje. Lieve, kleine Saar, jouw glimlachjes maakten de laatste loodjes minder zwaar.

LIST OF PUBLICATIONS

1. Pijlman GP, de Vrij J, van den End FJ, Vlak JM, Martens DE. Evaluation of baculovirus expression vectors with enhanced stability in continuous cascaded insect-cell bioreactors. *Biotechnol Bioeng* 2004; **87**: 743-753.
2. Vellinga J, Uil TG, de Vrij J, Rabelink MJ, Lindholm L, Hoeben RC. A system for efficient generation of adenovirus protein IX-producing helper cell lines. *J Gene Med* 2006; **8**: 147-154.
3. Hoeben RC, Uil TG, de Vrij J, de Vries AAF, Vellinga J. Adenoviruses: The long march from "oncogenic" to "oncolytic" virus. *Chemtracts-Biochem and Mol Biol* 2006; **19**: 211-222.
4. Vellinga J, de Vrij J, Myhre S, Uil TG, Martineau P, Lindholm L, Hoeben RC. Efficient incorporation of a functional hyper-stable single-chain antibody fragment protein-IX fusion in the adenovirus capsid. *Gene Ther* 2007; **14**: 664-670.
5. Sebestyen Z, de Vrij J, Magnusson M, Debets R, Willemsen R. An oncolytic adenovirus redirected with a tumor-specific T-cell receptor. *Cancer Res* 2007; **67**: 11309-11316.
6. de Vrij J, Uil TG, van den Hengel SK, Cramer SJ, Koppers-Lalic D, Verweij MC, Wiertz EJ, Vellinga J, Willemsen RA, Hoeben RC. Adenovirus targeting to HLA-A1/MAGE-A1-positive tumor cells by fusing a single-chain T-cell receptor with minor capsid protein IX. *Gene Ther* 2008; **15**: 978-989.
7. Hoang-Le D, Smeenk L, Anraku I, Pijlman GP, Wang XJ, de Vrij J, Liu WJ, Le TT, Schroder WA, Khromykh AA, Suhrbier A. A Kunjin replicon vector encoding granulocyte macrophage colony-stimulating factor for intra-tumoral gene therapy. *Gene Ther* 2009; **16**: 190-199.
8. Uil TG, de Vrij J, Vellinga J, Rabelink MJ, Cramer SJ, Chan OY, Pugnali M, Magnusson M, Lindholm L, Boulanger P, Hoeben RC. A lentiviral vector-based adenovirus fiber-pseudotyping approach for expedited functional assessment of candidate retargeted fibers. *J Gene Med* 2009; **11**: 990-1004.
9. De Vrij J, Willemsen RA, Lindholm L, Hoeben RC, and the GIANT consortium. Adenovirus-derived vectors for prostate cancer gene therapy. *Hum Gene Ther* 2010; **7**: 795-805.
10. Uil TG, Vellinga J, de Vrij J, van den Hengel SK, Rabelink MJ, Cramer SJ, Eekels JJ, Ariyurek Y, van Galen M, Hoeben RC. Directed adenovirus evolution using engineered mutator viral polymerases. *Nucleic Acids Res* 2010; **39**: e30.
11. Van den Hengel SK, de Vrij J, Uil TG, Lamfers ML, Sillevius Smitt PA, Hoeben RC. Truncating the i-leader open reading frame enhances release of human adenovirus type 5 in glioma cells. *Virology* 2011; **8**: 162.
12. De Vrij J, van den Hengel SK, Uil TG, Koppers-Lalic D, Dautzenberg IJ, Stassen OM, Bárcena M, Yamamoto M, de Ridder CM, Kraaij R, Kwappenberg KM, Schilham MW, Hoeben RC. Enhanced transduction of CAR-negative cells by protein IX-gene deleted adenovirus 5 vectors. *Virology* 2011; **410**: 192-200.

13. De Vrij J, Dautzenberg IJ, van den Hengel SK, Magnusson MK, Uil TG, Cramer SJ, Vellinga J, Verissimo CS, Lindholm L, Koppers-Lalic D, Hoeben RC. A cathepsin-cleavage site between the adenovirus capsid protein IX and a tumor-targeting ligand improves targeted transduction. *Gene Ther* 2012; doi: 10.1038/gt.2011.162.
14. De Vrij J, Maas SLN, Hegmans JP, Lamfers ML, Dirven CMF, Broekman MLD. Exosomes and cancer. *Ned Tijdschr Geneeskd* 2011; A3677R2.

CURRICULUM VITAE

Jeroen de Vrij werd geboren in Stolwijk op 1 december 1979. Na het behalen van het VWO diploma aan de Goudse Scholen Gemeenschap te Gouda, werd in 1998 begonnen met de studie Bioprocestechnologie aan de Wageningen Universiteit (WUR). Tijdens de afstudeerfase werd bij het Laboratorium voor Virologie en de afdeling Proceskunde van het WUR onderzoek gedaan naar recombinant baculovirussen voor de productie van vaccins in cellen in een bioreactorsysteem, onder leiding van dr. G.P. Pijlman en dr. D.E. Martens. Tevens werd een onderzoeksstage doorlopen bij het Sir Albert Sakzewski Virus Research Center te Brisbane, Australia, met tot doel 'het ontwikkelen van Flavivirus vectoren voor genterapeutische toepassingen'. Alvorens af te studeren in 2004 werd een afstudeervak gevolgd bij de afdeling Moleculaire Celbiologie, Virus- en Stamcelbiologie groep, van het Leids Universitair Medisch Centrum, onder supervisie van dr. J. Vellinga en prof. dr. R.C. Hoeben. Het daar opgezette onderzoek, betreffende een haalbaarheidsstudie naar het gebruik van adenovirus manteleiwit IX voor koppeling van tumor-targeting eiwitten, kon vervolgens worden voortgezet als promotiestudie, uiteindelijk resulterend in dit proefschrift. Als zijnde onderdeel van het Europese project GIANT ('Gene Therapy, an Integrated Approach to Neoplastic Treatment') werd een groot deel van de promotiestudie uitgevoerd in samenwerking en overleg met verscheidene nationale en internationale onderzoekers. Sinds februari 2010 is Jeroen werkzaam als post-doc onderzoeker op de afdeling Neurochirurgie van het Erasmus Medisch Centrum te Rotterdam. Hier wordt in samenwerking met dr. M.L.D. Broekman, dr. M.L. Lamfers en prof. C.M.F. Dirven onderzoek verricht aan oncolytische adenovirussen voor de behandeling van hersenkanker en wordt nagegaan op welke wijze hersentumoren de (micro)omgeving beïnvloeden.

